Convergence analysis of numerical methods for fractional differential and integro-differential equations

Sandip Maji

Convergence analysis of numerical methods for fractional differential and integro-differential equations

Thesis submitted to

Indian Institute of Technology Guwahati

for the award of the degree

of

Doctor of Philosophy

by

Sandip Maji

(Roll Number: 196123008)

under the guidance of

Professor Natesan Srinivasan

DEPARTMENT OF MATHEMATICS

INDIAN INSTITUTE OF TECHNOLOGY GUWAHATI

February 2024

Department of Mathematics
Indian Institute of Technology Guwahati
Guwahati, Assam-781039, India

Declaration

It is certified that the work contained in this thesis entitled "**Convergence analysis of numerical methods for fractional differential and integro-differential equations**" has done by me, under the supervision of Dr. Natesan Srinivasan, Professor, Department of Mathematics, Indian Institute of Technology Guwahati for the award of the degree of Doctor of Philosophy and this work has not been submitted elsewhere for a degree.

IIT Guwahati
February 2024

Sandip Maji
Roll No. 196123008

Department of Mathematics
Indian Institute of Technology Guwahati
Guwahati, Assam-781039, India

Certificate

This is to certify that this thesis entitled "**Convergence analysis of numerical methods for fractional differential and integro-differential equations**" submitted by **Sandip Maji**, to the Indian Institute of Technology Guwahati, is a record of bona fide research work carried out under my supervision and is worthy of consideration for award of the degree of Doctor of Philosophy of the Institute.

IIT Guwahati
February 2024

Dr. Natesan Srinivasan
Professor
Department of Mathematics
Indian Institute of Technology Guwahati.

Dedicated to

"My family members"

and

"My thesis supervisor"

Acknowledgment

It gives me tremendous pleasure and honor to express my gratitude to all of the people who have supported me on my path. I want to start by thanking Professor Natesan Srinivasan for supervising my thesis. Throughout my stay, his assistance, mentorship, and patience during my research work have served as a beacon of hope for me. He never left my side and was there for me in all situations. There were times when I struggled, but he was always that source of inspiration whose optimistic energy I absorbed. His never-ending perseverance, tolerance, inspiration, and excitement have inspired me. This dissertation would not have been possible without his direction and constant assistance. He has been my friend, mentor, and critic, and he has always assured me to get the best out of me.

Along with my supervisor, I would like to express my gratitude to the rest of my doctoral committee members, Prof. D. C. Dalal, Prof. R. K. Sinha, and Prof. S. N. Bora, for their cooperation and insightful feedback while my research work progressed.

The Indian Institute of Technology Guwahati deserves my heartfelt gratitude for providing me with the resources I needed for my research. I am appreciative that the Ministry of Human Resource Development, Government of India, helped me out financially so that I could finish my thesis. The picturesque campus was the highlight of my entire stay throughout all these years. It exudes freshness with its melting beauty and upbeat atmosphere.

I appreciate the help I received from the department's office staff, Mr. Sridhar Samal, Mrs. Trishna Choudhury, Mr. Phatik Kumar, and Mr. Jayanta Kumar Kalita, as well as our technical superintendent, Mr. Pranpratim Borgohain, Mr. Santanu Majumdar, Mr. Pranab Jyoti Boro.

I would like to thank Prof. Satyajit Roy (Dept. of Math, IIT Madras), Dr. Ratikanta Behera (Dept. of CDS, IISC), and Dr. Swarup Kumar Panda (Dept. of Math, IIT KGP) for inspiring me and providing valuable suggestions to pursue further study in mathematics during my postgraduate and project periods. I want to express my gratitude

especially to Mr. Sumanta Pradhan, a teacher from my high school who never fails to inspire me in mathematics and have faith in me.

I appreciate my research colleagues for creating a stimulating and enjoyable workplace. I want to express my gratitude to my seniors, Dr. Gautam Singh, Dr. Avijit Das, and Dr. Mrityunjoy Barman, who have been by my side continually and have taught me a lot of the fundamentals of this subject. I also like to express my gratitude to my friends Matap, Abhijit, Aniruddha, Sagar, Mijanur, Saikat, and Abhradeep for their lovely and amiable company throughout my research career. For sharing all the special moments, my juniors Saurabh, Sachin, Aayushman, Ramesh, Suraj, Arijit and many others deserve my gratitude. I am also thankful to my college friends Puspendu, Parimal, Sourav, Subhankar, Snehasis, and Koushik, as well as my high school friends Sovan, Batakrishna, Subrata, Subhajit, and Anup, for their amazing company that provided me strength in any situation. This area is too little for me to express my gratitude to all of my incredible friends, but I will always treasure the wonderful times we have shared over the past few years.

I will always be appreciative to my parents, Mrs. Pratima Maji, Mr. Swapan Maji and my brother Mr. Sudip Maji, and my sister Mrs. Suparna Maji Das. They have been my pillar of support and have always had faith in me. My uncle Mr. Nimai Chand Maji, who was my first teacher and encouraged me in mathematics from an early age, deserves a special mention as well. I would praise God for his kindness. This journey will always hold special meaning.

February 2024 **Sandip Maji**

"We cannot solve problems with the same thinking we used to create them." - Albert Einstein

"If you want to have good ideas, you must have many ideas."
- Linus Pauling

"There is a universe of mathematics lying between the complete differentiations and integrations."
- O. Heaviside

Abstract

This thesis mainly focuses on the numerical solutions for the various types of fractional order differential and integro-differential equations. We have discussed the ordinary, partial, and integro-partial differential equations involving RLC-type and Caputo-type fractional derivatives. The numerical methods we have proposed in this thesis are mainly the shooting method, the cubic spline, and the discontinuous Galerkin finite element method. Besides finding the numerical solutions, we have discussed the well-posedness of some of the problems.

The thesis begins with the introduction providing the basic definitions, detailed literature survey and describing the outline of the rest of the chapters. First, we have studied the shooting technique for the steady-state linear and semi-linear fractional BVPs of RLC-type. Then, we have considered a class of one-dimensional linear and semi-linear time-fractional diffusion IBVPs. Here, we used the Sumudu decomposition approach and the maximum-minimum principle to demonstrate the existence and uniqueness of the analytical solution of the linear IBVP, respectively. Also, using L1-discretization for the fractional temporal derivative and the cubic spline approximation for the spatial variables, we provide a numerical scheme for both the linear and semi-linear diffusion IBVP. The same analytic and numerical solution approach is applied to a class of linear fractional integro-differential equation (FIDE).

Then, for the linear and semi-linear time-fractional diffusion problem, we obtained the numerical solution by applying the non-symmetric interior penalty Galerkin (NIPG) method for the spatial direction on a uniform mesh and the L1-discretization for the time derivative on a graded mesh. Also, we have studied the superconvergence of error estimates in the discrete energy-norm. After that, we discuss an efficient numerical method for solving nonlinear FIDE, where we first use the Newton's linearization process and then apply the NIPG method for discretizing the spatial variable and both the L1-discretization and L2-discretization for the time-fractional derivative and the trapezoidal rule for the integral term. Next, we suggest a fully discrete numerical solution approach for the time-fractional Burgers' equation, by considering the L2-discretization formula in the temporal direction and the NIPG method for the spatial variable. Finally, we proposed an alternating direction implicit (ADI) type operator splitting discontinuous Galerkin finite element method to solve a class of two-dimensional time-factional diffusion equations, numerically. For solving both the sub-problems obtained by splitting technique, we use the L2-discretization in time discretization and the NIPG approach for spatial variable.

The thesis concludes with a summary and suggestions for further research.

Abbreviation

ADI	Alternating direction implicit
BO	Baumann-Oden
BVP	Boundary-value problem
DDG	Direct discontinuous Galerkin
DGM	Discontinuous Galerkin method
FDM	Finite difference method
FEM	Finite element method
FVM	Finite volume method
FDE	Fractional differential equation
FIDE	Fractional integro-differential equation
IVP	Initial-value problem
IBVP	Initial-boundary-value problem
IPG	Interior penalty Galerkin
IDE	Integro-differential equation
LDG	Local discontinuous Galerkin
LOD	Locally one-dimensional
MSM	Multiple shooting method
NIPG	Non-symmetric interior penalty Galerkin
ODE	Ordinary differential equation
PDE	Partial differential equation
RKDG	Runge-Kutta discontinuous Galerkin
RLC	Riemann-Liouville-Caputo

SSM	Simple shooting method
SIPG	Symmetric interior penalty Galerkin
TF-ADR	Time-fractional advection-diffusion-reaction
TF-PDE	Time-fractional partial differential equation
TF-IPDE	Time-fractional integro-partial differential equation
VIE	Volterra integral equation
VIDE	Volterra integro-differential equation

Nomenclature

α	Order of fractional derivative
$\mathbb{N}$	Set of natural numbers
$\mathbb{R}$	Set of real numbers
M	Number of sub-intervals in spatial direction
N	Number of sub-intervals in temporal direction
$\Omega, \Omega_x, \Omega_y$	Spatial domain
$\overline{\Omega}_M$	Discrete spatial domain
x, x_m, x_i, y, y_j	Continuous and discrete spatial variables
G	Temporal domain
$\overline{G}^N$	Discrete temporal domain
t, t_n	Continuous and discrete temporal variables
Q	$\Omega \times G$
h	Mesh-size in spatial direction
τ_n, τ	Mesh-size in temporal direction
C	Generic positive constant independent of the mesh
$\|\cdot\|_{\overline{\Omega}_M}$	Discrete maximum-norm on the mesh $\overline{\Omega}_M$
$\|\cdot\|_{\omega}$	Maximum-norm on the domain ω
$\|\cdot\|$	L^2-norm on the domain Ω
$\|\!\|\!\|\cdot\|\!\|\!\|_{DG}, \|\!\|\!\|\cdot\|\!\|\!\|_{DG,x}, \|\!\|\!\|\cdot\|\!\|\!\|_{DG,y}$	DG energy-norm
$\|\!\|\!\|\cdot\|\!\|\!\|$	Discrete energy-norm
$PC[0,T]$	Space of all piece-wise continuous functions on $[0,T]$

$AC[a,b]$	Space of functions which are absolutely continuous on $[a,b]$
$\mathcal{C}^n(\omega)$	Space of n times continuously differentiable functions defined on the domain ω
$\mathcal{C}(\omega)$	Space of continuous functions defined on the domain ω
$\mathcal{C}_x^2(\Omega)$	The set of functions that are twice continuously differentiable with respect to x on the domain Ω
$L^1(\omega)$	The space of integrable function on the domain ω
$W_t^1((0,T))$	The space of functions $v \in \mathcal{C}^1((0,T])$ such that $v' \in L^1((0,T))$
I_x^α	Riemann-Liouville integral in x variable
${}^{RLC}\mathcal{D}_x^\alpha$	RLC-type fractional derivative in x variable
${}^{C}\mathcal{D}_t^\alpha$	Caputo-type fractional derivative in t variable
$\mathcal{L}, \mathcal{L}^N$	Spatial differential operators
$\mathcal{I}_t$	Integral operator
I	Identity operator
$\mathcal{R}_M^m, \mathcal{R}_N^n, \mathcal{R}^n, \mathcal{R}_1^n, \mathcal{R}_2^n$	Truncation error
E_M, $E_{M,N}, \mathcal{E}_{M,N}, \mathcal{E}_{M,N}^1, \mathcal{E}_{M,N}^2$	Error
$\mathcal{D}_M, \mathcal{D}_{M,N}$	Maximum two-mesh differences
$R_M, R_{M,N}, R_{M,N}^1, R_{M,N}^2$	Order of convergence

List of Figures

List of Tables

Contents

CHAPTER 1

Introduction

This chapter discusses the basic information about fractional calculus and numerical solution techniques, which is followed by a section outlining the goals and motivation behind the solution techniques we will use throughout the thesis. Next, we provide the preliminary information that are used in the thesis.

1.1 Background

Since the invention of calculus by Newton and Leibniz at the end of the seventeenth century, differential equations involving integer order derivatives have been studied. Since then, several models, including ordinary differential equations (ODEs) and partial differential equations (PDEs), have been used to successfully describe problems in the real world. The integer order derivative at a point is a type of local descriptor that is solely influenced or decided by its neighborhood, as is widely known. However, due to their local nature, these models may no longer be accurate for the majority of real-world issues, particularly those that call for "memory". This encourages scientists to look for a different but better tool to replace the integer order derivative. The fractional order derivative accomplishes this.

1.1.1 Fractional calculus

Fractional calculus (which includes fractional order integration and fractional order differentiation) is as old as its counterpart, classical calculus (which includes integer order integration and integer order differentiation). It took a while for it to develop slowly. However, due to its applications in science and engineering, fractional calculus is currently receiving much more attention. As a result, fractional differential equation mod-

els have been constructed in many applicable disciplines. Fractional derivatives have provided good tools to describe numerous materials and processes with memory and hereditary features, among other things.

Calculus is a formal tool that scientists use to think quantitatively. The conventional rules of analysis, such as determining causation and producing verifiable predictions, become difficult to apply to the study of complicated phenomena, especially those that vary over time. Through the systematic use of fractal operators, fractional calculus, and fractional differential equations, one can anticipate the improbable and prepare for unintended effects. However, we also need to include in the discussion some of the more conventional ideas of complexity, including unpredictability. As a result, we begin our exploration of the tools necessary to think differently about complexity with a quick overview of random walks using fractional differential equations. These fractional random walks have been used to represent a variety of complicated events, from climate change to changes in the financial markets.

Since the greater scientific community just saw the need for fractional calculus recently, its application in the physical, social, and life sciences has lagged. In the past, it was believed that the classical calculus of Newton and Leibniz, and the analytic functions used to solve the differential equations brought on by Newton's force laws were essential and sufficient to provide an accurate and thorough mechanical description of the physical universe. However, the analytical functions we have come to rely on in physics are unable to explain a wide variety of physical, biological, and social events, according to experiments. These functions cannot capture the complex dynamics of frequent natural occurrences like earthquakes and hurricanes [103], common social phenomena like group consensus [107] and economic unpredictability like stock market crashes [104], high-frequency finance [29], and healthcare networks [105], or psychological processes like habituation and cognition [115]. The classic nineteenth-century analysis, which has served as the mathematical foundation of physics and engineering ever since cannot adequately account for the inherent complexity of these events. Complexity must be viewed as an extended class of issues with shared structural and mathematical traits, necessitating new ways of thinking and problem-solving.

It was believed that non-integer order integrals and/or derivatives were interesting curiosities that belonged outside of the realm of mainstream science. The vast amount of data made available by social media, the improved data processing methods, and the ever-improving computational capabilities, however, have all contributed to the expansion of science in such a way that those phenomena that were once thought to be outliers are now center stage. A new mathematical approach is necessary to create a fundamen-

tal understanding of these strange processes, which are now referred to as exotic scaling phenomena. The fractional calculus, which can measure the connection of fluctuations in phenomena over highly disparate scales in both space and time, may very well offer such a perspective.

1.1.2 Fractional differential and integro-differential equations

A fractional differential equation (FDE) is an equation involving an unknown function of one or more variables and certain of its derivatives with at least one fractional derivative. If a FDE contains more than one fractional order derivative, then it's called a multi-term FDE. If the unknown function in a FDE is a function of only one variable, then the FDE is an ordinary FDE. Otherwise, we often call it partial FDE. FDE can be classified according to its linearity in a similar way as in the case of differential equations involving only integer order derivatives. A fractional integro-differential equation (FIDE) is an equation which involves fractional derivatives and some integral-term.

1.1.2.1 Analytic solution approach for fractional differential and integro-differential equations

Many analytical techniques, including the Fourier transform method, the Laplace transform method, the Mellin transform method, the Sumudu decomposition method, and the Green's function approach, can be used to resolve highly particular (usually linear) fractional differential equations.

1.1.2.2 Numerical methodology for fractional differential and integro-differential equations

Numerical simulation is now playing a crucial role and has become one of the three basic tools in science and technology, in addition to experimentation and theory. Numerical simulation offers a relatively modest and effective technique to aid in the comprehension of the physical world and the advancement of technology. There are various numerical approaches available in the field of study of the fractional differential equations. Here, we will give a short description of some of the numerical methods that will be the focus of this study.

1.1.2.2.1 Shooting method

Many scholars have given and explored a wide range of methods for handling boundary-value problems (BVPs). Solving initial-value problems (IVPs) is a simple task compared

to BVPs, as there are numerous easy ways to handle IVPs. A system of equations in linear algebra is produced from the BVP by the finite difference method (FDM). However, if the step length is very small in FDM, there are a large number of equations to be solved, which means it will take a lot of time and memory to solve the problem. The shooting technique overcomes all these difficulties, and also it is good in handling nonlinear BVPs. By assuming initial values that would have been provided if the ordinary differential equation had been an initial value problem, the shooting technique reduces the BVP to finding the solution of an equivalent IVP. Next, the computed boundary value and the actual boundary value are compared. One tries to approach the computed boundary value as closely as feasible to the actual boundary value by scientific methods or trial and error process. Morrison et al. [81] initially proposed the idea of multiple shooting, and Keller [57] later advanced it by creating and evaluating both a multiple shooting method (MSM) [60] and a simple shooting method (SSM) [56]. Liu proposed the Lie-group shooting method [69, 71, 70]. The shooting method was also applied to solve fractional BVPs, for example, one can refer to Diethelm and Ford [32], Al-Mdallal et al. [3], Huang et al. [48] and Cen et al. [18, 19, 20].

1.1.2.2.2 Cubic splines

Raggett and Wilson [88] have examined the use of cubic splines for the numerical solution of the one-dimensional wave equation. Raggett [87] has demonstrated how this technique could be extended to solve more general one-dimensional, constant-coefficient, hyperbolic partial differential equations.

1.1.2.2.3 Discontinuous Galerkin method

In the early 1970s, partial differential equations were numerically solved with the use of discontinuous piecewise polynomial approximations. This method, which was afterward named the discontinuous Galerkin method (DGM), emerged independently for elliptic and parabolic problems as well as for hyperbolic ones. More than ten primary approaches were developed in less than 30 years.

In 1973, Reed and Hill [89] employed the DGM for the first time to solve the neutron transport equation. Lasaint and Raviart [62] studied the numerical analysis of the DGM in 1974, from which they derived estimates of sub-optimal error. Improved error estimates were presented in [54] by Johnson and Pitkäranta in 1986, over a decade later. Richter also established the best order of convergence for a linear first-order hyperbolic equation in $\mathbb{R}^2$ in 1988 [90], and he expanded the analysis to include the situation of a

constant linear diffusion in 1992 [91].

A rapid development of the DGM occurred between 1989 and 1998, sparked by a series of studies using the DGM for nonlinear conservation laws, written by Cockburn, Shu, and their colleagues [23, 24, 25, 26]. Their methods combine the Runge-Kutta time discretization with the space DG discretization. This technique is referred to as the Runge-Kutta discontinuous Galerkin (RKDG) technique. The RKDG approach was applied to the system of compressible Navier-Stokes equations in 1997 by Bassi and Rebay [9]. They considered the solution itself and its gradient as independent variables. This strategy is often referred to as the BR method. Similar to mixed techniques in conforming finite element method (FEM), Cockburn and Shu [27] presented the local discontinuous Galerkin (LDG) method in 1998 as a generalization of the BR method.

The DGM was developed simultaneously, though very separately, for the numerical solution of parabolic and second-order elliptic equations. Several discontinuous approximation variations were put forth and investigated by Douglas and Dupont in 1976 [35], Baker in 1977 [8], Wheeler in 1978 [116], and Arnold in 1982 [5]. The interior penalty Galerkin (IPG) method was the term commonly used to describe these methods. Eventually, they were referred to as the symmetric interior penalty Galerkin (SIPG) method in the literature. The advancement of the DGM for hyperbolic equations did not influence the development of these techniques. The Baumann-Oden (BO) approach is a novel form of DGM that was first presented in the publications of 1999 [12, 11]. An expansion of the BO approach that incorporates both the interior and boundary penalty is the non-symmetric interior penalty Galerkin (NIPG) method, which Riviere, Wheeler, and Girault proposed in 1999 [94]. One may refer to [63, 93] for further information.

1.2 Objective and motivation

Despite being first introduced several decades ago, fractional calculus has only lately started to become much more popular and important in a range of scientific and engineering sectors because of its practical applications in problem solving. It has been found that some complicated diffusion processes, such as those occurring in inhomogeneous or heterogeneous media, *e.g.*, porous media, cannot be well described by using standard diffusion equations. The anomalous diffusion phenomenon is described using fractional diffusion equations. It can be found in many different areas of science and engineering, including elasticity [113], rheology [50], quantitative biology [78], porous or fractured media [14], geothermal heat transport [75], biochemical applications [92], etc. The analytical and numerical solutions of fractional differential equations have attracted

the attention of numerous researchers in the past few years. The theoretical and numerical approaches for fractional differential equations can be seen in the books [31, 59] and [65], respectively.

Shkhanukov et al. [98] were probably the first ones who introduced the finite difference method in the study of heat conduction equation with a fractional derivative along with boundary conditions. In [97], Shkhanukov developed the finite difference method for BVPs with a Riemann-Liouville fractional derivative. Diethelm and Walz [33] applied an extrapolation algorithm for numerical solution of ordinary differential equations with the so called Caputo fractional derivative. Gracia et al. [38] studied a steady-state fractional advection-dispersion-reaction equation with the highest-order derivative of Riemann-Liouville-Caputo (RLC) fractional type, in which they solved the problem by using a finite difference scheme.

In recent years, time-fractional partial differential equations (TF-PDEs) have been successfully used to simulate a variety of processes and systems. To characterize the extremely slow diffusion process in a porous medium with the type of fractal geometry (Koch's tree), Nigmatullin [83] proposed a time-fractional diffusion equation. Several researchers have studied the analytical aspects, such as existence and uniqueness, maximum principle, stability bound, etc. of autonomous time-fractional advection-diffusion-reaction (TF-ADR) equations, and developed some numerical techniques. They have used the separation of variables method and the Mittag-Leffler analysis to establish the existence of the solution to the autonomous TF-ADR equation. However, these methods are not sufficient for proving the existence of a solution for non-autonomous TF-ADR equations, and therefore, one has to use some other suitable techniques. Zahra and Elkholy [120] solved a class of fractional BVPs using the combination of the cubic spline function approximation method and the shooting method. To solve numerically a class of nonlinear variable-order fractional equations with delay, Yaghoobi et al. [118] proposed a robust, and effective approach based on cubic spline interpolation.

Efficient numerical methods for time-fractional problems have drawn the attention of several scholars over the past few decades. Li et al. [66] investigated the L1-Galerkin finite element method for solving time fractional nonlinear diffusion problems. The existence, uniqueness, and regularity of the nonlinear time-fractional diffusion problem were provided by Jin et al. [53]. Huang et al. [47] established the error analysis for the direct discontinuous Galerkin (DDG) finite element method for the time-fractional reaction-diffusion problem.

Vito Volterra introduced Volterra integral equations (VIEs) and Volterra integro-differential equations (VIDEs) for the study of functional analysis. Numerous scientific

and engineering domains, such as the theory of radiative transfer [17], heat transfer in hybrid nano-fluid [96], etc., use these equations. Numerous studies have been conducted recently to solve FIDEs both analytically and numerically. To name a few, the numerical solution of the time-fractional integro-partial differential equation (TF-IPDE) on a uniform mesh was obtained by Santra and Mohapatra [95]. For the nonlinear TF-IPDE, Guo et al. [40] presented a finite difference approach. A spline collocation method was used by Pedas et al. in [85] for solving numerically a class of linear FIDEs. Luo et al. [77] proposed a compact finite difference scheme for a TF-IPDE.

Recently, Singh and Natesan investigated the NIPG approach for singularly perturbed problems in their papers [99, 100]. Xu and Hesthaven [117] suggested a DGM for fractional convection-diffusion equations. A hybridized DGM was proposed by Wang et al. [108] to solve 2D fractional convection-diffusion equations. To construct a fully discrete method for time-fractional diffusion equations, Mustapha et al. [82] used the continuous Galerkin approach in space and the DGM in time. A fully discrete DDG approach was suggested by Huang et al. [45] for the time-fractional diffusion equation.

Bateman [10] introduced the Burgers' equation, and he described it as important to research and offered steady solutions. Later on, Burgers used it as a mathematical model for turbulent fluid motion in his works [15, 16]. After that, it is observed that it is worthy of study and such an equation is referred to as Burgers' equation. In recent years, several researchers have shown interest in developing efficient methods for solving the time-fractional Burgers' equations. Here we cite a few of them. A linear implicit finite difference method was presented by Li et al. [67] to solve the generalized time-fractional Burgers' equation. Qiu et al. [86] used the three-point centered formula to approximate the second-order spatial derivative and the Galerkin method based on piecewise linear test functions to approximate the nonlinear convection term, while Li et al. [64] used the LDG method for the space derivative and the L1-discretization for the time derivative to approximate the generalized time-fractional Burgers' equation.

On a higher-dimensional domain, the computations of a time-dependent convection-diffusion-reaction problem are incredibly time-consuming and storage-intensive. Several strategies are described in the literature for removing this complexity and straightforward analyses. The alternating direction implicit (ADI) type operator splitting approach is one of them. The basic idea behind this operator splitting method, the ADI or locally one-dimensional (LOD), is to break the original two-dimensional problem into two separate ones. Then each one-dimensional problem will be solved effectively using proper techniques. The operator splitting approach initially appeared in the 1960s in the works of Yanenko, Dyakonov, Marchuk, Samarskii, and others who devoted con-

siderable time to this research, for more details one can see [37, 43, 109, 110, 119]. This prompts us to think about LOD techniques, which are effective at simultaneously solving multi-dimensional PDEs. We aim to solve higher-dimensional time-fractional convection-diffusion equations by combining the local one-dimensional technique with the L2-NIPG method.

In recent years, researchers have shown much interest in the numerical solution using the operator splitting approach for integer order convection-diffusion problems [7, 21, 28, 36, 41, 42, 61, 76]. Gradually this interest is now moving towards solving fractional differential equations. In the study of time-dependent two-dimensional two-sided space fractional diffusion equations, Song and Xu [102] presented a numerical algorithm that consists of a spectral method for the spatial discretization combined with a direction splitting scheme in time, which implies the solution of a series of one-dimensional fractional diffusion problems. To solve the time-fractional Perona-Malik model, Mazloum and Hadian Siahkal-Mahalle [79] devised a strong and precise local meshless algorithm. A suitable combination of the operator splitting technique and the compactly supported radial basis function method is proposed to overcome the complexity of the problem and transform a complex time-fractional partial differential equation into sparse linear algebraic systems that can be solved by standard solvers.

1.3 Basic definitions and preliminaries

This section covers certain fundamental concepts and well-known results that will appear frequently in the theoretical justifications for this thesis.

1.3.1 Some special functions

A tour of some necessary but relatively easy mathematical definitions will emerge in the study of fractional calculus, which will help to simplify and clarify the understanding of definitions and the application of fractional calculus. This subsection provides a brief discussion of several of these, including the gamma function, the Mittag-Leffler function and contraction mapping.

The factorial notation is thought to be generalized by the gamma function $\Gamma(z)$.

Definition 1.1 *If z is a complex number with a positive real part (i.e., $\mathbf{Re}\, z > 0$), then the absolutely convergent integral*

$$\Gamma(z) = \int_0^\infty t^{z-1} e^{-t} dt, \tag{1.1}$$

is known as the gamma function, or the second-kind Euler integral equation.

Obviously, $\Gamma(1) = 1$. $\Gamma(z+1) = z\Gamma(z)$ and when $z \in \mathbb{N}$, $\Gamma(z) = (z-1)!$ are fundamental characteristics of the gamma function.

The Mittag-Leffler function is a generalization of the exponential function and naturally arises in the closed-form solution of some fractional differential equations, especially in the case where the fractional time derivative appears as a convergent power series of the Mittag-Leffler case. It is found in the solution of fractional differential equations or fractional order integral equations, and in particular in the investigations of the fractional generalization of the Lévy process, random walks, kinetic equations, super-diffusive processes, and in the study of complex and spatiotemporal dynamical systems.

Definition 1.2 *The one-parameter Mittag-Leffler function, which was first introduced by Mittag-Leffler [80], is defined as a power series expansion*

$$E_{\delta_1}(z) = \sum_{i=0}^{\infty} \frac{z^i}{\Gamma(\delta_1\, i + 1)}, \quad \textit{for} \quad \delta_1, z \in \mathbb{R} \quad \textit{with} \quad \delta_1 > 0.$$

The two-parameter Mittag-Leffler function, generalization of the one parameter Mittag-Leffler function, which plays an important role in fractional calculus and was first introduced by R. P. Agarwal [2], is defined by the series expansion

$$E_{\delta_1,\delta_2}(z) = \sum_{i=0}^{\infty} \frac{z^i}{\Gamma(\delta_1 i + \delta_2)}, \quad \textit{for} \quad \delta_1, \delta_2, z \in \mathbb{R} \quad \textit{with} \quad \delta_1 > 0,\, \delta_2 > 0.$$

The next definition of contraction mapping is important to the study of the fixed point theorem.

Definition 1.3 *Suppose $(\mathcal{E}, d)$ be a non-empty metric space and $0 \leq C < 1$. If*

$$d(F(u_1), F(u_2)) \leq C d(u_1, u_2), \quad \forall u_1, u_2 \in \mathcal{E},$$

then the mapping $F : \mathcal{E} \to \mathcal{E}$ is called a contraction mapping.

Next, we define a space of functions, which will be useful in the later chapter.

Definition 1.4 *Let $\Omega = (0, \ell)$. For each positive integer r and $-\infty < \mu < 1$, let us define the space*

$$\mathcal{C}^{r,\mu}(0,\ell] := \left\{ y \in \mathcal{C}(\overline{\Omega}) : y^{(r)} \in \mathcal{C}(0,\ell] \text{ with } \|y\|_{r,\mu} < \infty \right\},$$

where

$$\|y\|_{r,\mu} := \sup_{0<x\leq\ell} |y(x)| + \sum_{i=1}^{r} \sup_{0<x\leq\ell} \left[x^{i-(1-\mu)}|y^{(i)}(x)|\right].$$

1.3.2 Fractional integral and derivatives

After the initial inquisition by Leibniz and L'Hopital, fractional calculus was mostly studied by the brightest minds in mathematics. L. Euler (1730), P. S. Laplace (1812), J. B. J. Fourier (1822), N. H. Abel (1823–1826), J. Liouville (1832-1837), B. Riemann (1847), A. K. Grünwald (1867), A. V. Letnikov (1868–1872), H. Laurent (1884), J. Hadamard (1892), O. Heaviside (1892–1922), G. H. Hardy and J. E. Littlewood (1917–1928), H. Weyl (1917), P. Lévy (1923), H. Riesz (1936–1949), and many more are among the outstanding mathematicians who experimented with fractional calculus and made significant contributions until this century. Later on, fractional differential operators such as the Riemann-Liouville, Grünwald-Letnikov, Hadamard, Caputo, Riesz, Atangana–Baleanu, and Caputo–Fabrizio were introduced, and fractional calculus began to draw interest from engineers, mathematicians, and physicists.

Fractional integration often means the Riemann-Liouville integral, which combines the definitions proposed by Riemann and Liouville.

Definition 1.5 *The Riemann-Liouville fractional integral of order $\alpha \geq 0$ for any function v is defined by*

$$(I_x^{\alpha} v)(x) = \frac{1}{\Gamma(\alpha)} \int_a^x (x-s)^{\alpha-1} v(s) ds, \quad x > a. \tag{1.2}$$

Definition 1.6 *The Riemann-Liouville fractional derivative of order $\alpha \in [m-1, m)$ for any function v is defined by*

$${}^{RL}\mathcal{D}_x^{\alpha} v(x) = \frac{d^m}{dx^m}\left(I_x^{m-\alpha} v\right)(x) = \frac{1}{\Gamma(m-\alpha)} \frac{d^m}{dx^m} \left(\int_a^x (x-s)^{m-\alpha-1} v(s) ds \right), \quad x > a. \tag{1.3}$$

Definition 1.7 *For $\alpha \in [m-1, m)$, ${}^{C}\mathcal{D}_x^{\alpha} v(x)$ is the Caputo fractional derivative of order α for any function v, which is defined as*

$${}^{C}\mathcal{D}_x^{\alpha} v(x) = I_x^{m-\alpha} \left(\frac{d^m v}{dx^m}\right)(x) = \frac{1}{\Gamma(m-\alpha)} \int_a^x (x-s)^{m-\alpha-1} \frac{d^m v(s)}{ds^m} ds, \quad x > a. \tag{1.4}$$

The RLC fractional derivative [38, 51], also known as the Patie-Simon fractional derivative [58, 84], was first introduced by Pierre Patie and Thomas Simon in the study of asymmetric α-stable Lévy processes. The spectrally positive (or spectrally negative) α-stable Lévy process is reflected at its running supremum using this derivative as the infinitesimal generator.

Definition 1.8 *For $1 < \alpha < 2$, the RLC fractional derivative is defined by*

$$ {}^{RLC}\mathcal{D}_x^{\alpha} v(x) := \frac{d}{dx}\left({}^{C}\mathcal{D}_x^{\alpha-1} v(x)\right) = \frac{d}{dx}\left(\int_a^x \frac{(x-s)^{1-\alpha}}{\Gamma(2-\alpha)}\frac{dv}{dx}ds\right), \quad x > a. \tag{1.5} $$

The following properties of fractional derivatives and integrals will be used in our later analysis:

1. For any $\beta \in \mathbb{R}$ and $0 < \alpha < 1$, we have

$$ {}^{C}\mathcal{D}_x^{\alpha} x^{\beta} = \begin{cases} 0, & \beta \leq 0, \\ \dfrac{\Gamma(\beta+1)}{\Gamma(\beta-\alpha+1)} x^{\beta-\alpha}, & \beta > 0. \end{cases} \tag{1.6} $$

2. Fractional integrals and derivatives satisfy the linearity property :

   (a) $I_x^{\alpha}(c_1 v_1 \pm c_2 v_2)(x) = c_1 I_x^{\alpha} v_1(x) \pm c_2 I_x^{\alpha} v_2(x)$,

   (b) ${}^{C}\mathcal{D}_x^{\alpha}(c_1 v_1 \pm c_2 v_2)(x) = c_1 {}^{C}\mathcal{D}_x^{\alpha} v_1(x) \pm c_2 {}^{C}\mathcal{D}_x^{\alpha} v_2(x)$,

where c_1, c_2 are positive constants and provided that the integrals and derivatives exist for any v_1, v_2.

1.3.3 Sumudu transformation and its properties

Differential and integral equations can be solved using a variety of integral transforms. The Laplace transformation is the most often utilized for these purposes. Watugala [112] proposed a novel integral transform (called the Sumudu transformation) and used it in the solution of control engineering and ordinary differential equations because of its numerous intriguing qualities that facilitate visualization. The Sumudu transform of partial derivatives was then derived by Weerakoon [114], who also supplied the complex inversion transform and used it to solve three distinct partial differential equations.

Definition 1.9 *Consider the space*

$$\mathcal{B} = \left\{ v : v \in PC[0,T],\ \forall T > 0 \, and \, |v(t)| < M \exp\left(\frac{|t|}{\nu}\right),\ M > 0, \nu > 0,\ t \in \mathbb{R} \right\}, \tag{1.7}$$

where $PC[0,T]$ is the space of all piece-wise continuous functions on every finite interval $[0,T]$. The Sumudu transformation of $v \in \mathcal{B}$ is defined by

$$\boldsymbol{G}(\mu) = \mathbb{S}[v(t)] = \int_0^\infty v(\mu t) \exp(-t) dt, \quad \mu \in (-\nu, \nu). \tag{1.8}$$

For fundamental properties and applications of the Sumudu transformation, one can refer to [13]. Katatbeh and Belgacem [55] extended the Sumudu transform to fractional integrals and derivatives. The Sumudu transform for fractional integral is described in the following lemma.

Lemma 1.1 *[55, Theorem 3] If $\boldsymbol{G}(\mu)$ is the Sumudu transform of $v(t)$, then the Sumudu transformation of the fractional integral of $v(t)$ of order α, $I_t^\alpha(v(t))$ is given by*

$$\mathbb{S}[I_t^\alpha(v(t))] = \mu^\alpha \boldsymbol{G}(\mu), \quad \mathbf{Re}\, \alpha > 0.$$

In the next lemma, we describe the Sumudu transform for the Caputo fractional derivative.

Lemma 1.2 *[55, Theorem 5] If for a positive integer n, $n-1 < \alpha \leq n$, and $\boldsymbol{G}(\mu)$ be the Sumudu transform of the function $v(t)$, then the Sumudu transform ${}^C\boldsymbol{G}^\alpha(\mu)$ of the Caputo fractional derivative of $v(t)$ of order α, ${}^C\mathcal{D}_t^\alpha v(t)$, is given by*

$${}^C\boldsymbol{G}^\alpha(\mu) = \mathbb{S}[{}^C\mathcal{D}_t^\alpha v(t)] = s\mu^{-\alpha} \left[\boldsymbol{G}(\mu) - \sum_{j=0}^{n-1} \mu^j \left[\frac{d^j v(t)}{dt^j} \right]_{t=0} \right].$$

Definition 1.10 *The convolution operation $*$ between two functions f and g is defined by*

$$(f * g)(t) = \int_0^t f(t-s)\, g(s) ds.$$

Lemma 1.3 *[6, Theorem 2.3] Let $\boldsymbol{F}(\mu)$ and $\boldsymbol{G}(\mu)$ be the Sumudu transforms of $f(t)$ and $g(t)$, respectively. If $h(t) = (f*g)(t)$, then the Sumudu transform of $h(t)$ is $\mu\, \boldsymbol{F}(\mu)\, \boldsymbol{G}(\mu)$.*

1.3.4 Domain discretization

We consider the spatial domain Ω (for $\Omega \subset \mathbb{R}$, $\Omega = (0, \ell)$, and for $\Omega \subset \mathbb{R}^2$, $\Omega = \Omega_x \times \Omega_y$, where $\Omega_x = (\ell_1, \ell_2)$, $\Omega_y = (\ell_3, \ell_4)$). For the one-dimensional case, Ω is discretized uniformly as $\overline{\Omega}_M = \{x_m = (m-1)h : 1 \leq m \leq M+1,\ h = \ell/M\}$ and denote the partition of the domain Ω as $\mathcal{P}_M = \{\mathcal{K}_m = (x_m, x_{m+1}) : m = 1, \cdots, M\}$. For the two-dimensional case, we solve the problem as two one-dimensional problems separately using the operator splitting approach and similarly discretize each one-dimensional domain.

Discretize the time domain $G = (0, T]$ as $\overline{G}^N = \{t_n : 1 \leq n \leq N+1\}$, where N is a positive integer. Define $\tau_n = t_{n+1} - t_n, 1 \leq n \leq N$ and $\tau_{\max} = \max\limits_{1 \leq n \leq N} \tau_n$.

1.3.5 Basic definitions related to finite element methods

The broken Sobolev space of order $k \geq 0$ associated with the family $\mathcal{P}_M$ is defined as

$$H^k(\Omega, \mathcal{P}_M) = \left\{ v \in L^2(\Omega) : v|_{\mathcal{K}_m} \in H^k(\mathcal{K}_m),\ \forall \mathcal{K}_m \in \mathcal{P}_M \right\}.$$

The related broken Sobolev norm and semi-norm are defined by

$$\|v\|^2_{i,\mathcal{P}_M} = \sum_{m=1}^{M} \|v\|^2_{i,\mathcal{K}_m}, \quad |v|^2_{i,\mathcal{P}_M} = \sum_{m=1}^{M} |v|^2_{i,\mathcal{K}_m}, \quad (\forall i \leq k),$$

where the normal Sobolev norm and semi-norm are defined over the domain $\mathcal{K}_m$, respectively as, $\|.\|_{i,\mathcal{K}_m}$ and $|.|_{i,\mathcal{K}_m}$. We also define the inner product in $H^k(\Omega, \mathcal{P}_M)$ as $\langle v_1, v_2 \rangle_{k,\mathcal{P}_M} = \sum\limits_{i \leq k} \sum\limits_{m=1}^{M} \int\limits_{\mathcal{K}_m} \frac{d^i v_1}{dx^i} \frac{d^i v_2}{dx^i} dx = \sum\limits_{i \leq k} \left\langle \frac{d^i v_1}{dx^i}, \frac{d^i v_2}{dx^i} \right\rangle$, where $\langle \cdot, \cdot \rangle$ denotes the inner product on $L^2(\Omega)$.

The finite element space $V_h^k(\Omega)$ for a fixed $k \geq 1$ associated with the family $\mathcal{P}_M$ will be defined as follows:

$$V_h^k(\Omega) = \left\{ v_{_h} \in L^2(\Omega) : v_{_h}|_{\mathcal{K}_m} \in \mathbb{P}^k(\mathcal{K}_m),\ \forall \mathcal{K}_m \in \mathcal{P}_M \right\}, \text{ and}$$

$$V_{0,h}^k(\Omega) = \left\{ v_{_h} \in V_h^k(\Omega) : v_{_h}|_{\partial\Omega} = 0 \right\},$$

where $\mathbb{P}^k(\mathcal{K}_m)$ stands for the space of polynomials of degree at most k on $\mathcal{K}_m$. We also use the following notations to denote the left and right limits, jump, and average as

$$v_m^{\pm} = v(x_m \pm 0),\ [v_m] = v_m^+ - v_m^-,\ \{v_m\} = \frac{v_m^+ + v_m^-}{2}.$$

and

$$[v(x_1)] = v(x_1),\ \{v(x_1)\} = v(x_1),\ [v(x_{M+1})] = -v(x_{M+1}),\ \{v(x_{M+1})\} = v(x_{M+1}).$$

Definition 1.11 *Let* $\mathbf{P} : H^1(\Omega, \mathcal{P}_M) \to V_{0,h}^k(\Omega)$ *be the* L^2*-projection operator, which is defined as follows: for* $u \in H^1(\Omega, \mathcal{P}_M)$, $\mathbf{P}u(x) \in V_h^k(\Omega)$ *is the unique polynomial satisfying*

$$\int_{\mathcal{K}_m} (\mathbf{P}u(x) - u(x))\, v(x)dx = 0, \quad \forall v \in V_h^k(\Omega), \quad \forall \mathcal{K}_m \in \mathcal{P}_M,$$

with $\mathbf{P}u(x_m) = u(x_m)$, $\forall x_m$.

Let us denote the maximum-norm on Ω as $\|\cdot\|_\Omega$, the discrete maximum-norm on $\overline{\Omega}_M$ as $\|\cdot\|_{\overline{\Omega}_M}$ and the L^2-norm on Ω as $\|\cdot\|$.

Lemma 1.4 *[72, Lemma 3.1] Let* $u \in H^{k+1}(\mathcal{K}_m)$ *for* $m = 1, 2, \cdots, M$ *and* $k \geq 0$. *Then we have the following estimates:*

$$(i) \quad |\mathbf{P}u - u|_{i,\mathcal{K}_m} \leq Ch^{k+1-i}|u|_{k+1,\mathcal{K}_m}, \quad i \leq k+1,$$

$$(ii) \quad \left|\frac{\partial^i}{\partial x^i}(\mathbf{P}u - u)(x_m)\right| \leq Ch^{k+\frac{1}{2}-i}|u|_{k+1,\mathcal{K}_{m+\frac{1}{2}}}, \quad i \leq k+\frac{1}{2},$$

where $\mathcal{K}_{m+\frac{1}{2}} = \mathcal{K}_m \cup \mathcal{K}_{m+1}$ *and the positive constant* C *is independent of* h.

1.3.6 Discretization of the time-fractional derivatives

L1-discretization: The Caputo fractional derivative ${}^C\mathcal{D}_t^\alpha v(t)$ at $t = t_n$ is discretized using the standard L1-approximation as:

$$\begin{aligned} {}^C\mathcal{D}_t^\alpha v(t_n) \approx {}_{L1}^{C}\mathcal{D}_N^\alpha v^n &:= \frac{1}{\Gamma(1-\alpha)} \sum_{j=1}^{n-1} \frac{v^{j+1} - v^j}{\tau_j} \int_{t_j}^{t_{j+1}} (t_n - s)^{-\alpha} ds \\ &= \sum_{j=1}^{n-1} [v^{j+1} - v^j]\, \widehat{d}_{n,j} \\ &= \widehat{d}_{n,n-1} v^n + \sum_{j=2}^{n-1} [\widehat{d}_{n,j-1} - \widehat{d}_{n,j}] v^j - \widehat{d}_{n,1}\, v^1, \end{aligned} \tag{1.9}$$

where

$$\widehat{d}_{n,j} = \frac{(t_n - t_j)^{1-\alpha} - (t_n - t_{j+1})^{1-\alpha}}{\tau_j\,\Gamma(2-\alpha)}, \quad 1 \le j \le n-1, \quad 2 \le n \le N+1. \tag{1.10}$$

Lemma 1.5 *[106, Lemma 5.2] For each t_n, $n = 2, \cdots, N+1$, we have the following:*

$$\left\| \left({}_{L1}^{C}D_N^{\alpha} - {}^{C}D_t^{\alpha} \right) u(t_n) \right\| \le C\tau^{2-\alpha}.$$

L2-discretization: One can discretize the Caputo fractional derivative ${}^{C}\mathcal{D}_t^{\alpha} v(t)$ at $t = t_{n+1}$ over the uniform time grid $\overline{G}^N$ with step length τ by using the standard L2-approximation as:

$${}^{C}\mathcal{D}_t^{\alpha} v(t_{n+1}) \approx \int_{t_1}^{t_3} \frac{\Pi_{2,2} v(s)}{(t_{n+1}-s)^{\alpha}} ds + \sum_{j=3}^{n} \int_{t_j}^{t_{j+1}} \frac{\Pi_{2,j} v(s)}{(t_{n+1}-s)^{\alpha}} ds,$$

where on each interval $[t_j, t_{j+1}]$, $2 \le j \le n$, $\Pi_{2,j} v(s)$ is the quadratic interpolation of $v(s)$ using three points $(t_{j-1}, v(t_{j-1}))$, $(t_j, v(t_j))$ and $(t_{j+1}, v(t_{j+1}))$. Hence, for $j \ge 2$, we have

$$\Pi_{2,j} v(s) = v(t_{j-1}) \frac{(s-t_j)(s-t_{j+1})}{2\tau^2} + v(t_j) \frac{(s-t_{j-1})(t_{j+1}-s)}{\tau^2} + v(t_{j+1}) \frac{(s-t_j)(s-t_{j-1})}{2\tau^2},$$

and $(\Pi_{2,j} v(s))' = \Delta u^j + \nabla \Delta u^j (s - t_{j+1/2})$, where $\Delta u^j = (v(t_{j+1}) - v(t_j))/\tau$, $\nabla u^j = (v(t_j) - v(t_{j-1}))/\tau$, and $\nabla \Delta u^j = (\Delta u^j - \nabla u^j)/\tau = (v(t_{j+1}) - 2v(t_j) + v(t_{j-1}))/\tau^2$.

Therefore, for $n \ge 2$, we have

$${}^{C}\mathcal{D}_t^{\alpha} v(t_{n+1}) \approx {}_{L2}^{C}\mathcal{D}_N^{\alpha} v^{n+1} := \sum_{j=1}^{n+1} D_{n,j}^{(\alpha)} v^j, \tag{1.11}$$

where

$$\tau^{\alpha}\Gamma(2-\alpha) D_{2,j}^{(\alpha)} = \begin{cases} d_2^1 + d_2^2 - d_1^2, & j = 1, \\ d_1^2 - d_1^1 - 2d_2^1 - 2d_2^2, & j = 2, \\ d_2^1 + d_2^2 + d_1^1, & j = 3, \end{cases}$$

$$\tau^{\alpha}\Gamma(2-\alpha)D_{3,j}^{(\alpha)} = \begin{cases} d_2^2 + d_2^3 - d_1^3, & j = 1, \\ d_1^3 - d_1^2 - 2d_2^2 - 2d_2^3 + d_2^1, & j = 2, \\ d_1^2 + d_2^2 - d_1^1 + d_2^3 - 2d_2^1, & j = 3, \\ d_2^1 + d_1^1, & j = 4, \end{cases}$$

and for $n \geq 4$,

$$\tau^{\alpha}\Gamma(2-\alpha)D_{n,j}^{(\alpha)} = \begin{cases} d_2^{n-1} + d_2^n - d_1^n, & j = 1, \\ d_1^n - d_1^{n-1} - 2d_2^n - 2d_2^{n-1} + d_2^{n-2}, & j = 2, \\ d_1^{n-1} - d_1^{n-2} + d_2^n + d_2^{n-1} - 2d_2^{n-2} + d_2^{n-3}, & j = 3, \\ d_1^{n-j+2} - d_1^{n-j+1} + d_2^{n-j+2} + d_2^{n-j} - 2d_2^{n-j+1}, & 4 \leq j \leq n-1, \\ d_1^2 - d_1^1 + d_2^2 - 2d_2^1, & j = n, \\ d_2^1 + d_1^1, & j = n+1, \end{cases}$$

with $d_1^j = j^{1-\alpha} - (j-1)^{1-\alpha}$, $d_2^j = \dfrac{1}{2-\alpha}[j^{2-\alpha} - (j-1)^{2-\alpha}] - \dfrac{1}{2}[j^{1-\alpha} + (j-1)^{1-\alpha}]$, $j \geq 1$.

Lemma 1.6 *[4, Lemma 2.1] For any $\alpha \in (0,1)$, $n = 2, 3, \cdots, N$ and $u(t) \in \mathcal{C}^3[0, t_{n+1}]$, we have the following truncation error bound:*

$$\left|\left({}^{C}\mathcal{D}_t^{\alpha} - {}_{L2}^{C}\mathcal{D}_N^{\alpha}\right) u(t_{n+1})\right| \leq C\tau^{3-\alpha},$$

where C is a positive constant.

Remark 1.1 *In order to utilize L2-discretization in (1.11), we need the value of u^2 which will be obtain by using the L1-discretization on $[0, \tau]$ with step size $\widehat{\tau} = \mathcal{O}\left(\tau^{\frac{3-\alpha}{2-\alpha}}\right)$ with overall order of accuracy in time $\mathcal{O}(\tau^{3-\alpha})$.*

1.3.7 Some special Theorem and Lemmas

In the following, we present the classical Banach fixed point theorem in a complete metric space.

Theorem 1.2 *[59, Theorem 1.9] Let $(\mathcal{E}, d)$ be a nonempty complete metric space and $F : \mathcal{E} \to \mathcal{E}$ a contraction mapping, then F has a unique fixed point u^* in $\mathcal{E}$.*

The maximum-minimum principle will be studied by using the following theorem.

Theorem 1.3 *[74, Theorem 1] Let $t = t_0 \in G$ be a maximum point over $\overline{G}$ for the function $v \in W_t^1((0,T)) \cap \mathcal{C}(\overline{G})$. Then the Caputo fractional derivative of the function v is nonnegative at the point t_0 for any α, $0 < \alpha \leq 1$:*

$$ {}^{C}\mathcal{D}_t^{\alpha} v(t_0) \geq 0. $$

To establish the stability estimate for the spatially discretized scheme we recall the following well-known Gronwall inequality.

Lemma 1.7 *(Discrete Gronwall inequality, [101]) Let $\{w_n\}$ be a sequence of nonnegative real numbers, which satisfies*

$$ w_n \leq \mu_n + \sum_{i=1}^{n-1} \eta_i w_i, \quad n \geq 1, \tag{1.12} $$

where $\{\mu_n\}$ denotes a non-decreasing sequence of nonnegative numbers, and $\eta_i \geq 0$. Then the following inequality holds for $n \geq 1$,

$$ w_n \leq \mu_n \exp\left(\sum_{i=1}^{n-1} \eta_i\right). $$

The generalized discrete Gronwall inequality is presented in the following lemma and will be used for further investigation.

Lemma 1.8 *(Generalized discrete Gronwall inequality [34, Theorem 6.1]) Suppose $z_j \geq 0\,(1 \leq j \leq N)$, and $\psi_j \geq 0\,(1 \leq j \leq N)$ is a monotonically increasing real numbers satisfying*

$$ z_j \leq \psi_j + Mh^{1-\alpha} \sum_{i=1}^{j-1} \frac{z_k}{(j-i)^{\alpha}}, \quad 1 \leq j \leq N, \tag{1.13} $$

where $0 < \alpha < 1, M > 0$ is constant independently of h. Then

$$ z_j \leq \psi_j E_{1-\alpha,1}\left(M\Gamma(1-\alpha)(jh)^{1-\alpha}\right), \quad 1 \leq j \leq N. \tag{1.14} $$

1.4 Model problems

The model problems studied in this thesis are briefly mentioned in this section. At the beginning of the following chapters, we comprehensively present these model problems with relevant details for clarity of presentation.

The following model problems are taken into consideration, and summaries of each are provided below:

1.4.1 Linear fractional steady-state BVP with RLC derivative

Consider the following class of steady-state linear fractional advection-diffusion-reaction BVPs with the highest order derivative of RLC fractional type:

$$\begin{cases} -{}^{RLC}\mathcal{D}_x^{\alpha} u(x) + (bu)'(x) + c(x)u(x) = f(x), \quad x \in \Omega = (0, \ell), \\ {}^{C}\mathcal{D}_x^{\alpha-1} u(0) = \gamma, \quad u(\ell) + \beta_1 u'(\ell) = \gamma_1, \end{cases} \tag{1.15}$$

where $1 < \alpha < 2$, the constants $\gamma, \beta_1, \gamma_1$ and the functions b, c, f are known. We assume that for $r \in \mathbb{N}$ and some $\nu \in (-\infty, 1)$,

$$b, c, f \in \mathcal{C}^{r,\nu}(0, \ell], \quad c + b' \geq 0, \quad \beta_1, \gamma_1 \geq 0.$$

1.4.2 Semi-linear fractional steady-state BVP with RLC derivative

Here, we consider the following class of steady-state semi-linear fractional advection-diffusion-reaction BVPs with the highest order derivative of RLC fractional type:

$$\begin{cases} -{}^{RLC}\mathcal{D}_x^{\alpha} u(x) + (bu)'(x) = f(x, u(x)), \quad x \in \Omega = (0, \ell), \\ {}^{C}\mathcal{D}_x^{\alpha-1} u(0) = \gamma, \quad u(\ell) + \beta_1 u'(\ell) = \gamma_1, \end{cases} \tag{1.16}$$

where $1 < \alpha < 2$, $f \in \mathcal{C}^2(\Omega \times \mathbb{R})$ and $b \in \mathcal{C}^{r,\nu}(0, \ell]$ $(r \in \mathbb{N}, \nu \in (-\infty, 1))$ are known. It is also assumed that there exist two positive constants $\lambda_i (i = 1, 2)$ such that

$$0 \leq \lambda_1 \leq \frac{\partial f}{\partial u}(x, u(x)) \leq \lambda_2, \quad \forall x \in (0, \ell], \quad \forall u \in \mathbb{R}.$$

1.4.3 Linear non-autonomous time-fractional IBVP

We focus on the following class of non-autonomous time-fractional advection-diffusion-reaction initial-boundary-value problems (IBVPs):

$$\begin{cases} {}^{C}\mathcal{D}_t^{\alpha} u(x,t) + \mathcal{L}(u(x,t)) = f(x,t), \quad (x,t) \in Q := \Omega \times G,\ 0 < \alpha < 1, \\ u(x,0) = g(x), \quad \forall x \in \overline{\Omega}, \\ u(0,t) = \psi_1(t), \quad u(\ell,t) = \psi_2(t), \quad \forall t \in \overline{G}, \end{cases} \tag{1.17}$$

where $\Omega = (0,\ell)$, $G = (0,T]$ and $\mathcal{L}(u(x,t)) = p(t)\left[-\dfrac{\partial}{\partial x}\left(a(x)\dfrac{\partial u}{\partial x}\right) + b(x)u\right](x,t)$ with

$$\begin{cases} a \in \mathcal{C}^1(\overline{\Omega}), \quad b \in \mathcal{C}(\overline{\Omega}), \quad a(x) > 0, \quad b(x) \geq 0, \quad \forall x \in \overline{\Omega}, \\ p \in \mathcal{C}(\overline{G}), \quad p(t) > 0, \quad \forall t \in G. \end{cases}$$

Further, we assume that the compatibility conditions $g(0) = \psi_1(0)$ and $g(\ell) = \psi_2(0)$ hold.

1.4.4 Semi-linear non-autonomous time-fractional IBVP

Here, we deal with the following class of semi-linear non-autonomous time-fractional advection-diffusion-reaction equations:

$$\begin{cases} {}^{C}\mathcal{D}_t^{\alpha} u(x,t) + \mathcal{L}(u(x,t)) = f(x,t), \quad (x,t) \in Q := \Omega \times G,\ 0 < \alpha < 1, \\ u(x,0) = g(x), \quad \forall x \in \overline{\Omega}, \\ u(0,t) = \psi_1(t), \quad u(\ell,t) = \psi_2(t), \quad \forall t \in \overline{G}, \end{cases} \tag{1.18}$$

where $\Omega = (0,\ell)$, $G = (0,T]$ and $\mathcal{L}(u(x,t)) = p(t)\left[-\dfrac{\partial}{\partial x}\left(a(x)\dfrac{\partial u}{\partial x}(x,t)\right) + b(x,u)\right]$ with

$$\begin{cases} a \in \mathcal{C}^1(\overline{\Omega}),\ b \in \mathcal{C}^1(\Omega \times \mathbb{R}),\ a(x) > 0,\ b_u \geq 0, \quad \forall x \in \overline{\Omega}, \\ p \in \mathcal{C}(\overline{G}),\ p(t) > 0, \quad \forall t \in G. \end{cases}$$

Further, we assume that for sufficiently smooth functions $b(x,u), f(x,t)$ and $g(x)$, and that the compatibility conditions $g(0) = \psi_1(0)$ and $g(\ell) = \psi_2(0)$ hold.

1.4.5 Linear time-fractional integro-partial differential equations

We focus on the following class of linear time-fractional integro-partial differential equations:

$$\begin{cases} {}^{C}\mathcal{D}_t^{\alpha} u(x,t) + \mathcal{L}u(x,t) + \lambda \int_0^t K(x,t-s)u(x,s)ds = f(x,t), \quad (x,t) \in Q := \Omega \times G, \\ u(x,0) = g(x), \quad \forall x \in \overline{\Omega}, \\ u(0,t) = \psi_1(t), \quad u(\ell,t) = \psi_2(t), \quad \forall t \in G, \end{cases} \tag{1.19}$$

where $\Omega = (0,\ell)$, $G = (0,T]$, $0 < \alpha < 1$, and

$$\mathcal{L}u(x,t) = -a(x,t)\frac{\partial^2 u}{\partial x^2}(x,t) + b(x,t)\frac{\partial u}{\partial x}(x,t) + c(x,t)u(x,t),$$

with sufficiently smooth functions a, b, c, f on $\overline{Q}$, $\lambda > 0$ such that

$$a(x,t) > 0, \;\; c(x,t) \geq 0, \;\; K(x,t) \geq 0, \quad \forall (x,t) \in Q.$$

Further, we assume that g, ψ_1, ψ_2 are smooth functions and the kernel $K \in \mathcal{C}^2(Q)$, and the admissible conditions $g(0) = \psi_1(0)$, $g(\ell) = \psi_2(0)$ hold.

1.4.6 Nonlinear time-fractional integro-partial differential equations

We will study the following class of nonlinear time-fractional integro-partial differential equations:

$$\begin{cases} {}^{C}\mathcal{D}_t^{\alpha} u(x,t) + \mathcal{L}u(x,t) + \mathcal{I}_t u(x,t) = g(x,t), \quad (x,t) \in Q := \Omega \times G, \\ u(x,0) = g(x), \quad \forall x \in \overline{\Omega}, \\ u(0,t) = u(\ell,t) = 0, \quad \forall t \in G, \end{cases} \tag{1.20}$$

where $\Omega = (0, \ell)$, $G = (0, T]$, $0 < \alpha < 1$, and

$$\mathcal{L}u(x,t) := -\frac{\partial}{\partial x}\left(a(x,t)\frac{\partial u}{\partial x}(x,t)\right) + b(u(x,t)),$$
$$\mathcal{I}_t u(x,t) := \lambda \int_0^t K(x, t-s)u(x,s)ds.$$

Further, we assume that the functions a, b, f, g are sufficiently smooth, $\lambda > 0$ as well as

$$0 < a_* < a(x,t) \leq a^*, \frac{\partial b}{\partial u} \geq 0, f(x,t) \geq 0, \quad \forall (x,t) \in Q,$$

and the initial value $g(\cdot)$ satisfies the compatibility conditions $g(0) = g(\ell) = 0$, and the IBVP (6.1) admits a unique solution.

1.4.7 Nonlinear time-fractional Burgers' equation

Consider the following nonlinear time-fractional Burgers' equation:

$$\begin{cases} {}^C\mathcal{D}_t^\alpha u(x,t) + \dfrac{\partial}{\partial x}\left(\dfrac{u^2}{2}\right)(x,t) = \mu \dfrac{\partial^2 u}{\partial x^2}(x,t) + f(x,t), \ (x,t) \in \Omega \times (0,T], \\ u(x,0) = g(x), \quad \forall x \in \overline{\Omega}, \\ u(0,t) = u(\ell,t) = 0, \quad \forall t \in (0,T], \end{cases} \tag{1.21}$$

where $\Omega = (0, \ell)$, $\mu > 0$, and $0 < \alpha < 1$. Furthermore, we assume that $\dfrac{\partial u}{\partial x} \geq \nu^* > 0$, and $g(0) = g(\ell) = 0$.

1.4.8 Two-dimensional linear time-fractional diffusion equations

We take into account the following two-dimensional time-fractional diffusion IBVP for $0 < \alpha < 1$:

$$\begin{cases} {}^C\mathcal{D}_t^\alpha u(x,y,t) + \mathcal{L}u(x,y,t) = f(x,y,t), \ (x,y,t) \in \Omega \times (0,T], \\ u(x,y,0) = g(x,y), \quad (x,y) \in \overline{\Omega}, \\ u(x,y,t) = 0, \quad (x,y) \in \partial\Omega, \ t \in (0,T], \end{cases} \tag{1.22}$$

where $\Omega = \Omega_x \times \Omega_y \subset \mathbb{R}^2$ with $\Omega_x = (\ell_1, \ell_2)$, $\Omega_y = (\ell_3, \ell_4)$, $p > 0$, $\mathbf{a}(x, y) = (a_1(x, y), a_2(x, y))$ and $b = b_1 + b_2$, and

$$\mathcal{L}u(x, y, t) := -p\Delta u(x, y, t) + \mathbf{a}(x, y) \cdot \nabla u(x, y, t) + b(x, y)u(x, y, t),$$

We also assume that

$$a_1 \geq a_1^* > 0,\ a_2 \geq a_2^* > 0, \quad b_1, b_2 \geq 0 \quad \text{in } \overline{\Omega},$$
$$b_1 - \frac{1}{2}\frac{\partial a_1}{\partial x} \geq \gamma_1 > 0, \quad b_2 - \frac{1}{2}\frac{\partial a_2}{\partial y} \geq \gamma_2 > 0.$$

1.5 Thesis organization

This thesis consists of nine chapters. **Chapter 1** describes the general introduction along with the historical background of the related work done in the field of fractional calculus and fractional differential equations. It also provides the motivation and objective for solving fractional differential and integro-differential equations in one and two dimensions. The rest of the thesis is structured as follows:

Chapter 2 focuses on a numerical method to solve the linear BVP (1.15) and semi-linear BVP (1.16). We first discuss the well-posedness of the linear BVP. Then, by applying the shooting technique, we convert the linear BVP (1.15) into an equivalent IVP. Later, the IVP is converted into an integral equation of the Volterra type to avoid a potential singularity in the exact solution. Next, to substantially approximate the integral equation, we construct an integral discretization scheme. The process is then repeated with the initial condition modified until the solution satisfies the right boundary condition with the requisite accuracy. Using a modified Gronwall's inequality and the truncation error estimate, the discretization scheme's convergence analysis is provided. We extend the method to the semi-linear BVP (1.16). To demonstrate how effective and accurate the suggested approach is, numerical assessments are conducted.

In **Chapter 3** of the thesis, we establish the existence and uniqueness of the solution of the linear non-autonomous time-fractional IBVP (1.17) by using the Sumudu decomposition method and the maximum-minimum principle. We also propose a numerical technique for solving the IBVP (1.17) based on L1-discretization for fractional temporal derivative and cubic spline approximation for spatial variables. First, we semi-discretize the IBVP (1.17) with respect to the time variable by using the L1-discretization for the fractional-time derivative term and discussed the stability and convergence of the semi-

discretized scheme. Next, we use the cubic spline approximation to discretize the spatial derivative of the semi-discrete problem and finally, we obtain the fully discrete scheme for the IBVP (1.17). The proposed method is of $O\big(N^{-(2-\alpha)} + M^{-2}\big)$, where N and M are respectively the number of sub-intervals in temporal and spatial direction. Also, we have applied the proposed method to solve semi-linear IBVP (1.18) after linearizing by the Newton linearization process. Numerical experiments support the theoretical results.

In **Chapter 4** of the thesis, our main aim is to solve the linear TF-IPDE (1.19) analytically and numerically. First, we obtain the analytical solution of the IBVP (1.19) by using the Sumudu decomposition technique. Then, we prove the uniqueness results of the analytical solution of the IBVP (1.19) by utilizing the maximum-minimum principle. Further, we propose a numerical technique for solving the IBVP (1.19), which comprises of the L1-discretization for the fractional-time derivative and the cubic spline approximation for the spatial derivatives. To obtain the numerical solution of the FIDE (1.19), first, we apply the L1-discretization for the fractional-time derivative and trapezoidal rule for the integral term to semi-discretize the IBVP (1.19) with respect to the time variable, and we investigate the stability and convergence of the semi-discrete problem. Then, we apply the cubic spline method to discretize the spatial derivative appearing in the resultant semi-discrete problem to obtain the fully discrete scheme for the IBVP (1.19). The stability of the fully discrete scheme is analyzed through the discrete maximum principle, and error estimates are obtained. Theoretical results are validated through several numerical examples.

In **Chapter 5** of the thesis, we consider a class of non-autonomous TF-ADR equations (1.17) with homogeneous boundary conditions. To obtain the numerical solution of the model problem, we apply the NIPG method in space on a uniform mesh and the L1-discretization in time on a graded mesh. It is demonstrated that the computed solution is discretely stable. Superconvergence of error estimates for the proposed method is obtained using the discrete energy-norm. Also, we have applied the proposed method to solve the semi-linear problems (1.18) with homogeneous boundary conditions obtained after linearizing the nonlinear problem by the Newton linearization process. The theoretical results are verified through numerical experiments.

The main objective of **Chapter 6** is to obtain the numerical solution of the nonlinear time-fractional integro-partial differential IBVP (1.20) by using the L1-NIPG (L1-discretization for the time-fractional derivative and NIPG for the spatial variable) and L2-NIPG (L2-discretization for the time-fractional derivative and NIPG for the spatial variable) methods. As a first step, by applying Newton's linearization process

to the nonlinear model problem, we obtain a sequence of linear problems. Then, for resultant linear problems, we apply the NIPG method for the spatial variable to obtain the semi-discrete problem. Finally, to obtain the fully discrete schemes, we use both L1-discretization and L2-discretization for the time-fractional derivative, and the trapezoidal rule for the integral term that appears in the semi-discrete problem. Further, we study the L^2-norm stability of the proposed method and derive the required error estimates. In the study of convergence analysis, we will find that when we discretize the Caputo derivative using the L1-discretization, the order of convergence for the suggested technique is $(2-\alpha)$ in the time direction, however, the order will increase by one, *i.e.*, $(3-\alpha)$ when we do the same using the L2-discretization. To support the proposed approach and demonstrate the theoretical error bounds, numerical experiments will be carried out.

The major goal of **Chapter 7** of the thesis is to arrive at a numerical solution for the nonlinear time-fractional Burgers' equation (1.21) by applying the NIPG approach for spatial variable and the L2-discretization for time derivative discretization. We further examine the suggested method's stability under the L^2-norm, and we calculate the necessary error estimates with an order of convergence of $(h^{k+1}+\tau^{3-\alpha})$, where h and τ are the step-lengths in space and time, respectively. Numerical experiments will be carried out to validate the suggested approach and show the theoretical error bounds.

In **Chapter 8** of the thesis, the alternating direction implicit type operator splitting discontinuous Galerkin finite element method is proposed to solve a class of two-dimensional time-factional diffusion equations (1.22), numerically. By using the operator splitting method, the two-dimensional diffusion problem is split into two separate one-dimensional problems. The time-fractional derivative term is discretized over uniform mesh using the well-known L2-discretization and for the discretization of the spatial derivatives, the discontinuous Galerkin finite element method is used for both one-dimensional problems over the uniform mesh. The stability and the error estimate of the proposed scheme are addressed. Finally, we give some numerical experiments to validate the proposed method.

CHAPTER 2

Shooting technique for solving ordinary fractional boundary-value problem with RLC fractional derivative

This chapter provides a numerical solution to the steady-state fractional advection-diffusion-reaction problem. We also study the existence and uniqueness of the solution to the BVP using the Banach fixed point theorem. The proposed numerical approach includes the shooting method, transformation of differential equation into an equivalent integral equation, and integral discretization over uniform mesh. Stability analysis and error estimates are given for the suggested scheme. To support the theoretical results, numerical results are presented.

2.1 Introduction

In this chapter, we consider the following steady-state fractional advection-diffusion-reaction equation with the highest order derivative of RLC fractional type:

$$\begin{cases} -{}^{RLC}\mathcal{D}_x^{\alpha} u(x) + (bu)'(x) + c(x)u(x) = f(x), \quad x \in \Omega = (0, \ell), \\ {}^{C}\mathcal{D}_x^{\alpha-1} u(0) = \gamma, \quad u(\ell) + \beta_1 u'(\ell) = \gamma_1, \end{cases} \tag{2.1}$$

where $1 < \alpha < 2$, and the constants $\gamma, \beta_1, \gamma_1$ and the functions b, c, f are known.

We assume that for $r \in \mathbb{N}$ and some $\nu \in (-\infty, 1)$,

$$b, c, f \in \mathcal{C}^{r,\nu}(0, \ell], \quad c + b' \geq 0, \quad \beta_1, \gamma_1 \geq 0. \tag{2.2}$$

Here, we propose a numerical method to solve the BVP (2.1). More precisely, first, by applying the shooting technique, we convert the BVP into an equivalent IVP. Later,

the IVP is changed into an integral equation of the Voltera type to avoid a potential singularity in the exact solution. Next, in order to substantially approximate the integral equation, we construct an integral discretization scheme. The process is then repeated with the initial condition modified until the solution satisfies the right boundary condition with the requisite accuracy. Using a modified Gronwall's inequality and the truncation error estimate, the discretization scheme's convergence analysis is provided. In order to demonstrate how effective and accurate the suggested approach is, numerical assessments are conducted.

The chapter is arranged as follows: in Section 2.2, we discuss the well-posedness of the continuous solution for the given BVP and the numerical solution technique which consists of a shooting method based on the secant method with integral discretization of the equivalent integral equation of the IVP (IVP is transformed from BVP using the shooting technique). Here, we also study the convergence of the secant method used in the shooting technique. Section 2.3 deals with the error estimate and convergence analysis. In Section 2.4, we extend the proposed method to the semi-linear BVPs. Finally, numerical experiments are presented in Section 2.5.

2.2 Proposed method

In this section, we will discuss some sequential approximation methods for solving the BVP (2.1) numerically.

2.2.1 Shooting technique

First, by using the shooting technique, we convert the given BVP (2.1) into the following IVP:

$$\begin{cases} -{}^{RLC}\mathcal{D}_x^{\alpha} u(x) + (bu)'(x) + c(x)u(x) = f(x), \quad x \in \Omega, \\ u(0) = \eta, \quad {}^{C}\mathcal{D}_x^{\alpha-1} u(0) = \gamma, \end{cases} \tag{2.3}$$

where η is an initial guess which will be adjusted so that the solution satisfies the required boundary condition at $x = \ell$ as given in (2.1). This shooting technique is based on the secant iterative method.

Instead of solving (2.3) directly, we will transform it into an equivalent integral equation, by assuming some regularity conditions on u. The following statement yields the equivalence of the equation (2.3) and an integral equation.

Theorem 2.1 *Let us assume the conditions given in (2.2) holds true. If $u \in \mathcal{C}^1(\overline{\Omega})$, then $u(x)$ satisfies the equation (2.3) if, and only if, $u(x)$ satisfies the Volterra integral equation with a weakly singular kernel:*

$$\begin{cases} u(x) = u(0) + \left(\dfrac{{}^{C}\mathcal{D}_x^{\alpha-1}u(0) - b(0)u(0)}{\Gamma(\alpha)} \right) x^{\alpha-1} + \dfrac{1}{\Gamma(\alpha-1)} \displaystyle\int_0^x (x-s)^{\alpha-2}(bu)(s)ds \\ \qquad\quad + \dfrac{1}{\Gamma(\alpha)} \displaystyle\int_0^x (x-s)^{\alpha-1}(cu-f)(s)ds, \quad x \in \Omega, \\ u(0) = \eta, \quad {}^{C}\mathcal{D}_x^{\alpha-1}u(0) = \gamma. \end{cases} \tag{2.4}$$

Proof. From (2.3), we have

$$\frac{d}{dx}\left({}^{C}\mathcal{D}_x^{\alpha-1}u(x)\right) = g(x,u(x)), \text{ where } g(x,u(x)) = \big((bu)' + cu - f\big)(x).$$

Since $u \in \mathcal{C}(\overline{\Omega})$ and $b, c, f \in \mathcal{C}^{r,\nu}(0,\ell]$, then $g \in \mathcal{C}^{r,\nu}(0,\ell]$. By integrating it over $[0,x]$, we get

$${}^{C}\mathcal{D}_x^{\alpha-1}u(x) - {}^{C}\mathcal{D}_x^{\alpha-1}u(0) = \int_0^x g(t,u(t))dt = (bu)(x) - (bu)(0) + (I_x^1(cu-f))(x). \tag{2.5}$$

Multiplying both sides of the equation (2.5) by $I_x^{\alpha-1}$ and using the fact that

$$({}^{C}\mathcal{D}_x^{\alpha-1}u(0))(x) = 0, \quad I_x^{\alpha-1} \cdot I_x^1 u(x) = I_x^{\alpha}u(x),$$

and

$$(I_x^{\beta} \cdot {}^{C}\mathcal{D}_x^{\beta}H)(x) = H(x), \text{ provided } H(0) = 0,\ \beta \geq 0,$$

we have

$$u(x) - u(0) = I_x^{\alpha-1}({}^{C}\mathcal{D}_x^{\alpha-1}u(0) - (bu)(0)) + I_x^{\alpha-1}(bu)(x) + I_x^{\alpha}(cu-f)(x).$$

Hence, we get the integral equation (2.4), and thus the necessity is proved.

Now let $u(x) \in \mathcal{C}(\overline{\Omega})$ be the solution of the integral equation (2.4). By differentiating on both sides of the equation (2.4) with respect to x, we get

$$u'(x) = \frac{{}^{C}\mathcal{D}_x^{\alpha-1}u(0) - b(0)u(0)}{\Gamma(\alpha-1)}x^{\alpha-2} + I_x^{\alpha-2}(bu)(x) + I_x^{\alpha-1}(cu-f)(x), \quad x > 0. \tag{2.6}$$

Using (2.6), ${}^{RLC}\mathcal{D}_x^{\alpha}u(x)$ can be expressed as follows:

$$\begin{aligned} {}^{RLC}\mathcal{D}_x^{\alpha}u(x) = {}^{RL}\mathcal{D}_x^{\alpha-1}(u'(x)) &= {}^{RL}\mathcal{D}_x^{\alpha-1}\left(I_x^{\alpha-2}(bu)(x)\right) + {}^{RL}\mathcal{D}_x^{\alpha-1}\left(I_x^{\alpha-1}(cu-f)(x)\right) \\ &= (bu)'(x) + (cu-f)(x), \end{aligned}$$

where we have used the fact that ${}^{RL}\mathcal{D}_x^{\alpha-1}(x^{\alpha-2}) = 0$. Thus we arrive at equation (2.3) and the sufficiency is proved. □

2.2.2 Existence and uniqueness of the solution of the BVP

Next, we will show that the one and only solution of the BVP (2.1) exists using the Banach fixed point theorem.

Theorem 2.2 *Suppose the conditions given in (2.2) holds true. If* $\left(\frac{\|b\|_\Omega\,\ell^{\alpha-1}}{\Gamma(\alpha)} + \frac{\|c\|_\Omega\,\ell^{\alpha}}{\Gamma(\alpha+1)}\right) < 1$, *then there exists a unique solution* $u(x) \in \mathcal{C}(\overline{\Omega})$ *to the BVP (2.1).*

Proof. From Theorem 2.1 we observe that if u is the solution to the BVP (2.1), then u satisfies the following : $u(x) = \mathcal{H}u(x)$, $\forall x \in \overline{\Omega}$, where

$$\begin{aligned} \mathcal{H}u(x) &= u(0) + \left(\frac{{}^{C}\mathcal{D}_x^{\alpha-1}u(0) - b(0)u(0)}{\Gamma(\alpha)}\right)x^{\alpha-1} + \frac{1}{\Gamma(\alpha-1)}\int_0^x (x-s)^{\alpha-2}(bu)(s)ds \\ &\quad + \frac{1}{\Gamma(\alpha)}\int_0^x (x-s)^{\alpha-1}(cu-f)(s)ds. \end{aligned} \tag{2.7}$$

Then, for $u_1, u_2 \in \mathcal{C}(\overline{\Omega})$, we have

$$\begin{aligned} \|\mathcal{H}u_1 - \mathcal{H}u_2\|_\Omega &\le \left\| \int_0^x \frac{b(s)(x-s)^{\alpha-2}}{\Gamma(\alpha-1)}(u_1-u_2)(s)ds + \int_0^x \frac{c(s)(x-s)^{\alpha-1}}{\Gamma(\alpha)}(u_1-u_2)(s)ds \right\|_\Omega \\ &\le \frac{\|b\|_\Omega}{\Gamma(\alpha-1)}\|u_1-u_2\|_\Omega \int_0^x (x-s)^{\alpha-2}ds + \frac{\|c\|_\Omega}{\Gamma(\alpha)}\|u_1-u_2\|_\Omega \int_0^x (x-s)^{\alpha-1}ds \\ &\le \left(\frac{\|b\|_\Omega\,\ell^{\alpha-1}}{\Gamma(\alpha)} + \frac{\|c\|_\Omega\,\ell^{\alpha}}{\Gamma(\alpha+1)}\right)\|u_1-u_2\|_\Omega. \end{aligned} \tag{2.8}$$

Since $\left(\frac{\|b\|_\Omega\,\ell^{\alpha-1}}{\Gamma(\alpha)} + \frac{\|c\|_\Omega\,\ell^{\alpha}}{\Gamma(\alpha+1)}\right) < 1$ is given, then we have $\|\mathcal{H}u_1 - \mathcal{H}u_2\|_\Omega < \|u_1-u_2\|_\Omega$.

Therefore, $\mathcal{H}$ is a contraction mapping and $(\mathcal{C}(\overline{\Omega}), \|.\|_\Omega)$ is a Banach space. Hence by Theorem 1.2 one can conclude that BVP (2.1) has a unique solution u in $\overline{\Omega}$. □

Here, we establish the following stability result for the exact solution $u(x)$ to the BVP (2.1).

Lemma 2.1 *Let $u(x)$ be the exact solution of the BVP (2.1) with the assumptions given in (2.2) and $\left(\frac{\|b\|_\Omega \ell^{\alpha-1}}{\Gamma(\alpha)} + \frac{\|c\|_\Omega \ell^\alpha}{\Gamma(\alpha+1)}\right) < 1$. Then we have*

$$\|u\|_\Omega \leq C(|\eta| + |\gamma| + \|f\|_\Omega). \tag{2.9}$$

Proof. Theorem 2.2 guarantees that the BVP (2.1) has a solution $u \in \mathcal{C}(\Omega)$, and then from Theorem 2.1, one can observe that u satisfies the integral equation (2.4). Now, from (2.4), for $x \in \Omega$, we have

$$\begin{aligned} |u(x)| &\leq |\eta| + \frac{|\gamma| + |\eta b(0)|}{\Gamma(\alpha)}|x|^{\alpha-1} + \frac{\|f\|_\Omega}{\Gamma(\alpha+1)}|x|^\alpha \\ &\quad + \left(\frac{\|b\|_\Omega}{\Gamma(\alpha-1)} + \frac{\ell\,\|c\|_\Omega}{\Gamma(\alpha)}\right)\int_0^x (x-s)^{\alpha-2}|u(s)|ds \\ &= h(x) + \lambda\int_0^x (x-s)^{\alpha-2}|u(s)|ds, \end{aligned} \tag{2.10}$$

where $h(x) = |\eta| + \frac{|\gamma| + |\eta b(0)|}{\Gamma(\alpha)}|x|^{\alpha-1} + \frac{\|f\|_\Omega}{\Gamma(\alpha+1)}|x|^\alpha$ and $\lambda = \frac{\|b\|_\Omega}{\Gamma(\alpha-1)} + \frac{\ell\,\|c\|_\Omega}{\Gamma(\alpha)}$.

Here, $h(x)$ is a non-decreasing function on $\overline{\Omega}$. Applying the generalized Gronwall inequality given in [34, Theorem 3.1] to (2.10), we can obtain that

$$|u(x)| \leq h(x)E_{\alpha-1,1}(\lambda\Gamma(\alpha-1)x^{\alpha-1}). \tag{2.11}$$

The expression of $E_{\alpha-1,1}(\lambda\Gamma(\alpha-1)x^{\alpha-1})$ with $1 < \alpha < 2$ and $x \in \overline{\Omega}$ is convergent [31, Theorem 4.1] and

$$E_{\alpha-1,1}(\lambda\Gamma(\alpha-1)x^{\alpha-1}) \leq E_{\alpha-1,1}(\lambda\Gamma(\alpha-1)\ell^{\alpha-1}), \quad \forall x \in \overline{\Omega}. \tag{2.12}$$

It is obvious that

$$h(x) \leq C(|\eta| + |\gamma| + \|f\|_\Omega).$$

Hence, from (2.11), we have

$$|u(x)| \leq C(|\eta| + |\gamma| + \|f\|_\Omega),$$

and then from the definition of the maximum norm we can obtain the required result (2.9). □

Lemma 2.2 *Let us consider the assumptions given in (2.2). Then* $u(x;\eta)$ *and* $\dfrac{\partial u}{\partial x}(x;\eta)$ *are both twice continuously differentiable with respect to* η*, and satisfy the following:*

$$\left|\frac{\partial^{i+j} u}{\partial \eta^i \partial x^j}(x;\eta)\right| \leq C, \quad i = 1, 2,\ j = 0, 1.$$

Proof. Differentiating both sides of equation (2.4) with respect to x and using the fact that

$$I_x^{\alpha-1}(bu)(x) = \frac{b_0\eta}{\Gamma(\alpha-1)}x^\alpha + I_x^\alpha(bu)'(x) \quad \text{(using integration by parts)},$$

we obtain

$$\begin{aligned} u'(x) &= \frac{\gamma - b_0\eta}{\Gamma(\alpha-1)}x^{\alpha-2} + \frac{b_0\eta}{\Gamma(\alpha-1)}x^{\alpha-2} + I_x^{\alpha-1}((bu)' + cu - f)(x) \\ &= \frac{\gamma}{\Gamma(\alpha-1)}x^{\alpha-2} + I_x^{\alpha-1}((bu)' + cu - f)(x). \end{aligned} \tag{2.13}$$

From the expressions of u and $\dfrac{\partial u}{\partial x}$ respectively given in (2.4) and (2.13), for $i = 1, 2$ we have

$$\frac{\partial^i u}{\partial \eta^i}(x;\eta) = d_i + \int_0^x (x-s)^{\alpha-2}\left[\frac{b(s)}{\Gamma(\alpha-1)} + \frac{c(s)(x-s)}{\Gamma(\alpha)}\right]\frac{\partial^i u}{\partial \eta^i}(s;\eta)ds, \tag{2.14}$$

and

$$\frac{\partial^{i+1} u}{\partial \eta^i \partial x}(x;\eta) = D_i + \int_0^x \frac{(x-s)^{\alpha-2}}{\Gamma(\alpha-1)}\left[\left(b' + c\right)(s)\frac{\partial^i u}{\partial \eta^i}(s;\eta) + b(s)\frac{\partial^{i+1} u}{\partial \eta^i \partial x}(s;\eta)\right]ds, \tag{2.15}$$

where $d_1 = 1 - \dfrac{b_0 x^{\alpha-1}}{\Gamma(\alpha)}$, $d_2 = 0$ and $D_1 = D_2 = 0$.

From (2.14) and (2.15), one can observe that $u(x;\eta)$ and $\dfrac{\partial u}{\partial x}(x;\eta)$ are both con-

tinuously differentiable with respect to η. By taking the modulus on both sides of (2.14)-(2.15) and using simultaneously the triangle inequality and general Gronwall inequality (in a similar way as in the proof of Lemma 2.1), one can obtain the required results. □

In general, it is quite difficult to find out the exact value of η, we have to look at some approximation method for finding η in such a way that $u(\ell;\eta)+\beta_1 u'(\ell;\eta)-\gamma_1 = 0$, where $u(x;\eta)$ is the solution of (2.3) for each $u(0) = \eta$. We use the secant method to compute η iteratively, by finding the solution of $\phi(\eta) = 0$, where

$$\phi(\eta) = u(\ell;\eta) + \beta_1 u'(\ell;\eta) - \gamma_1. \tag{2.16}$$

Firstly, we take the values η_0 and η_1, namely $\eta_0 = \gamma, \eta_1 = \gamma_1$ (if $\gamma \neq \gamma_1$) and $\eta_0 = \gamma, \eta_1 = \gamma_1 + 1$ (if $\gamma = \gamma_1$), and iteratively compute $\eta_i (i \geq 2)$ using the secant method [30, equation (6.2.3)] as

$$\eta_{i+1} = \eta_i - \frac{\eta_i - \eta_{i-1}}{\phi(\eta_i) - \phi(\eta_{i-1})}\phi(\eta_i), \quad i \geq 1. \tag{2.17}$$

Let $\varepsilon_i = \eta_i - \eta$ be the error due to the secant method, where η is such that $\phi(\eta) = 0$ and η_i defined in (2.17). Then by a simple calculation as given in [30, equation (6.2.6)], one can show that

$$\varepsilon_{i+1} = -\frac{1}{2}\frac{\phi''(\xi_i)}{\phi'(\xi_i')}\varepsilon_i\varepsilon_{i-1}, \ \xi_i \in int(\eta, \eta_{i-1}, \eta_i) \text{ and } \xi_i' \in int(\eta_{i-1}, \eta_i), \tag{2.18}$$

where $int(a, b)$ = the interval form by a and b and $int(a, b, c)$ = the interval form by a, b and c.

In the following theorem we will show the convergence of the secant method.

Theorem 2.3 *Assume that the conditions given in (2.2) holds true and $\phi'(\eta) \neq 0$. Then the function ϕ defined by the equation (2.16) satisfies the following:*

$$\left|\frac{\phi''(\xi_i)}{2\phi'(\xi_i')}\right| \leq C, \tag{2.19}$$

and hence the secant method given in (2.17) converges, i.e., $\eta_i \to u(0)$ with the order of convergence 1.618.

Proof. From Lemma 2.2, we can observe that $\phi(\xi), \phi'(\xi)$, and $\phi''(\xi)$ are continuous for all values of $\xi \in \mathcal{I} = [\eta - \epsilon, \eta + \epsilon]$ with some $\epsilon > 0$. Also, $\phi'(\xi) \neq 0$, $\xi \in \mathcal{I}$. Then by

defining

$$C = \frac{\max\limits_{\xi\in\mathcal{I}} |\phi''(\xi)|}{2\min\limits_{\xi\in\mathcal{I}} |\phi'(\xi)|},$$

one can show that $\left|\frac{\phi''(\xi_i)}{2\phi'(\xi_i')}\right| \leq C$. Hence by following [30, Theorem 6.2.1], the secant method given in (2.17) converges. □

2.2.3 Discretization scheme

The problem (2.4) is approximated on the uniform mesh $\overline{\Omega}_M$ as follows:

$$\begin{aligned} u(x_m) &= u_0 + \frac{{}^C\mathcal{D}_x^{\alpha-1}u(0) - b_0u_0}{\Gamma(\alpha)}x_m^{\alpha-1} + \frac{1}{\Gamma(\alpha-1)}\int_0^{x_m}(x_m-s)^{\alpha-2}(bu)(s)ds \\ &\quad + \frac{1}{\Gamma(\alpha)}\int_0^{x_m}(x_m-s)^{\alpha-1}(cu-f)(s)ds \\ &\approx \eta + \frac{\gamma-\eta b_0}{\Gamma(\alpha)}x_m^{\alpha-1} + \frac{1}{\Gamma(\alpha-1)}\sum_{i=2}^{m}\int_{x_{i-1}}^{x_i}(x_m-s)^{\alpha-2}b_iu_ids \\ &\quad + \frac{1}{\Gamma(\alpha)}\sum_{i=2}^{m}\int_{x_{i-1}}^{x_i}(x_m-s)^{\alpha-1}(c_iu_i-f_i)ds. \end{aligned} \tag{2.20}$$

Let u_m^M be the computed solution of the problem (2.4) at the point x_m. As a result, the discretization approach (2.4) is as follows:

$$\begin{aligned} u_m^M &= \eta + \frac{\gamma-\eta b_0}{\Gamma(\alpha)}x_m^{\alpha-1} + \frac{1}{\Gamma(\alpha)}\sum_{i=2}^{m}b_iu_i^M[(x_m-x_{i-1})^{\alpha-1} - (x_m-x_i)^{\alpha-1}] \\ &\quad + \frac{1}{\Gamma(\alpha+1)}\sum_{i=2}^{m}(c_iu_i^M - f_i)[(x_m-x_{i-1})^{\alpha} - (x_m-x_i)^{\alpha}], \quad m = 2,3,\cdots,M+1, \end{aligned}$$

which is equivalent to

$$\begin{aligned} u_m^M &= d_m\eta + \frac{\gamma-\eta b_0}{\Gamma(\alpha)}d_mx_m^{\alpha-1} + \frac{d_m}{\Gamma(\alpha)}\sum_{i=2}^{m-1}b_iu_i^M[(x_m-x_{i-1})^{\alpha-1} - (x_m-x_i)^{\alpha-1}] \\ &\quad + \frac{d_m}{\Gamma(\alpha+1)}\sum_{i=2}^{m-1}(c_iu_i^M - f_i)[(x_m-x_{i-1})^{\alpha} - (x_m-x_i)^{\alpha}] - \frac{d_mf_m}{\Gamma(\alpha+1)}h^{\alpha}, \end{aligned} \tag{2.21}$$

where $d_m = \left(1 - \frac{b_m h^{\alpha-1}}{\Gamma(\alpha)} - \frac{c_m h^{\alpha}}{\Gamma(\alpha+1)}\right)^{-1}$ and $2 \le m \le M+1$. For sufficiently small h, $d_m > 0$.

2.3 Convergence analysis

In this section, we establish the error estimate for the discrete scheme (2.21) by finding the truncation error, stability analysis, and convergence of the computed solution.

Let $e_m^M := u_m^M - u_m, (2 \le m \le M+1)$, where u_m^M be the solution of the numerical scheme (2.21) and u_m be the analytic solution of the problem (2.4) at $x = x_m$. Then the error e_m^M satisfies

$$e_m^M - \sum_{i=2}^{m} \frac{b_i e_i^M}{\Gamma(\alpha)}[(x_m - x_{i-1})^{\alpha-1} - (x_m - x_i)^{\alpha-1}] - \sum_{i=2}^{m} \frac{c_i e_i^M}{\Gamma(\alpha+1)}[(x_m - x_{i-1})^{\alpha} - (x_m - x_i)^{\alpha}] =: \mathcal{R}_M^m, \tag{2.22}$$

where $\mathcal{R}_M^m$ is the truncation error at $x = x_m$ defined by

$$\mathcal{R}_M^m = \sum_{i=2}^{m} \int_{x_{i-1}}^{x_i} [b_i u_i - (bu)(s)] \frac{(x_m - s)^{\alpha-2}}{\Gamma(\alpha-1)} ds + \sum_{i=2}^{m} \int_{x_{i-1}}^{x_i} [(c_i u_i - f_i) - (cu - f)(s)] \frac{(x_m - s)^{\alpha-1}}{\Gamma(\alpha)} ds. \tag{2.23}$$

The following lemma provides bound for the truncation error.

Lemma 2.3 *Let us assume that the conditions given in (2.2) holds true. Then the truncation error $\mathcal{R}_M^m$ defined in (2.23) satisfies the following bound:*

$$|\mathcal{R}_M^m| \le CM^{-1}, \quad 2 \le m \le M+1.$$

Proof. From the hypothesis given in (2.2), and by applying the mean-value theorem to (2.23), we have

$$\begin{aligned} |\mathcal{R}_M^m| &\le \frac{1}{\Gamma(\alpha-1)} \sum_{i=2}^{m} \int_{x_{i-1}}^{x_i} |b_i u_i - (bu)(s)| (x_m - s)^{\alpha-2} ds \\ &\quad + \frac{1}{\Gamma(\alpha)} \sum_{i=2}^{m} \int_{x_{i-1}}^{x_i} |(c_i u_i - f_i) - (cu - f)(s)| (x_m - s)^{\alpha-1} ds \\ &\le \frac{Ch}{\Gamma(\alpha-1)} \sum_{i=2}^{m} \int_{x_{i-1}}^{x_i} (x_m - s)^{\alpha-2} ds + \frac{Ch}{\Gamma(\alpha)} \sum_{i=2}^{m} \int_{x_{i-1}}^{x_i} (x_m - s)^{\alpha-1} ds \end{aligned}$$

$$
\begin{aligned}
&= \frac{C}{M}\sum_{i=2}^{m}\left\{\frac{[(x_m - x_{i-1})^{\alpha-1} - (x_m - x_i)^{\alpha-1}]}{\Gamma(\alpha)} + \frac{[(x_m - x_{i-1})^{\alpha} - (x_m - x_i)^{\alpha}]}{\Gamma(\alpha+1)}\right\} \\
&= \frac{C}{M\,\Gamma(\alpha)}x_m^{\alpha-1} + \frac{C}{M\,\Gamma(\alpha+1)}x_m^{\alpha} \\
&\leq CM^{-1},
\end{aligned}
$$

which is the required result. □

In the next lemma, we present the stability analysis of the discrete scheme (2.21) on the mesh $\overline{\Omega}_M$ by using the generalized discrete Gronwall inequality.

Lemma 2.4 *(Discrete stability estimate) The computed solution* $\{u_m^M\}_{m=1}^{M+1}$ *of the scheme (2.21) on the mesh* $\overline{\Omega}_M$ *satisfies*

$$\|u^M\|_{\overline{\Omega}_M} \leq C(|\eta| + |\gamma| + \|f\|_{\overline{\Omega}_M}),$$

provided the assumptions given in (2.2) holds true.

Proof. From (2.21), we have

$$
\begin{cases}
|u_2^M| \leq |d_2|p_2, \\
|u_m^M| \leq |d_m|p_m + \sum_{i=2}^{m-1} w_{i,m}\,|u_i^M|, \quad 3 \leq m \leq M+1,
\end{cases}
\tag{2.24}
$$

where for $2 \leq m \leq M+1$,

$$d_m = \left[1 - \frac{b_m h^{\alpha-1}}{\Gamma(\alpha)} - \frac{c_m h^{\alpha}}{\Gamma(\alpha+1)}\right]^{-1},$$

$$p_m = |\eta| + \frac{|\gamma| + |\eta b_0|}{\Gamma(\alpha)}x_m^{\alpha-1} + \frac{1}{\Gamma(\alpha+1)}\sum_{i=2}^{m}|f_i|[(x_m - x_{i-1})^{\alpha} - (x_m - x_i)^{\alpha}],$$

and for $3 \leq m \leq M+1,\ 2 \leq i \leq m-1$,

$$w_{i,m} = \frac{|d_m||b_i|}{\Gamma(\alpha)}[(x_m - x_{i-1})^{\alpha-1} - (x_m - x_i)^{\alpha-1}] + \frac{|d_m||c_i|}{\Gamma(\alpha+1)}[(x_m - x_{i-1})^{\alpha} - (x_m - x_i)^{\alpha}].$$

Using a straightforward calculation, one may now arrive at the following result for a positive constant C:

$$p_m \leq C(|\eta| + |\gamma| + \|f\|_{\overline{\Omega}_M}).$$

By using the assumptions on b and c given in (2.2), for some positive constant C_1, we have

$$|d_m| \leq \left[1 - \frac{h^{\alpha-1}\|b\|_{\overline{\Omega}_M}}{\Gamma(\alpha)} - \frac{h^{\alpha}\|c\|_{\overline{\Omega}_M}}{\Gamma(\alpha+1)}\right]^{-1} \leq C_1. \tag{2.25}$$

Furthermore, for $2 \leq i \leq m-1$, using the mean-value theorem with $\chi_i, \mu_i \in (x_{i-1}, x_i)$, the inequality $k \leq 2(k-1)$ for $2 \leq k (\in \mathbb{N})$ and the assumptions $b, c \in \mathcal{C}^{r,\nu}(0, \ell]$, we have

$$\begin{aligned}
w_{i,m} &\leq C_1 \left(\frac{\|b\|_{\overline{\Omega}_M}}{\Gamma(\alpha)} [(x_m - x_{i-1})^{\alpha-1} - (x_m - x_i)^{\alpha-1}] \right. \\
&\qquad \left. + \frac{\|c\|_{\overline{\Omega}_M}}{\Gamma(\alpha+1)} [(x_m - x_{i-1})^{\alpha} - (x_m - x_i)^{\alpha}] \right) \\
&\leq C_1 \frac{\|b\|_{\overline{\Omega}_M}}{\Gamma(\alpha-1)} h(x_m - \chi_i)^{\alpha-2} + C_1 \frac{\|c\|_{\overline{\Omega}_M}}{\Gamma(\alpha)} h(x_m - \mu_i)^{\alpha-1} \\
&\leq C_1 \frac{\|b\|_{\overline{\Omega}_M}}{\Gamma(\alpha-1)} h(x_m - x_i)^{\alpha-2} + C_1 \frac{\|c\|_{\overline{\Omega}_M}}{\Gamma(\alpha)} h(x_m - x_{i-1})^{\alpha-1} \\
&\leq C_1 \frac{\|b\|_{\overline{\Omega}_M}}{\Gamma(\alpha-1)} h(x_m - x_i)^{\alpha-2} + C_1 \frac{\|c\|_{\overline{\Omega}_M} 2^{\alpha-1}}{\Gamma(\alpha)} h(x_m - x_i)^{\alpha-1} \\
&\leq C_1 \left[\frac{\|b\|_{\overline{\Omega}_M}}{\Gamma(\alpha-1)} + \frac{\|c\|_{\overline{\Omega}_M} 2^{\alpha-1}\ell}{\Gamma(\alpha)} \right] h(x_m - x_i)^{\alpha-2} \\
&\leq Ch(x_m - x_i)^{\alpha-2} \\
&= Ch^{\alpha-1}(m-i)^{\alpha-2}.
\end{aligned} \tag{2.26}$$

Now, combining (2.24)-(2.26), we have

$$\begin{cases} |u_2^M| \leq \psi_2, \\ |u_m^M| \leq \psi_m + Ch^{\alpha-1} \displaystyle\sum_{i=2}^{m-1} \frac{|u_i^M|}{(m-i)^{2-\alpha}}, \quad 3 \leq m \leq M+1, \end{cases} \tag{2.27}$$

where $\psi_m = C(|\eta| + |\gamma| + \|f\|_{\overline{\Omega}_M})$, $2 \leq m \leq M+1$, a monotonically increasing sequence of non-negative real numbers and $0 < 2 - \alpha < 1$. Hence by applying Lemma 1.8 and using the fact given in (2.12), we get the required result. □

The estimated error for the numerical solution is given by the next theorem.

Theorem 2.4 *Let u and $\{u_m^M\}_{m=1}^{M+1}$ be the solution of (2.4) and (2.21) respectively. Then, from the assumptions given in (2.2), we get*

$$|u_m^M - u_m| \leq CM^{-1}, \quad 1 \leq m \leq M+1,$$

for sufficiently large M.

Proof. From (2.22) and (2.23), we have

$$\begin{cases} |e_2^M| \le p_2, \\ |e_m^M| \le p_m + \sum_{i=2}^{m-1} w_{i,m} |e_i^M|, \quad 3 \le m \le M+1, \end{cases} \tag{2.28}$$

where

$$p_m = |d_m||\mathcal{R}_M^m|, \quad d_m = \left[1 - \frac{b_m h^{\alpha-1}}{\Gamma(\alpha)} - \frac{c_m h^{\alpha}}{\Gamma(\alpha+1)}\right]^{-1}, \quad 2 \le m \le M+1,$$

and for $2 \le i \le m-1$, $3 \le m \le M+1$,

$$w_{i,m} = \frac{|d_m||b_i|}{\Gamma(\alpha)}[(x_m - x_{i-1})^{\alpha-1} - (x_m - x_i)^{\alpha-1}] + \frac{|d_m||c_i|}{\Gamma(\alpha+1)}[(x_m - x_{i-1})^{\alpha} - (x_m - x_i)^{\alpha}].$$

In a similar way to (2.25), for large M, we have

$$|d_m| \le C_1, \quad 2 \le m \le M+1. \tag{2.29}$$

Thus, from Lemma 2.3 and (2.29), we have

$$0 < p_m \le CM^{-1}, \quad 2 \le m \le M+1. \tag{2.30}$$

Hence, combining (2.26) with (2.28)-(2.30), we have

$$\begin{cases} |e_1^M| = 0 \le \psi_1, \\ |e_m^M| \le \psi_m + Ch^{\alpha-1} \sum_{i=1}^{m-1} \frac{|e_i^M|}{(m-i)^{2-\alpha}}, \quad 2 \le m \le M+1, \end{cases} \tag{2.31}$$

where $\psi_m = CM^{-1}$, $1 \le m \le M+1$, a monotonically increasing sequence of non-negative real numbers and $0 < 2-\alpha < 1$. Applying Lemma 1.8 on (2.31) and using the fact given in (2.12), we can obtain

$$|e_m^M| \le CM^{-1}, \quad 1 \le m \le M+1,$$

which is the required estimate. □

Remark 2.5 *The bound CM^{-1} of Theorem 2.4 is better than the convergence result of*

$CM^{-1}\ln M$ that was obtained in reference [38] for their finite difference scheme, but also points out that [38] is for the original problem (2.1) whereas Theorem 2.4 is for the problem (2.4) where the value of η cannot be deduced a priori from (2.3).

2.4 Semi-linear BVPs

Here, in this section, we extend the results presented in Section 2.2 and Section 2.3 with some essential modification to the semi-linear BVPs.

Consider the following semi-linear BVP:

$$\begin{cases} -{}^{RLC}\mathcal{D}_x^{\alpha}u(x) + (bu)'(x) = f(x,u(x)), \quad x \in \Omega = (0,\ell), \\ {}^{C}\mathcal{D}_x^{\alpha-1}u(0) = \gamma, \quad u(\ell) + \beta_1 u'(\ell) = \gamma_1, \end{cases} \tag{2.32}$$

where $f \in \mathcal{C}^2(\Omega \times \mathbb{R})$ and $b \in \mathcal{C}^{r,\nu}(0,\ell]$ $(r \in \mathbb{N}, \nu \in (-\infty, 1))$ are known. Assume that there exist two positive constants $\lambda_i (i = 1, 2)$ such that

$$0 \le \lambda_1 \le \frac{\partial f}{\partial u}(x,u(x)) \le \lambda_2, \quad \forall x \in (0,\ell], \quad \forall u \in \mathbb{R}. \tag{2.33}$$

Using the shooting technique, we convert the semi-linear BVP (2.32) into an IVP similar to (2.3) with $u(0) = \eta$, and then as in Theorem 2.1 we get an integral equation similar to (2.4), wherein both the IVP and integral equation $(cu - f)(x)$ is replaced by $-f(x,u(x))$ and the integral equation is equivalent to (2.32). Using the above conditions on b and f, one can establish the existence and uniqueness of the solution of (2.32), by finding the same for the equivalent integral equation as discussed in the proof of [59, Theorem 3.14]. Using the condition given in (2.33) and the linear affine approximation of the Taylor series expansion $f(x,u(x)) = f(x,0) + f_u(x,\beta u(x))u(x)$ with $0 < \beta < 1$, we can obtain the following result.

Lemma 2.5 *Let $u(x)$ represent the exact solution to the problem (2.32). Then, we have*

$$\|u\|_{\Omega} \le C(|\eta| + |\gamma| + \|f(\cdot,0)\|_{\Omega}). \tag{2.34}$$

Proof. From Lemma 2.1, the proof can be deduced. □

In the same way, as discussed in Lemma 2.2 and Theorem 2.3, one can establish the convergence of the secant method in the shooting method for a semi-linear problem.

To solve the semi-linear BVP (2.32) numerically, we discretize the equivalent integral equation over the uniform mesh $\overline{\Omega}_M$ in a similar way as followed in (2.20), we obtain

for $m = 2, 3, \cdots, M+1$:

$$\begin{aligned} u_m^M &= \eta + \frac{\gamma - \eta b_0}{\Gamma(\alpha)} x_m^{\alpha-1} + \frac{1}{\Gamma(\alpha)} \sum_{i=2}^{m} b_i u_i^M [(x_m - x_{i-1})^{\alpha-1} - (x_m - x_i)^{\alpha-1}] \\ &\quad - \frac{1}{\Gamma(\alpha+1)} \sum_{i=2}^{m} f(x_i, u_i^M)[(x_m - x_{i-1})^{\alpha} - (x_m - x_i)^{\alpha}]. \end{aligned} \tag{2.35}$$

Let $e_m^M := u_m^M - u_m, (2 \le m \le M+1)$, where u_m^M be the solution of the numerical scheme (2.35) and u_m be the analytic solution of the problem (2.32) at $x = x_m$. Then we have

$$\begin{aligned} e_m^M &- \sum_{i=2}^{m} \frac{b_i e_i^M}{\Gamma(\alpha)} [(x_m - x_{i-1})^{\alpha-1} - (x_m - x_i)^{\alpha-1}] \\ &+ \sum_{i=2}^{m} \frac{f(x_i, u_i^M) - f(x_i, u_i)}{\Gamma(\alpha+1)} [(x_m - x_{i-1})^{\alpha} - (x_m - x_i)^{\alpha}] =: \mathcal{R}_M^m, \end{aligned} \tag{2.36}$$

where $\mathcal{R}_M^m$ is the truncation error at $x = x_m$ defined by

$$\begin{aligned} \mathcal{R}_M^m &= \sum_{i=2}^{m} \int_{x_{i-1}}^{x_i} [b_i u_i - (bu)(s)] \frac{(x_m - s)^{\alpha-2}}{\Gamma(\alpha-1)} ds \\ &\quad - \sum_{i=2}^{m} \int_{x_{i-1}}^{x_i} [f(x_i, u_i) - f(s, u(s))] \frac{(x_m - s)^{\alpha-1}}{\Gamma(\alpha)} ds. \end{aligned} \tag{2.37}$$

The results of the convergent analysis presented in Section 2.3 can be deduced for the semi-linear problems in a similar way, which is stated in the following Lemma.

Lemma 2.6 *Let $b \in \mathcal{C}^{r,\nu}(0, L]$ and condition given in (2.33) holds true. Then we have the following results :*

(a) The truncation error $\mathcal{R}_M^m$ defined in (2.37) satisfies the following

$$|\mathcal{R}_M^m| \le C M^{-1}, \quad 2 \le m \le M+1.$$

(b) The computed solution $\{u_m^M\}_{m=1}^{M+1}$ of the scheme (2.35) on the mesh $\overline{\Omega}_M$ satisfies

$$\|u^M\|_{\overline{\Omega}_M} \le C(|\eta| + |\gamma| + \|f(\cdot, 0)\|_{\overline{\Omega}_M}).$$

(c) We have the following error bound

$$|u_m^M - u_m| \leq CM^{-1}, \quad 1 \leq m \leq M+1,$$

for sufficiently large M.

2.5 Numerical examples

In this section, we carry out the numerical experiments for the proposed discrete schemes (2.21) and (2.35) with examples to validate the theoretical statements like accuracy and efficiency. We applied the shooting technique based on the secant iterative method to solve the discrete schemes (2.21) and (2.35), particularly in all the examples.

For the numerical experiments, we have taken $\varepsilon = 10^{-6}$ and

$$\phi(\eta_i) = u_{M+1}^{M,i} + \beta_1 \frac{u_{M-1}^{M,i} - 4u_M^{M,i} + 3u_{M+1}^{M,i}}{2h} - \gamma_1,$$

where $u_m^{M,i}$ be the numerical solution of (2.21) and (2.35) at x_m for each η_i, and iteratively compute η_i until $|\eta_i - \eta_{i-1}| < \varepsilon$..

Remark 2.6 *The order of convergence of the numerical solution to the BVPs (2.1) and (2.32) will depend on the shooting method that transformed them into the IVPs and the numerical discretization of the IVPs. As the shooting method is based on the secant method with an order of convergence of 1.618 and approximation of $u'(\ell)$ in the definition of ϕ using a backward difference formula with three points (second order of convergence), the order of convergence for the shooting method will be 1.618. In Theorem 2.4 and Lemma 2.6, we discussed the error estimate for the numerical solution to the IVP and observed that the numerical solution has first-order convergence. Therefore, the numerical solution to the BVPs has a first-order of convergence.*

Example 2.7 *[38] Take into account the subsequent two-point BVP:*

$$\begin{cases} -{}^{RLC}\mathcal{D}_x^{\alpha} u(x) - 0.5u' = 1, \quad x \in (0,1), \\ {}^{C}\mathcal{D}_x^{\alpha-1} u(0) = 0, \quad u(1) = 0. \end{cases} \tag{2.38}$$

The exact solution of this problem is $u(x) = -x^{\alpha} E_{\alpha-1,\alpha+1}(-0.5x^{\alpha-1}) + u(0)$.

Table 2.1: *Maximum errors E_M and order of convergence R_M for Example 2.7.*

	Method / R_M	$M = 64$	$M = 128$	$M = 256$	$M = 512$	$M = 1024$	$M = 2048$
$\alpha = 1.2$	Shooting	1.340e-03	7.086e-04	3.712e-04	1.930e-04	9.972e-05	5.126e-05
	R_M	0.9187	0.9326	0.9437	0.9527	0.9600	
	FDM [38]	9.207e-03	4.605e-03	2.303e-03	1.152e-03	5.759e-04	2.880e-04
	R_M	0.9994	0.9997	0.9998	0.9999	0.9999	
$\alpha = 1.4$	Shooting	1.814e-03	9.311e-04	4.748e-04	2.409e-04	1.218e-04	6.141e-05
	R_M	0.9619	0.9716	0.9788	0.9841	0.9880	
	FDM [38]	9.681e-03	4.852e-03	2.430e-03	1.216e-03	6.085e-04	3.044e-04
	R_M	0.9966	0.9977	0.9985	0.9990	0.9993	
$\alpha = 1.6$	Shooting	1.882e-03	9.514e-04	4.793e-04	2.408e-04	1.208e-04	6.053e-05
	R_M	0.9839	0.9893	0.9929	0.9953	0.9969	
	FDM [38]	9.902e-03	4.994e-03	2.513e-03	1.263e-03	6.338e-04	3.178e-04
	R_M	0.9875	0.9906	0.9929	0.9946	0.9959	
$\alpha = 1.8$	Shooting	1.715e-03	8.607e-04	4.313e-04	2.159e-04	1.081e-04	5.405e-05
	R_M	0.9948	0.9969	0.9981	0.9989	0.9993	
	FDM [38]	9.236e-03	4.711e-03	2.396e-03	1.216e-03	6.156e-04	3.111e-04
	R_M	0.9711	0.9754	0.9789	0.9819	0.9844	

The maximum error and the order of convergence are respectively determined by

$$E_M := \|u^M - u\|_{\overline{\Omega}_M} = \max_{1 \le m \le M+1} |u_m^M - u(x_m)|, \quad R_M := \log_2 \left(\frac{E_M}{E_{2M}} \right).$$

The exact solution and the computed solution of Example 2.7 for $M = 256$ and $\alpha = 1.3, 1.6$ are shown in Figure 2.1. In Figure 2.2 we justified that our scheme has better accuracy than the FDM used in Gracia et al. [38] for $M = 256$. The numerical results for Example 2.7 by using the proposed method and FDM in Gracia et al. [38], are shown in Table 2.1 which indicates that the shooting method is more efficient than FDM for all values of α, and where we find out that our scheme is of first-order convergence which also shown in Figure 2.3 for $\alpha = 1.9$ by using the log-log plot. In Table 2.1, for each α and M, the number of iterations required by the shooting method is 4.

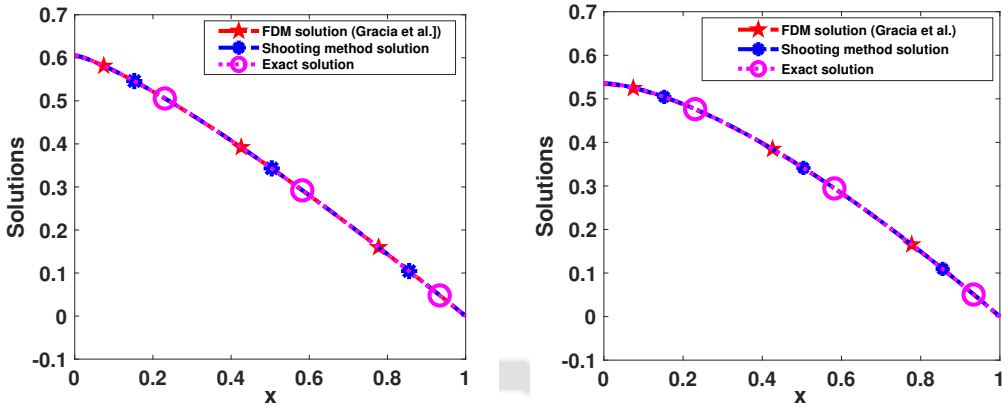

(a) $\alpha = 1.3$. *(b)* $\alpha = 1.6$.

Figure 2.1: *Exact and computed solutions for Example 2.7.*

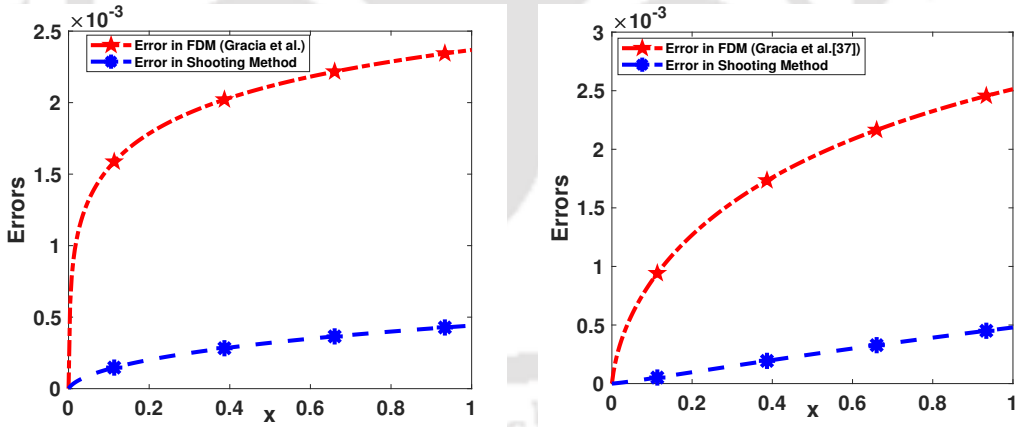

(a) $\alpha = 1.3$. *(b)* $\alpha = 1.6$.

Figure 2.2: *Comparison of errors for Example 2.7.*

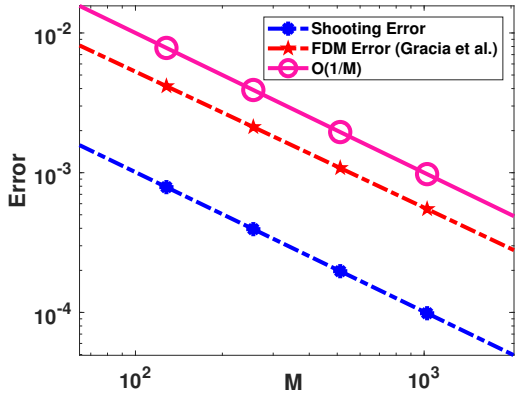

Figure 2.3: *Log-log plot of M vs. maximum errors for Example 2.7 with $\alpha = 1.9$.*

Example 2.8 *Consider the following problem:*

$$\begin{cases} -{}^{RLC}\mathcal{D}_x^{\alpha} u(x) - (1+x^2)u' + xu = -e^x, \quad x \in (0,1), \\ {}^{C}\mathcal{D}_x^{\alpha-1} u(0) = 0, \quad u(1) + u'(1) = 1. \end{cases} \tag{2.39}$$

We utilize the two-mesh approach to calculate the maximum two-mesh differences and order of convergence because the exact solution to the problem (2.39) is unknown. Let $\{u_m^M\}_{m=1}^{M+1}$ and $\{v_m^{2M}\}_{m=1}^{2M+1}$ be computed solutions of the problem (2.39) with the scheme (2.21) on the uniform meshes $\{x_m\}_{m=1}^{M+1}$ and $\{y_m\}_{m=1}^{2M+1}$ respectively. The maximum two-mesh differences $\mathcal{D}_M$ and the order of convergence R_M are respectively calculated by

$$\mathcal{D}_M := \max_{1 \le m \le M+1} |u_m^M - v_{2m-1}^{2M}| \quad \text{and} \quad R_M := \log_2 \left(\frac{\mathcal{D}_M}{\mathcal{D}_{2M}} \right).$$

The computed solutions of Example 2.8 for $M = 256$ and $\alpha = 1.3, 1.6$ by using the FDM Gracia et al. [38] and the shooting method are shown in Figure 2.4. Also, Figure 2.5 shows the error comparison between the above two methods for $M = 256$, which again reveals the performance of the present method. Table 2.2 contains the numerical results for Example 2.8, from where we can observe the almost first-order convergence. In Figure 2.6, we have shown the first-order convergence of the scheme for $\alpha = 1.1$ by using the log-log plot. As like in the previous example, 4 iterations are required for the shooting technique for each α and M to obtain the values in Table 2.2.

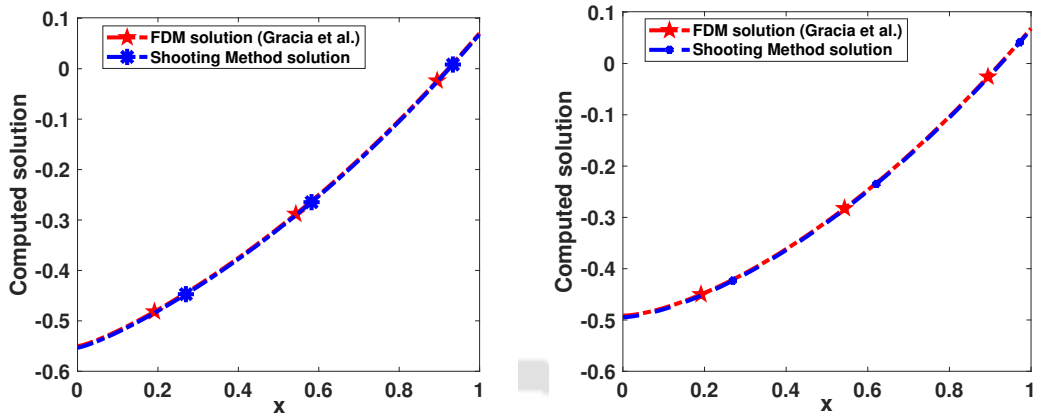

(a) $\alpha = 1.3$. *(b)* $\alpha = 1.6$.

Figure 2.4: *The computed solutions for Example 2.8 with* $M = 256$.

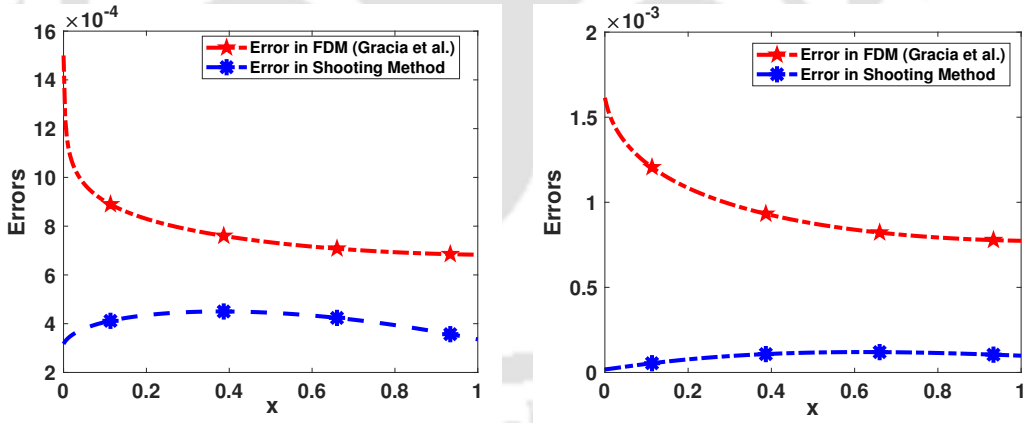

(a) $\alpha = 1.3$. *(b)* $\alpha = 1.6$.

Figure 2.5: *Comparison of errors for Example 2.8 with* $M = 256$.

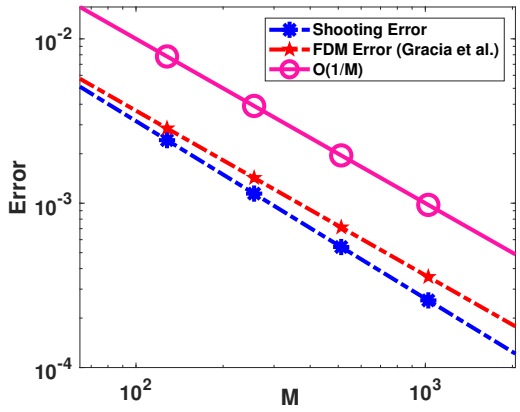

Figure 2.6: *Log-log plot of M vs. maximum errors for Example 2.8 with $\alpha = 1.1$.*

Table 2.2: *$\mathcal{D}_M$ and R_M for Example 2.8.*

Order	Method / R_M	M=64	M=128	M=256	M=512	M=1024	M=2048
α=1.2	Shooting	3.517e-03	1.582e-03	7.135e-04	3.229e-04	1.467e-04	6.688e-05
	R_M	1.1526	1.1486	1.1439	1.1386	1.1328	
	FDM [38]	5.859e-03	2.925e-03	1.462e-03	7.306e-04	3.653e-04	1.826e-04
	R_M	1.0022	1.0009	1.0004	1.0001	1.0000	
α=1.4	Shooting	1.622e-03	6.778e-04	2.883e-04	1.249e-04	5.511e-05	2.478e-05
	R_M	1.2584	1.2336	1.2071	1.1799	1.1532	
	FDM [38]	6.146e-03	3.076e-03	1.540e-03	7.707e-04	3.856e-04	1.929e-04
	R_M	0.9986	0.9983	0.9985	0.9988	0.9991	
α=1.6	Shooting	7.053e-04	2.844e-04	1.198e-04	5.248e-05	2.380e-05	1.110e-05
	R_M	1.3101	1.2480	1.1903	1.1408	1.1010	
	FDM [38]	6.381e-03	3.210e-03	1.614e-03	8.110e-04	4.071e-04	2.041e-04
	R_M	0.9910	0.9918	0.9932	0.9945	0.9957	
α=1.8	Shooting	2.326e-04	8.807e-05	3.607e-05	2.082e-05	1.123e-05	5.849e-06
	R_M	1.4012	1.2879	0.7928	0.8908	0.94086	
	FDM [38]	6.366e-03	3.223e-03	1.632e-03	8.255e-04	4.170e-04	2.104e-04
	R_M	0.9819	0.9820	0.9833	0.9851	0.9868	

Example 2.9 *Consider the following semi-linear problem with* $1 < \alpha < 2$ *:*

$$\begin{cases} -{}^{RLC}\mathcal{D}_x^{\alpha} u(x) + u'(x) - \sin(u(x)) = 0, \quad x \in \Omega = (0,1), \\ {}^{C}\mathcal{D}_x^{\alpha-1} u(0) = 0, \quad u(1) + u'(1) = 1. \end{cases} \tag{2.40}$$

First, we solve the semi-linear problem (2.40) by using the shooting method with the scheme (2.35). Here, the nonlinear system of equations (2.35) is solved by using the Newton's method with $uold_m^M$ $(m = 1, \cdots, M+1)$ as an initial guess and the shooting method, then we iteratively compute $unew^M$ using the Newton's method until

$$\max_{1 \le m \le M+1} |unew_m^M - uold_m^M| \le \text{Tol},$$

where Tol denotes the tolerance bound. For the numerical computations, we have taken $\text{Tol} = 1.0e-07$ and $uold_m^M = 0.5\,(m = 1, \cdots, M+1)$.

Additionally, we employ the Newton linearization method to solve (2.40) using the FDM outlined in Gracia et al. [38]. This allows us to derive the sequence $\{u^{(q)}\}_{q \ge 1}$ for the initial guess $u^{(0)}$ fulfilling the boundary conditions of the problem. Here, we define $u^{(q+1)}$, $q \ge 0$ to be the solution of the following linear BVP:

$$\begin{cases} -{}^{RLC}\mathcal{D}_x^{\alpha} u^{(q+1)}(x) + (u^{(q+1)})'(x) - cos(u^{(q)}(x)) u^{(q+1)}(x) \\ \qquad = \sin(u^{(q)}(x)) - u^{(q)}(x)\cos(u^{(q)}(x)), \quad x \in \Omega = (0,1), \\ {}^{C}\mathcal{D}_x^{\alpha-1} u^{(q+1)}(0) = 0, \quad u^{(q+1)}(1) + (u^{(q+1)})'(1) = 1. \end{cases} \tag{2.41}$$

Hence for a fixed q, we solve (2.41) using the numerical scheme given in Gracia et al. [38] and then, the convergence criterion listed below is employed for the Newton linearization process:

$$\max_{x_m \in \overline{\Omega}_M} |u^{(q+1)}(x_m) - u^{(q)}(x_m)| \le \text{Tol}, \quad q \ge 0.$$

For the numerical computations, we have taken $\text{Tol} = 1.0e-07$ and $u_m^{(0)} = 0.5\,(m = 1, 2, \cdots, M+1)$.

Since the exact solution is unknown, we use the two-mesh principle to find the maximum errors and order of convergence for both methods. The numerical results for Example 2.9 are given in Table 2.3. The computed solutions and comparison of errors

for Example 2.9 with $M = 512$, $\alpha = 1.8$ are shown in Figure 2.7, which again reveal the performance of the present method. In Figure 2.8 we have shown the first-order of convergence of the scheme for $\alpha = 1.6$ through the log-log plot.

Table 2.3: $\mathcal{D}_M$ and R_M for Example 2.9

Order	Method / R_M	$M = 64$	$M = 128$	$M = 256$	$M = 512$	No of iterations
α=1.4	Shooting	2.653e-03	1.420e-03	7.464e-04	3.872e-04	6
	R_M	0.9014	0.9280	0.9468		(shooting)
	FDM [38]	9.261e-03	4.680e-03	2.357e-03	1.184e-03	5
	R_M	0.9848	0.9895	0.9932		(Newton)
α=1.6	Shooting	2.893e-03	1.496e-03	7.651e-04	3.882e-04	7
	R_M	0.9508	0.9679	0.9789		(shooting)
	FDM [38]	1.171e-02	5.820e-03	2.917e-03	1.466e-03	5
	R_M	1.0083	0.9964	0.9924		(Newton)
α=1.8	Shooting	5.217e-03	2.661e-03	1.346e-03	6.769e-04	7
	R_M	0.9709	0.9840	0.9912		(shooting)
	FDM [38]	2.070e-02	1.021e-02	5.134e-03	2.600e-03	6
	R_M	1.0192	0.9920	0.9814		(Newton)

2.6 Conclusion

In this chapter, we proposed an efficient numerical technique for solving linear and semi-linear fractional differential equations of RLC type. First, the given BVP is converted into an IVP by using the shooting technique based on the secant method. Then the numerical solution of the resultant IVP is obtained by finding the numerical solution of an equivalent Volterra integral equation. Stability of the proposed scheme is studied and error analysis is carried out. The numerical outcomes show that the current method is more effective and accurate than the prior result Gracia et al. [38].

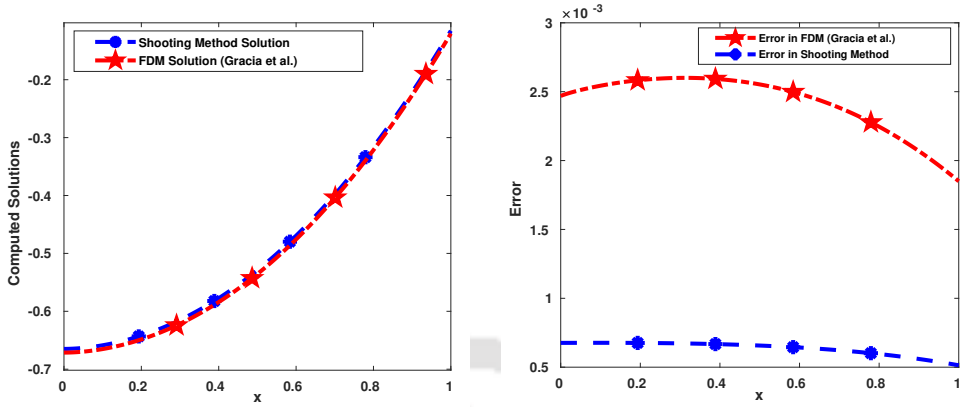

(a) Computed solutions. *(b) Comparison of Errors.*

Figure 2.7: *Computed solutions and comparison of errors for Example 2.9 with* $M = 512, \alpha = 1.8$.

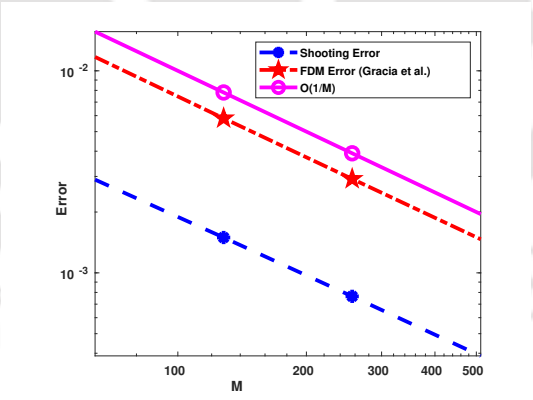

Figure 2.8: *Log-log plot of* M *vs. maximum errors for Example 2.9 with* $\alpha = 1.6$.

CHAPTER 3

Cubic spline approximation method for linear and semi-linear time-fractional convection-diffusion-reaction equation

In this chapter, we focus on the analytical and numerical solutions of a class of non-autonomous time-fractional diffusion problems. The Sumudu decomposition method and maximum-minimum principle are used for the study of the existence and uniqueness of the analytical solutions, whereas the cubic spline approach with L1-discretization is used for the numerical solution of the problem.

3.1 Introduction

In this chapter, we consider the following non-autonomous TF-ADR IBVP with time fractional derivative of Caputo-type:

$$\begin{cases} {}^{C}\mathcal{D}_t^{\alpha} u(x,t) + \mathcal{L}(u(x,t)) = f(x,t), \quad (x,t) \in Q, \\ u(x,0) = g(x), \quad \forall x \in \overline{\Omega}, \\ u(0,t) = \psi_1(t), \quad u(\ell,t) = \psi_2(t), \quad \forall t \in \overline{G}, \end{cases} \tag{3.1}$$

where $Q := \Omega \times G$, $\Omega = (0,\ell)$, $G = (0,T]$, $0 < \alpha < 1$, and

$$\mathcal{L}(u(x,t)) = p(t)\left[-\frac{\partial}{\partial x}\left(a(x)\frac{\partial u}{\partial x}\right) + b(x)u\right](x,t)$$

with

$$\begin{cases} a \in \mathcal{C}^1(\overline{\Omega}), \quad b \in \mathcal{C}(\overline{\Omega}), \quad a(x) > 0, \quad b(x) \geq 0, \quad \forall x \in \overline{\Omega}, \\ p \in \mathcal{C}(\overline{G}), \quad p(t) > 0, \quad \forall t \in G. \end{cases} \tag{3.2}$$

Further, we assume that the compatibility conditions $g(0) = \psi_1(0)$ and $g(\ell) = \psi_2(0)$ hold.

We establish the existence and uniqueness of the solution of the IBVP (3.1) by using the Sumudu decomposition method and the maximum-minimum principle. Further, we semi-discretize the IBVP (3.1) with respect to the time variable by using the L1-discretization for the time-fractional Caputo derivative term and discuss the stability and convergence of the semi-discretized scheme. Next, we use the cubic spline approximation to discretize the spatial derivatives of the semi-discrete problem and finally, we obtain the fully discrete scheme for the IBVP (3.1). The proposed method is of $O\big(N^{-(2-\alpha)}+M^{-2}\big)$. By applying the Newton's linearization technique, we obtain a sequence of linearized IBVPs from semi-linear IBVP and then we use the proposed method for the numerical solution of the semi-linear IBVP. Numerical experiments support the theoretical results.

We organize the rest of the chapter as follows: We establish the existence and uniqueness of the solution of IBVP (3.1) in Section 3.2. Section 3.3 deals with the discretization of the problem and convergence analysis of the discretized scheme. In Section 3.4, we extend the results of linear problems to semilinear problems by using the Newton's linearization approach. Finally, numerical experiments are presented in Section 3.5.

3.2 Continuous problem

The existence and uniqueness of the analytical solution of the IBVP (3.1) is discussed in this section.

3.2.1 Existence of the solution

In this subsection, we investigate the solution of the IBVP (3.1) analytically in the form of a series, obtained by using the Sumudu decomposition method.

By taking the Sumudu transform on both sides of the IBVP (3.1) with respect to the time variable, and using the initial condition and Lemma 1.2, we have

$$\mu^{-\alpha}\big(\mathbb{S}_t[u(x,t)] - g(x)\big) + \mathbb{S}_t[\mathcal{L}(u(x,t))] = \mathbb{S}_t[f(x,t)]. \tag{3.3}$$

By simplifying and using the linearity property of $\mathbb{S}_t$, we get

$$\begin{aligned}\mathbb{S}_t[u(x,t)] &= g(x) + \mu^\alpha \left(\mathbb{S}_t[f(x,t)] - \mathbb{S}_t[\mathcal{L}(u(x,t))]\right) \\ &= g(x) + \mu^\alpha \, \mathbb{S}_t \left[f(x,t) - \mathcal{L}(u(x,t))\right]. \end{aligned} \tag{3.4}$$

The Adomian decomposition method [1] consists of looking for the solution of the IBVP (3.1) in the series form:

$$u(x,t) = \sum_{j=0}^{\infty} u_j(x,t), \tag{3.5}$$

provided the infinite series of functions converges uniformly.

Substituting (3.5) in (3.4), and using the linearity of $\mathcal{L}$ and uniform convergence of the infinite series, we obtain

$$\begin{aligned}\mathbb{S}_t\left[\sum_{j=0}^{\infty} u_j(x,t)\right] &= g(x) + \mu^\alpha \, \mathbb{S}_t \left[f(x,t) - \mathcal{L}\left(\sum_{j=0}^{\infty} u_j(x,t)\right)\right] \\ &= g(x) + \mu^\alpha \, \mathbb{S}_t \left[f(x,t) - \sum_{j=0}^{\infty} \mathcal{L}\left(u_j(x,t)\right)\right]. \end{aligned} \tag{3.6}$$

Operating with the Sumudu inverse transform on both sides of (3.6) and using the properties of $\mathbb{S}_t$ and Lemma 1.1, we get

$$\begin{aligned}\sum_{j=0}^{\infty} u_j(x,t) &= \mathbb{S}_t^{-1}\left(g(x)\right) + \mathbb{S}_t^{-1}\left(\mu^\alpha \, \mathbb{S}_t \left[f(x,t) - \sum_{j=0}^{\infty} \mathcal{L}\left(u_j(x,t)\right)\right]\right) \\ &= g(x) + I_t^\alpha \left(f(x,t) - \sum_{j=0}^{\infty} \mathcal{L}\left(u_j(x,t)\right)\right) \\ &= g(x) + I_t^\alpha \left(f(x,t)\right) - \sum_{j=0}^{\infty} I_t^\alpha \mathcal{L}\left(u_j(x,t)\right). \end{aligned} \tag{3.7}$$

In order to obtain u_j, we define the following recurrence equations by Adomian relation :

$$\begin{aligned} u_0(x,t) &= g(x) + I_t^\alpha f(x,t), \\ u_{j+1}(x,t) &= -I_t^\alpha \mathcal{L}\left(u_j(x,t)\right) \end{aligned} \tag{3.8}$$

$$= \quad (-I_t^\alpha \mathcal{L})^{j+1} g(x) + \left(I_t^\alpha (-I_t^\alpha \mathcal{L})^{j+1}\right) f(x,t), \ j \geq 0. \tag{3.9}$$

Finally, the solution $U_J(x,t)$ can be approximated by the truncated series

$$U_J(x,t) = \sum_{j=0}^{J} u_j(x,t), \quad J \in \mathbb{N}, \tag{3.10}$$

and we define the solution of the IBVP (3.1) as

$$\begin{aligned} u(x,t) &= \lim_{J\to\infty} U_J(x,t) = \sum_{j=0}^{\infty} u_j(x,t) \\ &= g(x) + I_t^\alpha f(x,t) + \sum_{j=1}^{\infty} (-I_t^\alpha \mathcal{L})^j g(x) + \sum_{j=1}^{\infty} \left(I_t^\alpha (-I_t^\alpha \mathcal{L})^j\right) f(x,t). \end{aligned} \tag{3.11}$$

The convergence of the Adomian series obtained by the Adomian decomposition method was investigated by several authors, for example, one can see [22, 44], and they obtained some results about the speed of convergence of this method.

Assume that for sufficiently smooth functions f and g, the solution $u(x,t)$ defined in (3.11) is the classical solution of the IBVP (3.1), *i.e.*, $u \in \mathcal{C}(\overline{Q}) \cap W_t^1((0,T)) \cap \mathcal{C}_x^2(\Omega)$, and satisfies the following bounds for all $(x,t) \in \overline{\Omega} \times G$:

$$\begin{cases} \left|\dfrac{\partial^i u}{\partial x^i}(x,t)\right| \leq C, & \text{for } i = 0,1,2,3,4, \\ \left|\dfrac{\partial^i u}{\partial t^i}(x,t)\right| \leq C(1+t^{\alpha-i}), & \text{for } i = 0,1,2. \end{cases} \tag{3.12}$$

Now, we apply the technique mentioned above to obtain the analytical solution of the following example.

Example 3.1 *Consider the following IBVP:*

$$\begin{cases} {}^C\mathcal{D}_t^\alpha u(x,t) - t\dfrac{\partial^2 u}{\partial x^2}(x,t) = xt^2, \quad (x,t) \in Q := (0,\pi) \times (0,1], \\ u(x,0) = \sin x, \quad x \in [0,\pi], \\ u(0,t) = 0, \quad u(\pi,t) = \dfrac{2\pi t^{\alpha+2}}{\Gamma(\alpha+3)}, \quad t \in [0,1]. \end{cases} \tag{3.13}$$

Solution.

By taking the Sumudu transform on both sides of the problem (3.13), and using the properties of the Sumudu transform along with the initial condition, we get

$$\mathbb{S}_t[u(x,t)] = \sin x + s^\alpha \left(\mathbb{S}_t[xt^2] + \mathbb{S}_t \left[t \frac{\partial^2 u}{\partial x^2}(x,t) \right] \right). \tag{3.14}$$

Using the Adomian decomposition technique given in (3.5)-(3.9), we arrive at the following recurrence relation:

$$u_0(x,t) = \sin x + \frac{2xt^{\alpha+2}}{\Gamma(\alpha+3)}, \tag{3.15}$$

$$u_{j+1}(x,t) = I_t^\alpha \left(t \frac{\partial^2 u_j}{\partial x^2}(x,t) \right), \quad j \geq 0. \tag{3.16}$$

By simplifying (3.16), we obtain that

$$u_j(x,t) = D_j \frac{(-t^{\alpha+1})^j \sin x}{\Gamma(j(\alpha+1)+1)}, \quad j \geq 1, \tag{3.17}$$

where $D_1 = 1$, $D_j = \prod_{i=2}^{j} \big((i-1)(\alpha+1) + \lfloor i/2 \rfloor\big)$, $(j \geq 2)$, with $\lfloor i \rfloor$ denotes the function which takes the greatest integer value $\leq i$. We can observe that $\sum_{j=0}^{\infty} u_j(x,t)$ is a power series in t-variable, for each $x \in \Omega$.

Now for all $(x,t) \in Q$ and for $j \geq 1$, we have

$$\lim_{j\to\infty} \left| \frac{u_{j+1}(x,t)}{u_j(x,t)} \right| = |t|^{\alpha+1} \lim_{j\to\infty} \frac{D_{j+1}}{D_j} \cdot \frac{\Gamma(j(\alpha+1)+1)}{\Gamma(j(\alpha+1)+\alpha+2)} = 0.$$

Therefore, the domain of convergence of the power series $\sum_{j=0}^{\infty} u_j(x,t)$ contains Q, and the series converges uniformly on Q.

Hence the solution of the problem (3.13) is given by

$$u(x,t) = \sum_{j=0}^{\infty} u_j(x,t), \tag{3.18}$$

where u_j's are given in (3.15) and (3.17).

3.2.2 Uniqueness of the solution

The uniqueness of the solution of the IBVP (3.1) will be proved by using the maximum-minimum principle. The maximum principle for the IBVP (3.1) which is stated in the following theorem, can be proved in the same way as discussed in [74, Theorem 2].

Theorem 3.2 *Let $u \in \mathcal{C}(\overline{Q}) \cap W_t^1((0,T)) \cap \mathcal{C}_x^2(\Omega)$ be a solution of the IBVP (3.1) in the domain Q and $f(x,t) \leq 0$, $(x,t) \in Q$. Then we have the following:*

$$u(x,t) \leq \max\{0, \max_{(x,t)\in S} u(x,t)\}, \quad \forall\, (x,t) \in \overline{Q}, \tag{3.19}$$

where $S := \big(\overline{\Omega} \times \{0\}\big) \cup \big(\{0,\ell\} \times \overline{G}\big)$.

Replacing u by $-u$ and assuming $f \geq 0$ in Theorem 3.2, the minimum principle can be obtained, which is stated below.

Theorem 3.3 *Let $u \in \mathcal{C}(\overline{Q}) \cap W_t^1((0,T)) \cap \mathcal{C}_x^2(\Omega)$ be the solution of the IBVP (3.1) in the domain Q and $f(x,t) \geq 0$, $(x,t) \in Q$. Then we have the following:*

$$u(x,t) \geq \min_{(x,t)\in S} u(x,t), \quad \forall\, (x,t) \in \overline{Q}, \tag{3.20}$$

where $S := \big(\overline{\Omega} \times \{0\}\big) \cup \big(\{0,\ell\} \times \overline{G}\big)$.

The maximum-minimum principle is used to demonstrate the well-known stability result, which is given in the following theorem, if the IBVP (3.1) has a solution, then the solution continually relies on the data provided in the problem.

Theorem 3.4 *Let u be a classical solution of the IBVP (3.1), i.e., $u \in \mathcal{C}(\overline{Q}) \cap W_t^1((0,T)) \cap \mathcal{C}_x^2(\Omega)$, and $f \in \mathcal{C}(\overline{Q})$, then it satisfies the following bound:*

$$\|u\|_Q \leq \max\{\|g\|_\Omega, \|\psi_1\|_G, \|\psi_2\|_G\} + \frac{T^\alpha}{\Gamma(1+\alpha)}\|f\|_Q. \tag{3.21}$$

Proof. Let us consider the function v defined by

$$v(x,t) := u(x,t) - \frac{\|f\|_Q}{\Gamma(1+\alpha)}t^\alpha, \quad (x,t) \in \overline{Q}.$$

Then the function v is the classical solution of the IBVP (3.1) with the functions

$$\widehat{f}(x,t) := f(x,t) - \|f\|_Q - \frac{\|f\|_Q\ p(t)}{\Gamma(1+\alpha)}b(x)t^\alpha, \quad \widehat{\psi}_i(x,t) := \psi_i(x,t) - \frac{\|f\|_Q}{\Gamma(1+\alpha)}t^\alpha$$

instead of f and ψ_i $(i = 1, 2)$, respectively. The function $\widehat{f}$ satisfies the condition $\widehat{f}(x,t) \leq 0$, $(x,t) \in \overline{Q}$. Then applying the maximum principle given in Theorem 3.2 to the classical solution v, we obtain that

$$v(x,t) \leq \max\left\{\|g\|_\Omega, \|\widehat{\psi}_1\|_G, \|\widehat{\psi}_2\|_G\right\}, \quad (x,t) \in \overline{Q}.$$

Since $\dfrac{\|f\|_Q}{\Gamma(1+\alpha)}t^\alpha \geq 0$, we have $\|\widehat{\psi}_i\|_G \leq \|\psi_i\|_G$, $i = 1, 2$. Hence, we obtain the following bound:

$$v(x,t) \leq \max\left\{\|g\|_\Omega, \|\psi_1\|_G, \|\psi_2\|_G\right\}, \quad (x,t) \in \overline{Q}. \tag{3.22}$$

Therefore, from (3.22), for all $(x,t) \in \overline{Q}$, we have the following estimate:

$$u(x,t) = v(x,t) + \frac{\|f\|_Q}{\Gamma(1+\alpha)}t^\alpha \leq \max\{\|g\|_\Omega, \|\psi_1\|_G, \|\psi_2\|_G\} + \frac{\|f\|_Q}{\Gamma(1+\alpha)}T^\alpha. \tag{3.23}$$

By applying Theorem 3.3 to the function

$$v(x,t) := u(x,t) + \frac{\|f\|_Q}{\Gamma(1+\alpha)}t^\alpha, \quad (x,t) \in \overline{Q},$$

we obtain the following

$$u(x,t) \geq -\max\{\|g\|_\Omega, \|\psi_1\|_G, \|\psi_2\|_G\} - \frac{\|f\|_Q}{\Gamma(1+\alpha)}T^\alpha, \quad (x,t) \in \overline{Q}. \tag{3.24}$$

Combining (3.23) and (3.24), we get the required result. □

In the next theorem, we will establish the uniqueness of the solution to the IBVP (3.1).

Theorem 3.5 *The IBVP (3.1) has a unique classical solution, provided f, g are sufficiently smooth.*

Proof. In Subsection 3.2.1, by using the Sumudu decomposition method, we have shown the existence of the classical solution to the IBVP (3.1), when f, g are sufficiently smooth.

Now, we prove the uniqueness of the solution, for that assume v_1 and v_2 are two solutions of the IBVP (3.1). Then $v_1 - v_2$ is the solution of the IBVP (3.1) with $f = 0$, $g = 0$, $\psi_1 = \psi_2 = 0$. Therefore, from Theorem 3.4, we have $\|v_1 - v_2\|_Q = 0$. Hence, $v_1 = v_2$, which proves the uniqueness of the solution. □

3.3 Discrete problem and convergence analysis

In this section, we discretize the IBVP (3.1) to find the numerical approximate solution and investigate the convergence analysis of the corresponding discretized scheme.

3.3.1 The temporal semi-discretization

Consider the temporal graded mesh $\overline{G}^N = \{t_n : 1 \le n \le N+1\}$ with $t_n = T\left(\frac{n-1}{N}\right)^r$, for $n = 1, 2, \cdots, N+1$, where the constant $r \ge 1$ in the mesh grading is chosen by the user and N is a fixed positive integer. The mesh will be uniform when $r = 1$. Let $\tau_n = t_{n+1} - t_n$, for $n = 1, 2, \cdots, N$. To obtain the numerical approximate solution of the IBVP (3.1), first, we discretize the temporal derivative by using the classical L1-scheme. Let $\widehat{u}^n(x)$ denotes the approximation of the exact solution $u(x,t)$ at the time level $t_n \in \overline{G}^N$.

Now, using L1-discretization (1.10) of the Caputo fractional derivative in (3.1) the temporal semi-discretization of the IBVP (3.1) over $\Omega \times \overline{G}^N$ is given by

$$\begin{cases} (\widehat{d}_{n,n-1} I + \mathcal{L}^N)\widehat{u}^n(x) = \displaystyle\sum_{j=2}^{n-1} [\widehat{d}_{n,j} - \widehat{d}_{n,j-1}]\, \widehat{u}^j(x) + \widehat{d}_{n,1} g(x) + f^n(x), \\ \widehat{u}^n(0) = \psi_1^n, \quad \widehat{u}^n(\ell) = \psi_2^n, \quad \text{for } n = 2, 3, \cdots, N+1, \end{cases} \tag{3.25}$$

where I is the identity operator and

$$\mathcal{L}^N\left(\widehat{u}^n(x)\right) = p(t_n)\left[-\frac{\partial}{\partial x}\left(a(x)\frac{\partial \widehat{u}^n}{\partial x}\right) + b(x)\widehat{u}^n\right].$$

Let $\mathcal{R}_N^n(x)$ denotes the truncation error due to the temporal semi-discretization, which is given by:

$$\mathcal{R}_N^n(x) := \left({}_{L1}^{C}\mathcal{D}_N^\alpha - {}^{C}\mathcal{D}_t^\alpha\right) u(x, t_n) = \sum_{j=1}^{n-1} \mathcal{E}_{n,j}, \tag{3.26}$$

$$\text{where} \quad \mathcal{E}_{n,j} = \frac{1}{\Gamma(1-\alpha)} \int_{s=t_j}^{t_{j+1}} (t_n - s)^{-\alpha} \left[\frac{u(x, t_{j+1}) - u(x, t_j)}{\tau_j} - \frac{\partial u}{\partial s}(x, s)\right] ds.$$

In the next lemma we will discuss the truncation error bound for the semi-discretized scheme (3.25).

Lemma 3.1 *Assume that the solution of the semi-discrete problem (3.25) satisfies the derivative bounds given in (3.12). Then for each* $(x, t_n) \in \Omega \times \overline{G}^N$, $n = 2, 3, \cdots, N+1$, *we have the following truncation error bound:*

$$\|\mathcal{R}_N^n\|_\Omega \leq C n^{-\min\{2-\alpha, r\alpha\}}.$$

Proof. The detailed proof is available in [106, Lemma 5.2]. □

The next lemma presents the stability bound for the semi-discrete problem (3.25).

Lemma 3.2 *The solution of the semi-discrete problem (3.25) satisfies the following:*

$$\begin{aligned}\|\widehat{u}^n\|_\Omega \;\leq\; & C\tau_{n-1}^\alpha \left(\|a\|_\Omega + \|a'\|_\Omega + \|f^n\|_\Omega\right) + \tau_{n-1}^\alpha \Gamma(2-\alpha)\widehat{d}_{n,1}\|g\|_\Omega \\ & + \tau_{n-1}^\alpha \Gamma(2-\alpha) \sum_{j=2}^{n-1} [\widehat{d}_{n,j} - \widehat{d}_{n,j-1}] \|\widehat{u}^j\|_\Omega. \end{aligned} \tag{3.27}$$

Proof. Using the mean-value theorem, we can see that $\widehat{d}_{n,j}$ defined in (1.10) satisfies the following:

$$\widehat{d}_{n,j} \geq \widehat{d}_{n,j-1}, \quad 2 \leq j \leq n-1, \quad 2 \leq n \leq N+1. \tag{3.28}$$

Using (3.12) and (3.28) in (3.25), we get

$$\begin{aligned}\left[\widehat{d}_{n,n-1} + p(t_n)b(x)\right] \|\widehat{u}^n\|_\Omega \;\leq\; & C\left(\|a\|_\Omega + \|a'\|_\Omega + \|f^n\|_\Omega\right) + \widehat{d}_{n,1}\|g\|_\Omega \\ & + \sum_{j=2}^{n-1} \left[\widehat{d}_{n,j} - \widehat{d}_{n,j-1}\right] \|\widehat{u}^j\|_\Omega. \end{aligned} \tag{3.29}$$

By using the assumption given in (3.2), we get

$$\widehat{d}_{n,n-1}\|\widehat{u}^n\|_\Omega \leq C\left(\|a\|_\Omega + \|a'\|_\Omega + \|f^n\|_\Omega\right) + \widehat{d}_{n,1}\|g\|_\Omega + \sum_{j=2}^{n-1} \left[\widehat{d}_{n,j} - \widehat{d}_{n,j-1}\right] \|\widehat{u}^j\|_\Omega. \tag{3.30}$$

Hence by simplifying (3.30), we get our desired result. □

The real numbers $\vartheta_{n,j}$ for $n = 2, 3, \cdots, N+1$ and $j = 2, 3, \cdots, n-1$ can be defined by

$$\vartheta_{n,n} = 1, \quad \vartheta_{n,j} = \sum_{i=1}^{n-j} \tau_{n-i-1}^\alpha \vartheta_{n-i,j} \left[\widehat{d}_{n,n-i} - \widehat{d}_{n,n-i-1}\right]. \tag{3.31}$$

The next lemma provides a weighted bound for $\|\widehat{u}^n\|_\Omega$ in terms of the given data $\|g\|_\Omega, \|a\|_\Omega, \|a'\|_\Omega$ and $\|f^j\|_\Omega$ for $j = 2, 3, \cdots, n$.

Lemma 3.3 *The solution of the semi-discrete problem (3.25) satisfies the following bound:*

$$\|\widehat{u}^n\|_\Omega \leq \|g\|_\Omega + C\tau_{n-1}^\alpha \sum_{j=2}^{n} \vartheta_{n,j} \left(\|a\|_\Omega + \|a'\|_\Omega + \|f^j\|_\Omega\right), \quad 2 \leq n \leq N+1. \tag{3.32}$$

Proof. We will complete this proof by using induction on n. For $n = 2$, (3.32) becomes

$$\|\widehat{u}^2\|_\Omega \leq \tau_1^\alpha \Gamma(2-\alpha)\widehat{d}_{2,1}\|g\|_\Omega + C\tau_1^\alpha \vartheta_{2,2}(\|a\|_\Omega + \|a'\|_\Omega + \|f^2\|_\Omega),$$

which is identical to (3.27).

Now we assume that (3.32) is valid for $i = 2, 3, \cdots, (n-1)$ with some fixed $n \in \{3, \cdots, N+1\}$. Then from (3.27) and induction hypothesis, we can show that

$$\begin{aligned}
\|\widehat{u}^n\|_\Omega &\leq C\tau_{n-1}^\alpha(\|a\|_\Omega + \|a'\|_\Omega + \|f^n\|_\Omega) + \tau_{n-1}^\alpha\Gamma(2-\alpha)\widehat{d}_{n,1}\|g\|_\Omega \\
&\quad + \tau_{n-1}^\alpha\Gamma(2-\alpha)\sum_{j=2}^{n-1}[\widehat{d}_{n,j} - \widehat{d}_{n,j-1}] \left\{\|g\|_\Omega + C\tau_{j-1}^\alpha \sum_{i=2}^{j} \vartheta_{j,i}\left(\|a\|_\Omega + \|a'\|_\Omega + \|f^i\|_\Omega\right)\right\} \\
&= C\tau_{n-1}^\alpha(\|a\|_\Omega + \|a'\|_\Omega + \|f^n\|_\Omega) + \tau_{n-1}^\alpha\Gamma(2-\alpha)\widehat{d}_{n,n-1}\|g\|_\Omega \\
&\quad + C\tau_{n-1}^\alpha \sum_{j=2}^{n-1}\left(\|a\|_\Omega + \|a'\|_\Omega + \|f^j\|_\Omega\right)\sum_{i=1}^{n-j}\tau_{n-i-1}^\alpha\,\vartheta_{n-i,j}\,[\widehat{d}_{n,n-i} - \widehat{d}_{n,n-i-1}] \\
&= \|g\|_\Omega + C\tau_{n-1}^\alpha \sum_{j=2}^{n} \vartheta_{n,j}\left(\|a\|_\Omega + \|a'\|_\Omega + \|f^j\|_\Omega\right),
\end{aligned}$$

where we have used (3.31) to handle $\vartheta_{n-i,j}$. Thus by the principle of induction, (3.32) holds true for $2 \leq n \leq N+1$ and we have reached our goal. □

To estimate the convergence of the semi-discrete problem we will use the following bounds for a weighted sum of $\vartheta_{n,j}$.

Lemma 3.4 *For $n = 2, 3, \cdots, N+1$, we have the following bound for $\vartheta_{n,j}$:*

$$\tau_{n-1}^\alpha \sum_{j=2}^{n} j^{-\varrho}\vartheta_{n,j} \;\leq\; CT^\alpha N^{-\varrho}, \tag{3.33}$$

where ϱ is a parameter satisfying $\varrho \leq r\alpha$ and $C \geq \Gamma(1-\alpha)$.

Proof. One can prove the lemma by following the ideas given in [106, Lemma 4.3]. □

The following lemma provides the error bound for the semi-discretized scheme (3.25).

Lemma 3.5 *Let $E_N^n(x) = u(x,t_n) - \widehat{u}^n(x), (n = 1, 2, \cdots, N+1)$ denotes the error associated with the semi-discretized scheme (3.25), where $u(x,t_n)$ and $\widehat{u}^n(x)$ be the solutions of (3.1) and (3.25) respectively, at the point (x,t_n). Then, we have the following bound:*

$$\max_{n\leq N+1} \|u(\cdot,t_n) - \widehat{u}^n\|_\Omega \leq CN^{-\min\{2-\alpha, r\alpha\}}. \tag{3.34}$$

Proof. If we define the temporal semi-discretization in (3.25) by $\mathbf{L}^N\widehat{u}^n(x) = f^n(x)$, then we get a similar equation for $E_N^n(x)$ as

$$\mathbf{L}^N E_N^n(x) = \mathcal{R}_N^n(x),$$

(observe that for all x, $E_N^1(x) = 0$ and $a(x) = 0$ in the expression of $\mathbf{L}^N E_N^n(x)$). Hence, invoking Lemma 3.3, and Lemma 3.4 with $\varrho = \min\{2-\alpha, r\alpha\}$, we can obtain that

$$\begin{aligned} \|E_N^n\|_\Omega \leq C\tau_{n-1}^\alpha \sum_{j=2}^{n} \vartheta_{n,j} \|\mathcal{R}_N^j\|_\Omega &\leq C\tau_{n-1}^\alpha \sum_{j=2}^{n} \vartheta_{n,j}\, j^{-\min\{2-\alpha, r\alpha\}} \\ &\leq CN^{-\min\{2-\alpha, r\alpha\}}. \end{aligned}$$

By taking maximum over $n \leq N+1$ we get the required result. □

3.3.2 Fully discrete scheme

To find out the numerical solution of the semi-discrete problem (3.25), at each time step t_n, we will apply the cubic spline approximation on the uniform mesh $\overline{\Omega}_M$ to approximate (3.25). Finally, we obtain the fully discrete scheme.

Let $S^n(x)$ denotes the cubic spline approximation of the exact solution $\widehat{u}^n(x)$ of the semi-discrete problem (3.25) at the n-th time level which has the following form at each sub-interval $[x_m, x_{m+1}]$, $m = 1, 2, \cdots, M$:

$$S^n(x) = A_m^n + B_m^n(x - x_m) + C_m^n(x - x_m)^2 + D_m^n(x - x_m)^3, \tag{3.35}$$

where A_m^n, B_m^n, C_m^n, and D_m^n are constants to be determined.

Using the notation $\widehat{u}_m^n$ for approximation of $\widehat{u}^n(x)$ at mesh point x_m and $S^n(x_m) = \widehat{u}_m^n$, $S^n(x_{m+1}) = \widehat{u}_{m+1}^n$ as interpolation constraints. From simple algebraic calculation,

we can obtain that

$$\begin{cases} A_m^n = \widehat{u}_m^n, \quad B_m^n = \dfrac{\widehat{u}_{m+1}^n - \widehat{u}_m^n}{h} - \dfrac{h}{6}(2\mathcal{M}_m^n + \mathcal{M}_{m+1}^n), \\ C_m^n = \dfrac{\mathcal{M}_m^n}{2}, \quad D_m^n = \dfrac{1}{6h}(\mathcal{M}_{m+1}^n - \mathcal{M}_m^n), \end{cases} \tag{3.36}$$

where $\mathcal{M}_m^n = (S^n)''(x_m)$. Using the continuity of the first derivative at the mesh point x_m, we obtain the following equation:

$$\mathcal{M}_{m+1}^n + 4\mathcal{M}_m^n + \mathcal{M}_{m-1}^n = \frac{6}{h^2}\left(\widehat{u}_{m+1}^n - 2\widehat{u}_m^n + \widehat{u}_{m-1}^n\right). \tag{3.37}$$

From (3.25), we get that

$$p^n a_m \mathcal{M}_m^n = \left[\widehat{d}_{n,n-1} + p^n b_m\right]\widehat{u}_m^n - p^n a_m' \frac{d\widehat{u}^n}{dx}(x_m) - f_m^n - \widehat{d}_{n,1} g_m + \sum_{j=2}^{n-1}[\widehat{d}_{n,j-1} - \widehat{d}_{n,j}]\widehat{u}_m^j. \tag{3.38}$$

The first-order derivative of $\widehat{u}^n$ can be approximated at the points x_{m-1}, x_m and x_{m+1} by the following finite difference approximations:

$$\begin{cases} \dfrac{d\widehat{u}^n}{dx}(x_m) \approx \dfrac{\widehat{u}_{m+1}^n - \widehat{u}_{m-1}^n}{2h} + O(h^2), \\ \dfrac{d\widehat{u}^n}{dx}(x_{m+1}) \approx \dfrac{3\widehat{u}_{m+1}^n - 4\widehat{u}_m^n + \widehat{u}_{m-1}^n}{2h} + O(h^2), \\ \dfrac{d\widehat{u}^n}{dx}(x_{m-1}) \approx \dfrac{-\widehat{u}_{m+1}^n + 4\widehat{u}_m^n - 3\widehat{u}_{m-1}^n}{2h} + O(h^2). \end{cases} \tag{3.39}$$

Using (3.38) and (3.39) in (3.37) and from the boundary conditions given in (3.25), we get the following fully discrete scheme:

$$\begin{cases} \mathcal{L}_M^N \widehat{u}_m^n = \mathcal{G}_m^n, \quad 2 \le m \le M, \\ \widehat{u}_1^n = \psi_1^n, \quad \widehat{u}_{M+1}^n = \psi_2^n, \end{cases} \tag{3.40}$$

where

$$\begin{aligned} \mathcal{L}_M^N \widehat{u}_m^n \;=\; & \left\{\frac{1}{a_{m-1}}[\widehat{d}_{n,n-1} + p^n b_{m-1}] - \frac{6p^n}{h^2} - \frac{\sigma_{m+1}^n}{2h} + \frac{2\sigma_m^n}{h} + \frac{3\sigma_{m-1}^n}{2h}\right\}\widehat{u}_{m-1}^n \\ & + \left\{\frac{4}{a_m}[\widehat{d}_{n,n-1} + p^n b_m] + \frac{12p^n}{h^2} + \frac{2\sigma_{m+1}^n}{h} - \frac{2\sigma_{m-1}^n}{h}\right\}\widehat{u}_m^n \\ & + \left\{\frac{1}{a_{m+1}}[\widehat{d}_{n,n-1} + p^n b_{m+1}] - \frac{6p^n}{h^2} - \frac{3\sigma_{m+1}^n}{2h} - \frac{2\sigma_m^n}{h} + \frac{\sigma_{m-1}^n}{2h}\right\}\widehat{u}_{m+1}^n, \end{aligned} \tag{3.41}$$

$$\text{and} \quad \mathcal{G}_m^n = \left(\frac{f_{m+1}^n}{a_{m+1}} + 4\frac{f_m^n}{a_m} + \frac{f_{m-1}^n}{a_{m-1}}\right) + \left(\frac{g_{m+1}}{a_{m+1}} + 4\frac{g_m}{a_m} + \frac{g_{m-1}}{a_{m-1}}\right)\widehat{d}_{n,1} + \sum_{j=2}^{n-1}[\widehat{d}_{n,j} - \widehat{d}_{n,j-1}]\left(\frac{\widehat{u}_{m+1}^j}{a_{m+1}} + 4\frac{\widehat{u}_m^j}{a_m} + \frac{\widehat{u}_{m-1}^j}{a_{m-1}}\right), \tag{3.42}$$

with $\sigma_m^n = \dfrac{p^n a'_m}{a_m}$.

For each time step t_n, the unknowns $v^n := [\widehat{u}_2^n, \widehat{u}_3^n, \cdots, \widehat{u}_M^n]^T$ are the solution of the system of linear algebraic equations:

$$\mathcal{A}\, v^n = \mathcal{F}, \tag{3.43}$$

where $\mathcal{F} := \left[\gamma_0^n + \mathcal{G}_2^n, \mathcal{G}_3^n, \cdots, \mathcal{G}_{M-1}^n, \gamma_1^n + \mathcal{G}_M^n\right]^T$ with the boundary terms γ_0^n, γ_1^n which are extracted from $\mathcal{L}_M^N$ and $\mathcal{A} = [\mathcal{A}_{i,m}]_{i,m=1}^{M-1}$ denotes the $(M-1)\times(M-1)$ stiffness matrix corresponding to the discretization (3.40) and (3.41).

The operator $\mathcal{L}_M^N$ defined in (3.41) satisfies the discrete maximum principle, as shown in the following lemma.

Lemma 3.6 *(Discrete maximum principle) Assume that the conditions given in (3.2) hold, and the mesh width h satisfies the following condition:*

$$0 < h < \frac{-H + \sqrt{H^2 + 24Ja_*P_*}}{2J}, \tag{3.44}$$

where $J = \widehat{d}_{\max} + \|b\|_\Omega \|p\|_G$, $H = \dfrac{a_*}{2}(7\Sigma^* - \sigma_*)$, $a_* = \min\limits_m a_m$, $\Sigma^* = \max\limits_{m,n} |\sigma_m^n|$, $\sigma_* = \min\limits_{m,n} |\sigma_m^n|$, $P_* = \min\limits_n p^n$, $\widehat{d}_{\max} = \max\limits_n \widehat{d}_{n,n-1}$. *Then the operator $\mathcal{L}_M^N$ defined in (3.41) satisfies the discrete maximum principle.*

Proof. Here we have to show that the stiffness matrix $\mathcal{A}$ (defined in (3.43)) associated with $\mathcal{L}_M^N$ is an M-matrix. From (3.44), it is clear that

$$\widehat{d}_{\max} + |b\|_\Omega \|p\|_G + \frac{a_*}{2h}(7\Sigma^* - \sigma_*) < \frac{6a_*P_*}{h^2}. \tag{3.45}$$

By using the inequality (3.45), for $3 \le m \le M$, we have

$$\mathcal{A}_{m-1,m-2} = \frac{1}{a_{m-1}}\left[\widehat{d}_{n,n-1} + p^n b_{m-1}\right] - \frac{6p^n}{h^2} - \frac{\sigma_{m+1}^n}{2h} + \frac{2\sigma_m^n}{h} + \frac{3\sigma_{m-1}^n}{2h}$$

$$\begin{aligned}
&\leq \frac{1}{a_*}\left[\widehat{d}_{\max} + |b|_\Omega \|p\|_G\right] - \frac{6p^n}{h^2} - \frac{\sigma_{m+1}^n}{2h} + \frac{2\sigma_m^n}{h} + \frac{3\sigma_{m-1}^n}{2h} \\
&< \frac{6P_*}{h^2} - \frac{1}{2h}\left(7\Sigma^* - \sigma_*\right) - \frac{6p^n}{h^2} - \frac{\sigma_{m+1}^n}{2h} + \frac{2\sigma_m^n}{h} + \frac{3\sigma_{m-1}^n}{2h} \\
&= \frac{6}{h^2}(P_* - p^n) + \frac{1}{2h}\left(\sigma_* - \sigma_{m+1}^n\right) - \frac{2}{h}\left(\Sigma^* - \sigma_m^n\right) - \frac{3}{2h}\left(\Sigma^* - \sigma_{m-1}^n\right) \\
&\leq 0. \qquad (3.46)
\end{aligned}$$

For $2 \leq m \leq M-1$, we have

$$\begin{aligned}
\mathcal{A}_{m-1,m} &= \frac{1}{a_{m+1}}[\widehat{d}_{n,n-1} + p^n b_{m+1}] - \frac{6p^n}{h^2} - \frac{3\sigma_{m+1}^n}{2h} - \frac{2\sigma_m^n}{h} + \frac{\sigma_{m-1}^n}{2h} \\
&\leq \frac{1}{a_*}[\widehat{d}_{\max} + |b|_\Omega \|p\|_G] - \frac{6p^n}{h^2} - \frac{3\sigma_{m+1}^n}{2h} - \frac{2\sigma_m^n}{h} + \frac{\sigma_{m-1}^n}{2h} \\
&< \frac{6P_*}{h^2} - \frac{1}{2h}\left(7\Sigma^* - \sigma_*\right) - \frac{6p^n}{h^2} - \frac{3\sigma_{m+1}^n}{2h} - \frac{2\sigma_m^n}{h} + \frac{\sigma_{m-1}^n}{2h} \\
&\leq \frac{6P_*}{h^2} - \frac{1}{2h}\left(\Sigma^* - 7\sigma_*\right) - \frac{6p^n}{h^2} - \frac{3\sigma_{m+1}^n}{2h} - \frac{2\sigma_m^n}{h} + \frac{\sigma_{m-1}^n}{2h} \\
&= \frac{6}{h^2}(P_* - p^n) - \frac{1}{2h}\left(\Sigma^* - \sigma_{m-1}^n\right) + \frac{2}{h}\left(\sigma_* - \sigma_m^n\right) + \frac{3}{2h}\left(\sigma_* - \sigma_{m+1}^n\right) \\
&\leq 0, \qquad (3.47)
\end{aligned}$$

where we have used the inequality (3.45) and the fact that $(7\Sigma^* - \sigma_*) \geq (\Sigma^* - 7\sigma_*)$.

By using (3.46) and (3.47), for $3 \leq m \leq M-1$, we have

$$\begin{aligned}
&\mathcal{A}_{m-1,m-1} - |\mathcal{A}_{m-1,m-2}| - |\mathcal{A}_{m-1,m}| \\
&= \frac{4}{a_m}[\widehat{d}_{n,n-1} + p^n b_m] + \frac{12p^n}{h^2} + \frac{2\sigma_{m+1}^n}{h} - \frac{2\sigma_{m-1}^n}{h} \\
&\quad + \frac{1}{a_{m-1}}[\widehat{d}_{n,n-1} + p^n b_{m-1}] - \frac{6p^n}{h^2} - \frac{\sigma_{m+1}^n}{2h} + \frac{2\sigma_m^n}{h} + \frac{3\sigma_{m-1}^n}{2h} \\
&\quad + \frac{1}{a_{m+1}}[\widehat{d}_{n,n-1} + p^n b_{m+1}] - \frac{6p^n}{h^2} - \frac{3\sigma_{m+1}^n}{2h} - \frac{2\sigma_m^n}{h} + \frac{\sigma_{m-1}^n}{2h} \\
&= \left(\frac{1}{a_{m+1}} + \frac{4}{a_m} + \frac{1}{a_{m-1}}\right)\widehat{d}_{n,n-1} + p^n\left(\frac{b_{m+1}}{a_{m+1}} + \frac{4b_m}{a_m} + \frac{b_{m-1}}{a_{m-1}}\right) \\
&> 0, \qquad (3.48)
\end{aligned}$$

where we have used $\widehat{d}_{n,n-1} > 0$ and the conditions given in (3.2). Therefore, $\mathcal{A}_{m-1,m-1} > |\mathcal{A}_{m-1,m-2}| + |\mathcal{A}_{m-1,m+}| > 0$, for $3 \leq m \leq M-1$.

By using the inequality (3.45) and the conditions given in (3.2), for $m = 2$, M, we

have

$$\begin{aligned}\mathcal{A}_{m-1,m-1} &= \frac{4}{a_m}[\widehat{d}_{n,n-1}+p^n b_m]+\frac{12p^n}{h^2}+\frac{2\sigma^n_{m+1}}{h}-\frac{2\sigma^n_{m-1}}{h}\\ &> \frac{2}{a_*}\left[\widehat{d}_{\max}+|b|_\Omega\,\|p\|_G+\frac{a_*}{2h}\left(7\Sigma^*-\sigma_*\right)\right]+\frac{2\sigma_*}{h}-\frac{2\Sigma^*}{h}\\ &= \frac{2}{a_*}\left[\widehat{d}_{\max}+|b|_\Omega\,\|p\|_G\right]+\frac{1}{h}\left(5\Sigma^*+\sigma_*\right)\\ &> 0, \end{aligned} \tag{3.49}$$

where we have used the fact that $\frac{4}{a_m}[\widehat{d}_{n,n-1}+p^n b_m]>0$ in the first inequality. Hence the stiffness matrix $\mathcal{A}$ associated with $\mathcal{L}^N_M$ is an M-matrix and therefore $\mathcal{L}^N_M$ satisfies the discrete maximum principle. □

The stability estimate for the spatially discretized scheme (3.40), as stated in the following corollary, is established by using Lemma 3.6 and Lemma 1.7.

Corollary 3.6 *For each time step t_n, the solution of the spatially discretized scheme (3.40) satisfies:*

$$\|\widehat{u}^n\|_{\overline{\Omega}_M}\le C\left[6\left(\|g\|_{\overline{\Omega}_M}+\|f^n\|_{\overline{\Omega}_M}\right)+\sum_{j=2}^{n}\left(\widehat{d}_{n,j}-\widehat{d}_{n,j-1}\right)\left(\left|\psi_1^j\right|+\left|\psi_2^j\right|\right)\right], \tag{3.50}$$

where $C=\frac{1}{a_*}\exp\left(\frac{6\,\widehat{d}_{\max}}{a_*}\right)$, $a_*=\min_m a_m$, $\widehat{d}_{\max}=\max_n \widehat{d}_{n,n-1}$.

Proof. From the spatially discretized scheme (3.40), for each time step t_n, we have

$$\begin{aligned}\left|\mathcal{L}^N_M\widehat{u}^n_m\right|=|\mathcal{G}^n_m| &\le \frac{6}{a_*}\|f^n\|_{\overline{\Omega}_M}+\frac{6\widehat{d}_{n,1}}{a_*}\|g\|_{\overline{\Omega}_M}+\frac{1}{a_*}\sum_{j=2}^{n-1}\left(\widehat{d}_{n,j}-\widehat{d}_{n,j-1}\right)\\ &\quad\times\left(\left|\widehat{u}^j_{m-1}\right|+4\left|\widehat{u}^j_m\right|+\left|\widehat{u}^j_{m+1}\right|\right),\ m=2,\cdots,M. \end{aligned} \tag{3.51}$$

By simplifying (3.51) and considering the boundary term corresponding to $m=1,M+1$, one may derive the following for $m=2,\cdots,M$ and for each time step t_n:

$$\begin{aligned}\left|\mathcal{L}^N_M\widehat{u}^n_m\right| &\le \frac{6}{a_*}\left(\|f^n\|_{\overline{\Omega}_M}+\widehat{d}_{n,1}\|g\|_{\overline{\Omega}_M}\right)+\frac{1}{a_*}\sum_{j=2}^{n-1}\left(\widehat{d}_{n,j}-\widehat{d}_{n,j-1}\right)\left[\left|\psi_1^j\right|+\left|\psi_2^j\right|\right]\\ &\quad+\frac{6}{a_*}\sum_{j=2}^{n-1}\left(\widehat{d}_{n,j}-\widehat{d}_{n,j-1}\right)\|\widehat{u}^j\|_{\overline{\Omega}_M}. \end{aligned} \tag{3.52}$$

By using the discrete maximum principle stated in Lemma 3.6 and then taking maximum over $\overline{\Omega}_M$ on the left side, we get

$$\|\widehat{u}^n\|_{\overline{\Omega}_M} \leq \mu_n + \sum_{j=2}^{n-1} \eta_j \left\|\widehat{u}^j\right\|_{\overline{\Omega}_M}, \tag{3.53}$$

where $\mu_n = \dfrac{6}{a_*}\left(\|f^n\|_{\overline{\Omega}_M} + \widehat{d}_{n,1}\|g\|_{\overline{\Omega}_M}\right) + \dfrac{1}{a_*}\displaystyle\sum_{j=2}^{n-1}\left(\widehat{d}_{n,j} - \widehat{d}_{n,j-1}\right)\left[\left|\psi_1^j\right| + \left|\psi_2^j\right|\right]$ and $\eta_j = \dfrac{6}{a_*}\left(\widehat{d}_{n,j} - \widehat{d}_{n,j-1}\right)$, $2 \leq j \leq n-1$.

It is obvious that $\{\mu_n\}$ is a non-decreasing sequence of non-negative numbers and $\eta_j \geq 0$. Also $\displaystyle\sum_{j=2}^{n-1}\eta_j = \frac{6}{a_*}\left(\widehat{d}_{n,n-1} - \widehat{d}_{n,1}\right) \leq \frac{6\widehat{d}_{\max}}{a_*}$. By using Lemma 1.7, for each time step t_n we have

$$\|\widehat{u}^n\|_{\overline{\Omega}_M} \;\leq\; \mu_n \exp\left(\sum_{j=2}^{n-1}\eta_j\right) \;\leq\; \mu_n \exp\left(\frac{6\widehat{d}_{\max}}{a_*}\right), \tag{3.54}$$

which is the required bound. □

The error bound for the spatially discretized scheme (3.40) is provided in the following result.

Lemma 3.7 *Let $\widehat{u}^n(x)$ be the solution of the semi-discretized scheme (3.25) and $\{\widehat{u}_m^n\}$ be the solution of the spatially discretized scheme (3.40). Then for each time step t_n, we have the following error estimate :*

$$\|\widehat{u}^n(x_m) - \widehat{u}_m^n\|_{\overline{\Omega}_M} \leq Ch^2, \;\; 1 \leq n \leq N+1. \tag{3.55}$$

Proof. For each time step t_n, the following results are obtained from the equations (3.40)-(3.41) and (3.25) :

$$\begin{aligned}\mathcal{L}_M^N\left(\widehat{u}^n(x_m)\right) \;=\; & \frac{1}{a_{m+1}}\left[f^n + \widehat{d}_{n,1}g + \sum_{j=2}^{n-1}\left(\widehat{d}_{n,j} - \widehat{d}_{n,j-1}\right)\widehat{u}^j\right](x_{m+1}) \\ & + \frac{4}{a_m}\left[f^n + \widehat{d}_{n,1}g + \sum_{j=2}^{n-1}\left(\widehat{d}_{n,j} - \widehat{d}_{n,j-1}\right)\widehat{u}^j\right](x_m)\end{aligned}$$

$$
\begin{aligned}
&+\frac{1}{a_{m-1}}\left[f^n+\widehat{d}_{n,1}g+\sum_{j=2}^{n-1}\left(\widehat{d}_{n,j}-\widehat{d}_{n,j-1}\right)\widehat{u}^j\right](x_{m-1})\\
=\;&\left[\widehat{d}_{n,n-1}I+\mathcal{L}^N\right]\frac{\widehat{u}^n(x_{m+1})}{a_{m+1}}+4\left[\widehat{d}_{n,n-1}I+\mathcal{L}^N\right]\frac{\widehat{u}^n(x_m)}{a_m}\\
&+\left[\widehat{d}_{n,n-1}I+\mathcal{L}^N\right]\frac{\widehat{u}^n(x_{m-1})}{a_{m-1}}. \qquad (3.56)
\end{aligned}
$$

Therefore, by taking the difference of (3.56) and (3.41), we have

$$
\begin{aligned}
\left|\mathcal{L}_M^N\left(\widehat{u}^n(x_m)-\widehat{u}_m^n\right)\right| &= \left|\left[\widehat{d}_{n,n-1}I+\mathcal{L}^N\right]\frac{\widehat{u}^n(x_{m+1})}{a_{m+1}}+4\left[\widehat{d}_{n,n-1}I+\mathcal{L}^N\right]\frac{\widehat{u}^n(x_m)}{a_m}\right.\\
&\quad\left.+\left[\widehat{d}_{n,n-1}I+\mathcal{L}^N\right]\frac{\widehat{u}^n(x_{m-1})}{a_{m-1}}-\mathcal{L}_M^N\widehat{u}_m^n\right|\\
&\le |p^n|\left|\frac{6}{h^2}\left(\widehat{u}_{m+1}^n-2\widehat{u}_m^n+\widehat{u}_{m-1}^n\right)-\frac{d^2\widehat{u}^n}{dx^2}(x_{m+1})-4\frac{d^2\widehat{u}^n}{dx^2}(x_m)-\frac{d^2\widehat{u}^n}{dx^2}(x_{m-1})\right|\\
&\quad+|\sigma_{m+1}^n|\left|\frac{d\widehat{u}^n}{dx}(x_{m+1})-\frac{3\widehat{u}_{m+1}^n-4\widehat{u}_m^n+\widehat{u}_{m-1}^n}{2h}\right|\\
&\quad+4|\sigma_m^n|\left|\frac{d\widehat{u}^n}{dx}(x_m)-\frac{\widehat{u}_{m+1}^n-\widehat{u}_{m-1}^n}{2h}\right|\\
&\quad+|\sigma_{m-1}^n|\left|\frac{d\widehat{u}^n}{dx}(x_{m-1})-\frac{-\widehat{u}_{m+1}^n+4\widehat{u}_m^n-3\widehat{u}_{m-1}^n}{2h}\right|\\
&\le \left(|\sigma_{m+1}^n|+4|\sigma_m^n|+|\sigma_{m-1}^n|\right)Ch^2\\
&\le Ch^2, \qquad (3.57)
\end{aligned}
$$

where in the second inequality we have used (3.37) and (3.39). Hence, using the discrete maximum principle for $\mathcal{L}_M^N$ given in Lemma 3.6, we can obtain the required result. □

Next theorem establishes the error estimate for the fully discretization of the IBVP (3.1).

Theorem 3.7 *Let $u(x_m,t_n)$ be the exact solution of the IBVP (3.1) and let $\widehat{u}_m^n$ be the discrete solution of the fully discrete scheme (3.40) at (x_m,t_n). Then the global error satisfies*

$$
\|u(x_m,t_n)-\widehat{u}_m^n\|_{\overline{\Omega}_M}\le C\left(N^{-\min\{2-\alpha,r\alpha\}}+h^2\right),\ 1\le n\le N+1. \qquad (3.58)
$$

Proof. The error at each time step t_n can be decomposed as

$$
\|u(x_m,t_n)-\widehat{u}_m^n\|_{\overline{\Omega}_M}\le\|u(x_m,t_n)-\widehat{u}^n(x_m)\|_{\overline{\Omega}_M}+\|\widehat{u}^n(x_m)-\widehat{u}_m^n\|_{\overline{\Omega}_M}. \qquad (3.59)
$$

From Lemma 3.5 and Lemma 3.7, we can obtain

$$\|u(x_m,t_n)-\widehat{u}_m^n\|_{\overline{\Omega}_M}\leq C(N^{-\min\{2-\alpha,r\alpha\}}+h^2). \tag{3.60}$$

Hence, the proof is complete. □

3.4 Semi-linear non-autonomous TF-ADR equations

In this section, we consider the following semi-linear non-autonomous TF-ADR problem:

$$\begin{cases} {}^{C}\mathcal{D}_t^{\alpha}u(x,t)+\mathcal{L}(u(x,t))=f(x,t), \quad (x,t)\in Q:=\Omega\times G,\\ u(x,0)=g(x), \quad \forall x\in\overline{\Omega},\\ u(0,t)=\psi_1(t), \quad u(\ell,t)=\psi_2(t), \quad \forall t\in\overline{G}, \end{cases} \tag{3.61}$$

where $\Omega=(0,\ell)$, $G=(0,T]$ and $\mathcal{L}(u(x,t))=p(t)\left[-\dfrac{\partial}{\partial x}\left(a(x)\dfrac{\partial u}{\partial x}(x,t)\right)+b(x,u)\right]$ with

$$\begin{cases} a\in\mathcal{C}^1(\overline{\Omega}),\ b\in\mathcal{C}^1(\Omega\times\mathbb{R}),\ a(x)>0,\ b_u\geq 0, \quad \forall x\in\overline{\Omega},\\ p\in\mathcal{C}(\overline{G}),\ p(t)>0, \quad \forall t\in G. \end{cases} \tag{3.62}$$

Further, we assume that for sufficiently smooth functions $b(x,u)$, $f(x,t)$, and $g(x)$, the problem (3.61) admits a unique solution $u(x,t)$ satisfying the conditions given in (3.12) and that the compatibility conditions $g(0)=\psi_1(0)$ and $g(\ell)=\psi_2(0)$ hold.

To obtain the numerical solution of the problem (3.61), first, we convert the semi-linear problem into a sequence of linear problems by using the Newton's linearization process. In other words, we arrive at a sequence of approximate solutions $\{u^{(q)}\}$ for the initial guess $u^{(0)}$ satisfying the initial and boundary conditions of the semi-linear problem (3.61). Thus, we define the following linear non-autonomous TF-ADR problem's solution as $u^{(q+1)}$ for each fixed q:

$$\begin{cases} {}^{C}\mathcal{D}_t^{\alpha}u^{(q+1)}(x,t)+\mathcal{L}^q(u^{(q+1)}(x,t))=F^q(x,t), \quad \forall (x,t)\in Q,\\ u^{(q+1)}(x,0)=g(x), \quad \forall x\in\overline{\Omega},\\ u^{(q+1)}(0,t)=\psi_1(t), \quad u^{(q+1)}(\ell,t)=\psi_2(t), \quad \forall t\in G, \end{cases} \tag{3.63}$$

where

$$\mathcal{L}^q(u^{(q+1)}(x,t)) = p(t)\left[-\frac{\partial}{\partial x}\left(a(x)\frac{\partial u^{(q+1)}}{\partial x}\right) + b_u(x,u^{(q)})u^{(q+1)}\right](x,t),$$

$$F^q(x,t) = f(x,t) - p(t)\left[b(x,u^{(q)}) - b_u(x,u^{(q)})u^{(q)}(x,t)\right].$$

Hence for each fixed q, we solve (3.63) by using the numerical method discussed in the above section and then, for the Newton linearization process, the following convergence criterion is used :

$$\max_{(x_m,t_n)} |u^{(q+1)}(x_m,t_n) - u^{(q)}(x_m,t_n)| \leq \text{Tol}, \quad q \geq 0.$$

For computational purpose we have used $\text{Tol} = 1.0e-07$. The next section provides numerical results for the semi-linear problem (3.61).

3.5 Numerical experiments

To validate the theoretical error estimates, we conduct numerical experiments in this section using the proposed numerical approach for a variety of test problems. The numerical results are presented as tables of maximum errors and convergence rates, surface plots of the numerical solution, and log-log plots of the maximum errors.

The maximum error and the rate of convergence are determined by

$$E_{M,N} = \max_{m,n} |u(x_m,t_n) - \widehat{u}_m^n|, \quad \text{and} \quad R_{M,N} = \log_2\left(\frac{E_{M,N}}{E_{2M,2N}}\right),$$

where $u(x_m,t_n)$ is the exact solution and $\widehat{u}_m^n$ is the approximate solution at the point (x_m,t_n). We have used $r = (2-\alpha)/\alpha$ for the numerical experiments.

Example 3.8 *Consider the following IBVP:*

$$\begin{cases} {}^C\mathcal{D}_t^\alpha u(x,t) - \dfrac{\partial^2 u}{\partial x^2} = f(x,t), \quad (x,t) \in (0,\pi)\times(0,1], \\ u(x,0) = 0, \quad x \in [0,\pi], \\ u(0,t) = 0, \quad u(\pi,t) = 0, \quad t \in (0,1]. \end{cases} \tag{3.64}$$

We choose $f(x,t)$ so that the exact solution is $u(x,t) = t^3 \sin x$. Figure 3.1 (a)

displays the surface plot of the numerical solution for $\alpha = 0.6$, and Figure 3.1 (b) shows the errors at final time $T = 1$ for various values of α for Example 3.8 with $M = N = 64$, which demonstrates that the errors increase for large values of α.

Tables 3.1 and 3.2 show the numerical results for the proposed scheme and the method outlined in [106] for Example 3.8, where one can find that the maximum error is less in the proposed method than the method given in [106]. The log-log plots of the maximum errors are depicted in Figure 3.2 corresponding to Tables 3.1 and 3.2.

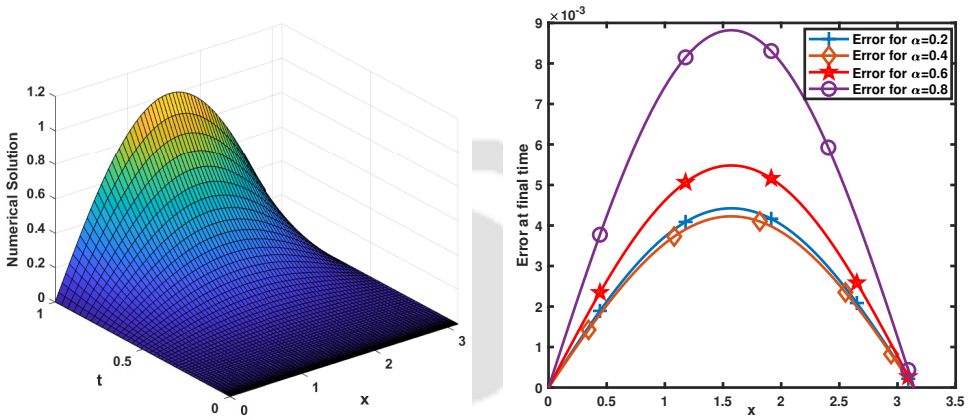

(a) Numerical Solution for $\alpha = 0.6$. *(b) Errors at time $T = 1$.*

Figure 3.1: *Plots of numerical results for Example 3.8 with $M = N = 64$.*

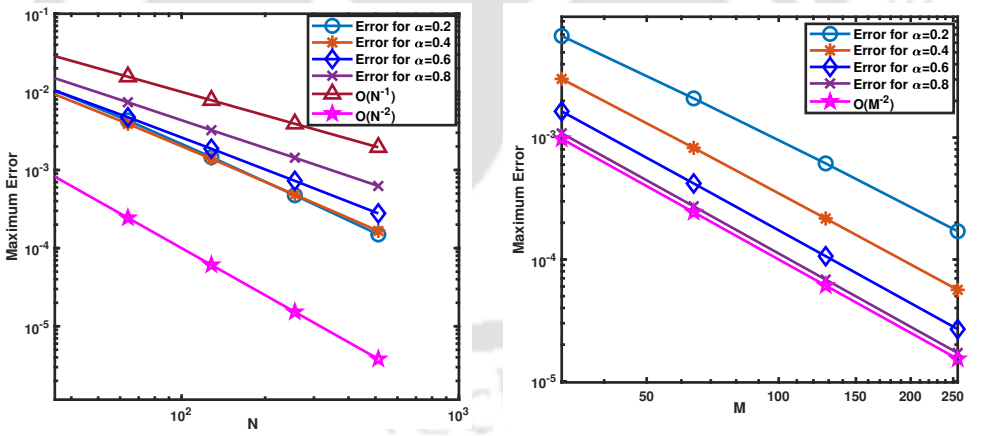

(a) Corresponding to Table 3.1. *(b) Corresponding to Table 3.2.*

Figure 3.2: *Log-log plots of the maximum error for Example 3.8.*

Example 3.9 *Consider the following problem over the domain* $(0,\pi)\times(0,1]$:

$$\begin{cases} {}^{C}\mathcal{D}_t^{\alpha}u(x,t)+(t^2+1)\left[-\dfrac{\partial}{\partial x}\left((x+1)\dfrac{\partial u}{\partial x}\right)+u\right](x,t)=f(x,t), \\ u(x,0)=0, \quad x\in[0,\pi], \\ u(0,t)=t^{\alpha}, \quad u(\pi,t)=t^{\alpha}, \quad t\in(0,1]. \end{cases} \tag{3.65}$$

In (3.65), the RHS function $f(x,t)$ is chosen in such a way that the exact solution of the problem is $u(x,t)=t^{\alpha}(1-x\sin x)$. Figure 3.3 shows the numerical solution of Example 3.9 for $\alpha=0.2$ and $\alpha=0.6$ with $M=N=64$, where we can observe that the solution for $\alpha=0.2$ has a strong singularity around $t=0$ than the solution for $\alpha=0.6$. Figure 3.4 shows the errors at final time $T=1$ for several values of α for Example 3.9. The maximum errors and the corresponding rate of convergence for Example 3.9 are shown in Tables 3.3 and 3.4, the same results are plotted in Figure 3.5 in the log-log scale for better understanding.

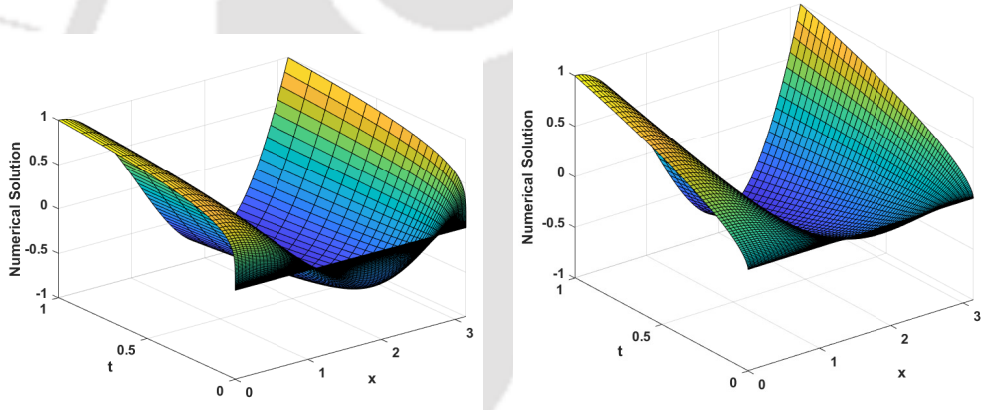

(a) Numerical solution for $\alpha=0.2$. *(b) Numerical solution for* $\alpha=0.6$.

Figure 3.3: *Numerical Solutions of Example 3.9 with* $M=N=64$.

Example 3.10 *Consider the semi-linear problem:*

$$\begin{cases} {}^{C}\mathcal{D}_t^{\alpha}u(x,t)-\dfrac{\partial^2 u}{\partial x^2}-\exp(-u)=f(x,t),\ (x,t)\in(0,\pi)\times(0,1], \\ u(x,0)=0, \quad x\in[0,\pi], \\ u(0,t)=t^3, \quad u(\pi,t)=-t^3, \quad t\in(0,1]. \end{cases} \tag{3.66}$$

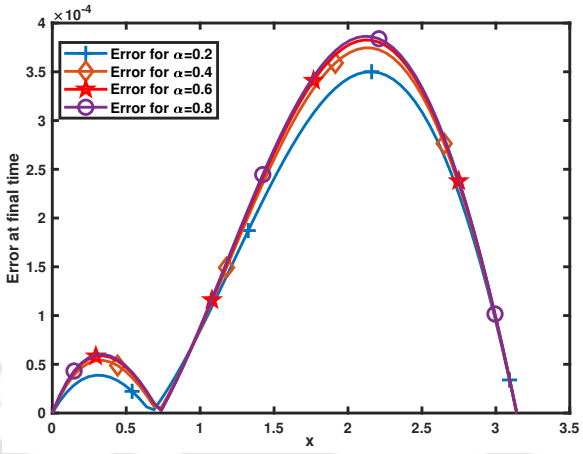

Figure 3.4: *Error at final time $T = 1$ for Example 3.9 with $M = N = 64$.*

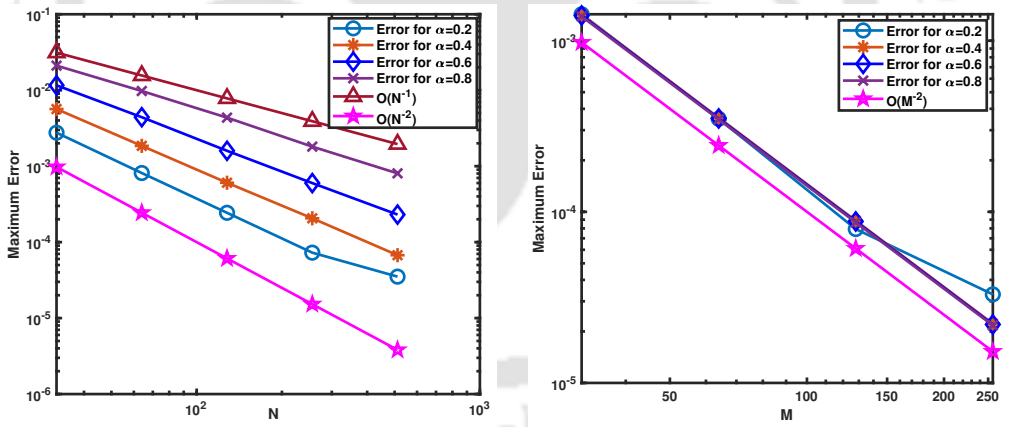

(a) Corresponding to Table 3.3. *(b) Corresponding to Table 3.4.*

Figure 3.5: *Log-log plots of the maximum error for Example 3.9.*

The function $f(x,t)$ in the problem (3.66) is computed in such a way that the exact solution of the problem is $u(x,t) = t^3 \cos x$. To solve this problem numerically, we first apply the Newton's linearization method given in (3.63) to the semi-linear problem (3.66) and obtain the following sequence of linear problems:

$$\begin{cases} {}^{C}\mathcal{D}_t^{\alpha} u^{(q+1)}(x,t) + \mathcal{L}^q(u^{(q+1)}(x,t)) = F^q(x,t), \quad \forall (x,t) \in (0,\pi) \times (0,1], \\ u^{(q+1)}(x,0) = 0, \quad x \in [0,\pi], \\ u^{(q+1)}(0,t) = t^3, \quad u^{(q+1)}(\pi,t) = -t^3, \quad t \in (0,1], \end{cases} \tag{3.67}$$

where for $i \geq 0$,

$$\mathcal{L}^q(u^{(q+1)}(x,t)) = -\frac{\partial^2 u^{(q+1)}}{\partial x^2}(x,t) + \exp(-u^{(q)}(x,t))u^{(q+1)}(x,t),$$

$$F^q(x,t) = f(x,t) + \exp(-u^{(q)}(x,t))(1 + u^{(q)}(x,t)).$$

Then we use the proposed numerical technique (3.40) to the sequence of linear problems (3.67) and obtain the approximate solution for the problem (3.10). For computation purpose, we take the initial guess $u^{(0)}(x,t) = 1$, $(x,t) \in (0,\pi) \times (0,1]$.

Figure 3.6 (a) displays the surface plot of the numerical solution for $\alpha = 0.4$, and Figure 3.6 (b) shows the errors at final time $T = 1$ for various values of α for Example 3.10 with $M = N = 64$, which demonstrates that the errors increase for large values of α.

Tables 3.5 and 3.6 present the numerical results for the proposed scheme for Example 3.10. The log-log plots of the maximum errors are given in Figure 3.7 corresponding to Tables 3.5 and 3.6.

3.6 Conclusion

The analytical and numerical solutions of linear non-autonomous TF-ADR IBVPs with a fractional derivative of Caputo-type are obtained in this chapter. We have used the Sumudu decomposition method and the maximum-minimum principle to prove the existence and uniqueness of the analytical solution to these problems. To obtain the numerical solution of the fractional diffusion IBVP, we have developed a computational scheme. Precisely, we have used the fully discrete scheme, which comprises the L1-approximation for the fractional-time derivative and the cubic spline approximation

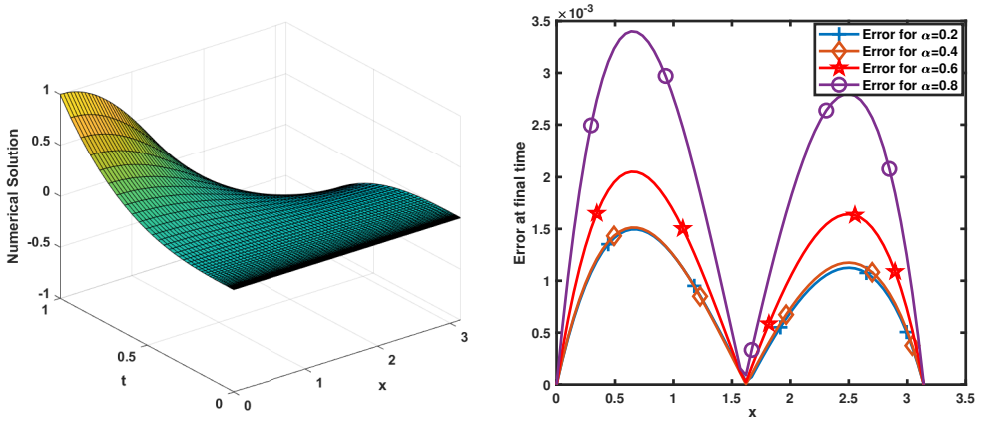

(a) Numerical Solution with $\alpha = 0.4$. *(b) Errors at time $T = 1$.*

Figure 3.6: *Plots of numerical results for Example 3.10 with $M = N = 64$.*

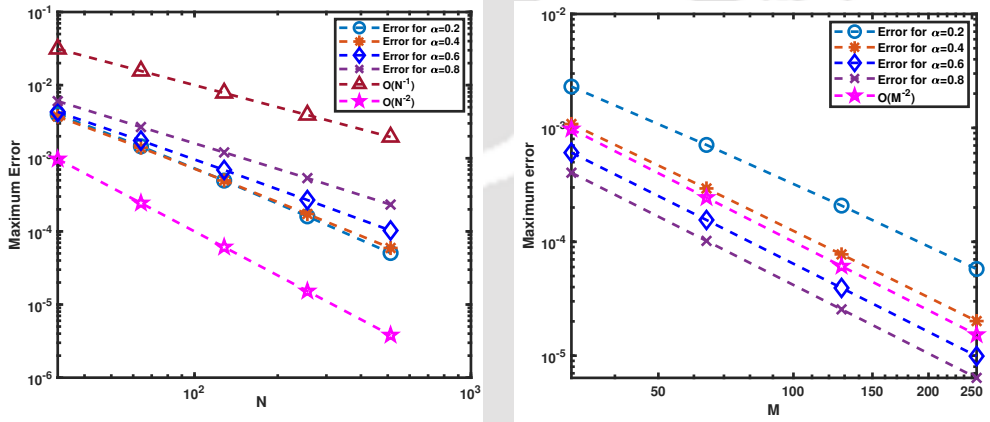

(a) Corresponding to Table 3.5. *(b) Corresponding to Table 3.6.*

Figure 3.7: *Log-log plots of the maximum error for Example 3.10.*

technique for the spatial derivatives, to get the numerical solution of the IBVP. Further, we have provided the convergence analysis and obtained $(2-\alpha)-$order error estimates for the temporal variable and second-order error estimates for the spatial variable. In addition, we applied the proposed method to solve semi-linear problems after linearizing them by the Newton linearization procedure. To validate the proposed technique, numerical examples are carried out, and the results are compared to previous methods available in the literature.

Table 3.1: *$E_{M,N}$ and $R_{M,N}$ of Example 3.8 with* $M = \left\lceil N^{\frac{2-\alpha}{2}} \right\rceil$.

Order	Method		$N = 32$	$N = 64$	$N = 128$	$N = 256$	$N = 512$
α=0.2	Present Method	$E_{M,N}$	1.1777e-02	4.3078e-03	1.4631e-03	4.7485e-04	1.4973e-04
		$R_{M,N}$	1.4510	1.5579	1.6235	1.6651	–
		CPU (s)	0.019412	0.020987	0.087494	0.438177	2.221987
	Method in [106]	$E_{M,N}$	1.3169e-02	4.7194e-03	1.5787e-03	5.0817e-04	1.5932e-04
		$R_{M,N}$	1.4805	1.5798	1.6354	1.6734	–
		CPU (s)	0.021787	0.016842	0.048370	0.183913	0.706914
α=0.4	Present Method	$E_{M,N}$	1.0519e-02	3.9044e-03	1.3932e-03	4.8397e-04	1.6603e-04
		$R_{M,N}$	1.4298	1.4867	1.5254	1.5434	–
		CPU (s)	0.005894	0.021298	0.056679	0.240133	1.195108
	Method in [106]	$E_{M,N}$	1.2995e-02	4.6999e-03	1.6512e-03	5.7162e-04	1.9463e-04
		$R_{M,N}$	1.4673	1.5091	1.5304	1.5543	–
		CPU (s)	0.002227	0.009050	0.027097	0.086044	0.403864
α=0.6	Present Method	$E_{M,N}$	1.1643e-02	4.7343e-03	1.8734e-03	7.2628e-04	2.7847e-04
		$R_{M,N}$	1.2983	1.3375	1.3671	1.3830	–
		CPU (s)	0.002735	0.008479	0.031054	0.135503	0.605563
	Method in [106]	$E_{M,N}$	1.6033e-02	6.3583e-03	2.4534e-03	9.4288e-04	3.6173e-04
		$R_{M,N}$	1.3343	1.3739	1.3796	1.3822	–
		CPU (s)	0.001411	0.004399	0.015428	0.057712	0.197916
α=0.8	Present Method	$E_{M,N}$	1.6548e-02	7.3598e-03	3.2355e-03	1.4340e-03	6.2436e-04
		$R_{M,N}$	1.1689	1.1857	1.1740	1.1996	–
		CPU (s)	0.001877	0.005182	0.021065	0.080570	0.328021
	Method in [106]	$E_{M,N}$	2.3550e-02	1.0387e-02	4.5641e-03	1.9800e-03	8.6642e-04
		$R_{M,N}$	1.1810	1.1864	1.2048	1.1923	–
		CPU (s)	0.001474	0.005401	0.010509	0.034653	0.122255

Table 3.2: *$E_{M,N}$ and $R_{M,N}$ of Example 3.8 with* $N = \left[M^{\frac{2}{2-\alpha}}\right]$.

Order	Method		$M = 32$	$M = 64$	$M = 128$	$M = 256$
α=0.2	Present Method	$E_{M,N}$	6.8258e-03	2.0963e-03	6.1374e-04	1.7045e-04
		$R_{M,N}$	1.7031	1.7721	1.8483	–
		CPU (s)	0.028577	0.059233	0.287157	1.831610
	Method in [106]	$E_{M,N}$	7.5389e-03	2.2727e-03	6.5771e-04	1.8143e-04
		$R_{M,N}$	1.7299	1.7889	1.8580	–
		CPU (s)	0.031185	0.025488	0.122571	0.575517
α=0.4	Present Method	$E_{M,N}$	3.0301e-03	8.2306e-04	2.1687e-04	5.6314e-05
		$R_{M,N}$	1.8803	1.9241	1.9453	–
		CPU (s)	0.021310	0.115084	0.790927	6.561508
	Method in [106]	$E_{M,N}$	3.6379e-03	9.7418e-04	2.5460e-04	6.5742e-05
		$R_{M,N}$	1.9008	1.9360	1.9533	–
		CPU (s)	0.012593	0.047385	0.268328	1.494471
α=0.6	Present Method	$E_{M,N}$	1.6405e-03	4.2040e-04	1.0639e-04	2.6803e-05
		$R_{M,N}$	1.9643	1.9824	1.9889	–
		CPU (s)	0.036924	0.298415	3.046025	47.366416
	Method in [106]	$E_{M,N}$	2.1500e-03	5.4733e-04	1.3810e-04	3.4727e-05
		$R_{M,N}$	1.9738	1.9867	1.9915	–
		CPU (s)	0.019232	0.108610	0.721873	6.348350
α=0.8	Present Method	$E_{M,N}$	1.0843e-03	2.7298e-04	6.8373e-05	1.7106e-05
		$R_{M,N}$	1.9899	1.9973	1.9989	–
		CPU (s)	0.129191	1.735907	32.166463	1212.732655
	Method in [106]	$E_{M,N}$	1.5019e-03	3.7711e-04	9.4391e-05	2.3610e-05
		$R_{M,N}$	1.9937	1.9983	1.9993	–
		CPU (s)	0.054928	0.556113	4.665823	107.654040

Table 3.3: $E_{M,N}$ *and* $R_{M,N}$ *of Example 3.9 with* $M = \left\lceil N^{\frac{2-\alpha}{2}} \right\rceil$.

Order		$N = 32$	$N = 64$	$N = 128$	$N = 256$	$N = 512$
	$E_{M,N}$	2.7603e-03	8.1278e-04	2.4349e-04	7.2713e-05	3.5165e-05
α=0.2	$R_{M,N}$	1.7639	1.7390	1.7436	1.0481	–
	CPU (s)	0.043553	0.048450	0.133439	0.436299	2.154235
	$E_{M,N}$	5.6513e-03	1.8514e-03	6.0497e-04	2.0601e-04	6.7307e-05
α=0.4	$R_{M,N}$	1.6100	1.6137	1.5541	1.6139	–
	CPU (s)	0.005764	0.029302	0.064758	0.373181	1.191567
	$E_{M,N}$	1.1596e-02	4.4129e-03	1.5945e-03	5.9897e-04	2.3063e-04
α=0.6	$R_{M,N}$	1.3938	1.4687	1.4125	1.3769	–
	CPU (s)	0.002662	0.009768	0.036711	0.210328	0.644767
	$E_{M,N}$	2.1075e-02	9.7578e-03	4.3548e-03	1.8091e-03	8.0492e-04
α=0.8	$R_{M,N}$	1.1109	1.1639	1.2674	1.1683	–
	CPU (s)	0.002456	0.008295	0.021789	0.084085	0.363875

Table 3.4: $E_{M,N}$ *and* $R_{M,N}$ *of Example 3.9 with* $N = \left\lceil M^{\frac{2}{2-\alpha}} \right\rceil$.

Order		$M = 32$	$M = 64$	$M = 128$	$M = 256$
α=0.2	$E_{M,N}$	1.4276e-03	3.4963e-04	7.9295e-05	3.2927e-05
	$R_{M,N}$	2.0296	2.1405	1.2680	–
	CPU (s)	0.108210	0.081524	0.324150	1.834651
α=0.4	$E_{M,N}$	1.4181e-03	3.5491e-04	8.8764e-05	2.2199e-05
	$R_{M,N}$	1.9984	1.9994	1.9995	–
	CPU (s)	0.031361	0.149114	0.785984	6.717388
α=0.6	$E_{M,N}$	1.4043e-03	3.5135e-04	8.7855e-05	2.1966e-05
	$R_{M,N}$	1.9989	1.9997	1.9999	–
	CPU (s)	0.043056	0.337707	3.240722	48.240723
α=0.8	$E_{M,N}$	1.3862e-03	3.4683e-04	8.6726e-05	2.1683e-05
	$R_{M,N}$	1.9989	1.9997	1.9999	–
	CPU (s)	0.143179	1.755215	4.472064	1266.924966

Table 3.5: $E_{M,N}$ *and* $R_{M,N}$ *of Example 3.10 with* $M = \left\lfloor N^{\frac{2-\alpha}{2}} \right\rfloor$.

Order		$N = 32$	$N = 64$	$N = 128$	$N = 256$	$N = 512$
α=0.2	$E_{M,N}$	3.9817e-03	1.4564e-03	4.9505e-04	1.6070e-04	5.0673e-05
	$R_{M,N}$	1.4509	1.5568	1.6232	1.6651	–
	CPU (s)	0.190928	0.120067	0.421776	1.900274	9.711752
α=0.4	$E_{M,N}$	3.7266e-03	1.3952e-03	4.9796e-04	1.7289e-04	5.9333e-05
	$R_{M,N}$	1.4174	1.4863	1.5262	1.5429	–
	CPU (s)	0.032472	0.094245	0.271906	1.025281	5.162946
α=0.6	$E_{M,N}$	4.3054e-03	1.7462e-03	6.9230e-04	2.6869e-04	1.0291e-04
	$R_{M,N}$	1.3019	1.3347	1.3654	1.3845	–
	CPU (s)	0.011486	0.041810	0.154947	0.673295	2.905099
α=0.8	$E_{M,N}$	6.0446e-03	2.6739e-03	1.2032e-03	5.3534e-04	2.3278e-04
	$R_{M,N}$	1.1767	1.1521	1.1684	1.2015	–
	CPU (s)	0.008258	0.028072	0.099975	0.396093	1.638752

Table 3.6: $E_{M,N}$ *and* $R_{M,N}$ *of Example 3.10 with* $N = \left\lfloor M^{\frac{2}{2-\alpha}} \right\rfloor$.

Order		$M = 32$	$M = 64$	$M = 128$	$M = 256$
α=0.2	$E_{M,N}$	2.3047e-03	7.0860e-04	2.0769e-04	5.7685e-05
	$R_{M,N}$	1.7015	1.7705	1.8482	–
	CPU (s)	0.151657	0.275728	1.345684	7.839140
α=0.4	$E_{M,N}$	1.0816e-03	2.9394e-04	7.7497e-05	2.0121e-05
	$R_{M,N}$	1.8795	1.9233	1.9454	–
	CPU (s)	0.096089	0.527870	3.372298	27.900680
α=0.6	$E_{M,N}$	6.0573e-04	1.5536e-04	3.9321e-05	9.9059e-06
	$R_{M,N}$	1.9631	1.9822	1.9889	–
	CPU (s)	0.200186	1.588399	15.046314	210.336490
α=0.8	$E_{M,N}$	4.0400e-04	1.0181e-04	2.5505e-05	6.3814e-06
	$R_{M,N}$	1.9885	1.9970	1.9988	–
	CPU (s)	0.654505	7.996733	134.303628	3850.248545

CHAPTER 4

Efficient numerical techniques for solving time-fractional integro-partial differential equation

This chapter studies solution techniques for a class of time-fractional integro-differential equations. The existence and uniqueness of the analytical solution of the problem are obtained by using the Sumudu decomposition method and the maximum-minimum principle. Cubic spline approximation and L1-discretization are used for the numerical solution for the time-fractional integro-differential equation.

4.1 Introduction

In this chapter, we consider the following TF-IPDE with Caputo-type time fractional derivative:

$$\begin{cases} {}^{C}\mathcal{D}_t^{\alpha} u(x,t) + \mathcal{L}u(x,t) + \lambda \int_0^t K(x,t-s)u(x,s)ds = f(x,t), \quad (x,t) \in Q := \Omega \times G, \\ u(x,0) = g(x), \quad \forall x \in \overline{\Omega}, \\ u(0,t) = \psi_1(t), \quad u(\ell,t) = \psi_2(t), \quad \forall t \in G, \end{cases} \tag{4.1}$$

where $\Omega = (0,\ell)$, $G = (0,T]$, $0 < \alpha < 1$, and

$$\mathcal{L}u(x,t) = -a(x,t)\frac{\partial^2 u}{\partial x^2}(x,t) + b(x,t)\frac{\partial u}{\partial x}(x,t) + c(x,t)u(x,t), \tag{4.2}$$

with sufficiently smooth functions a, b, c, f on $\overline{Q}$, $\lambda > 0$ such that

$$a(x,t) > 0, \;\; c(x,t) \geq 0, \;\; K(x,t) \geq 0, \qquad \forall (x,t) \in Q. \tag{4.3}$$

Further, we assume that g, ψ_1, ψ_2 are smooth functions and the kernel $K \in \mathcal{C}^2(Q)$, and the admissible conditions $g(0) = \psi_1(0)$, $g(\ell) = \psi_2(0)$ hold.

In this chapter, our main aim is to solve the FIDE given in (4.1) analytically and numerically. First, we obtain the analytical solution of the IBVP (4.1) by using the Sumudu decomposition technique. More precisely, we prove the existence and uniqueness results of the analytical solution of the IBVP (4.1) by utilizing the Sumudu decomposition method and the maximum-minimum principle. Further, we propose a numerical technique for solving the IBVP (4.1), which comprises the L1-discretization for the fractional-time derivative and the cubic spline approximation for the spatial derivatives. To obtain the numerical solution of the FIDE (4.1), first, we apply the L1-discretization for the fractional-time derivative and trapezoidal rule for the integral term to semi-discretize the IBVP (4.1) with respect to the time variable, and we investigate the stability and convergence of the semi-discrete problem. Then, we apply the cubic spline method to discretize the spatial derivatives appearing in the resultant semi-discrete problem to obtain the fully discrete scheme for the IBVP (4.1). The stability of the fully discrete scheme is analyzed through the discrete maximum principle, and error estimates are obtained. Theoretical results are validated through several numerical examples. To show the efficiency and accuracy of the proposed numerical scheme, we have compared our results with the numerical results given in [95].

We organize the remaining part of this chapter as follows: We present the existence and uniqueness results of the analytical solution of the IBVP (4.1) in Section 4.2. The discretization of the problem and convergence analysis of the numerical solution are discussed in section 4.3. Finally, in Section 4.4, numerical experiments are carried out.

4.2 Continuous problem

In this section, we study the existence and uniqueness of the analytical solution for IBVP (4.1).

4.2.1 Existence of the solution

Here, we investigate the analytical solution of the IBVP (4.1) in the series form using the Sumudu decomposition method.

By applying the Sumudu transformation to the IBVP (4.1) with respect to t, and using the initial condition and Theorem 1.2, we obtain the following:

$$\mu^{-\alpha}\big(\mathbb{S}_t[u(x,t)] - g(x)\big) + \mathbb{S}_t[\mathcal{L}(u(x,t)) + \lambda\big(K(x,\cdot) * u(x,\cdot)\big)(t)] = \mathbb{S}_t[f(x,t)]. \tag{4.4}$$

By simplifying (4.4) and using the linearity and convolution property (Lemma 1.3) of $\mathbb{S}_t$, we get

$$\mathbb{S}_t[u(x,t)] = g(x) + \mu^{\alpha}\,\mathbb{S}_t\left[f(x,t) - \mathcal{L}(u(x,t))\right] - \lambda\mu^{\alpha+1}\mathbb{S}_t[K(x,t)]\mathbb{S}_t[u(x,t)]. \tag{4.5}$$

The Adomian decomposition method [1] consists of seeking the solution of the IBVP (4.1) in the series form:

$$u(x,t) = \sum_{j=0}^{\infty} u_j(x,t), \tag{4.6}$$

provided the infinite series of functions converges uniformly.

Substituting (4.6) in (4.5), and using the linearity of $\mathcal{L}$ and uniform convergence of the infinite series, we obtain that

$$\begin{aligned}\mathbb{S}_t\left[\sum_{j=0}^{\infty} u_j(x,t)\right] &= g(x) + \mu^{\alpha}\,\mathbb{S}_t\left[f(x,t) - \sum_{j=0}^{\infty}\mathcal{L}\left(u_j(x,t)\right)\right] \\ &\quad -\lambda\mu^{\alpha+1}\mathbb{S}_t[K(x,t)]\mathbb{S}_t\left[\sum_{j=0}^{\infty} u_j(x,t)\right] \\ &= g(x) + \mu^{\alpha}\,\mathbb{S}_t\left[f(x,t) - \sum_{j=0}^{\infty}\mathcal{L}\left(u_j(x,t)\right)\right] - \lambda\mu^{\alpha}\mathbb{S}_t\left[\sum_{j=0}^{\infty}\big(K(x,\cdot) * u_j(x,\cdot)\big)(t)\right]. \end{aligned} \tag{4.7}$$

Operating with the Sumudu inverse transform on both sides of (4.7) and using the properties of $\mathbb{S}_t$ and Theorem 1.1, we get

$$\begin{aligned}\sum_{j=0}^{\infty} u_j(x,t) &= g(x) + I_t^{\alpha}\left(f(x,t) - \sum_{j=0}^{\infty}\mathcal{L}\left(u_j(x,t)\right)\right) - \lambda I_t^{\alpha}\left[\sum_{j=0}^{\infty}\big(K(x,\cdot) * u_j(x,\cdot)\big)(t)\right] \\ &= g(x) + I_t^{\alpha} f(x,t) - \sum_{j=0}^{\infty} I_t^{\alpha}\mathcal{L}\left(u_j(x,t)\right) - \lambda\sum_{j=0}^{\infty} I_t^{\alpha}\big(K(x,\cdot) * u_j(x,\cdot)\big)(t).\end{aligned}$$

In order to obtain u_j, we define the following recurrence equations by Adomian

relation:

$$\begin{aligned} u_0(x,t) &= g(x) + I_t^\alpha f(x,t), \\ u_{j+1}(x,t) &= -\mathcal{L}\left(I_t^\alpha u_j(x,t)\right) - \lambda I_t^\alpha \left(K(x,\cdot) * u_j(x,\cdot)\right)(t), \quad j \geq 0. \end{aligned}$$

Finally, the truncated series solution $U_J(x,t), J \in \mathbb{N}$, can be approximated by

$$U_J(x,t) \approx \sum_{j=0}^{J} u_j(x,t),$$

and we define the solution of the IBVP (4.1) as

$$u(x,t) = \lim_{J\to\infty} U_J(x,t) = \sum_{j=0}^{\infty} u_j(x,t). \tag{4.8}$$

The convergence related results of the Adomian series (4.8) can be obtained in a similar way as discussed in [22, 44].

Assume that for sufficiently smooth f and g, the solution $u(x,t)$ is the analytical solution of the IBVP (4.1), *i.e.*, $u \in \mathcal{C}(\overline{Q}) \cap W_t^1((0,T)) \cap \mathcal{C}_x^2(\Omega)$ satisfies the IBVP (4.1), and further, u satisfies the following bounds for all $(x,t) \in \overline{\Omega} \times G$:

$$\begin{cases} \left|\dfrac{\partial^i u}{\partial x^i}(x,t)\right| \leq C, & \text{for } i = 0,1,2,3,4, \\ \left|\dfrac{\partial^i u}{\partial t^i}(x,t)\right| \leq C(1+t^{\alpha-i}), & \text{for } i = 0,1,2. \end{cases} \tag{4.9}$$

Example 4.1 *Consider the following problem :*

$$\begin{cases} {}^C\mathcal{D}_t^\alpha u(x,t) - \dfrac{\partial^2 u}{\partial x^2} + \displaystyle\int_0^t u(x,s)ds = t\sin(x)E_{\alpha,2}(-t^\alpha), \quad (x,t) \in (0,\pi) \times (0,1], \\ u(x,0) = \sin(x), \quad x \in [0,\pi], \\ u(0,t) = 0 = u(\pi,t), \quad t \in [0,1]. \end{cases} \tag{4.10}$$

This is a particular case of the IBVP (4.1) with $a = 1$, $b = c = 0$, $K = 1$, $\lambda = 1$, $\ell = \pi$ and $T = 1$. One can easily verify that $u(x,t) = E_{\alpha,1}(-t^\alpha)\sin(x)$ is the solution of the IBVP (4.10). Now one can compute the derivatives of u and can see that they satisfy

the bounds given in (4.9). From (4.9), we can see that u has a singularity along $t = 0$.

Figure 4.1 (a) illustrates the surface plot of the analytical solution $u(x,t)$ and Figure 4.1 (b) displays its cross section along $x = \frac{\pi}{4}$ for $\alpha = 0.4$. From these figures, we can observe that there is an initial layer in u along $t = 0$, as stated in (4.9).

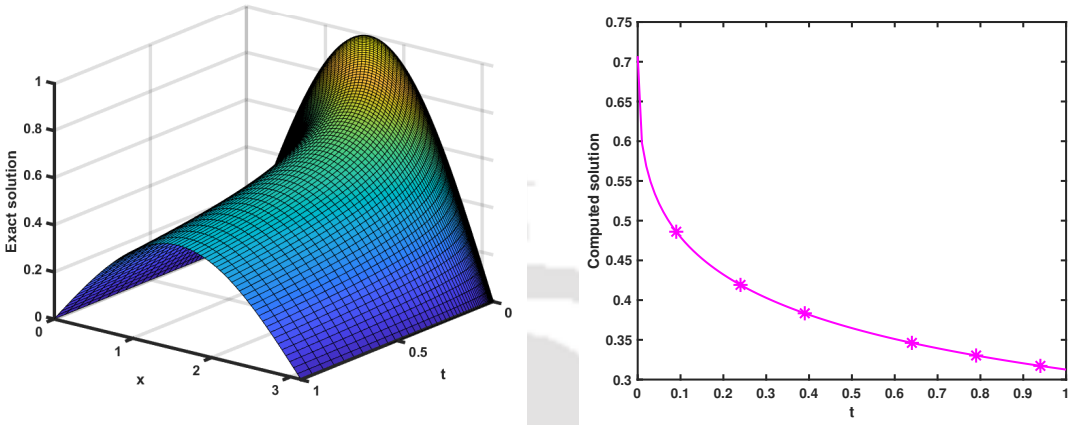

(a) Surface plot. *(b) Cross section of the solution along $x = \pi/4$.*

Figure 4.1: *Analytical solution for Example 4.1 with $\alpha = 0.4$.*

In general, like Example 4.1, the IBVP (4.1) will have a solution u with singularity along $t = 0$, whose presence leads to some difficulties in the numerical methods for solving the IBVP (4.1).

4.2.2 Uniqueness of the solution

The uniqueness of the solution for the IBVP (4.1) will be established here by using the maximum-minimum concept. The maximum principle for the IBVP (4.1) is stated in the following Theorem.

Theorem 4.2 *Let $u \in \mathcal{C}(\overline{Q}) \cap W_t^1((0,T)) \cap \mathcal{C}_x^2(\Omega)$ be a solution of the IBVP (4.1) with $f(x,t) \leq 0$, $(x,t) \in Q$. Then we have the following :*

$$u(x,t) \leq \max\left\{0, \max_{(x,t)\in S} u(x,t)\right\}, \quad \forall\,(x,t) \in \overline{Q},$$

where $S := \left(\overline{\Omega} \times \{0\}\right) \cup \left(\{0,\ell\} \times \overline{G}\right)$.

Proof. We will establish the result by using contradiction. Assume that the statement of the theorem does not hold true, *i.e.*, $\exists\,(x_0, t_0) \in Q$ with the property that

$$u(x_0, t_0) > \max_{(x,t)\in S}\{0, u(x,t)\} = \Phi_S \geq 0. \tag{4.11}$$

Let us consider $\varepsilon := u(x_0, t_0) - \Phi_S > 0$ and define the function v as

$$v(y,s) := u(y,s) + \frac{\varepsilon}{2}\left(\frac{T-s}{T}\right),\ (y,s) \in \overline{Q}. \tag{4.12}$$

It is clear that for $(y,s) \in \overline{Q}$, $v(y,s) \leq u(y,s) + \dfrac{\varepsilon}{2}$; and for $(y,s) \in S$,

$$v(x_0,t_0) \geq u(x_0,t_0) = \varepsilon + \Phi_S \geq \varepsilon + u(y,s) \geq \varepsilon + v(y,s) - \frac{\varepsilon}{2} = v(y,s) + \frac{\varepsilon}{2}.$$

This leads to the fact that the function v attains its maximum on $(\overline{Q} \setminus S)$. Let (x_1, t_1) be the maximum point of the function v over $\overline{Q}$, then $x_1 \in \Omega$, $t_1 \in G$ and

$$v(x_1,t_1) \geq v(x_0,t_0) \geq \varepsilon + \Phi_S \geq \varepsilon. \tag{4.13}$$

From the necessary conditions for the existence of maximum value of v over Ω and Theorem 1.3, we have

$$\begin{cases} {}^{C}\mathcal{D}_t^{\alpha} v(x_1,t_1) \geq 0, \\ \\ v_x(x_1,t_1) = 0, \quad v_{xx}(x_1,t_1) \leq 0. \end{cases} \tag{4.14}$$

From (4.12) and the property ${}^{C}\mathcal{D}_t^{\alpha} t^{\beta} = \dfrac{\Gamma(1+\beta)}{\Gamma(1-\alpha+\beta)}\, t^{\beta-\alpha},\ \beta > 0$, we have

$${}^{C}\mathcal{D}_t^{\alpha} u(x,t) = {}^{C}\,\mathcal{D}_t^{\alpha} v(x,t) + \frac{\varepsilon}{2T}\frac{t^{1-\alpha}}{\Gamma(2-\alpha)}, \quad (x,t) \in \overline{Q}. \tag{4.15}$$

Let $w(s) = v(x_1,s) - \dfrac{\varepsilon}{2}\left(\dfrac{T-s}{T}\right),\ s \in [0,t_1]$. Since $v(x_1,s)$ attains its maximum at $s = t_1$, so $v_s(x_1,s) \geq 0$ for $s \in [0,t_1]$. Therefore, w is strictly an increasing function over $[0,t_1]$, and

$$w(s) > w(0) = v(x_1,0) - \frac{\varepsilon}{2} = u(x_1,0) > 0,$$

as $(x_1,0) \in S$ and here we have used (4.11). Also, $w(t_1) > \dfrac{\varepsilon}{2}$.

By using the formulae (4.2), (4.13)-(4.15), the condition (4.3) and (4.12), we arrive at the following conclusion, for the point (x_1, t_1):

$$\begin{aligned} & {}^{C}\mathcal{D}_t^{\alpha} u(x_1,t_1) + \mathcal{L}u(x_1,t_1) + \lambda \int_0^{t_1} K(x_1, t_1 - s)u(x_1,s)ds - f(x_1,t_1) \\ = \;& {}^{C}\mathcal{D}_t^{\alpha} v(x_1,t_1) + \frac{\varepsilon}{2T}\frac{{t_1}^{1-\alpha}}{\Gamma(2-\alpha)} + \mathcal{L}v(x_1,t_1) - c(x_1,t_1)\frac{\varepsilon}{2T}(T-t_1) \\ & \qquad + \lambda \int_0^{t_1} K(x_1, t_1 - s)w(s)ds - f(x_1,t_1) \\ > \;& \frac{\varepsilon}{2T}\frac{{t_1}^{1-\alpha}}{\Gamma(2-\alpha)} + c(x_1,t_1)\left[v(x_1,t_1) - \frac{\varepsilon}{2}\frac{T-t_1}{T}\right] \\ > \;& 0, \end{aligned}$$

which contradicts that u is the solution of the IBVP (4.1). Therefore our assumption taken in (4.11) is wrong and hence the proof is completed. □

If we replace u by $-u$ and assuming that $f \geq 0$ in Theorem 4.2, then we obtain the minimum principle in a similar way, which is stated below.

Theorem 4.3 *Let $u \in \mathcal{C}(\overline{Q}) \cap W_t^1((0,T)) \cap \mathcal{C}_x^2(\Omega)$ be a solution of the IBVP (4.1) and $f(x,t) \geq 0$, $(x,t) \in Q$. Then we have the following :*

$$u(x,t) \geq \min_{(x,t)\in S} u(x,t), \quad \forall\, (x,t) \in \overline{Q},$$

where $S := \big(\overline{\Omega} \times \{0\}\big) \cup \big(\{0, \ell\} \times \overline{G}\big)$.

In the following theorem, by using the maximum and minimum principles given in Theorems 4.2 and 4.3, respectively, we show that if the IBVP (4.1) has a solution, then the solution is continuously dependent on the given data of the problem, *i.e.*, the solution is stable.

Theorem 4.4 *Let u be the analytical solution of the IBVP (4.1), i.e., $u \in \mathcal{C}(\overline{Q}) \cap W_t^1((0,T)) \cap \mathcal{C}_x^2(\Omega)$, and $f \in \mathcal{C}(\overline{Q})$, then we have the following estimate:*

$$\|u\|_Q \leq \max\{\|g\|_\Omega, \|\psi_1\|_G, \|\psi_2\|_G\} + \frac{T^\alpha}{\Gamma(1+\alpha)}\|f\|_Q.$$

Proof. Let us consider the function W defined by

$$W(x,t) := u(x,t) - \frac{\|f\|_Q}{\Gamma(1+\alpha)}t^\alpha, \quad (x,t) \in \overline{Q}.$$

Then W is the analytical solution of the IBVP (4.1) with

$$\widehat{\psi}_i(x,t) := \psi_i(x,t) - \frac{\|f\|_Q}{\Gamma(1+\alpha)}t^\alpha,$$

and

$$\widehat{f}(x,t) := f(x,t) - \|f\|_Q - c(x,t)\frac{\|f\|_Q\, t^\alpha}{\Gamma(1+\alpha)} - \frac{\lambda\|f\|_Q}{\Gamma(1+\alpha)}\int_0^t s^\alpha K(x,t-s)ds,$$

instead of ψ_i $(i = 1,2)$ and f, respectively. The function $\widehat{f}$ satisfies the condition $\widehat{f}(x,t) \leq 0$, $(x,t) \in \overline{Q}$. Then applying the maximum principle given in Theorem 4.2 to the analytical solution W, we obtain

$$W(x,t) \leq \max\{\|g\|_\Omega, \|\psi_1\|_G, \|\psi_2\|_G\}, \quad (x,t) \in \overline{Q}. \tag{4.16}$$

Therefore, from (4.16), for all $(x,t) \in \overline{Q}$, we have the following

$$u(x,t) = W(x,t) + \frac{\|f\|_Q}{\Gamma(1+\alpha)}t^\alpha \leq \max\{\|g\|_\Omega, \|\psi_1\|_G, \|\psi_2\|_G\} + \frac{\|f\|_Q}{\Gamma(1+\alpha)}T^\alpha. \tag{4.17}$$

In a similar way as done above, by applying Theorem 4.3 to the function

$$W(x,t) := u(x,t) + \frac{\|f\|_Q}{\Gamma(1+\alpha)}t^\alpha, \quad (x,t) \in \overline{Q},$$

we can obtain the following

$$u(x,t) \geq -\max\{\|g\|_\Omega, \|\psi_1\|_G, \|\psi_2\|_G\} - \frac{\|f\|_Q}{\Gamma(1+\alpha)}T^\alpha, (x,t) \in \overline{Q}. \tag{4.18}$$

Combining (4.17) and (4.18) we get our required result. □

We will establish the uniqueness of the solution for the IBVP (4.1) in the following theorem.

Theorem 4.5 *For sufficiently smooth functions f and g, the IBVP given in (4.1) admits a unique analytical solution.*

Proof. In Subsection 4.2.1, for sufficiently smooth functions f, g, we have shown the existence of the analytical solution of the IBVP (4.1) by using the Sumudu decomposition method.

In order to prove the uniqueness, let us assume that there exist two solutions to the IBVP (4.1), namely v_1 and v_2. Then $v_1 - v_2$ will be the solution of the homogeneous IBVP of the form (4.1), *i.e.*, with $f = 0, g = 0, \psi_1 = \psi_2 = 0$. Hence, from Theorem 4.4, we have $\|v_1 - v_2\|_Q = 0$, *i.e.*, $v_1 \equiv v_2$, which shows that the IBVP (4.1) has a unique solution. □

4.3 Discrete problem and convergence analysis

In this section, we study the numerical discretization of the IBVP (4.1) and the corresponding convergence analysis.

4.3.1 The temporal semi-discretization

For finding the numerical approximate solution of the IBVP (4.1), first, we discretize the time fractional derivative by using the L1-discretization and the integral term by using trapezoidal rule. Set $t_n = T\left(\frac{n-1}{N}\right)^r$ for $n = 1, 2, \cdots, N+1$, where $r \geq 1$ is a constant and N is a fixed positive integer. Let $\overline{G}^N = \{t_n : 1 \leq n \leq N+1\}$ denotes the discretized time domain. The temporal graded mesh is given by $\overline{Q}^N = \{(x, t_n) : x \in \overline{\Omega},\, t_n \in \overline{G}^N\}$.

Since the solution of the IBVP (4.1) has singularities along $t = 0$ as seen in (4.9), we use graded mesh to discretize the temporal domain, which increases the accuracy in numerical solutions than the same over uniform mesh.

In order to approximate the integral term appearing in (4.1), we use the following composite trapezoidal rule on the graded mesh $\overline{Q}^N$:

$$\begin{aligned}\int_0^{t_n} K(x, t_n - s)u(x, s)ds &= \sum_{j=1}^{n-1} \int_{t_j}^{t_{j+1}} K(x, t_n - s)u(x, s)ds \\ &= \sum_{j=1}^{n-1} \frac{\tau_j}{2}[K(x, t_n - t_j)u(x, t_j) + K(x, t_n - t_{j+1})u(x, t_{j+1})] \\ &= \sum_{j=1}^{n} K(x, t_n - t_j)u(x, t_j)\, I_j, \end{aligned} \tag{4.19}$$

where

$$I_j = \begin{cases} \dfrac{\tau_1}{2}, & j = 1, \\ \dfrac{1}{2}(\tau_j + \tau_{j-1}), & 2 \le j \le n-1, \\ \dfrac{\tau_{n-1}}{2}, & j = n. \end{cases}$$

Now, using L1-discretization (1.10) for the Caputo fractional derivative and trapezoidal rule for the integral term in (4.1), we obtain the following semi-discrete scheme:

$$\begin{cases} (\widehat{d}_{n,n-1} I + \mathcal{L}^N)\widehat{u}^n(x) = \mathcal{F}^n(x), \\ \widehat{u}^n(0) = \psi_1^n, \quad \widehat{u}^n(\ell) = \psi_2^n, \quad \text{for} \quad n = 2, 3, \cdots, N+1, \end{cases} \tag{4.20}$$

where I is the identity operator, and

$$\mathcal{L}^N \widehat{u}^n(x) = -a^n(x)\frac{d^2\widehat{u}^n}{dx^2} + b^n(x)\frac{d\widehat{u}^n}{dx} + c^n(x)\widehat{u}^n(x) + \lambda K(x,0) I_n\, \widehat{u}^n(x),$$

and

$$\mathcal{F}^n(x) = f^n(x) + \widehat{d}_{n,1}\, g(x) + \sum_{j=2}^{n-1} [\widehat{d}_{n,j} - \widehat{d}_{n,j-1}]\, \widehat{u}^j(x) - \lambda \sum_{j=1}^{n-1} K(x, t_n - t_j) I_j\, \widehat{u}^j(x),$$

$\widehat{u}^n(x)$ denotes the approximation of $u(x,t)$ at $t = t_n$.

Let $\mathcal{R}^n(x)$ denotes the truncation error due to the temporal discretization, which is defined as:

$$\mathcal{R}^n(x) = \mathcal{R}_1^n(x) + \mathcal{R}_2^n(x), \tag{4.21}$$

where

$$\begin{aligned} \mathcal{R}_1^n(x) &:= ({}^{C}_{L1}\mathcal{D}_N^{\alpha} - {}^{C}\mathcal{D}_t^{\alpha})u(x,t_n) = \left| \sum_{j=1}^{n-1} \mathcal{E}_{n,j} \right|, \\ \mathcal{E}_{n,j} &= \frac{1}{\Gamma(1-\alpha)} \int_{s=t_j}^{t_{j+1}} (t_n - s)^{-\alpha} \left[\frac{u(x,t_{j+1}) - u(x,t_j)}{\tau_j} - \frac{\partial u}{\partial s}(x,s) \right] ds, \\ \mathcal{R}_2^n(x) &:= \lambda \sum_{j=1}^{n-1} \frac{-\tau_j^3}{12} \frac{\partial^2}{\partial t^2} \big[K(x, t_n - \xi_j) u(x, \xi_j) \big], \quad \xi_j \in (t_j, t_{j+1}). \end{aligned} \tag{4.22}$$

In the next lemma we discuss about the bounds of the truncation error $\mathcal{R}_1^n(x)$.

Lemma 4.1 *Assume that $\widehat{u}(x,t_n)$ is the solution of the semi-discrete problem (4.20), which satisfies the conditions given in (4.9) for $(x,t_n) \in \overline{Q}^N$. Then, for each $(x,t_n) \in \overline{Q}^N$, we have the following bound:*

$$\|\mathcal{R}_1^n\|_\Omega \leq Cn^{-\min\{2-\alpha, r\alpha\}}.$$

Proof. The detailed proof can be seen in [106, Lemma 5.2]. □

The following lemma provides the bounds of the truncation error $\mathcal{R}_2^n(x)$.

Lemma 4.2 *Assume that the solution $\widehat{u}(x,t_n)$ of (4.20) satisfies the conditions given in (4.9) for $(x,t_n) \in \overline{Q}^N$. Then, the remainder term $\mathcal{R}_2^n(x)$ for $n = 2, \cdots, N+1$ satisfies following inequality:*

$$\|\mathcal{R}_2^n\|_\Omega \leq \begin{cases} Cn^{-\min\{r(\alpha+1), 4-2r(\alpha+1)\}}, & r(\alpha+1) \neq 2, \\ Cn^{-2}\ln(n), & r(\alpha+1) = 2. \end{cases} \tag{4.23}$$

Proof. From the mean-value theorem, we have

$$\tau_j = T\left(\frac{j}{N}\right)^r - T\left(\frac{j-1}{N}\right)^r \leq CN^{-r}j^{r-1}, \quad j = 1, 2, \cdots, N. \tag{4.24}$$

From (4.9), (4.22) and (4.24) and using the fact that $K \in \mathcal{C}^2(Q)$, we have

$$\begin{aligned} |\mathcal{R}_2^n(x)| &\leq C\sum_{j=1}^{n-1}\tau_j^3 \sum_{i=0}^{2}\left|\frac{\partial^i u}{\partial t^i}(x,\xi_j)\right|, \quad \xi_j \in (t_j, t_{j+1}), \\ &\leq C\sum_{j=1}^{n-1}(N^{-r}j^{r-1})^3\,\xi_j^{\alpha-2} \\ &< C\sum_{j=1}^{n-1}N^{-3r}j^{3(r-1)}\left(\frac{j}{N}\right)^{r(\alpha-2)} \\ &= C\sum_{j=1}^{n-1}N^{-r(\alpha+1)}\,j^{r(\alpha+1)-3} \\ &\leq Cn^{-r(\alpha+1)}\sum_{j=1}^{n-1}j^{r(\alpha+1)-3}, \end{aligned}$$

here in the third inequality we have used $\xi_j^{\alpha-2} \leq t_j^{\alpha-2}$, as $\alpha < 2$.

From the well-known convergence outcomes of this kind, we have

$$|\mathcal{R}_2^n(x)| \leq \begin{cases} Cn^{-r(\alpha+1)}, & r(\alpha+1) < 2, \\ Cn^{-2}\ln(n), & r(\alpha+1) = 2, \\ Cn^{2r(\alpha+1)-4}, & r(\alpha+1) > 2. \end{cases}$$

Hence we get our required result. □

We have established the truncation error bound due to temporal semidiscretization of the IBVP (4.1) in the following lemma.

Lemma 4.3 *For each $n = 2, \cdots, N+1$, we have the following truncation error bound:*

$$\|\mathcal{R}^n\|_\Omega \leq Cn^{-\min\{2-\alpha, r\alpha, 4-2r(\alpha+1)\}}.$$

Proof. We have $n^{-r\alpha} \geq Cn^{-r(\alpha+1)}\ln(n)$, if $r(\alpha+1) \leq 2$ and $n^{-(2-\alpha)} \geq n^{-2}$, if $r(\alpha+1) > 2$. Therefore, by combining Lemma 4.1 and Lemma 4.2, we get the required result. □

The next lemma will be used in the stability estimate of the semi-discrete problem (4.20).

Lemma 4.4 *The solution of the semi-discrete problem (4.20) satisfies*

$$\|\widehat{u}^n\|_\Omega \leq C\tau_{n-1}^\alpha(\|a^n\|_\Omega + \|b^n\|_\Omega + \|f^n\|_\Omega) + \tau_{n-1}^\alpha\Gamma(2-\alpha)\left[\widehat{d}_{n,1} + \lambda I_1\|K(\cdot,t_n)\|_\Omega\right]\|g\|_\Omega$$
$$+\tau_{n-1}^\alpha\Gamma(2-\alpha)\sum_{j=2}^{n-1}\left[\widehat{d}_{n,j} - \widehat{d}_{n,j-1} + \lambda I_j\|K(\cdot,t_n-t_j)\|_\Omega\right]\|\widehat{u}^j\|_\Omega, \quad 2 \leq n \leq N+1.$$

Proof. From (4.20) and using (3.28), we have

$$\left[\widehat{d}_{n,n-1} + c^n(x) + \lambda K(x,0)I_n\right]\|\widehat{u}^n\|_\Omega \leq C\left(\|a^n\|_\Omega + \|b^n\|_\Omega + \|f^n\|_\Omega\right)$$
$$+\left[\widehat{d}_{n,1} + \lambda I_1\|K(\cdot,t_n)\|_\Omega\right]\|g\|_\Omega + \sum_{j=2}^{n-1}\left[\widehat{d}_{n,j} - \widehat{d}_{n,j-1} + \lambda I_j\|K(\cdot,t_n-t_j)\|_\Omega\right]\|\widehat{u}^j\|_\Omega.$$

By using the assumption given in (4.3) and (4.9), we get

$$\begin{aligned}\widehat{d}_{n,n-1}\|\widehat{u}^n\|_\Omega &\leq C\left(\|a^n\|_\Omega+\|b^n\|_\Omega+\|f^n\|_\Omega\right)+\left[\widehat{d}_{n,1}+\lambda I_1\|K(\cdot,t_n)\|_\Omega\right]\|g\|_\Omega\\ &\quad+\sum_{j=2}^{n-1}\left[\widehat{d}_{n,j}-\widehat{d}_{n,j-1}+\lambda I_j\|K(\cdot,t_n-t_j)\|_\Omega\right]\|\widehat{u}^j\|_\Omega.\end{aligned}$$

Thus, we get our desired result. □

For $n=2,3,\cdots,N+1$ and $j=2,3,\cdots,n$, we recall $\vartheta_{n,j}$ defined in (3.31). The next theorem presents the stability estimate for the solution of the semi-discrete problem.

Theorem 4.6 *The solution of the temporal semi-discretized scheme (4.20) satisfies the following stability estimate:*

$$\|\widehat{u}^n\|_\Omega\leq C\left(\|g\|_\Omega+\tau_{n-1}^{\alpha}\sum_{j=1}^{n}\vartheta_{n,j}\left(\|a^j\|_\Omega+\|b^j\|_\Omega+\|f^j\|_\Omega\right)\right),\quad 2\leq n\leq N+1.$$

Proof. It is clear that, $\widehat{d}_{n,1}<\dfrac{\tau_{n-1}^{-\alpha}}{\Gamma(1-\alpha)}$. Therefore, from Lemma 4.4, we can obtain

$$\begin{aligned}\|\widehat{u}^n\|_\Omega &\leq \left[(1-\alpha)+\frac{\lambda\tau_{\max}^{\alpha+1}}{2}\|K\|_Q\right]\|g\|_\Omega+C\tau_{n-1}^{\alpha}\sum_{j=2}^{n}\vartheta_{n,j}\left(\|a^j\|_\Omega+\|b^j\|_\Omega+\|f^j\|_\Omega\right)\\ &\quad+\tau_{n-1}^{\alpha}\Gamma(2-\alpha)\sum_{j=2}^{n-1}\left[\widehat{d}_{n,j}-\widehat{d}_{n,j-1}+\lambda I_j\|K(\cdot,t_n-t_j)\|_\Omega\right]\|\widehat{u}^j\|_\Omega\\ &= b_n+\sum_{j=2}^{n-1}\eta_j\|\widehat{u}^j\|_\Omega,\end{aligned}\tag{4.25}$$

where $b_n=\left[(1-\alpha)+\dfrac{\lambda\tau_{\max}^{\alpha+1}}{2}\|K\|_Q\right]\|g\|_\Omega+C\tau_{n-1}^{\alpha}\sum\limits_{j=2}^{n}\vartheta_{n,j}\left(\|a^j\|_\Omega+\|b^j\|_\Omega+\|f^j\|_\Omega\right)$, which is a non-decreasing sequence of non-negative numbers, and

$$\eta_j=\tau_{n-1}^{\alpha}\Gamma(2-\alpha)\left[\widehat{d}_{n,j}-\widehat{d}_{n,j-1}+\lambda I_j\|K(\cdot,t_n-t_j)\|_\Omega\right]\geq 0.$$

Now, we have

$$\sum_{j=2}^{n-1}\eta_j=\tau_{n-1}^{\alpha}\Gamma(2-\alpha)\left[\widehat{d}_{n,n-1}-\widehat{d}_{n,1}+\lambda\sum_{j=2}^{n-1}I_j\|K(\cdot,t_n-t_j)\|_\Omega\right]$$

$$\begin{aligned} &\leq 1+\lambda\tau_{\max}^{\alpha+1}\Gamma(2-\alpha)\sum_{j=2}^{n-1}\|K(\cdot,t_n-t_j)\|_\Omega \\ &\leq 1+C\lambda\tau_{\max}^{\alpha+1}\Gamma(2-\alpha) \;\leq\; C. \end{aligned} \tag{4.26}$$

Applying Lemma 1.7 to (4.25) and using (4.26), we have

$$\begin{aligned} &\|\widehat{u}^n\|_\Omega \leq b_n \exp\left(\sum_{j=2}^{n-1}\eta_j\right) \\ &\leq \exp(C)\left\{\left[(1-\alpha)+\frac{\lambda\tau^{\alpha+1}}{2}\|K\|_Q\right]\|g\|_\Omega + C\tau_{n-1}^{\alpha}\sum_{j=2}^{n}\vartheta_{n,j}\left(\|a^j\|_\Omega+\|b^j\|_\Omega+\|f^j\|_\Omega\right)\right\} \\ &\leq C\left(\|g\|_\Omega+\tau_{n-1}^{\alpha}\sum_{j=2}^{n}\vartheta_{n,j}\left(\|a^j\|_\Omega+\|b^j\|_\Omega+\|f^j\|_\Omega\right)\right), \end{aligned}$$

which is the required result. □

The error due to the temporal semi-discretization of the IBVP (4.1) satisfies the bound given in the following theorem.

Theorem 4.7 *Let $e_N^n(x) = u(x,t_n) - \widehat{u}^n(x), (n = 1,2,\cdots,N+1)$ denotes the error associated with the semi-discretized scheme (4.20), where $u(x,t_n)$ and $\widehat{u}^n(x)$ are the solutions of (4.1) and (4.20) respectively, at the point (x,t_n). Then, we have the following bound:*

$$\sup_{n\leq N+1}\|u(\cdot,t_n)-\widehat{u}^n\|_\Omega \leq CN^{-\varrho},$$

where $\varrho := \min\{2-\alpha, r\alpha, 4-2r(\alpha+1)\}$.

Proof. If we define the temporal semidiscretization in (4.20) as $\mathbf{L}^N\widehat{u}^n(x) = f^n(x)$, then we get a similar equation for $e_N^n(x)$ as

$$\mathbf{L}^N e_N^n(x) = \mathcal{R}^n(x),$$

(observe that $e_N^1(x) = 0$, for all x, and $a = b = 0$ in the expression of $\mathbf{L}^N e_N^n(x)$). Hence, invoking Theorem 4.6, and Lemma 3.4 with $\varrho = \min\{2-\alpha, r\alpha, 4-2r(\alpha+1)\}$, we can obtain that

$$\|e_N^n\|_\Omega \leq C\tau_{n-1}^{\alpha}\sum_{j=1}^{n}\vartheta_{n,j}\|\mathcal{R}^j\|_\Omega \leq C\tau_{n-1}^{\alpha}\sum_{j=1}^{n}\vartheta_{n,j}\,j^{-\varrho} \leq CN^{-\varrho}.$$

Thus, by taking maximum over $n \leq N+1$, we get the required result. □

4.3.2 The fully discrete scheme

To find out the numerical solution of the semi-discrete problem (4.20), the spatial discretization is performed on a uniform mesh $\overline{\Omega}_M$, and finally we reach a fully discrete scheme. We use cubic spline approximation to the solution of the semi-discrete problem (4.20) on $\overline{\Omega}_M$ at each time step t_n.

Let $S^n(x)$ be the cubic spline approximation of $\widehat{u}^n(x)$ of (4.20) at t_n. On $[x_m, x_{m+1}]$, $S^n(x)$ has the following form:

$$S^n(x) = A_m^n + B_m^n(x - x_m) + C_m^n(x - x_m)^2 + D_m^n(x - x_m)^3, \quad m = 1, 2, \cdots, M,$$

where A_m^n, B_m^n, C_m^n, and D_m^n are constants.

Assume that $\widehat{u}_m^n$ is the approximation of $\widehat{u}^n(x)$ at x_m and $S^n(x_m) = \widehat{u}_m^n$, $S^n(x_{m+1}) = \widehat{u}_{m+1}^n$. From a simple algebraic calculation, we can obtain

$$\begin{cases} A_m^n = \widehat{u}_m^n, \quad B_m^n = \dfrac{\widehat{u}_{m+1}^n - \widehat{u}_m^n}{h} - \dfrac{h}{6}(2\mathcal{M}_m^n + \mathcal{M}_{m+1}^n), \\ C_m^n = \dfrac{\mathcal{M}_m^n}{2}, \quad D_m^n = \dfrac{1}{6h}(\mathcal{M}_{m+1}^n - \mathcal{M}_m^n), \end{cases}$$

where $\mathcal{M}_m^n = (S^n)''(x_m)$. Using the continuity of the first-order derivative at the mesh point x_m, we obtain the following equation:

$$\mathcal{M}_{m+1}^n + 4\mathcal{M}_m^n + \mathcal{M}_{m-1}^n = \frac{6}{h^2}(\widehat{u}_{m+1}^n - 2\widehat{u}_m^n + \widehat{u}_{m-1}^n). \tag{4.27}$$

From (4.20), we get

$$\begin{aligned} \mathcal{M}_m^n = \frac{1}{a_m^n}\Bigg(& \big[\widehat{d}_{n,n-1} + c_m^n + \lambda I_n K(x_m, 0)\big]\widehat{u}_m^n + b_m^n \left.\frac{d\widehat{u}^n}{dx}\right|_{x_m} - f_m^n \Bigg) \\ & - \big[\widehat{d}_{n,1} - \lambda I_1 K(x_m, t_n)\big]\frac{g_m}{a_m^n} - \sum_{j=2}^{n-1}\big[\widehat{d}_{n,j} - \widehat{d}_{n,j-1} - \lambda I_j K(x_m, t_n - t_j)\big]\frac{\widehat{u}_m^j}{a_m^n}. \end{aligned} \tag{4.28}$$

Using (4.28) and (3.39) in (4.27), for each time step t_n, $n = 2, 3, \cdots, N+1$, we have

the following fully discrete scheme:

$$\begin{cases} \mathcal{L}_M^N \widehat{u}_m^n = \mathcal{G}_m^n, \quad m = 2, 3, \cdots, M, \\ \\ \widehat{u}_1^n = \psi_1^n, \quad \widehat{u}_{M+1}^n = \psi_2^n, \end{cases} \tag{4.29}$$

where

$$\begin{aligned} \mathcal{L}_M^N \widehat{u}_m^n = & \left\{ \frac{1}{a_{m+1}^n} [\widehat{d}_{n,n-1} + c_{m+1}^n + \lambda I_n K(x_{m+1}, 0)] - \frac{6}{h^2} + \frac{3\sigma_{m+1}^n}{2h} + \frac{2\sigma_m^n}{h} - \frac{\sigma_{m-1}^n}{2h} \right\} \widehat{u}_{m+1}^n \\ & + \left\{ \frac{4}{a_m^n} [\widehat{d}_{n,n-1} + c_m^n + \lambda I_n K(x_m, 0)] + \frac{12}{h^2} - \frac{2\sigma_{m+1}^n}{h} + \frac{2\sigma_{m-1}^n}{h} \right\} \widehat{u}_m^n \\ & + \left\{ \frac{1}{a_{m-1}^n} [\widehat{d}_{n,n-1} + c_{m-1}^n + \lambda I_n K(x_{m-1}, 0)] - \frac{6}{h^2} + \frac{\sigma_{m+1}^n}{2h} - \frac{2\sigma_m^n}{h} - \frac{3\sigma_{m-1}^n}{2h} \right\} \widehat{u}_{m-1}^n, \end{aligned} \tag{4.30}$$

and

$$\begin{aligned} \mathcal{G}_m^n = & \left(\frac{f_{m+1}^n}{a_{m+1}^n} + \frac{4f_m^n}{a_m^n} + \frac{f_{m-1}^n}{a_{m-1}^n} \right) + \frac{g_{m+1}}{a_{m+1}^n} \left[\widehat{d}_{n,1} - \lambda I_1 K(x_{m+1}, t_n) \right] \\ & + \sum_{j=2}^{n-1} \left[\widehat{d}_{n,j} - \widehat{d}_{n,j-1} - \lambda I_j K(x_{m+1}, t_n - t_j) \right] \frac{\widehat{u}_{m+1}^j}{a_{m+1}^n} + \frac{4g_m}{a_m^n} \left[\widehat{d}_{n,1} - \lambda I_1 K(x_m, t_n) \right] \\ & + 4 \sum_{j=2}^{n-1} \left[\widehat{d}_{n,j} - \widehat{d}_{n,j-1} - \lambda I_j K(x_m, t_n - t_j) \right] \frac{\widehat{u}_m^j}{a_m^n} + \frac{g_{m-1}}{a_{m-1}^n} \left[\widehat{d}_{n,1} - \lambda I_1 K(x_{m-1}, t_n) \right] \\ & + \sum_{j=2}^{n-1} \left[\widehat{d}_{n,j} - \widehat{d}_{n,j-1} - \lambda I_j K(x_{m-1}, t_n - t_j) \right] \frac{\widehat{u}_{m-1}^j}{a_{m-1}^n}, \end{aligned} \tag{4.31}$$

with $\sigma_m^n = \dfrac{b_m^n}{a_m^n}$.

For each time step n, the unknowns $v^n := [\widehat{u}_2^n, \widehat{u}_3^n, \cdots, \widehat{u}_M^n]^T$ are the solution of the linear system

$$\mathcal{A} v^n = \mathcal{P}^n, \tag{4.32}$$

where $\mathcal{P}^n := \left[\gamma_0^n + \mathcal{G}_2^n, \mathcal{G}_3^n, \cdots, \mathcal{G}_{M-1}^n, \mathcal{G}_M^n + \gamma_1^n\right]^T$ with the boundary terms γ_0^n, γ_1^n, which are extracted from $\mathcal{L}_M^N$ and $\mathcal{A} = [\mathcal{A}_{i,m}]_{i,m=1}^{M-1}$ denotes the $(M-1) \times (M-1)$ stiffness matrix corresponding to the discretization (4.29) and (4.30).

Lemma 4.5 *(Discrete maximum principle) Under the conditions given in (4.3), along*

with the assumption on the mesh width h:

$$0 < h < \frac{-H + \sqrt{H^2 + 24Ja_*}}{2J}, \tag{4.33}$$

where $J = \widehat{d}_{\max} + \|c\|_Q + \frac{\lambda}{2}\tau K^*$, $H = \frac{a_*}{2}(7\Sigma^* - \sigma_*)$, $a_* = \min_{m,n} a_m^n$, $\Sigma^* = \max_{m,n} |\sigma_m^n|$, $\sigma_* = \min_{m,n} |\sigma_m^n|$, $K^* = \max_m K(x_m, 0)$, $\widehat{d}_{\max} = \max_n \widehat{d}_{n,n-1}$, *one can prove that the operator* $\mathcal{L}_M^N$ *defined in (4.30) satisfies the discrete maximum principle.*

Proof. Here we have to show that the stiffness matrix $\mathcal{A}$ (defined in (4.32)) associated with $\mathcal{L}_M^N$ is an M-matrix. From (4.33), it is clear that

$$\widehat{d}_{\max} + \|c\|_Q + \frac{\lambda}{2}\tau K^* + \frac{a_*}{2h}(7\Sigma^* - \sigma_*) < \frac{6a_*}{h^2}. \tag{4.34}$$

For $3 \le m \le M$, we have

$$\begin{aligned}
\mathcal{A}_{m-1,m-2} &= \frac{1}{a_{m-1}^n}\left[\widehat{d}_{n,n-1} + c_{m-1}^n + \lambda I_n K(x_{m-1}, 0)\right] - \frac{6}{h^2} + \frac{\sigma_{m+1}^n}{2h} - \frac{2\sigma_m^n}{h} - \frac{3\sigma_{m-1}^n}{2h} \\
&\le \frac{1}{a_*}\left[\widehat{d}_{\max} + \|c\|_Q + \frac{\lambda}{2}\tau K^*\right] - \frac{6}{h^2} + \frac{\sigma_{m+1}^n}{2h} - \frac{2\sigma_m^n}{h} - \frac{3\sigma_{m-1}^n}{2h} \\
&< \frac{6}{h^2} - \frac{1}{2h}(7\Sigma^* - \sigma_*) - \frac{6}{h^2} + \frac{\sigma_{m+1}^n}{2h} - \frac{2\sigma_m^n}{h} - \frac{3\sigma_{m-1}^n}{2h} \\
&\le -\frac{1}{2h}(\Sigma^* - 7\sigma_*) + \frac{\sigma_{m+1}^n}{2h} - \frac{2\sigma_m^n}{h} - \frac{3\sigma_{m-1}^n}{2h} \\
&= -\frac{1}{2h}\left(\Sigma^* - \sigma_{m+1}^n\right) + \frac{2}{h}(\sigma_* - \sigma_m^n) + \frac{3}{2h}\left(\sigma_* - \sigma_{m-1}^n\right) \\
&\le 0,
\end{aligned} \tag{4.35}$$

where we have used the inequality (4.34) and the fact that $(7\Sigma^* - \sigma_*) \ge (\Sigma^* - 7\sigma_*)$.

By using the inequality (4.34), for $2 \le m \le M-1$, we have

$$\begin{aligned}
\mathcal{A}_{m-1,m} &= \frac{1}{a_{m+1}^n}\left[\widehat{d}_{n,n-1} + c_{m+1}^n + \lambda I_n K(x_{m+1}, 0)\right] - \frac{6}{h^2} + \frac{3\sigma_{m+1}^n}{2h} + \frac{2\sigma_m^n}{h} - \frac{\sigma_{m-1}^n}{2h} \\
&\le \frac{1}{a_*}\left[\widehat{d}_{\max} + \|c\|_Q + \frac{\lambda}{2}\tau K^*\right] - \frac{6}{h^2} + \frac{3\sigma_{m+1}^n}{2h} + \frac{2\sigma_m^n}{h} - \frac{\sigma_{m-1}^n}{2h} \\
&< \frac{6}{h^2} - \frac{1}{2h}(7\Sigma^* - \sigma_*) - \frac{6}{h^2} + \frac{3\sigma_{m+1}^n}{2h} + \frac{2\sigma_m^n}{h} - \frac{\sigma_{m-1}^n}{2h} \\
&= -\frac{3}{2h}\left(\Sigma^* - \sigma_{m+1}^n\right) - \frac{2}{h}(\Sigma^* - \sigma_m^n) + \frac{1}{2h}\left(\sigma_* - \sigma_{m-1}^n\right) \\
&\le 0.
\end{aligned} \tag{4.36}$$

By using (4.35) and (4.36), for $3 \leq m \leq M-1$, we have

$$\begin{aligned}
& \mathcal{A}_{m-1,m-1} - |\mathcal{A}_{m-1,m-2}| - |\mathcal{A}_{m-1,m}| \\
= \; & \frac{4}{a_m^n}\left[\widehat{d}_{n,n-1} + c_m^n + \lambda I_n K(x_m,0)\right] + \frac{12}{h^2} - \frac{2\sigma_{m+1}^n}{h} + \frac{2\sigma_{m-1}^n}{h} \\
& + \frac{1}{a_{m-1}^n}[\widehat{d}_{n,n-1} + c_{m-1}^n + \lambda I_n K(x_{m-1},0)] - \frac{6}{h^2} + \frac{\sigma_{m+1}^n}{2h} - \frac{2\sigma_m^n}{h} - \frac{3\sigma_{m-1}^n}{2h} \\
& + \frac{1}{a_{m+1}^n}[\widehat{d}_{n,n-1} + c_{m+1}^n + \lambda I_n K(x_{m+1},0)] - \frac{6}{h^2} + \frac{3\sigma_{m+1}^n}{2h} + \frac{2\sigma_m^n}{h} - \frac{\sigma_{m-1}^n}{2h} \\
= \; & \left(\frac{1}{a_{m+1}^n} + \frac{4}{a_m^n} + \frac{1}{a_{m-1}^n}\right)\widehat{d}_{n,n-1} + \frac{1}{a_{m-1}^n}\left[c_{m-1}^n + \lambda I_n K(x_{m-1},0)\right] \\
& + \frac{4}{a_m^n}\left[c_m^n + \lambda I_n K(x_m,0)\right] + \frac{1}{a_{m+1}^n}\left[c_{m+1}^n + \lambda I_n K(x_{m+1},0)\right] \\
> \; & 0,
\end{aligned}$$

where we have used the fact that $\widehat{d}_{n,n-1} > 0$ and the conditions given in (4.3). Therefore, $\mathcal{A}_{m-1,m-1} > |\mathcal{A}_{m-1,m-2}| + |\mathcal{A}_{m-1,m}| > 0$, for $3 \leq m \leq M-1$.

By using the inequality (4.34) and the conditions given in (4.3), for $m = 2, M$, we have

$$\begin{aligned}
\mathcal{A}_{m-1,m-1} &= \frac{4}{a_m^n}\left[\widehat{d}_{n,n-1} + c_m^n + \lambda I_n K(x_m,0)\right] + \frac{12}{h^2} - \frac{2\sigma_{m+1}^n}{h} + \frac{2\sigma_{m-1}^n}{h} \\
&> \frac{2}{a_*}\left[\widehat{d}_{\max} + \|c\|_Q + \frac{\lambda}{2}\tau K^* + \frac{a_*}{2h}\left(7\Sigma^* - \sigma_*\right)\right] - \frac{2}{h}\left(\Sigma^* - \sigma_*\right) \\
&= \frac{2}{a_*}\left[\widehat{d}_{\max} + \|c\|_Q + \frac{\lambda}{2}\tau K^*\right] + \frac{1}{h}\left(5\Sigma^* + \sigma_*\right) \\
&> 0,
\end{aligned}$$

where we have used the fact that $\frac{4}{a_m^n}\left[\widehat{d}_{n,n-1} + c_m^n + \lambda I_n K(x_m,0)\right] > 0$ and the inequality (4.34) in the first inequality. Hence the stiffness matrix $\mathcal{A}$ associated with $\mathcal{L}_M^N$ is an M-matrix and therefore $\mathcal{L}_M^N$ satisfies the discrete maximum principle. □

From the discrete maximum principle given in Lemma 4.5, one can conclude that the fully discrete scheme (4.29) is stable in the maximum-norm. In the following theorem we establish the error estimate due to the spatial discretization by using the discrete maximum principle.

Theorem 4.8 *Let $\widehat{u}^n(x)$ be the solution of the semi-discrete problem (4.20) and $\{\widehat{u}_m^n\}$ be the solution of the fully discrete scheme (4.29). Then for each time step t_n, we have*

the following error estimate:

$$\|\widehat{u}^n(x_m) - \widehat{u}^n_m\|_{\overline{\Omega}_M} \leq Ch^2, \quad 1 \leq n \leq N+1.$$

Proof. From (4.29)-(4.30) and using equation (4.20), we have

$$\begin{aligned}\mathcal{L}^N_M\left(\widehat{u}^n(x_m)\right) &= \frac{1}{a^n_{m+1}}\left[\widehat{d}_{n,n-1}I + \mathcal{L}^N\right]\widehat{u}^n(x_{m+1}) + \frac{4}{a^n_m}\left[\widehat{d}_{n,n-1}I + \mathcal{L}^N\right]\widehat{u}^n(x_m) \\ &\quad + \frac{1}{a^n_{m-1}}\left[\widehat{d}_{n,n-1}I + \mathcal{L}^N\right]\widehat{u}^n(x_{m-1}). \qquad (4.37)\end{aligned}$$

Therefore, by taking the difference of (4.37) and (4.30), we have

$$\begin{aligned}&\left|\mathcal{L}^N_M\left(\widehat{u}^n(x_m) - \widehat{u}^n_m\right)\right| \\ &\leq \left|\frac{6}{h^2}\left(\widehat{u}^n_{m+1} - 2\widehat{u}^n_m + \widehat{u}^n_{m-1}\right) - \frac{d^2\widehat{u}^n}{dx^2}(x_{m+1}) - 4\frac{d^2\widehat{u}^n}{dx^2}(x_m) - \frac{d^2\widehat{u}^n}{dx^2}(x_{m-1})\right| \\ &\quad + \left|\sigma^n_{m+1}\right|\left|\frac{d\widehat{u}^n}{dx}(x_{m+1}) - \frac{3\widehat{u}^n_{m+1} - 4\widehat{u}^n_m + \widehat{u}^n_{m-1}}{2h}\right| \\ &\quad + 4\left|\sigma^n_m\right|\left|\frac{d\widehat{u}^n}{dx}(x_m) - \frac{\widehat{u}^n_{m+1} - \widehat{u}^n_{m-1}}{2h}\right| \\ &\quad + \left|\sigma^n_{m-1}\right|\left|\frac{d\widehat{u}^n}{dx}(x_{m-1}) - \frac{-\widehat{u}^n_{m+1} + 4\widehat{u}^n_m - 3\widehat{u}^n_{m-1}}{2h}\right| \\ &\leq \left(\left|\sigma^n_{m+1}\right| + 4\left|\sigma^n_m\right| + \left|\sigma^n_{m-1}\right|\right)Ch^2 \\ &\leq Ch^2,\end{aligned}$$

where we have used the equations (4.27) and (3.39). Hence, using the discrete maximum principle for $\mathcal{L}^N_M$ given in Lemma 4.5, we have obtained the required result. □

Next theorem established the error estimate for the fully discretization of the IBVP (4.1).

Theorem 4.9 *Let $u(x,t)$ be the exact solution of the IBVP (4.1) and $\widehat{u}^n_m$ be the discrete solution at (x_m, t_n) of the fully discrete scheme (4.29). Then the global error of the fully discrete scheme satisfies*

$$\|u(x_m,t_n) - \widehat{u}^n_m\|_{\overline{\Omega}_M} \leq C(N^{-\varrho} + h^2), \quad 1 \leq n \leq N+1,$$

where $\varrho = \min\{2-\alpha, r\alpha, 4-2r(\alpha+1)\}$.

Proof. The error at time level t_n can be decomposed as

$$\|u(x_m,t_n)-\widehat{u}_m^n\|_{\overline{\Omega}_M} \le \|u(x_m,t_n)-\widehat{u}^n(x_m)\|_{\overline{\Omega}_M} + \|\widehat{u}^n(x_m)-\widehat{u}_m^n\|_{\overline{\Omega}_M}\,.$$

From Theorem 4.7 and Theorem 4.8, we can obtain that

$$\|u(x_m,t_n)-\widehat{u}_m^n\|_{\overline{\Omega}_M} \le C\left(N^{-\varrho}+h^2\right).$$

Hence, the proof is complete. □

4.4 Numerical experiments

In this section, we conduct several numerical experiments to validate the proposed numerical method and the theoretical error estimates. The numerical results are compared with those produced by prior techniques available in the literature. We have used $r=(2-\alpha)/\alpha$ for the numerical experiments.

Example 4.10 *Consider the following IBVP on the domain* $Q:=(0,1)\times(0,1]$ *:*

$$\begin{cases} {}^{C}\mathcal{D}_t^{\alpha}u(x,t)-\dfrac{\partial^2 u}{\partial x^2}+\displaystyle\int_0^t x(t-s)u(x,s)ds=f(x,t),\ (x,t)\in Q,\\ u(x,0)=0,\quad \forall x\in[0,1],\\ u(0,t)=t+t^{\alpha},\quad u(1,t)=0,\quad \forall t\in(0,1]. \end{cases} \tag{4.38}$$

Here $f(x,t)$ is chosen in such a way that the exact solution of the problem (4.38) is $u(x,t)=(1-x^2)(t+t^{\alpha})$. Let $E_{M,N}=\max\limits_{m,n}|u(x_m,t_n)-\widehat{u}_m^n|$ denotes the computed maximum error and $R_{M,N}=\log_2\left(\dfrac{E_{M,N}}{E_{2M,2N}}\right)$ denotes the order of convergence.

Figure 4.2 displays the numerical solution of Example 4.10 for $\alpha=0.4$ and $\alpha=0.8$ with $M=N=64$. Table 4.1 presents the maximum error and order of convergence of the present numerical method on the graded mesh for the time domain and uniform mesh for the spatial domain and the method given in [95] on the uniform mesh. The errors as well as the order of convergence given in Table 4.1 reveal that the proposed approximation technique performs far better than the earlier method described in [95]. Figure 4.3 displays the comparison of the maximum errors (in time) of the present method with the method in [95] for Example 4.10 for various values of α, with $M=N=64$. The log-log plot of N vs. maximum errors for both the methods is depicted in

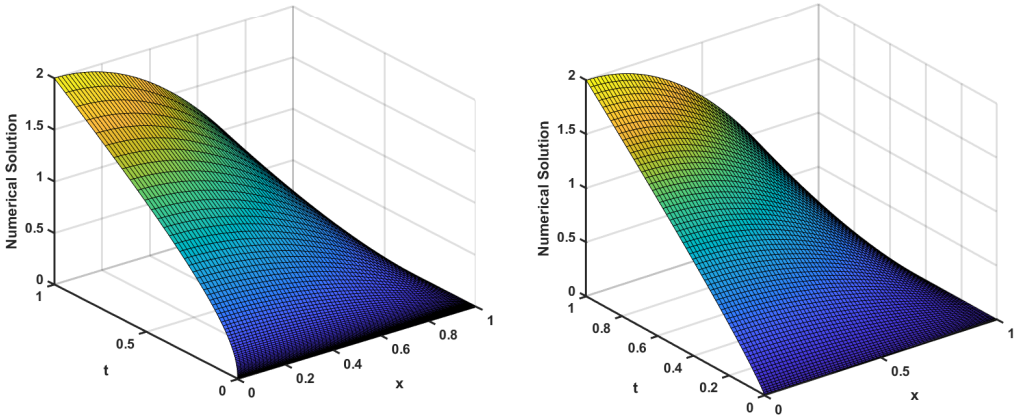

(a) For $\alpha = 0.4$. *(b) For $\alpha = 0.8$.*

Figure 4.2: *Surface plots of the numerical solutions for Example 4.10 with $M = N = 64$.*

Figure 4.4 corresponding to Table 4.1 with $N = M$.

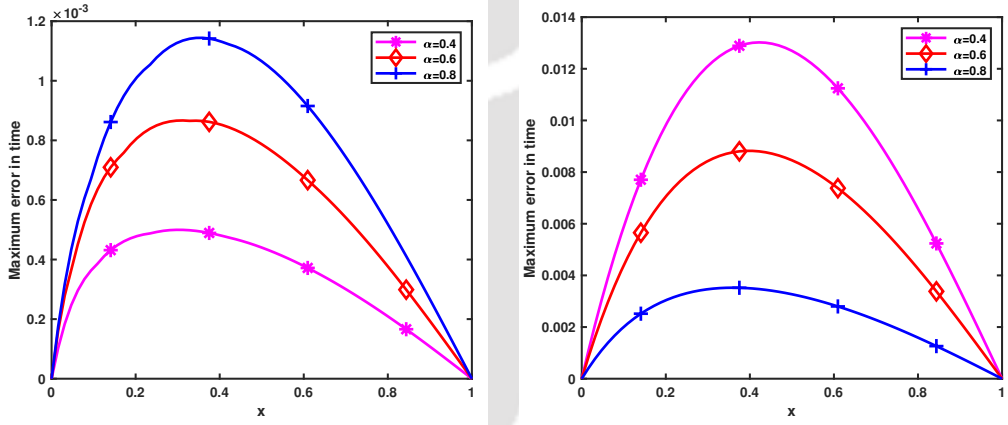

(a) By the proposed method. *(b) By the method given in [95].*

Figure 4.3: *Comparison of the maximum errors (in time) for Example 4.10.*

Finally, we apply the proposed method to the following most general time-fractional integro-partial diffusion-advection-reaction IBVP, to verify the accuracy and efficiency.

Table 4.1: $E_{M,N}$ *and* $R_{M,N}$ *for Example 4.10 with* $M = N$.

Order	Method		$N = 64$	$N = 128$	$N = 256$	$N = 512$	$N = 1024$
α=0.4	Present method	$E_{M,N}$	4.9969e-04	1.8612e-04	6.6651e-05	2.3306e-05	8.0331e-06
		$R_{M,N}$	1.4248	1.4815	1.5160	1.5367	–
		CPU (s)	0.147146	0.188501	0.997198	6.267940	144.459022
	Method in [95]	$E_{M,N}$	1.3022e-02	1.1640e-02	1.0214e-02	8.7980e-03	7.4440e-03
		$R_{M,N}$	0.1619	0.1885	0.2153	0.2411	–
		CPU (s)	0.29660	0.064791	0.478599	3.697276	31.355178
α=0.6	Present method	$E_{M,N}$	8.6677e-04	3.8105e-04	1.6002e-04	6.5240e-05	2.6039e-05
		$R_{M,N}$	1.1857	1.2517	1.2944	1.3251	–
		CPU (s)	0.110102	0.696580	3.251924	20.557401	147.909691
	Method in [95]	$E_{M,N}$	8.8219e-03	6.8197e-03	5.0877e-03	3.6865e-03	2.6110e-03
		$R_{M,N}$	0.3714	0.4227	0.4648	0.4977	–
		CPU (s)	0.013038	0.094350	0.495960	3.857545	32.105124
α=0.8	Present method	$E_{M,N}$	1.1441e-03	5.9561e-04	2.9922e-04	1.4623e-04	6.9895e-05
		$R_{M,N}$	0.9417	0.9932	1.0330	1.0649	–
		CPU (s)	0.107447	0.516708	3.161052	20.519396	117.658320
	Method in [95]	$E_{M,N}$	3.5240e-03	2.2877e-03	1.4296e-03	8.9469e-04	5.4590e-04
		$R_{M,N}$	0.6233	0.6783	0.6761	0.7127	–
		CPU (s)	0.012549	0.063796	0.484713	3.908563	32.355230

Example 4.11 *Consider the following IBVP for* $(x,t) \in Q := (0,2) \times (0,1]$*:*

$$\begin{cases} {}^{C}\mathcal{D}_t^{\alpha} u(x,t) + \mathcal{L}u(x,t) + 3\int_0^t \exp(-x(t-s))u(x,s)ds = f(x,t), \\ u(x,0) = 0, \quad \forall x \in [0,2], \\ u(0,t) = 0, \quad u(2,t) = 0, \quad \forall t \in (0,1], \end{cases}$$

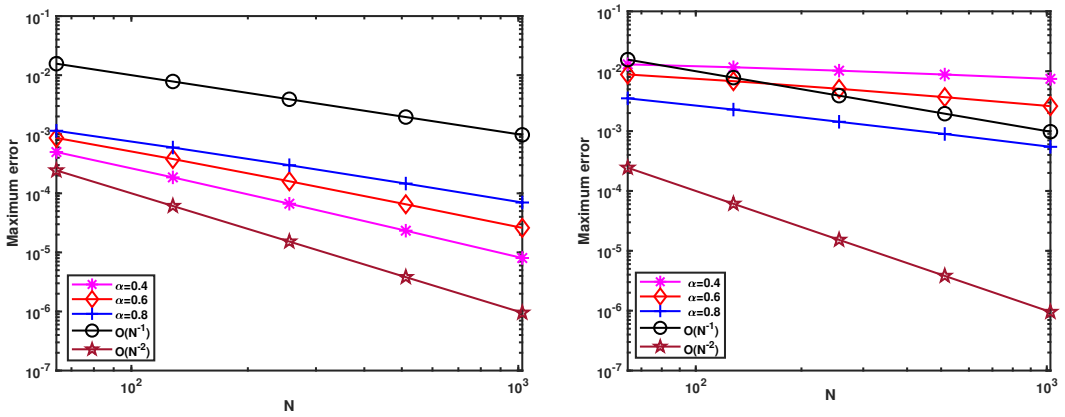

(a) By the present method. *(b) By the method given in [95].*

Figure 4.4: *Log-log plots for comparison of the order of convergence for Example 4.10.*

where $f(x,t) = \Gamma(1+\alpha)\sin\left(x+\dfrac{\pi x}{2}\right) + \dfrac{t^{3+\alpha}}{1+\alpha}\exp(x(1+t))$, *and*

$$\mathcal{L}u(x,t) = -(2+\sin(xt))\frac{\partial^2 u}{\partial x^2}(x,t) + (-3x^2t^4)\frac{\partial u}{\partial x}(x,t) + (2+t^2\exp(x))u(x,t).$$

The two-mesh principle described below will be used to calculate the error and the order of convergence, because the exact solution of Example 4.11 is not known. Let u_m^n $(m = 1, 2, \cdots, M+1,\ n = 1, 2, \cdots N+1)$ be the approximate solution of Example 4.11 obtained by using the proposed scheme (4.29) over the mesh $\{(x_m, t_n)\}$. Now consider another mesh $\{(\widehat{x}_m, \widehat{t}_n) : m = 1, 2, \cdots, 2M+1,\ n = 1, 2, \cdots, 2N+1\}$, where $\widehat{x}_m = (m-1)/(2M)$ and $\widehat{t}_n = ((n-1)/(2N))^r$, $r \geq 1$, and denote the computed solution of Example 4.11 over this mesh by z_m^n. It is easy to see that $x_m = \widehat{x}_{2m-1}$, $t_n = \widehat{t}_{2n-1}$ for $m = 1, \cdots, M+1$, $n = 1, \cdots, N+1$. Then, the maximum two-mesh differences are determined by

$$\mathcal{D}_{M,N} := \max_{\substack{1\leq n\leq N+1,\\ 1\leq m\leq M+1}} \left|u_m^n - z_{2m-1}^{2n-1}\right|,$$

and the rate of convergence is estimated by the formula:

$$R_{M,N} = \log_2\left(\frac{\mathcal{D}_{M,N}}{\mathcal{D}_{2M,2N}}\right).$$

Table 4.2 presents the maximum two-mesh differences and the corresponding order of convergence for Example 4.11 for $\alpha = 0.4, 0.6, 0.8$. The numerical solutions of Example

Table 4.2: $\mathcal{D}_{M,N}$ *and* $R_{M,N}$ *for Example 4.11 with* $M = N$.

Order		$N = 64$	$N = 128$	$N = 256$	$N = 512$	$N = 1024$
α=0.4	$\mathcal{D}_{M,N}$	1.0469e-03	6.3368e-04	3.5441e-04	1.8955e-04	9.8779e-05
	$R_{M,N}$	0.7243	0.8383	0.9028	0.9403	–
	CPU (s)	0.476189	1.844733	12.289036	65.663274	555.214601
α=0.6	$\mathcal{D}_{M,N}$	5.3066e-04	2.3939e-04	1.1118e-04	6.6933e-05	3.7766e-05
	$R_{M,N}$	1.1484	1.1065	0.7321	0.8256	–
	CPU (s)	0.231646	1.327460	9.077288	67.743251	657.712070
α=0.8	$\mathcal{D}_{M,N}$	8.3327e-04	4.2367e-04	2.0666e-04	9.8029e-05	4.5608e-05
	$R_{M,N}$	0.9758	1.0357	1.0759	1.1039	–
	CPU (s)	0.230143	1.394742	9.185984	68.491994	665.737263

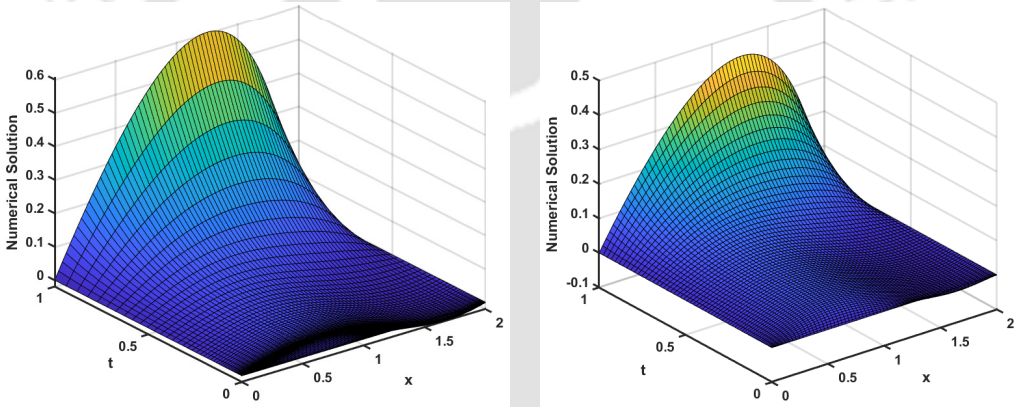

(a) For $\alpha = 0.4$. *(b) For* $\alpha = 0.8$.

Figure 4.5: *Surface plots of the numerical solution of Example 4.11 with* $M = N = 64$.

4.11 for $\alpha = 0.4$ and $\alpha = 0.8$ with $M = N = 64$ are shown in Figure 4.5. Figure 4.6 (a) displays the maximum errors (in time) for various values of α for Example 4.11 with $M = N = 64$, and log-log plot of N vs. maximum errors corresponding to Table 4.2 with $N = M$ is depicted in Figure 4.6 (b).

The numerical results presented in this section validate the theoretical error estimates given in Theorem 4.9. Also, one can observe that the proposed method is more accurate and efficient for TF-IPDEs.

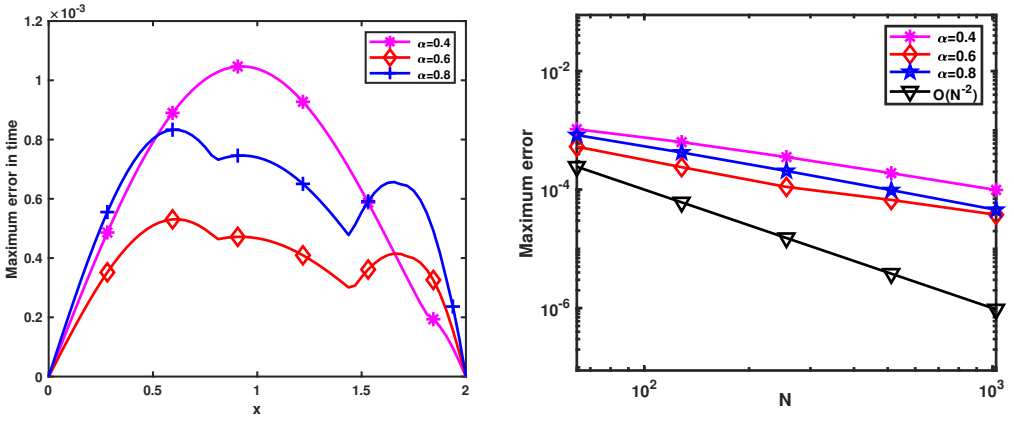

(a) Maximum error (in time). *(b) Log-log plot of N vs. $\mathcal{D}_{M,N}$.*

Figure 4.6: *Plots of numerical results for Example 4.11.*

4.5 Conclusion

In this chapter, we obtained the analytical and numerical solutions of non-autonomous time-fractional integro-partial differential equations. The existence and uniqueness of the analytical solution of the IBVP (4.1) are proved by using the Sumudu decomposition method and the maximum-minimum principle. To obtain the numerical solution of the IBVP (4.1), first we semi-discretize the IBVP (4.1) in the temporal direction by discretizing the time-fractional derivative and the integral term using L1-discretization and trapezoidal rule, respectively. And then we obtain the fully discrete scheme by discretizing the spatial derivatives by using the cubic spline approximation. In order to tackle the singularity in the solution along $t = 0$, we used the graded mesh in the time direction, which increases the accuracy of the computed solution over those obtained by using uniform mesh. Theoretical error estimates are derived and numerical experiments are carried out to demonstrate the efficiency and accuracy of the present numerical method over the previous method described in [95].

CHAPTER 5

Study of interior penalty discontinuous Galerkin method for time-fractional diffusion problem

This chapter studies the superconvergence of error estimates for the discontinuous Galerkin method for a class of non-autonomous time-fractional partial advection-diffusion-reaction equations. To obtain the numerical solution to the model problem, we apply the NIPG method in space on a uniform mesh and the L1-discretization in time on a graded mesh. It is demonstrated that the computed solution is discretely stable. Superconvergence of error estimates for the proposed method is obtained using the discrete energy-norm. Also, we have applied the proposed method to solve semi-linear problems after linearizing by Newton's linearization process. The theoretical results are verified through numerical experiments.

5.1 Introduction

The class of initial-boundary-value problems (IBVPs) with Caputo fractional derivative that we will be focusing on in this chapter is as follows:

$$\begin{cases} {}^{C}\mathcal{D}_t^{\alpha} u(x,t) + \mathcal{L}(u(x,t)) = f(x,t), \quad (x,t) \in Q := \Omega \times (0,T], \\ u(x,0) = g(x), \quad \forall x \in \overline{\Omega}, \\ u(0,t) = u(\ell,t) = 0, \quad \forall t \in (0,T], \end{cases} \tag{5.1}$$

where $\Omega = (0,\ell)$, $\mathcal{L}(u(x,t)) = p(t)\left[-\dfrac{\partial}{\partial x}\left(a(x)\dfrac{\partial u}{\partial x}\right) + b(x)u\right](x,t)$ with $a \in \mathcal{C}^1(\overline{\Omega})$, $b \in \mathcal{C}(\overline{\Omega})$, $p \in \mathcal{C}([0,T])$, $a, p > 0$, $b \geq 0$ and $0 < \alpha < 1$. The compatibility restrictions

$g(0) = g(\ell) = 0$ are likewise assumed to be valid. The presence of the unique solution to the IBVP (5.1) is discussed in Section 3.2 of Chapter 3.

The outline of the chapter is as follows. Section 5.2 deals with the proposed numerical scheme for the IBVP (5.1), whereas the L^2-norm stability is studied in Section 5.3. Section 5.4 discusses the superconvergence analysis of the proposed method. By utilizing the Newton linearization approach, we extend the results of linear problem to semi-linear problem in Section 5.5. Section 5.6 carries out numerical experiments.

5.2 Fully discrete formulation

This section provides the numerical scheme to solve the IBVP (5.1). We further demonstrate that the associated discretized scheme has the Galerkin orthogonality property.

5.2.1 Temporal semi-discretization

Consider the graded mesh $\overline{G}^N = \{t_n : 1 \le n \le N+1\}$ as described in the Subsection 3.3.1. Let $\widehat{u}^{\,n}$ be the approximation of $u(\cdot, t_n)$. The Caputo fractional derivative is discretized using the standard L1-discretization as in (1.10). From [106, Lemma 5.2], the bound for the truncation error at time $t = t_n$, $\mathcal{R}_N^n(x) := \left({}_{L1}^{C}\mathcal{D}_N^{\alpha} - {}^{C}\mathcal{D}_t^{\alpha}\right) u(x, t_n)$, is as follows:

$$|\mathcal{R}_N^n(x)| \le C n^{-\min\{2-\alpha, r\alpha\}}. \tag{5.2}$$

We generate the following semi-discrete problem by discretizing the temporal derivative in the IBVP (5.1): For $n \in \{2, 3, \cdots, N+1\}$,

$$\begin{cases} -\dfrac{\partial}{\partial x}\left(p(t_n) a \dfrac{\partial \widehat{u}^{\,n}}{\partial x}\right)(x) + (c^n \widehat{u}^{\,n})(x) = F^n(x), \quad x \in \Omega, \\ \widehat{u}^{\,1}(x) = g(x), \quad x \in \Omega, \\ \widehat{u}^{\,n}(0) = \widehat{u}^{\,n}(\ell) = 0, \end{cases} \tag{5.3}$$

where $c^n(x) = p(t_n)b(x) + \widehat{d}_{n,n-1}$, $f^n(x) = f(x, t_n)$ and $F^n(x) = \sum_{j=2}^{n-1} [\widehat{d}_{n,j} - \widehat{d}_{n,j-1}]\, \widehat{u}^{\,j}(x) + \widehat{d}_{n,1}\, \widehat{u}^{\,1}(x) + f^n(x)$.

Recall the error estimate for the temporal semi-discretization of the IBVP (5.1) discussed in Lemma 3.5 of Chapter 3.

Lemma 5.1 *The error resulting from temporal semi-discretization of IBVP (5.1) has the following bound:*

$$\|u^n - \widehat{u}^{\,n}\| \leq CN^{-\min\{2-\alpha, r\alpha\}}, \quad n = 1, 2, \cdots, N+1. \tag{5.4}$$

5.2.2 The fully discrete NIPG method

The spatial derivatives are discretized using the NIPG approach in this subsection. For a positive integer M, we consider spatial uniform mesh $\overline{\Omega}_M$. Denote the spatial approximation of $\widehat{u}^n$ in the finite element space $V_{0,h}^k$ as u_h^n.

The finite element approximation for the semi-discrete problem (5.3) is given by the following using the NIPG method for spatial variable:

$$\begin{cases} \text{Find } u_h^n \in V_{0,h}^k (n = 2, \cdots, N+1) \text{ so that} \\ B_h(u_h^n, v_h) = \langle F^n, v_h \rangle, \quad \forall v_h \in V_{0,h}^k, \\ \int\limits_{\Omega} u_h^1 v_h dx = \int\limits_{\Omega} g\, v_h dx, \quad \forall v_h \in V_{0,h}^k, \end{cases} \tag{5.5}$$

with $B_h(u_h^n, v_h) = B_1(u_h^n, v_h) + B_2(u_h^n, v_h) - B_2(v_h, u_h^n) + B_3(u_h^n, v_h)$, where

$$\begin{aligned} B_1(u_h^n, v_h) &= \sum_{m=1}^{M} \int\limits_{\mathcal{K}_m} (p(t_n)a(x)(u_h^n)_x(v_h)_x + c^n(x)u_h^n v_h)\, dx, \\ B_2(u_h^n, v_h) &= \sum_{m=1}^{M+1} \{p(t_n)a(x_m)(u_h^n)_x(x_m)\}[v_h(x_m)], \\ B_3(u_h^n, v_h) &= \sum_{m=1}^{M+1} \frac{\sigma_m}{h}[u_h^n(x_m)][v_h(x_m)], \\ \langle F^n, v_h \rangle &= \sum_{m=1}^{M} \int\limits_{\mathcal{K}_m} \Big(f^n + \widehat{d}_{n,1} u_h^1 + \sum_{j=2}^{n-1} (\widehat{d}_{n,j} - \widehat{d}_{n,j-1}) u_h^j \Big) v_h dx, \end{aligned}$$

and the stated discontinuity-penalization parameters $\sigma_m \geq 1$ $(m = 1, 2, \cdots, M+1)$ are connected to the node x_m.

Using the definitions of jump and average as well as integration by parts, one can now obtain the Galerkin orthogonality property for the bilinear form $B_h(\cdot, \cdot)$.

Lemma 5.2 *Let $\widehat{u}^n$ be the solution of the semi-discrete problem (5.3) and u_h^n be the solution of the fully discrete scheme (5.5). The Galerkin orthogonality property is then*

satisfied by the bilinear form $B_h(\cdot,\cdot)$*:*

$$B_h(\widehat{u}^{\,n} - u_h^n, v_h) = 0, \quad \forall v_h \in V_{0,h}^k(\Omega), \quad 1 \le n \le N+1.$$

Proof. Since $\widehat{u}^{\,n}$ is the solution of the semi-discrete problem (5.3), we have $[\widehat{u}^{\,n}(x_m)] = 0$, $1 \le m \le M+1$ and $[\widehat{u}_x^n(x_m)] = 0$, $2 \le m \le M$. Then for all $v_h \in V_{0,h}^k(\Omega)$, we have

$$B_h(\widehat{u}^{\,n}, v_h) = B_1(\widehat{u}^{\,n}, v_h) + B_2(\widehat{u}^{\,n}, v_h). \tag{5.6}$$

Using the definitions of jump and average as well as integration by parts, one can now obtain that

$$B_1(\widehat{u}^{\,n}, v_h) = \sum_{m=1}^{M} \int_{\mathcal{K}_m} \Big(-(p(t_n)a(\widehat{u}^{\,n})_x)_x + c^n \widehat{u}^{\,n}\Big) v_h dx - \sum_{m=1}^{M+1} \{p(t_n)a(x_m)(\widehat{u}^{\,n})_x(x_m)\}[v_h(x_m)]. \tag{5.7}$$

Thus from the equations (5.6), (5.7) and using the semi-discrete problem (5.3), we get the following for $v_h \in V_{0,h}^k(\Omega)$:

$$B_h(\widehat{u}^{\,n}, v_h) = \sum_{m=1}^{M} \int_{\mathcal{K}_m} \Big(- (p(t_n)a(\widehat{u}^{\,n})_x)_x + c^n \widehat{u}^{\,n}\Big) v_h dx = \langle F^n, v_h \rangle. \tag{5.8}$$

From equation (5.5) and equation (5.8), we obtained our required result. □

For the given bilinear form $B_h(\cdot,\cdot)$, we define the DG energy-norm as

$$|||v|||_{DG}^2 = \beta \sum_{m=1}^{M} \int_{\mathcal{K}_m} (|v_x|^2 + |v|^2) dx + \sum_{m=1}^{M+1} \sigma_m [v(x_m)]^2, \quad v \in V_{0,h}^k(\Omega),$$

and the discrete energy-norm as

$$|||v|||^2 = \frac{\beta h}{2} \sum_{m=1}^{M} \sum_{j=1}^{k} w_j |v_x(x_{mj})|^2 + \beta \|v\|^2 + \sum_{m=1}^{M+1} \sigma_m [v(x_m)]^2, \quad v \in V_{0,h}^k(\Omega),$$

where $\beta = \min\{p_* a_*, b_* p_*\}$, $p_* = \min\limits_{1 \le n \le N} p(t_n)$, $a_* = \min\limits_{x \in \Omega} a(x)$ $b_* = \min\limits_{x \in \Omega} b(x)$ and x_{mj} are the Gaussian points in element $\mathcal{K}_m$. Here, $\dfrac{hw_j}{2} > 0$ are weights for the k-point Gaussian quadrature rule on $\mathcal{K}_m$. It is obvious that the coercivity condition satisfied by the bilinear form provided in the fully discrete scheme (5.5) in both the energy-norm, i.e., $B_h(v,v) \ge |||v|||^2$ and $B_h(v,v) \ge |||v|||_{DG}^2$.

5.3 L^2-stability of the fully discrete scheme

This section establishes the L^2-stability for the fully discrete L1-NIPG scheme.

Lemma 5.3 *The following bound is satisfied for $n = 2, 3, \cdots, N+1$ by the solution u_h^n of the fully discrete scheme (5.5):*

$$\|u_h^n\| \leq \tau_{n-1}^{\alpha}\Gamma(2-\alpha)\Big(\|f^n\| + \widehat{d}_{n,1}\|u_h^1\| + \sum_{j=2}^{n-1}(\widehat{d}_{n,j} - \widehat{d}_{n,j-1})\|u_h^j\|\Big). \tag{5.9}$$

Proof. Fix $n \in \{2, 3, \cdots, N+1\}$. Letting $v = u_h^n$ in the fully discrete scheme (5.5) and using the condition given for a, b, p, we have

$$\begin{aligned}\widehat{d}_{n,n-1}\|u_h^n\|^2 &\leq |B_h(u_h^n, u_h^n)| = |\langle F, u_h^n\rangle| \\ &\leq \sum_{m=1}^{M}\int_{\mathcal{K}_m}\Big(|f^n| + \widehat{d}_{n,1}|u_h^1| + \sum_{j=2}^{n-1}(\widehat{d}_{n,j} - \widehat{d}_{n,j-1})|u_h^j|\Big)|u_h^n|dx.\end{aligned}$$

Using the Cauchy-Schwarz inequality on the right side of the aforementioned inequality results in

$$\widehat{d}_{n,n-1}\|u_h^n\|^2 \leq \Big(\|f^n\| + \widehat{d}_{n,1}\|u_h^1\| + \sum_{j=2}^{n-1}(\widehat{d}_{n,j} - \widehat{d}_{n,j-1})\|u_h^j\|\Big)\|u_h^n\|.$$

Then the equation (5.9) follows as $\widehat{d}_{n,n-1} > \dfrac{1}{\tau_{n-1}^{\alpha}\,\Gamma(2-\alpha)}$. Hence the proof is done. □

For $n = 2, 3, \cdots, N+1$ and $j = 2, 3, \cdots, n$, we recall $\vartheta_{n,j}$ defined in (3.31). The stability result for the fully discrete scheme (5.5) is given by the following lemma.

Lemma 5.4 *Let u_h^n be the solution of the fully discrete scheme (5.5). Then, we have*

$$\|u_h^n\| \leq \|u_h^1\| + C\,T^{\alpha}\max_{1\leq j\leq n}\|f^j\|, \quad \text{for } 2 \leq n \leq N+1. \tag{5.10}$$

Proof. By replicating the proof of [106, Lemma 4.2] in the Lemma 5.3, we have

$$\|u_h^n\| \leq \|u_h^1\| + C\tau_{n-1}^{\alpha}\sum_{j=1}^{n}\vartheta_{n,j}\|f^j\| \leq \|u_h^1\| + C\tau_{n-1}^{\alpha}\max_{1\leq j\leq n}\|f^j\|\sum_{j=1}^{n}\vartheta_{n,j}. \tag{5.11}$$

By Lemma 3.4 with $\varrho = 0$, we obtain our required result. □

Remark 5.1 *The NIPG approach is well posed, as shown by the aforementioned lemma, which states that if $f = u_h^1 = 0$, then one must have the trivial solution $u_h^n = 0$ in the fully discrete scheme (5.5). This also concludes the uniqueness of the discrete solution.*

5.4 Superconvergence analysis of proposed DG method

In this section, we will study the superconvergence analysis of the fully discrete scheme using discrete energy-norm rather than using the DG energy-norm. Let us first consider the Lobatto points $\{-1 = z_0^{(k)}, z_1^{(k)}, \cdots, z_{k-1}^{(k)}, z_k^{(k)} = 1\}$ on $[-1, 1]$, which are the $(k+1)$ zeros of the polynomial $\Phi_{k+1}(z) = \dfrac{d^{k-1}}{dz^{k-1}}(z^2-1)^k$. Let $\Pi v \in \mathbb{P}^k([-1,1])$ denotes the Lagrange interpolation of a continuous function v defined on $[-1, 1]$ by using the Lobatto nodes $\{z_j^{(k)}\}_{j=0}^k$. Then we have

$$(\Pi v - v)(z) = \frac{v^{(k+1)}(z)}{(2k)!}\Phi_{k+1}(z) + O(1)\int_{-1}^{1} |v^{(k+2)}(z)|dz, \tag{5.12}$$

$$(\Pi v - v)'(z) = \frac{v^{(k+1)}(z)}{(2k)!}\Psi_{k}(z) + O(1)\int_{-1}^{1} |v^{(k+2)}(z)|dz, \tag{5.13}$$

where $\Psi_k(z) = \dfrac{d^k}{dz^k}(z^2-1)^k$ is a multiple of the kth Legendre polynomial on $[-1, 1]$ and Gauss points are the zeros of $\Psi_k(z)$.

For $m = 1, 2, \cdots, M$, let $x_{m,j}^{(k)} = \dfrac{x_m + x_{m+1}}{2} + \dfrac{x_{m+1} - x_m}{2} z_j^{(k)}$, $j = 0, 1, \cdots, k$ be the nodes in $[x_m, x_{m+1}]$ corresponding to $z_j^{(k)}$. For $2 \le n \le N+1$, let $\pi_h u^n$ denotes the piecewise Lagrange interpolant of u^n using $\{x_{m,j}^{(k)}\}_{j=0}^k$ as node points on $[x_m, x_{m+1}]$. Then from equations (5.12) and (5.13), we have the following for $x \in [x_m, x_{m+1}]$ and $n = 1, 2, \cdots, N+1$:

$$(\pi_h u^n - u^n)(x) = \frac{(u^n)^{(k+1)}(x)}{(2k)!}\widehat{\Phi}_{m,k+1}(x) + O(h^{k+1})\int_{\mathcal{K}_m} \left|(u^n)^{(k+2)}(x)\right| dx, \tag{5.14}$$

$$(\pi_h u^n - u^n)'(x) = \frac{(u^n)^{(k+1)}(x)}{(2k)!}\widehat{\Psi}_{m,k}(x) + O(h^{k})\int_{\mathcal{K}_m} \left|(u^n)^{(k+2)}(x)\right| dx, \tag{5.15}$$

where $\widehat{\Phi}_{m,k+1}(x) = \dfrac{d^{k-1}}{dx^{k-1}}\left((x - x_{m+1/2})^2 - \dfrac{h^2}{4}\right)^k$ and $\widehat{\Psi}_{m,k}(x) = \widehat{\Phi}'_{m,k+1}(x)$.

Therefore, the equation (5.15) at the Gauss points x_{mj} becomes

$$(\pi_h u^n - u^n)'(x_{mj}) = O(h^k) \int_{\mathcal{K}_m} |(u^n)^{(k+2)}(x)|dx. \tag{5.16}$$

We have the following interpolation error estimate for any $u^n \in H^{k+1}(\Omega, \mathcal{P}_M)$ $(n = 1, 2, \cdots, N+1)$:

$$\|u^n - \pi_h u^n\|_{d_1, \mathcal{P}_M} \leq Ch^{k+1-d_1} |u^n|_{k+1, \mathcal{P}_M}, \quad 0 \leq d_1 \leq k+1. \tag{5.17}$$

Let u^n and u_h^n respectively, denote the solutions at $t = t_n$ of the equations (5.1) and (5.5), then we define the error e^n as

$$e^n := u^n - u_h^n = (u^n - \pi_h u^n) + (\pi_h u^n - u_h^n),\ n = 1, 2, \cdots, N+1.$$

Let's use the notation $\eta^n := u^n - \pi_h u^n$ for the interpolation error and $\xi^n := \pi_h u^n - u_h^n$ for the spatial discretization error.

The interpolation error in the DG energy-norm will be investigated in the following theorem.

Theorem 5.2 *The interpolation error can be bounded by*

$$|||\eta^n|||_{DG} \leq Ch^k, \quad n = 1, 2, \cdots, N+1.$$

Proof. Now, since $\eta^n(x_m) = 0$ for $m = 1, 2, \cdots, M+1$, which implies that $[\eta^n(x_m)] = 0$. Then for each $n = 1, 2, \cdots, N+1$, we have

$$|||\eta^n|||_{DG}^2 = \beta \sum_{m=1}^{M} \int_{\mathcal{K}_m} (|\eta_x^n|^2 + |\eta^n|^2)dx = \beta\Big(|\eta^n|_{1, \mathcal{P}_M}^2 + \|\eta^n\|^2\Big) \leq Ch^{2k}, \tag{5.18}$$

where we have used the estimate given in the equation (5.17). Hence the proof is done. □

The interpolation error in discrete energy-norm is a topic we'll explore in the following theorem.

Theorem 5.3 *The interpolation error can be bounded by*

$$|||\eta^n||| \leq Ch^{k+1}, \quad n = 1, 2, \cdots, N+1.$$

Proof. Now, since $\eta^n(x_m) = 0$ for $m = 1, 2, \cdots, M+1$, which implies that $[\eta^n(x_m)] = 0$. Then for each $n = 1, 2, \cdots, N+1$, we have

$$|||\eta^n|||^2 = \beta \sum_{m=1}^{M} \frac{h}{2} \sum_{j=1}^{k} w_j |(\eta^n)'(x_{mj})|^2 + \beta \|\eta^n\|^2. \tag{5.19}$$

By using equations (5.16) and (5.17) in the above equation (5.19) and then using the Hölder's inequality, we have the following

$$\begin{aligned} |||\eta^n|||^2 &\leq C \sum_{m=1}^{M} h^{2k+1} \left(\int_{\mathcal{K}_m} |(u^n)^{(k+2)}(x)| dx \right)^2 + Ch^{2k+2} \left(\sum_{m=1}^{M} \int_{\mathcal{K}_m} |(u^n)^{(k+1)}(x)| dx \right)^2 \\ &\leq Ch^{2k+2} |u^n|^2_{k+2,\mathcal{P}_M} + Ch^{2k+3} |u^n|^2_{k+1,\mathcal{P}_M} \\ &\leq Ch^{2k+2}. \end{aligned}$$

Hence the proof is done. □

The bound on the discretization error in the discrete energy-norm will be shown in the following.

Theorem 5.4 *The following bound is satisfied by the discretization error:*

$$|||\xi^n||| \leq C \left(h^{k+1} + n^{-\min\{2-\alpha, r\alpha\}} \right), \quad n = 1, 2, \cdots, N+1.$$

Proof. From the definition of ξ^n and η^n, and the linearity of $B_h(\cdot, \cdot)$, we have

$$B_h(\xi^n, \xi^n) = B_h(\widehat{u}^{\,n} - u_h^n, \xi^n) + B_h(u^n - \widehat{u}^{\,n}, \xi^n) - B_h(\eta^n, \xi^n). \tag{5.20}$$

From Lemma 5.2, we have $B_h(\widehat{u}^{\,n} - u_h^n, \xi^n) = 0$, as $\xi^n \in V_{0,h}^k(\Omega)$. Now, from the IBVP (5.1) and the semi-discrete problem (5.3), one can see that the following hold:

$$B_h(u^n - \widehat{u}^{\,n}, \xi^n) = \langle \mathcal{R}_N^n, \xi^n \rangle. \tag{5.21}$$

As $[\eta^n(x_m)] = 0$, we can estimate $B_2(\xi^n, \eta^n) = B_3(\eta^n, \xi^n) = 0$. So, $B_h(\eta^n, \xi^n) = B_1(\eta^n, \xi^n) + B_2(\eta^n, \xi^n)$. Now by using the Hölder's inequality, $B_1(\eta^n, \xi^n)$ can be written as

$$B_1(\eta^n, \xi^n) = \sum_{m=1}^{M} \int_{\mathcal{K}_m} \Big(p(t_n) a(x) \eta_x^n \xi_x^n + c^n(x) \eta^n \xi^n \Big) dx$$

$$\leq \quad C\Big(\|\eta^n\|_{1,\mathcal{P}_M}\|\xi^n\|_{1,\mathcal{P}_M} + \|\eta^n\|\|\xi^n\|\Big) \leq Ch^{k+1}|||\xi^n|||. \tag{5.22}$$

The remaining term $B_2(\eta^n, \xi^n)$ can be bounded by

$$B_2(\eta^n, \xi^n) = \sum_{m=1}^{M+1}\{p(t_n)a(x_m)\eta_x^n(x_m)\}[\xi^n(x_m)] \leq Ch^{k+1}|||\xi^n|||. \tag{5.23}$$

Therefore, by using the coercivity property and combining the equations (5.22) and (5.23), we have

$$\begin{aligned}|||\xi^n|||^2 \leq B_h(\xi^n, \xi^n) = \langle \mathcal{R}_N^n, \xi^n\rangle - B_h(\eta^n, \xi^n) \quad &\leq \quad \|\mathcal{R}_N^n\|\,\|\xi^n\| + |B_h(\eta^n, \xi^n)| \\ &\leq C\left(n^{-\min\{2-\alpha, r\alpha\}} + h^{k+1}\right)|||\xi^n|||. \end{aligned} \tag{5.24}$$

Therefore, $|||\xi^n||| \leq C\left(n^{-\min\{2-\alpha, r\alpha\}} + h^{k+1}\right)$. Hence, we can obtain the required result. □

The error bound resulting from the IBVP (5.1)'s fully discretization is shown in the following theorem.

Theorem 5.5 *Let u^n be the solution of the IBVP (5.1) and u_h^n be the solution of the fully discrete scheme (5.5) at $t = t_n$, then the error estimate is as follows:*

$$|||u^n - u_h^n||| \leq C\left(h^{k+1} + n^{-\min\{2-\alpha, r\alpha\}}\right), \quad 1 \leq n \leq N+1.$$

Proof. We know that for each $n = 1, 2, \cdots, N+1$,

$$|||u^n - u_h^n||| \leq |||\eta^n||| + |||\xi^n|||.$$

Now by combining the results given in Theorem 5.3 and Theorem 5.4, and we derive the necessary estimate by considering maximum over n. □

Remark 5.6 *As like the results given in Theorem 5.4 and Theorem 5.5, one can establish that $|||\xi^n|||_{DG} \leq C(h^k + n^{-\min\{2-\alpha, r\alpha\}})$ and $|||u^n - u_h^n|||_{DG} \leq C(h^k + n^{-\min\{2-\alpha, r\alpha\}})$. As a result, we have enhanced the order of convergence (spatial direction) by one, by utilizing the discrete energy-norm rather than the DG energy-norm.*

5.5 Semi-linear time-fractional IBVPs

We consider the following class of semi-linear time-fractional IBVPs in this section:

$$\begin{cases} {}^{C}\mathcal{D}_t^{\alpha} u(x,t) + \mathcal{L}(u(x,t)) = f(x,t), \quad (x,t) \in Q := \Omega \times (0,T], \\ u(x,0) = g(x), \quad \forall x \in \overline{\Omega}, \\ u(0,t) = u(\ell,t) = 0, \quad \forall t \in (0,T], \end{cases} \tag{5.25}$$

where $\Omega = (0,\ell)$ and $\mathcal{L}(u(x,t)) = p(t)\left[-\dfrac{\partial}{\partial x}\left(a(x)\dfrac{\partial u}{\partial x}(x,t)\right) + b(x,u)\right]$ with

$$\begin{cases} a \in \mathcal{C}^1(\overline{\Omega}),\ b \in \mathcal{C}^1(\Omega \times \mathbb{R}),\ a(x) > 0,\ b_u \geq 0, \quad \forall x \in \overline{\Omega}, \\ p \in \mathcal{C}([0,T]),\ p(t) > 0, \quad \forall t \in (0,T]. \end{cases} \tag{5.26}$$

We further assume that the problem (5.25) admits a unique solution $u(x,t)$ and that the compatibility conditions $g(0) = g(\ell) = 0$ hold true for suitably smooth functions $b(x,u)$, $f(x,t)$ and $g(x)$.

To arrive at the problem's numerical solution, we first apply the Newton linearization process to convert the semi-linear problem (5.25) into a sequence of linear problems and then we use the numerical approach described in the previous section. As a result, starting with the first guess $u^{(0)}$, we define the solution $u^{(q+1)}$, $q \geq 0$ of the following linear time-fractional IBVP:

$$\begin{cases} {}^{C}\mathcal{D}_t^{\alpha} u^{(q+1)}(x,t) + \mathcal{L}^q(u^{(q+1)}(x,t)) = F^q(x,t), \quad \forall (x,t) \in Q, \\ u^{(q+1)}(x,0) = g(x), \quad \forall x \in \overline{\Omega}, \\ u^{(q+1)}(0,t) = u^{(q+1)}(\ell,t) = 0, \quad \forall t \in (0,T], \end{cases} \tag{5.27}$$

where

$$\mathcal{L}^q(u^{(q+1)}(x,t)) = p(t)\left[-\frac{\partial}{\partial x}\left(a(x)\frac{\partial u^{(q+1)}}{\partial x}\right) + b_u(x,u^{(q)})u^{(q+1)}\right](x,t),$$

$$F^q(x,t) = f(x,t) - p(t)\left[b(x,u^{(q)}) - b_u(x,u^{(q)})u^{(q)}(x,t)\right].$$

We choose the convergence condition for $\{u^{(q)}\}_{q\geq 0}$ as:

$$\max_{(x_m,t_n)} |u^{(q+1)}(x_m,t_n) - u^{(q)}(x_m,t_n)| \;\leq\; \text{Tol}, \quad q \geq 0.$$

We used $\text{Tol} = 1.0e-07$ for computational purposes. The semi linear problem's numerical solutions are presented in the following section (5.25).

5.6 Numerical tests

To demonstrate the effectiveness and precision of the suggested numerical methodology, we conduct numerical experiments in this section. We consider three test examples: one with constant coefficients linear problem, a second one with variable coefficients linear problem, and another semi-linear problem. Tables and figures are used to present the numerical results.

The $L^\infty(L^2)$ error and the order of convergence can be calculated using

$$E_{M,N} = \max_{1\leq n\leq N+1} \|u^n - u_h^n\|, \quad \text{and} \quad R_{M,N} = \log_2\left(\frac{E_{M,N}}{E_{2M,2N}}\right).$$

For the numerical studies, we have taken $r = (2-\alpha)/\alpha$.

Example 5.7 *Consider the constant coefficient example:*

$$\begin{cases} {}^C\mathcal{D}_t^\alpha u(x,t) - \dfrac{\partial^2 u}{\partial x^2}(x,t) + u(x,t) = f(x,t), \quad (x,t) \in (0,\pi)\times(0,1] \\ u(x,0) = 0, \quad x \in [0,\pi], \\ u(0,t) = u(\pi,t) = 0, \quad t \in (0,1]. \end{cases} \tag{5.28}$$

In the IBVP (5.28), the function $f(x,t)$ is computed such that $u(x,t) = (t^\alpha + t^3)\sin x$.

The numerical solution's surface plot and the error curve at $t = 1$ of Example 5.7 for $\alpha = 0.6$ with $M = N = 64$ are displayed in Figure 5.1.

The $L^2(\Omega)$, $L^\infty(\Omega)$, $|||\cdot|||_{DG}$ and $|||\cdot|||$ errors and corresponding rate of convergence at $t = 1$ for $\alpha = 0.4, 0.6$ for Example 5.7 are provided in Table 5.1, where we observed that superconvergence of error occurring in $|||\cdot|||$ over $|||\cdot|||_{DG}$.

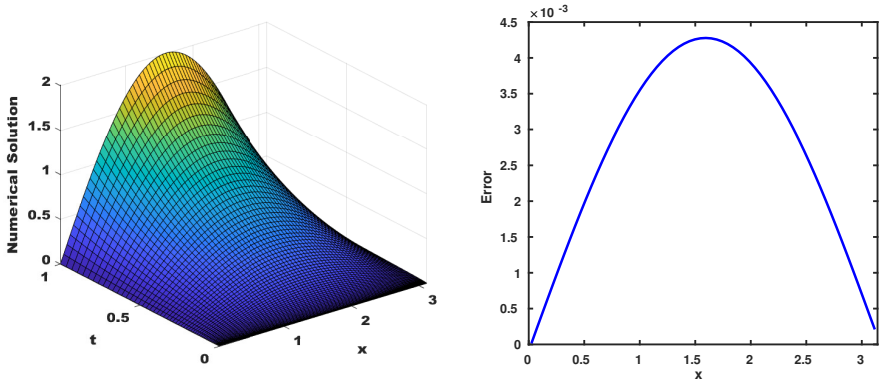

(a) Numerical solution. *(b) Error at $t = 1$.*

Figure 5.1: *Solution surface and error curve at $t = 1$ for Example 5.7.*

Example 5.8 *Consider the variable coefficient example over $(0, \pi) \times (0, 1]$:*

$$\begin{cases} {}^{C}\mathcal{D}_t^{\alpha} u(x,t) + (t^2+1)\left[-\dfrac{\partial}{\partial x}\left((x+1)\dfrac{\partial u}{\partial x}\right) + u\right](x,t) = f(x,t), \\ u(x,0) = 0, \quad x \in [0,\pi], \\ u(0,t) = u(\pi,t) = 0, \quad t \in (0,1]. \end{cases} \tag{5.29}$$

In the IBVP (5.29), the exact solution is $u(x,t) = t^{\alpha} x \sin x$, which will be utilized to determine the value of the function $f(x,t)$.

The numerical results for Example 5.8 are given in Figure 5.2, which depicts the numerical solution's surface plot, and the error curve at $t = 1$ for $\alpha = 0.6$ with $M = N = 64$. Also, the $L^2(\Omega)$, $L^{\infty}(\Omega)$, $|||\cdot|||_{DG}$ and $|||\cdot|||$ errors and corresponding rate of convergence at $t = 1$ for $\alpha = 0.4, 0.6$ for Example 5.8 are provided in Table 5.3, where we observe that superconvergence of error occurring in $|||\cdot|||$ over $|||\cdot|||_{DG}$.

Example 5.9 *Consider the semi-linear problem:*

$$\begin{cases} {}^{C}\mathcal{D}_t^{\alpha} u(x,t) - \dfrac{\partial^2 u}{\partial x^2} - \exp(-u(x,t)) = f(x,t), \ (x,t) \in (0,1) \times (0,1], \\ u(x,0) = x^2 - x, \quad x \in [0,1], \\ u(0,t) = u(1,t) = 0, \quad t \in (0,1]. \end{cases} \tag{5.30}$$

In the problem (5.30), the evaluation of $f(x,t)$ results in the exact solution, $u(x,t) =$

Table 5.1: *Errors and order of convergence at* $t = 1$ *for Example 5.7 with* $N = \left\lceil M^{\frac{2}{2-\alpha}} \right\rceil$, $\sigma_m = 1$ *and* $k = 1$.

$\alpha \downarrow$	$M \rightarrow$	20	40	80	160	320
0.4	$\|u - u_h\|_{L^2(\Omega)}$	1.3522e-02	3.5314e-03	9.1783e-04	2.3478e-04	5.9674e-05
	Order	1.9370	1.9439	1.9669	1.9761	–
	$\|u - u_h\|_{L^\infty(\Omega)}$	1.0732e-02	2.8109e-03	7.3151e-04	1.8722e-04	4.7601e-05
	Order	1.9328	1.9421	1.9661	1.9757	–
	$\|\|\|u - u_h\|\|\|_{DG}$	1.9758e-01	9.8536e-02	4.9231e-02	2.4611e-02	1.2305e-02
	Order	1.0037	1.0011	1.0003	1.0001	–
	$\|\|\|u - u_h\|\|\|$	1.5666e-02	4.1751e-03	1.1024e-03	2.8450e-04	7.2755e-05
	Order	1.9077	1.9212	1.9541	1.9673	–
0.6	$\|u - u_h\|_{L^2(\Omega)}$	1.0765e-02	2.7140e-03	6.8132e-04	1.7079e-04	4.2758e-05
	Order	1.9879	1.9940	1.9961	1.9980	–
	$\|u - u_h\|_{L^\infty(\Omega)}$	8.5329e-03	2.1588e-03	5.4281e-04	1.3617e-04	3.4104e-05
	Order	1.9828	1.9917	1.9950	1.9974	–
	$\|\|\|u - u_h\|\|\|_{DG}$	1.9725e-01	9.8484e-02	4.9224e-02	2.4610e-02	1.2304e-02
	Order	1.0020	1.0005	1.0001	1.0000	–
	$\|\|\|u - u_h\|\|\|$	1.1500e-02	2.9193e-03	7.3534e-04	1.8468e-04	4.6279e-05
	Order	1.9779	1.9892	1.9934	1.9966	–

$(t^\alpha + t^3 + 1)(x^2 - x)$. In order to numerically solve this problem, we first linearized the semi-linear problem (5.30) using Newton's approach described in equation (5.27), which results in the following linear problems:

$$\begin{cases} ({}^C\mathcal{D}_t^\alpha u^{(q+1)} + \mathcal{L}^q(u^{(q+1)}))(x,t) = F^q(x,t), \quad \forall\, (x,t) \in (0,1) \times (0,1], \\ u^{(q+1)}(x,0) = 0, \quad x \in [0,1], \\ u^{(q+1)}(0,t) = u^{(q+1)}(1,t) = 0, \quad t \in [0,1], \end{cases} \tag{5.31}$$

Table 5.2: *Errors and order of convergence at* $t = 1$ *for Example 5.7 with* $N = \left\lceil M^{\frac{2}{2-\alpha}} \right\rceil$, $\sigma_m = 1000$ *and* $k = 2$.

$\alpha \downarrow$	$M \rightarrow$	4	8	16	32	64
0.4	$\|u - u_h\|_{L^2(\Omega)}$	3.5126e-02	5.6404e-03	7.8277e-04	1.0309e-04	1.3153e-05
	Order	2.6387	2.8491	2.9247	2.9704	–
	$\|u - u_h\|_{L^\infty(\Omega)}$	2.9975e-02	4.5440e-03	6.2555e-04	8.2297e-05	1.0499e-05
	Order	2.7217	2.8608	2.9262	2.9706	–
	$\|\|\|u - u_h\|\|\|_{DG}$	1.6635e-01	3.7007e-02	8.6777e-03	2.0970e-03	5.1455e-04
	Order	2.1684	2.0924	2.0490	2.0269	–
	$\|\|\|u - u_h\|\|\|$	6.8309e-02	1.1059e-02	1.6621e-03	2.5421e-04	4.1639e-05
	Order	2.6269	2.7341	2.7089	2.6100	–
0.6	$\|u - u_h\|_{L^2(\Omega)}$	2.6859e-02	3.8755e-03	5.0604e-04	6.5118e-05	8.3524e-06
	Order	2.7929	2.9371	2.9581	2.9628	–
	$\|u - u_h\|_{L^\infty(\Omega)}$	2.2922e-02	3.1226e-03	4.0447e-04	5.1995e-05	6.6681e-06
	Order	2.8759	2.9486	2.9596	2.9630	–
	$\|\|\|u - u_h\|\|\|_{DG}$	1.6195e-01	3.7485e-02	9.2240e-03	2.3588e-03	6.1854e-04
	Order	2.1111	2.0229	1.9673	1.9311	–
	$\|\|\|u - u_h\|\|\|$	6.6898e-02	9.2170e-03	1.2128e-03	1.5645e-04	2.0078e-05
	Order	2.8596	2.9259	2.9546	2.9620	–

where for $q \geq 0$,

$$\mathcal{L}^q(u^{(q+1)}) = -\frac{\partial^2 u^{(q+1)}}{\partial x^2} + \exp(-u^{(q)})u^{(q+1)},$$

$$F^q = f + \exp(-u^{(q)})(1 + u^{(q)}).$$

The approximate solution to the problem (5.9) is then obtained by using the suggested numerical technique to (5.31). We utilize the initial supposition $u^{(0)}(x,t) = 0$, $(x,t) \in (0,1) \times (0,1]$ for computation.

The numerical solution surface and error curve at $t = 1$ are shown in Figure 5.3 with $M = N = 64$ and $\alpha = 0.5$. The numerical results for the suggested approach for Example 5.9 are presented in Table 5.4.

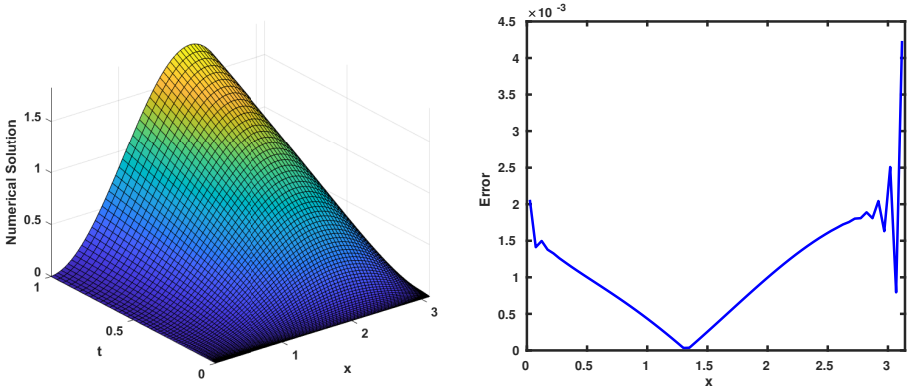

(a) Numerical solution. *(b) Error at $t = 1$.*

Figure 5.2: *Solution surface and error curve at $t = 1$ for Example 5.8.*

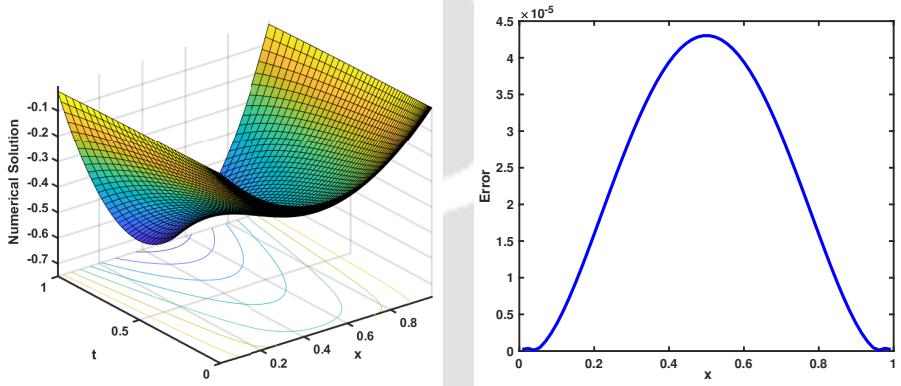

(a) Numerical solution. *(b) Error at $t = 1$.*

Figure 5.3: *Solution surface and error curve at $t = 1$ for Example 5.9.*

5.7 Conclusion

The present work examined the superconvergence of the NIPG approach for the non-autonomous TF-ADE (5.1). We developed a fully discrete scheme by discretizing the spatial variables using the NIPG technique and the time derivative using the L1-discretization. The suggested method is convergent with respect to the discrete energy-norm of order $(k+1)$ in the spatial direction and of order $\min\{2-\alpha, r\alpha\}$ in the temporal direction, where k represents the degree of the piecewise polynomial in the finite element space. Further, after linearizing the semi-linear problems by using the Newton's linearization process, we solved them by applying the present method. We validated the

Table 5.3: *Errors and order of convergence at* $t = 1$ *for Example 5.8 with* $N = \left\lceil M^{\frac{2}{2-\alpha}} \right\rceil$, $\sigma_m = 1$ *and* $k = 1$.

$\alpha \downarrow$	$M \rightarrow$	20	40	80	160	320
0.4	$\|u - u_h\|_{L^2(\Omega)}$	6.0297e-02	1.3814e-02	3.2707e-03	7.9315e-04	1.9511e-04
	Order	2.1259	2.0785	2.0439	2.0233	–
	$\|u - u_h\|_{L^\infty(\Omega)}$	1.0348e-01	2.6196e-02	6.5745e-03	1.6458e-03	4.1167e-04
	Order	1.9819	1.9944	1.9981	1.9993	–
	$\|\|\|u - u_h\|\|\|_{DG}$	3.2440e-01	1.5317e-01	7.4670e-02	3.6896e-02	1.8342e-02
	Order	1.0827	1.0365	1.0171	1.0083	–
	$\|\|\|u - u_h\|\|\|$	1.6262e-01	5.5796e-02	1.9477e-02	6.8469e-03	2.4143e-03
	Order	1.5433	1.5184	1.5082	1.5038	–
0.6	$\|u - u_h\|_{L^2(\Omega)}$	6.0228e-02	1.3801e-02	3.2678e-03	7.9247e-04	1.9495e-04
	Order	2.1257	2.0784	2.0439	2.0233	–
	$\|u - u_h\|_{L^\infty(\Omega)}$	1.0342e-01	2.6192e-02	6.5742e-03	1.6458e-03	4.1167e-04
	Order	1.9814	1.9942	1.9980	1.9992	–
	$\|\|\|u - u_h\|\|\|_{DG}$	3.2440e-01	1.5317e-01	7.4671e-02	3.6896e-02	1.8342e-02
	Order	1.0826	1.0365	1.0171	1.0083	–
	$\|\|\|u - u_h\|\|\|$	1.6250e-01	5.5780e-02	1.9474e-02	6.8466e-03	2.4143e-03
	Order	1.5426	1.5182	1.5081	1.5038	–

Table 5.4: $L^\infty(L^2)$ *error and the order of convergence for Example 5.9 with* $k = 2$ *and* $\sigma_m = 1$.

$\alpha \downarrow$	$M = N \rightarrow$	16	32	64	128	256
0.4	$E_{M,N}$	1.3177e-03	5.4129e-04	2.0350e-04	7.3971e-05	2.6366e-05
	$R_{M,N}$	1.2835	1.4114	1.4600	1.4883	–
0.6	$E_{M,N}$	1.9151e-03	8.8080e-04	3.7954e-04	1.5574e-04	6.2081e-05
	$R_{M,N}$	1.1206	1.2146	1.2851	1.3269	–
0.8	$E_{M,N}$	2.4319e-03	1.2029e-03	5.7275e-04	2.6515e-04	1.2052e-04
	$R_{M,N}$	1.0155	1.0706	1.1111	1.1375	–

theoretical results through various numerical experiments.

CHAPTER 6

Discontinuous Galerkin method for nonlinear time-fractional integro-partial differential equations

This chapter provides the numerical solution of the nonlinear time-fractional integro-partial differential equation. We linearize the nonlinear problem by applying the Newton's linearization process. For resultant linearized problem, we apply the NIPG method for the spatial variable and use both L1-discretization and L2-discretization for time-fractional derivative, and the trapezoidal rule for the integral term and obtain the fully discrete scheme. We then prove the stability and error estimate of the proposed method, and derive the required error estimates. To demonstrate the theoretical error bounds, numerical experiments will be carried out.

6.1 Introduction

Model problem for this chapter is the following initial-boundary-value problem (IBVP):

$$\begin{cases} {}^{C}\mathcal{D}_t^{\alpha} u(x,t) + \mathcal{L}u(x,t) + \mathcal{I}_t u(x,t) = f(x,t), \ (x,t) \in Q := \Omega \times G, \\ u(x,0) = g(x), \quad \forall x \in \overline{\Omega}, \\ u(0,t) = u(\ell,t) = 0, \quad \forall t \in G, \end{cases} \tag{6.1}$$

where $\Omega = (0,\ell)$, $G = (0,T]$, and $0 < \alpha < 1$, and

$$\mathcal{L}u(x,t) := -\frac{\partial}{\partial x}\left(a(x,t)\frac{\partial u}{\partial x}(x,t)\right) + b(u(x,t)), \tag{6.2}$$

$$\mathcal{I}_t u(x,t) := \lambda \int_0^t K(x,t-s)u(x,s)ds. \tag{6.3}$$

Further, we assume that the functions a, b, K, f are suitably smooth, $\lambda > 0$ as well as

$$0 < a_* < a(x,t) \leq a^*, \quad \frac{\partial b}{\partial u} \geq 0, \quad K(x,t) \geq 0, \quad \forall (x,t) \in Q, \tag{6.4}$$

and the initial value $g(\cdot)$ satisfies the compatibility conditions $g(0) = g(\ell) = 0$, and the IBVP (6.1) admits a unique solution.

This chapter is structured as follows: The detailed numerical method for the nonlinear IBVP (6.1) is given in Section 6.2. That is, here, by linearizing the nonlinear IBVP (6.1) and employing the NIPG method for the spatial variable, and both the L1-discretization and L2-discretization for the temporal derivative and the trapezoidal rule for the integral term, we develop the fully discrete schemes. The L^2-norm stability and uniform convergence of the fully discrete method are then examined in Sections 6.3 and 6.4, respectively. Numerical results are displayed in Section 6.5 to illustrate the theoretical convergence estimates.

6.2 Numerical method

This section describes the complete numerical procedure applied to solve the nonlinear time-fractional integro-partial differential IBVP (6.1).

6.2.1 Linearization of the nonlinear IBVP

We use the Newton linearization process and obtain the sequence $\{u^{(q)}(x,t)\}_{q\geq 0}$ for the initial guess $u^{(0)}(x,t)$ satisfying the initial and boundary conditions of the problem. Thus we define $u^{(q+1)}(x,t)$ for each fixed q, to be the solution of the following linear IBVP:

$$\begin{cases} {}^C\mathcal{D}_t^\alpha u^{(q+1)}(x,t) + \mathcal{L}^q u^{(q+1)}(x,t) + \mathcal{I}_t u^{(q+1)}(x,t) = \mathcal{G}^q(x,t), \quad \forall (x,t) \in Q, \\ u^{(q+1)}(x,0) = g(x), \quad \forall x \in \overline{\Omega}, \\ u^{(q+1)}(0,t) = u^{(q+1)}(\ell,t) = 0, \quad \forall t \in G, \end{cases} \tag{6.5}$$

where $\mathcal{L}^q u^{(q+1)}(x,t) := -\dfrac{\partial}{\partial x}\left(a\dfrac{\partial u^{(q+1)}}{\partial x}\right)(x,t) + b_u(u^{(q)})u^{(q+1)}(x,t)$, and $\mathcal{G}^q(x,t) = f(x,t) - b(u^{(q)}) + b_u(u^{(q)})u^{(q)}(x,t)$, $q \geq 0$.

Hence for a fixed q, we will solve (6.5) by using the L1-NIPG and the L2-NIPG methods. For the convergence of the Newton linearization process, we use the following criterion:

$$\max_{(x,t)\in Q} |u^{(q+1)}(x,t) - u^{(q)}(x,t)| \leq \text{Tol}, \quad q \geq 0.$$

For computational purpose we have taken $\text{Tol} = 1.0e-07$.

By denoting $u^{(q+1)}(x,t) = w(x,t)$, $b(u^{(q)}) = d(x,t)$, $b_u(u^{(q)}(x,t)) = c(x,t)$ and $b_u(u^{(q)})u^{(q)}(x,t) = \widetilde{c}(x,t)$, the linearized integro-differential equation (6.5) can be written in the following form:

$$\begin{cases} {}^C\mathcal{D}_t^\alpha w(x,t) + \widehat{\mathcal{L}}w(x,t) + \mathcal{I}_t w(x,t) = \mathcal{F}(x,t), \quad \forall (x,t) \in Q, \\ w(x,0) = g(x), \quad \forall x \in \overline{\Omega}, \\ w(0,t) = w(\ell,t) = 0, \quad \forall t \in G, \end{cases} \tag{6.6}$$

where $\widehat{\mathcal{L}}w(x,t) = -\dfrac{\partial}{\partial x}\left(a\dfrac{\partial w}{\partial x}\right)(x,t) + c(x,t)w(x,t)$ and $\mathcal{F}(x,t) = f(x,t) - d(x,t) + \widetilde{c}(x,t)$.

6.2.2 Spatial semi-discretization

In this subsection, we use the NIPG method to discretize the spatial variable and obtain the semi-discretized scheme. Let us first discretize the spatial domain uniformly as $\overline{\Omega}_M$. Now, the weak formulation of (6.6) on the spatial variable is given as: For each $t \in (0,T]$, find $w(\cdot,t) \in H^1(\Omega, \mathcal{P}_M)$ such that one has for all $v \in H^1(\Omega, \mathcal{P}_M)$,

$$\begin{cases} \left\langle \left({}^C\mathcal{D}_t^\alpha + \mathcal{I}_t + c(\cdot,t)\right) w, v \right\rangle - \displaystyle\sum_{m=1}^{M} a(x,t) w_x v|_{x=x_m}^{x_{m+1}} + \langle a w_x, v_x \rangle = \langle \mathcal{F}, v \rangle, \\ \langle w(x,0), v \rangle = \langle g, v \rangle, \end{cases} \tag{6.7}$$

with the conditions $w(0,t) = w(\ell,t) = 0$.

The semi-discretized scheme for the IBVP (6.6) using the NIPG method for the spatial variable is given by the following: Find $w_h(\cdot,t) \in V_{0,h}^k(\Omega)$ for each $t \in (0,T]$ and

$\forall v_{_h} \in V^k_{0,h}(\Omega)$ such that

$$\begin{cases} \left\langle {}^C\mathcal{D}^\alpha_t w_{_h}(\cdot,t), v_{_h} \right\rangle + \mathcal{A}(w_{_h}(\cdot,t), v_{_h}) + \left\langle (cw_{_h} + \mathcal{I}_t w_{_h})(\cdot,t), v_{_h} \right\rangle = \left\langle \mathcal{F}(\cdot,t), v_{_h} \right\rangle, \\ \left\langle w_{_h}(\cdot,0), v_{_h} \right\rangle = \left\langle \phi, v_{_h} \right\rangle, \end{cases} \tag{6.8}$$

with the conditions $w_{_h}(0,t) = w_{_h}(\ell,t) = 0$,

$$\mathcal{A}(w_{_h}(\cdot,t), v_{_h}) = \mathcal{A}_1(w_{_h}(\cdot,t), v_{_h}) + \mathcal{A}_2(w_{_h}(\cdot,t), v_{_h}) - \mathcal{A}_2(v_{_h}, w_{_h}(\cdot,t)) + \mathcal{A}_3(w_{_h}(\cdot,t), v_{_h}), \tag{6.9}$$

where

$$\mathcal{A}_1(w_{_h}(\cdot,t), v_{_h}) = \sum_{m=1}^{M} \int_{\mathcal{K}_m} a(x,t) \frac{\partial w_{_h}}{\partial x}(x,t) \frac{dv_{_h}}{dx} dx,$$

$$\mathcal{A}_2(w_{_h}(\cdot,t), v_{_h}) = \sum_{m=1}^{M+1} \{a(x_m,t)(w_{_h})_x(x_m,t)\}[v_{_h}(x_m)],$$

and $$\mathcal{A}_3(w_{_h}(\cdot,t), v_{_h}) = \sum_{m=1}^{M+1} \frac{\sigma_m}{h}[w_{_h}(x_m,t)][v_{_h}(x_m)].$$

Here $\sigma_m \geq 1$ are the penalty parameter for each m.

6.2.3 Fully discrete scheme

In this subsection, we study two discretization schemes for the time-fractional derivative, namely L1-discretization and L2-discretization. To discretize the integral term, we employ the composite trapezoidal rule.

6.2.3.1 Fully discrete scheme using L1-discretization

We obtain the fully discrete scheme by discretizing the temporal derivative using the L1-discretization and integral term using the trapezoidal rule in (6.8) over the graded mesh $\overline{G}^N$ with $t_n = T\left(\frac{n-1}{N}\right)^r$, $n = 1, \cdots, N+1$, and the constant $r \geq 1$ is arbitrary.

The Caputo fractional derivative ${}^C\mathcal{D}^\alpha_t w_{_h}(x,t_n), n \geq 2$ is approximated by using the L1-discretization as ${}^C\mathcal{D}^\alpha_t w_{_h}(x,t_n) \approx {}^C_{L1}\mathcal{D}^\alpha_N W^n_h(x)$. By using the composite trapezoidal rule as in (4.19) on the graded mesh, we obtain the following approximation of the integral term $\mathcal{I}_t w_{_h}$ appearing in (6.8) as $\mathcal{I}_t w_{_h}(x,t_n) \approx \mathcal{I}_N W^n_h(x)$. Using the L1-discretization and the trapezoidal rule in (6.8), we obtain the fully discrete scheme for

$2 \leq n \leq N+1$ and for all $v_{_h} \in V_{0,h}^k(\Omega)$:

$$\begin{cases} \left\langle {}_{L1}^{C}\mathcal{D}_N^{\alpha} W_h^n, v_{_h} \right\rangle + \mathcal{A}(W_h^n, v_{_h}) + \left\langle c^n W_h^n + \mathcal{I}_N W_h^n, v_{_h} \right\rangle = \left\langle \mathcal{F}^n, v_{_h} \right\rangle, \\ \left\langle W_h^1, v_{_h} \right\rangle = \left\langle g, v_{_h} \right\rangle, \end{cases} \tag{6.10}$$

with the conditions $W_h^n(0) = W_h^n(\ell) = 0$.

The truncation error $\mathcal{R}_N^n(x)$ for the discretization of the temporal derivative and integral term is

$$\mathcal{R}_N^n(x) := \left({}^{C}\mathcal{D}_t^{\alpha} + \mathcal{I}_t - {}_{L1}^{C}\mathcal{D}_N^{\alpha} - \mathcal{I}_N\right) w_h(x, t^n).$$

In the next lemma we will discuss the bound of $\mathcal{R}_N^n(x)$ as in Lemma 4.3.

Lemma 6.1 *For $x \in \Omega$ and $n = 2, \cdots, N+1$, a constant C exists such that we have the following bound:*

$$\|\mathcal{R}_N^n(x)\| \leq C n^{-\min\{2-\alpha, r\alpha, 4-2r(\alpha+1)\}}.$$

6.2.3.2 Fully discrete scheme using L2-discretization

Here, by discretizing the Caputo derivative with the L2-discretization [4] and integral term using trapezoidal rule in (6.8) over uniform mesh $\overline{G}^N$, we arrive at the fully discrete scheme, for $2 \leq n \leq N$ and for all $v_{_h} \in V_{0,h}^k(\Omega)$:

$$\begin{cases} \left\langle {}_{L2}^{C}\mathcal{D}_N^{\alpha} \widehat{W_h}^{n+1}, v_{_h} \right\rangle + \mathcal{A}(\widehat{W_h}^{n+1}, v_{_h}) + \left\langle c^{n+1} \widehat{W_h}^{n+1} + \mathcal{I}_N \widehat{W_h}^{n+1}, v_{_h} \right\rangle = \left\langle \mathcal{F}^{n+1}, v_{_h} \right\rangle, \\ \left\langle \widehat{W_h}^{1}, v_{_h} \right\rangle = \left\langle g, v_{_h} \right\rangle, \end{cases} \tag{6.11}$$

with the conditions $\widehat{W_h}^{n}(0) = \widehat{W_h}^{n}(\ell) = 0$.

Lemma 6.2 *[4, Lemma 2.1] For any $\alpha \in (0,1)$, $n = 2, 3, \cdots, N$ and $u(t) \in \mathcal{C}^3[0, t_{n+1}]$, we have the following truncation error bound:*

$$\left|\left({}^{C}\mathcal{D}_t^{\alpha} - {}_{L2}^{C}\mathcal{D}_N^{\alpha}\right) u(t_{n+1})\right| \leq C\tau^{3-\alpha},$$

where C is positive constant.

Remark 6.1 *We obtain the solution $\widehat{W_h}^{2}$ with the order of accuracy in time $\mathcal{O}(\tau^{3-\alpha})$, by using the L1-discretization on $[0, \tau]$ with step $\widehat{\tau} = \mathcal{O}\left(\tau^{\frac{3-\alpha}{2-\alpha}}\right)$.*

6.3 L^2-norm stability of the fully discrete scheme

In this part, we first examine the L^2-norm stability of the fully discrete scheme (6.10) derived from the IBVP (6.1) using the L1-NIPG approach. For the fully discrete scheme (6.11) generated by the L2-NIPG technique, the same can be established in a similar way.

Define the discrete energy-norm by

$$|||v_{_h}|||_{DG}^2 = \sum_{m=1}^{M} \int_{\mathcal{K}_m} |v_{_h}^{'}|^2 dx + \sum_{m=1}^{M+1} [v_{_h}(x_m)]^2, \quad \forall v_{_h} \in V_{0,h}^k(\Omega).$$

From (6.4) and (6.9), it is clear that there exists $\nu > 0$ such that

$$\mathcal{A}(v_{_h}, v_{_h}) \geq \nu |||v_{_h}|||_{DG}^2, \quad \forall v_{_h} \in V_{0,h}^k(\Omega). \tag{6.12}$$

We present the stability result in the following general framework. Suppose that for each $n = 2, 3, \cdots, N+1$ and $v_{_h} \in V_{0,h}^k(\Omega)$, the function $\gamma^n \in V_{0,h}^k(\Omega)$ satisfies the following:

$$\begin{cases} \left\langle {}_{L1}^{C}\mathcal{D}_N^{\alpha}\gamma^n, v_{_h} \right\rangle + \mathcal{A}(\gamma^n, v_{_h}) + \left\langle c^n\gamma^n + \mathcal{I}_N\gamma^n, v_{_h} \right\rangle = \left\langle \mathcal{G}^n, v_{_h} \right\rangle, \\ \left\langle \gamma^1, v_{_h} \right\rangle = \left\langle g, v_{_h} \right\rangle, \end{cases} \tag{6.13}$$

with $\gamma^n|_{\partial\Omega} = 0$, $1 \leq n \leq N+1$.

Define $\psi_{n,j}$ for $n = 2, 3, \cdots, N+1$, $j = 2, \cdots, n-1$ as

$$\psi_{n,n} = 1, \; \psi_{n,j} = \sum_{k=2}^{n-j+1} \tau_{n-k}^{\alpha} \, \psi_{n-k+1,j} \, (\widehat{d}_{n,n-k+1} - \widehat{d}_{n,n-k} + \lambda I_{n-k+1}^n). \tag{6.14}$$

Lemma 6.3 *The solution γ^n of the discrete scheme (6.13) satisfies the following bound:*

$$\|\gamma^n\| \leq C\Big(\|\gamma^1\| + \tau_{n-1}^{\alpha} \sum_{j=2}^{n} \psi_{n,j} \|\mathcal{G}^j\|\Big), \quad \textit{for } n = 2, 3, \cdots, N+1, \tag{6.15}$$

where C is a positive constant.

Proof. Letting $v_h = \gamma^n$ $(2 \le n \le N+1)$ in equation (6.13), we obtain that

$$\Big\langle {}^{C}_{L1}\mathcal{D}^{\alpha}_{N}\gamma^n, \gamma^n \Big\rangle + \mathcal{A}(\gamma^n, \gamma^n) + \Big\langle (c^n\gamma^n + \mathcal{I}_N\gamma^n), \gamma^n \Big\rangle = \Big\langle \mathcal{G}^n, \gamma^n \Big\rangle. \tag{6.16}$$

Using (6.4) and (6.12) in (6.16), we get

$$\big\langle {}^{C}_{L1}\mathcal{D}^{\alpha}_{N}\gamma^n + \mathcal{I}_N\gamma^n, \gamma^n \big\rangle \le \Big\langle \mathcal{G}^n, \gamma^n \Big\rangle. \tag{6.17}$$

Using the L1-discretization (1.10), trapezoidal rule (4.19) in (6.17), and then applying the Cauchy-Schwartz inequality, we obtain

$$\widehat{d}_{n,n-1}\|\gamma^n\| \le \|\mathcal{G}^n\| + C\Big(\widehat{d}_{n,1} + \lambda I_1^n\Big)\|\gamma^1\| + C\sum_{j=2}^{n-1}\Big(\widehat{d}_{n,j} - \widehat{d}_{n,j-1} + \lambda I_j^n\Big)\|\gamma^j\|,$$

which is equivalent to

$$\|\gamma^n\| \le C\tau_{n-1}^{\alpha}\Big(\|\mathcal{G}^n\| + \Big(\widehat{d}_{n,1} + \lambda I_1^n\Big)\|\gamma^1\| + \sum_{j=2}^{n-1}\Big(\widehat{d}_{n,j} - \widehat{d}_{n,j-1} + \lambda I_j^n\Big)\|\gamma^j\|\Big). \tag{6.18}$$

One can easily observe from (6.18) that the inequality (6.15) holds true for $n = 2$.

Now we assume that for $j = 2, 3, \cdots, n-1, (3 \le n \le N+1)$, the following holds:

$$\|\gamma^j\| \le C\Big(\|\gamma^1\| + \tau_{j-1}^{\alpha}\sum_{k=2}^{j}\psi_{j,k}\|\mathcal{G}^k\|\Big). \tag{6.19}$$

Then from (6.18) and (6.19), we have

$$\begin{aligned}
\|\gamma^n\| \;\le\;& C\tau_{n-1}^{\alpha}\Big(\|\mathcal{G}^n\| + \Big(\widehat{d}_{n,1} + \lambda I_1^n\Big)\|\gamma^1\|\Big) \\
&+C\tau_{n-1}^{\alpha}\sum_{j=2}^{n-1}\Big(\widehat{d}_{n,j} - \widehat{d}_{n,j-1} + \lambda I_j^n\Big)\Big(\|\gamma^1\| + \tau_{j-1}^{\alpha}\sum_{k=2}^{j}\psi_{j,k}\|\mathcal{G}^k\|\Big) \\
\le\;& C\tau_{n-1}^{\alpha}\Big(\|\mathcal{G}^n\| + \Big(\widehat{d}_{n,n-1} + \lambda\sum_{j=1}^{n-1}I_j^n\Big)\|\gamma^1\|\Big) \\
&+C\tau_{n-1}^{\alpha}\sum_{j=2}^{n-1}\Big(\widehat{d}_{n,j} - \widehat{d}_{n,j-1} + \lambda I_j^n\Big)\tau_{j-1}^{\alpha}\sum_{k=2}^{j}\psi_{j,k}\|\mathcal{G}^k\| \\
\le\;& C\tau_{n-1}^{\alpha}\|\mathcal{G}^n\| + C\Big(\frac{1}{\Gamma(2-\alpha)} + \lambda\tau_{\max}^{\alpha+1}\Big)\|\gamma^1\|
\end{aligned}$$

$$+C\tau_{n-1}^{\alpha}\sum_{j=2}^{n-1}\|\mathcal{G}^j\|\sum_{k=2}^{n-j+1}\tau_{n-k}^{\alpha}\Big(\widehat{d}_{n,n-k+1}-\widehat{d}_{n,n-k}+\lambda I_{n-k+1}^{n}\Big)\psi_{n-k+1,j}$$
$$\leq \quad C\Big(\|\gamma^1\|+\tau_{n-1}^{\alpha}\sum_{j=2}^{n}\psi_{n,j}\|\mathcal{G}^j\|\Big),$$

where in the last inequality we have used (6.14). Hence by using the induction principle, we have obtained the required result. □

In our analysis, the subsequent result is quite helpful.

Lemma 6.4 *For $n = 2, 3, \cdots, N+1$, we have the following bound for $\psi_{n,j}$:*

$$\tau_{n-1}^{\alpha}\sum_{j=2}^{n} j^{-\nu}\psi_{n,j} \;\leq\; C\,T^{\alpha}N^{-\nu},$$

where ν is a parameter satisfying $\nu \leq r\alpha$ and $C \geq \Gamma(1-\alpha)$.

Proof. The proof is similar to [106, Lemma 4.3].. □

Next lemma presents the stability result for the discrete scheme (6.13).

Lemma 6.5 *Let γ^n be the solution of (6.13). Then for $n = 2, 3, \cdots, N+1$, we have*

$$\|\gamma^n\| \leq C\Big(\|\gamma^1\| + \max_{2\leq j\leq n}\|\mathcal{G}^j\|\Big).$$

Proof. From Lemma 6.3 and Lemma 6.4 with $\nu = 0$, one can obtain the required result. □

One can establish the following result using Lemma 6.3, in the same way of proof as in [46, Lemma 4.4], which will be used in the error analysis.

Lemma 6.6 *Suppose that γ^n satisfies $\left\langle \left(\frac{C}{L1}\mathcal{D}_N^{\alpha}+\mathcal{I}_N\right)\gamma^n,\gamma^n\right\rangle \leq \langle \mathcal{G}^n,\gamma^n\rangle + (\mu^n)^2$, then for $1 \leq n \leq N+1$, we have*

$$\|\gamma^n\| \leq C\left(\|\gamma^1\| + \tau_{n-1}^{\alpha}\sum_{j=1}^{n}\psi_{n,j}\|\mathcal{G}^j\| + \max_{1\leq j\leq n}\|\mu^j\|\right).$$

6.4 Error estimates

In this section, we establish the error analysis for the L1-NIPG method. The error bound for the L2-NIPG method can be establish in a similar way. From the L^2-projection

definition and (6.10), we can have that $W_h^1(x) = \mathbf{P}\phi(x)$.

Let $w(x,t_n)$ and W_h^n be the solutions of (6.6) and (6.10) at $t = t_n$, respectively. Then denote the error $e^n(x)$, $n = 1, 2, \cdots, N+1$ as

$$e^n(x) = w(x,t_n) - W_h^n(x) =: \eta^n - \xi^n,$$

where $\eta^n = \mathbf{P}w(x,t_n) - W_h^n(x)$ and $\xi^n = \mathbf{P}w(x,t_n) - w(x,t_n)$.

From (6.7) and (6.8), we have the following for all $v_{_h}$:

$$\begin{aligned}\Big\langle \big({}_{L1}^{C}\mathcal{D}_N^{\alpha} + \mathcal{I}_N\big)\,\eta^n, v_{_h}\Big\rangle + \mathcal{A}(\eta^n, v_{_h}) + \langle c^n\eta^n, v_{_h}\rangle \\ = \Big\langle \big({}_{L1}^{C}\mathcal{D}_N^{\alpha} + \mathcal{I}_N\big)\,\xi^n, v_{_h}\Big\rangle + \mathcal{A}(\xi^n, v_{_h}) + \langle c^n\xi^n, v_{_h}\rangle - \langle \mathcal{R}_N^n, v_{_h}\rangle. \qquad (6.20)\end{aligned}$$

By using Lemma 1.4, we have the following estimate.

Lemma 6.7 *The projection error for each value of $n = 1, 2, \cdots, N+1$ is as follows:*

$$\|\mathbf{P}w(x,t_n) - w(x,t_n)\| \le Ch^{k+1},$$

where C is a positive constant.

In the next theorem we will find out the bound for the discretization error.

Theorem 6.2 *The bound for the discretization error for each $n = 1, 2, \cdots, N+1$ is as follows:*

$$\|\eta^n\| \le C\Big(h^k + N^{-\varrho}\Big), \qquad (6.21)$$

where $\varrho = \min\{2-\alpha, r\alpha, 4-2r(\alpha+1)\}$.

Proof. Taking $v_{_h} = \eta^n$ in (6.20), we have

$$\begin{aligned}\big\langle \big({}_{L1}^{C}\mathcal{D}_N^{\alpha} + \mathcal{I}_N\big)\,\eta^n, \eta^n\big\rangle + \mathcal{A}(\eta^n, \eta^n) + \langle c^n\eta^n, \eta^n\rangle \\ = \big\langle \big({}_{L1}^{C}\mathcal{D}_N^{\alpha} + \mathcal{I}_N\big)\,\xi^n, \eta^n\big\rangle + \mathcal{A}(\xi^n, \eta^n) + \langle c^n\xi^n, \eta^n\rangle - \langle \mathcal{R}_N^n, \eta^n\rangle. \qquad (6.22)\end{aligned}$$

Now from (6.4) and (6.9), we have

$$\begin{aligned}\mathcal{A}(\eta^n, \eta^n) &= \sum_{m=1}^{M} \int_{\mathcal{K}_m} a^n(\eta_x^n)^2 dx + \sum_{m=1}^{M+1} \sigma_m[\eta^n(x_m)]^2 \\ &\ge \frac{a_*}{2}\|\eta_x^n\|^2 + \sum_{m=1}^{M+1} \sigma_m[\eta^n(x_m)]^2. \qquad (6.23)\end{aligned}$$

It is clear that $[\xi^n(x_m)] = 0$. Then from (6.4) and (6.9) and using the Young's inequality, we have the following:

$$\begin{aligned}\mathcal{A}(\xi^n, \eta^n) &= \sum_{m=1}^{M} \int_{\mathcal{K}_m} a^n \xi_x^n \eta_x^n dx + \sum_{m=1}^{M+1} \{a^n(x_m)\xi_x^n(x_m)\}[\eta^n(x_m)] \\ &\leq a^* \sum_{m=1}^{M} \int_{\mathcal{K}_m} \xi_x^n \eta_x^n dx + a^* \sum_{m=1}^{M+1} \{\xi_x^n(x_m)\}[\eta^n(x_m)] \\ &\leq \left(\frac{a_*}{2}\|\eta_x^n\|^2 + \frac{a^*}{2a_*}\|\xi_x^n\|^2\right) + \sum_{m=1}^{M+1}\left([\eta^n(x_m)]^2 + \frac{a^{*2}}{4}\{\xi_x^n(x_m)\}^2\right). \end{aligned} \tag{6.24}$$

Using (6.23) and (6.24) in (6.22), we can obtain that

$$\left\langle \left({}_{L1}^{C}\mathcal{D}_N^{\alpha} + \mathcal{I}_N\right)\eta^n, \eta^n \right\rangle \leq \langle \chi^n, \eta^n \rangle + Ch^{2k}, \tag{6.25}$$

where $\chi^n = \left({}_{L1}^{C}\mathcal{D}_N^{\alpha} + \mathcal{I}_N\right)\xi^n + c^n\xi^n - \mathcal{R}_N^n$. It is clear that $\|\chi^n\| \leq C(h^{k+1} + n^{-\varrho})$. Now replacing $\gamma^n = \eta^n$, $\mathcal{G}^n = \chi^n$ and $\mu^n = \sqrt{C}h^k$ in Lemma 6.6, we have

$$\begin{aligned}\|\eta^n\| &\leq C\left(\|\eta^1\| + \tau_{n-1}^{\alpha}\sum_{j=1}^{n}\psi_{n,j}\|\chi^j\| + h^k\right) \\ &\leq C\left(h^{k+1} + \tau_{n-1}^{\alpha}\sum_{j=1}^{n}\psi_{n,j}(h^{k+1} + j^{-\varrho}) + h^k\right) \\ &\leq C(h^k + N^{-\varrho}),\end{aligned}$$

here we have used Lemma 6.4. □

Theorem 6.3 *Let $w(x, t_n)$ and W_h^n be the solutions of (6.6) and (6.10) at $t = t_n$, respectively. Then we have the following error bound due to the fully discretization of the IBVP (6.6):*

$$\max_{1\leq n\leq N+1}\|w(x, t_n) - W_h^n\| \leq C(h^k + N^{-\varrho}),$$

where $\varrho = \min\{2 - \alpha, r\alpha, 4 - 2r(\alpha + 1)\}$.

Proof. For each $n = 1, 2, \cdots, N + 1$, we have $\|w(x, t_n) - W_h^n\| \leq \|\eta^n\| + \|\xi^n\|$. We arrive at the necessary conclusion by combining Lemma 6.7 and Theorem 6.2. □

6.5 Numerical experiments

In this section, we carry out some numerical experiments to show the accuracy and efficiency of the proposed method, which will also validate the theoretical error bounds and order of convergence. The results are presented in tabular forms and figures, including error plots and log-log plots.

The errors and orders of convergence are determined by

$$\mathcal{E}^1_{M,N} = \max_{\substack{1\le n\le N+1,\\ 1\le m\le M+1}} |u(x_m,t_n) - W^n_h(x_m)|, \quad R^1_{M,N} = \log_2\left(\frac{\mathcal{E}^1_{M,N}}{\mathcal{E}^1_{2M,2N}}\right),$$
$$\mathcal{E}^2_{M,N} = \max_{1\le n\le N+1} \|u(\cdot,t_n) - W^n_h\|, \quad \text{and} \quad R^2_{M,N} = \log_2\left(\frac{\mathcal{E}^2_{M,N}}{\mathcal{E}^2_{2M,2N}}\right),$$

where v is the solution of IBVP (6.1) and W^n_h is the approximate solution of the fully discrete scheme (6.10) at $t = t_n$.

Example 6.4 *Consider the following problem:*

$$\begin{cases} {}^C\mathcal{D}^\alpha_t u(x,t) - \dfrac{\partial^2 u}{\partial x^2}(x,t) + \displaystyle\int_0^t x(t-s)u(x,s)ds = f(x,t),\ (x,t)\in(0,1)\times(0,1], \\ u(x,0) = 0, \quad x\in[0,1], \\ u(0,t) = u(1,t) = 0, \quad t\in(0,1]. \end{cases} \tag{6.26}$$

The solution of the IBVP (6.26) is $u(x,t) = (t^{5+\alpha} + t^{3+\alpha})x(1-x)$, which will be used to calculate the source term f. Tables 6.1 and 6.2 present the errors and the corresponding order of convergence for Example 6.4 using both L1-discretization and L2-discretization for the fractional-time derivative with $M = N$, where we see that L1-discretization gives order of convergence $(2-\alpha)$ and L2-discretization gives second order convergence results. Table 6.3 displays the same for Example 6.4 using the L2-discretization for the fractional-time derivative with $h^2 = \tau^{3-\alpha}$, where the order of convergence is $(3-\alpha)$. One can see from these Tables that the L2-discretization provides with higher accuracy and better order of convergence, which is further illustrated in Figure 6.1. Figure 6.2 depict log-log plots of N vs. errors for Example 6.4 for various values of α using $N = M$ and both L1-NIPG and L2-NIPG approaches.

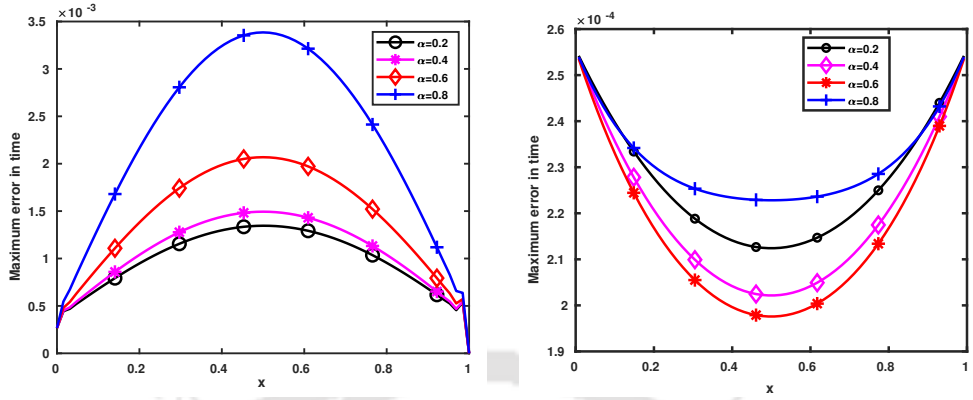

(a) Using L1-NIPG. *(b) Using L2-NIPG.*

Figure 6.1: *Errors for various values of α for Example 6.4 with $M = N = 64$.*

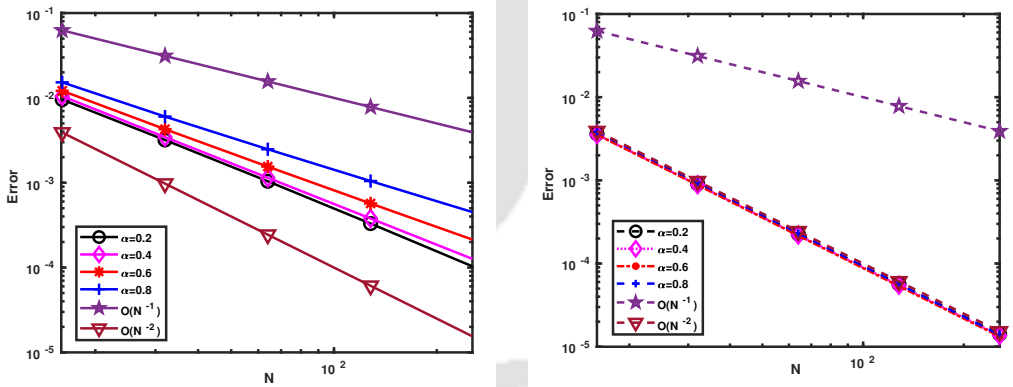

(a) Using L1-NIPG. *(b) Using L2-NIPG.*

Figure 6.2: *Log-log plots of errors N vs. $\mathcal{E}^2_{M,N}$ for various values of α for Example 6.4 with $M = N = 64$.*

Table 6.1: $\mathcal{E}^1_{M,N}$ *and* $R^1_{M,N}$ *for Example 6.4 using L1-NIPG with* $r = (2-\alpha)/\alpha$ *and L2-NIPG.*

$\alpha\downarrow$	Method	$N=M\rightarrow$	2^4	2^5	2^6	2^7	2^8
0.2	L1-NIPG	$\mathcal{E}^1_{M,N}$	1.1300e-02	3.9869e-03	1.3458e-03	4.3579e-04	1.3694e-04
		$R^1_{M,N}$	1.5030	1.5669	1.6267	1.6701	–
	L2-NIPG	$\mathcal{E}^1_{M,N}$	3.9994e-03	1.0111e-03	2.5419e-04	6.3723e-05	1.5953e-05
		$R^1_{M,N}$	1.9838	1.9920	1.9960	1.9980	–
0.4	L1-NIPG	$\mathcal{E}^1_{M,N}$	1.2644e-02	4.3678e-03	1.4939e-03	5.0534e-04	1.6954e-04
		$R^1_{M,N}$	1.5335	1.5478	1.5638	1.5756	–
	L2-NIPG	$\mathcal{E}^1_{M,N}$	3.9795e-03	1.0084e-03	2.5382e-04	6.3673e-05	1.5946e-05
		$R^1_{M,N}$	1.9805	1.9902	1.9950	1.9975	–
0.6	L1-NIPG	$\mathcal{E}^1_{M,N}$	1.5057e-02	5.5488e-03	2.0685e-03	7.7517e-04	2.9141e-04
		$R^1_{M,N}$	1.4402	1.4236	1.4160	1.4115	–
	L2-NIPG	$\mathcal{E}^1_{M,N}$	3.9697e-03	1.0067e-03	2.5354e-04	6.3631e-05	1.5940e-05
		$R^1_{M,N}$	1.9794	1.9893	1.9944	1.9971	–
0.8	L1-NIPG	$\mathcal{E}^1_{M,N}$	1.9545e-02	8.0294e-03	3.3852e-03	1.4470e-03	6.2323e-04
		$R^1_{M,N}$	1.2834	1.2461	1.2262	1.2152	–
	L2-NIPG	$\mathcal{E}^1_{M,N}$	3.9996e-03	1.0103e-03	2.5393e-04	6.3670e-05	1.5943e-05
		$R^1_{M,N}$	1.9850	1.9923	1.9958	1.9976	–

Table 6.2: $\mathcal{E}^2_{M,N}$ *and* $R^2_{M,N}$ *for Example 6.4 using L1-NIPG with* $r = (2-\alpha)/\alpha$ *and L2-NIPG.*

$\alpha\downarrow$	Method	$N=M\rightarrow$	2^4	2^5	2^6	2^7	2^8
0.2	L1-NIPG	$\mathcal{E}^2_{M,N}$	9.5527e-03	3.1861e-03	1.0401e-03	3.2985e-04	1.0222e-04
		$R^2_{M,N}$	1.5841	1.6152	1.6568	1.6902	–
	L2-NIPG	$\mathcal{E}^2_{M,N}$	3.6366e-03	9.0866e-04	2.2696e-04	5.6698e-05	1.4168e-05
		$R^2_{M,N}$	2.0008	2.0013	2.0010	2.0007	–
0.4	L1-NIPG	$\mathcal{E}^2_{M,N}$	1.0467e-02	3.4499e-03	1.1438e-03	3.7887e-04	1.2527e-04
		$R^2_{M,N}$	1.6011	1.5927	1.5941	1.5967	–
	L2-NIPG	$\mathcal{E}^2_{M,N}$	3.5547e-03	8.8445e-04	2.2011e-04	5.4833e-05	1.3674e-05
		$R^2_{M,N}$	2.0069	2.0066	2.0051	2.0036	–
0.6	L1-NIPG	$\mathcal{E}^2_{M,N}$	1.2125e-02	4.2748e-03	1.5485e-03	5.6975e-04	2.1167e-04
		$R^2_{M,N}$	1.5040	1.4649	1.4425	1.4285	–
	L2-NIPG	$\mathcal{E}^2_{M,N}$	3.5519e-03	8.7727e-04	2.1659e-04	5.3563e-05	1.3273e-05
		$R^2_{M,N}$	2.0175	2.0180	2.0157	2.0128	–
0.8	L1-NIPG	$\mathcal{E}^2_{M,N}$	1.5243e-02	6.0205e-03	2.4804e-03	1.0463e-03	4.4731e-04
		$R^2_{M,N}$	1.3402	1.2793	1.2452	1.2260	–
	L2-NIPG	$\mathcal{E}^2_{M,N}$	3.8217e-03	9.4289e-04	2.3132e-04	5.6679e-05	1.3898e-05
		$R^2_{M,N}$	2.0191	2.0272	2.0290	2.0279	–

Table 6.3: *Error and order of convergence for Example 6.4 using L2-NIPG with* $h^2 = \tau^{3-\alpha}$.

$\alpha\downarrow$	$N\rightarrow$	2^3	2^4	2^5	2^6
0.2	$\mathcal{E}^1_{M,N}$	3.1840e-03	4.3409e-04	6.3808e-05	9.1604e-06
	$R^1_{M,N}$	2.8748	2.7662	2.8003	–
	$\mathcal{E}^2_{M,N}$	2.9849e-03	4.0935e-04	6.0770e-05	8.8811e-06
	$R^2_{M,N}$	2.8663	2.7519	2.7745	–
0.4	$\mathcal{E}^1_{M,N}$	4.5787e-03	7.6086e-04	1.2622e-04	2.1041e-05
	$R^1_{M,N}$	2.5892	2.5917	2.5846	–
	$\mathcal{E}^2_{M,N}$	4.3919e-03	7.3606e-04	1.2335e-04	2.0757e-05
	$R^2_{M,N}$	2.5769	2.5770	2.5712	–
0.6	$\mathcal{E}^1_{M,N}$	7.1501e-03	1.3741e-03	2.6885e-04	5.1755e-05
	$R^1_{M,N}$	2.3795	2.3536	2.3770	–
	$\mathcal{E}^2_{M,N}$	7.0884e-03	1.3470e-03	2.6164e-04	5.0111e-05
	$R^2_{M,N}$	2.3957	2.3641	2.3844	–
0.8	$\mathcal{E}^1_{M,N}$	1.1489e-02	2.7096e-03	6.0862e-04	1.3396e-04
	$R^1_{M,N}$	2.0840	2.1545	2.1837	–
	$\mathcal{E}^2_{M,N}$	1.0977e-02	2.5584e-03	5.6953e-04	1.2454e-04
	$R^2_{M,N}$	2.1012	2.1674	2.1932	–

Example 6.5 *Consider the following nonlinear problem over the domain* $(0,1)\times(0,1]$:

$$\begin{cases} {}^{C}\mathcal{D}_t^{\alpha}u(x,t) - \dfrac{\partial^2 u}{\partial x^2}(x,t) + \exp(u(x,t)) + \displaystyle\int_0^t x(t-s)u(x,s)ds = f(x,t), \\ u(x,0) = x(1-x), \quad x\in[0,1], \\ u(0,t) = u(1,t) = 0, \quad t\in(0,1]. \end{cases} \tag{6.27}$$

The function $f(x,t)$ in the IBVP (6.27) will be selected in such a manner that $u(x,t) = x(1-x)(1+t^2+t^{3+\alpha})$ is the solution. The errors and the corresponding order of convergence for Example 6.5 are shown in Table 6.4 and Table 6.5 with $M = N$, where L2-discretization have better accuracy than L1-discretization. Figure 6.3 displays the maximum errors in time for both the schemes L1-NIPG and L2-NIPG with $M = N = 64$, where we can observe that the for each α the errors reduces when we use L2-discretization instead of L1-discretization. Table 6.6 demonstrates that, while $h^2 = \tau^{3-\alpha}$, the errors decreases, as it expected and the convergence order is $(3-\alpha)$. Figure 6.4 show log-log plots of N vs. errors for Example 6.5 for a range of α values, with $N = M$ and both schemes L1-NIPG and L2-NIPG.

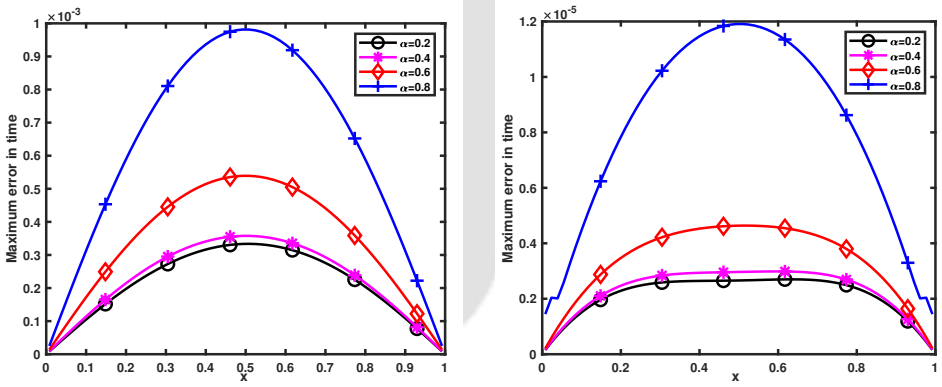

(a) Using L1-NIPG scheme. *(b) Using L2-NIPG scheme.*

Figure 6.3: *Errors for various values of* α *for Example 6.5 with* $M = N = 64$.

6.6 Conclusion

This chapter proposed and analyzed the convergence of the NIPG method for the nonlinear time-fractional integro-partial differential equations. After linearizing the IBVP

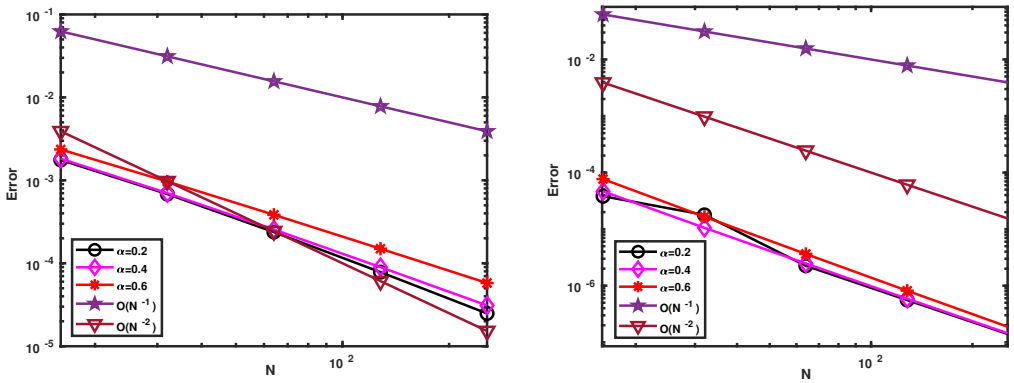

(a) Using L1-NIPG. *(b) Using L2-NIPG.*

Figure 6.4: *Log-log plots of errors N vs. $\mathcal{E}^2_{M,N}$ for various values of α for Example 6.5 with $M = N = 64$.*

Table 6.4: *$\mathcal{E}^1_{M,N}$ and $R^1_{M,N}$ for Example 6.5 using L1-NIPG with $r = (2-\alpha)/\alpha$ and L2-NIPG.*

$\alpha\downarrow$	Method	$N = M \rightarrow$	2^4	2^5	2^6	2^7	2^8
0.2	L1-NIPG	$\mathcal{E}^1_{M,N}$	2.4620e-03	9.5667e-04	3.3361e-04	1.0976e-04	3.4869e-05
		$R^1_{M,N}$	1.3637	1.5198	1.6038	1.6543	–
	L2-NIPG	$\mathcal{E}^1_{M,N}$	4.5991e-05	2.4589e-05	2.6995e-06	6.6692e-07	1.6560e-07
		$R^1_{M,N}$	0.9033	3.1873	2.0171	2.0098	–
0.4	L1-NIPG	$\mathcal{E}^1_{M,N}$	2.5427e-03	9.8123e-04	3.5766e-04	1.2610e-04	4.3555e-05
		$R^1_{M,N}$	1.3737	1.4560	1.5040	1.5337	–
	L2-NIPG	$\mathcal{E}^1_{M,N}$	5.7413e-05	1.2884e-05	2.9857e-06	7.0847e-07	1.7088e-07
		$R^1_{M,N}$	2.1558	2.1094	2.0753	2.0517	–
0.6	L1-NIPG	$\mathcal{E}^1_{M,N}$	3.2886e-03	1.3552e-03	5.3921e-04	2.1043e-04	8.1203e-05
		$R^1_{M,N}$	1.2790	1.3295	1.3575	1.3737	–
	L2-NIPG	$\mathcal{E}^1_{M,N}$	9.9599e-05	2.1339e-05	4.6379e-06	1.0251e-06	2.3053e-07
		$R^1_{M,N}$	2.2226	2.2020	2.1777	2.1528	–

Table 6.5: $\mathcal{E}^2_{M,N}$ *and* $R^2_{M,N}$ *for Example 6.5 using L1-NIPG with* $r = (2-\alpha)/\alpha$ *and L2-NIPG.*

$\alpha \downarrow$	Method	$N = M \rightarrow$	2^4	2^5	2^6	2^7	2^8
0.2	L1-NIPG	$\mathcal{E}^2_{M,N}$	1.7609e-03	6.8257e-04	2.3788e-04	7.8239e-05	2.4851e-05
		$R^2_{M,N}$	1.3672	1.5208	1.6042	1.6546	–
	L2-NIPG	$\mathcal{E}^2_{M,N}$	3.8311e-05	1.7871e-05	2.2527e-06	5.5696e-07	1.3836e-07
		$R^2_{M,N}$	1.1002	2.9879	2.0160	2.0092	–
0.4	L1-NIPG	$\mathcal{E}^2_{M,N}$	1.8228e-03	7.0073e-04	2.5510e-04	8.9893e-05	3.1040e-05
		$R^2_{M,N}$	1.3792	1.4578	1.5048	1.5341	–
	L2-NIPG	$\mathcal{E}^2_{M,N}$	4.6664e-05	1.0570e-05	2.4677e-06	5.8845e-07	1.4238e-07
		$R^2_{M,N}$	2.1424	2.0987	2.0682	2.0472	–
0.6	L1-NIPG	$\mathcal{E}^2_{M,N}$	2.3574e-03	9.6749e-04	3.8446e-04	1.4996e-04	5.7854e-05
		$R^2_{M,N}$	1.2849	1.3314	1.3582	1.3741	–
	L2-NIPG	$\mathcal{E}^2_{M,N}$	7.6813e-05	1.6590e-05	3.6468e-06	8.1577e-07	1.8561e-07
		$R^2_{M,N}$	2.2111	2.1856	2.1604	2.1359	–

by using the Newton linearization process, we have applied the NIPG method for spatial variable, and both L1-discretization and L2-discretization for time-fractional derivative, and the trapezoidal rule for the integral term, and finally obtained the fully discrete scheme. We derived L^2-norm stability and error analysis, and those are validated by numerical examples.

Table 6.6: *Error and order of convergence for Example 6.5 using L2-NIPG with* $h^2 = \tau^{3-\alpha}$.

$\alpha \downarrow$	$N \rightarrow$	2^3	2^4	2^5	2^6
0.2	$\mathcal{E}^1_{M,N}$	1.4885e-04	9.7500e-06	6.6692e-07	9.4822e-08
	$R^1_{M,N}$	3.9324	3.8698	2.8142	–
	$\mathcal{E}^2_{M,N}$	1.0870e-04	7.0765e-06	5.5696e-07	7.9234e-08
	$R^2_{M,N}$	3.9412	3.6674	2.8134	–
0.4	$\mathcal{E}^1_{M,N}$	6.6091e-05	9.4618e-06	1.4348e-06	2.2658e-07
	$R^1_{M,N}$	2.8043	2.7212	2.6628	–
	$\mathcal{E}^2_{M,N}$	5.3694e-05	7.7762e-06	1.1891e-06	1.8869e-07
	$R^2_{M,N}$	2.7876	2.7091	2.6559	–
0.6	$\mathcal{E}^1_{M,N}$	1.8936e-04	2.8686e-05	4.6379e-06	7.5995e-07
	$R^1_{M,N}$	2.7227	2.6288	2.6095	–
	$\mathcal{E}^2_{M,N}$	1.4587e-04	2.2258e-05	3.6468e-06	6.0619e-07
	$R^2_{M,N}$	2.7123	2.6096	2.5888	–
0.8	$\mathcal{E}^1_{M,N}$	6.3237e-04	1.3088e-04	2.5433e-05	4.8619e-06
	$R^1_{M,N}$	2.2725	2.3635	2.3871	–
	$\mathcal{E}^2_{M,N}$	4.7040e-04	9.6513e-05	1.8796e-05	3.6066e-06
	$R^2_{M,N}$	2.2851	2.3603	2.3817	–

CHAPTER 7

Non-symmetric interior penalty Galerkin method for nonlinear time-fractional Burgers' equation

This chapter focuses on the study of numerical solutions for the one-dimensional time-fractional Burgers' equation. We proposed a stable fully discrete scheme that comprises the L2-discretization for the time derivative and the NIPG method for the spatial variable. Convergence analysis are carried out. Numerical results show the accuracy and efficiency of the present method.

7.1 Introduction

This chapter takes into account the following nonlinear time-fractional Burgers' equation:

$$\begin{cases} {}^{C}\mathcal{D}_t^{\alpha} u(x,t) + \dfrac{\partial}{\partial x}\left(\dfrac{u^2}{2}\right)(x,t) = p\dfrac{\partial^2 u}{\partial x^2}(x,t) + f(x,t),\ (x,t) \in \Omega \times (0,T], \\ u(x,0) = g(x), \quad \forall x \in \overline{\Omega}, \\ u(0,t) = u(\ell,t) = 0, \quad \forall t \in (0,T], \end{cases} \tag{7.1}$$

where $\Omega = (0,\ell)$, $p > 0$, and $0 < \alpha < 1$. Furthermore, we assume that $\dfrac{\partial u}{\partial x} \geq \nu^* > 0$, and $g(0) = g(\ell) = 0$.

The major goal of this chapter is to arrive at a numerical solution for the nonlinear time-fractional Burgers' equation by applying the NIPG method for spatial variable and the L2-discretization for time derivative discretization. We further examine the suggested method's stability under the L^2-norm, and we calculate the necessary error

estimates with an order of convergence of $(h^{k+1} + \tau^{3-\alpha})$, where h and τ are the step-lengths in space and time, respectively. Numerical experiments will be carried out to validate the suggested approach and show the theoretical error bounds.

The rest of the chapter is organized as follows: In Section 7.2, we derive the L2-NIPG fully discrete scheme. Section 7.3 shows the L^2-stability of the fully discrete scheme. Section 7.4 establishes the convergence analysis of the proposed method. Finally, Section 7.5 shows the experimental studies for verifying the proposed results.

7.2 Derivation of the L2-NIPG scheme

This section outlines the numerical process of resolving the nonlinear time-fractional Burgers' equation (7.1).

7.2.1 Temporal semi-discretization

By discretizing the time derivative in (7.1) with the L2-discretization [4, 111] over the uniform temporal mesh $\overline{G}^N$ with temporal step length $\tau = T/N$, we arrive at the semi-discrete scheme. Let $U^{n+1}(x)$ be the approximate value of $u(x, t_{n+1})$. Now, L2-discretization for the discretization of ${}^{C}\mathcal{D}_t^{\alpha} u(x, t_{n+1}), n \geq 2$ is described as ${}^{C}\mathcal{D}_t^{\alpha} u(x, t_{n+1}) \approx {}_{L2}^{C}\mathcal{D}_N^{\alpha} U^{n+1}(x)$.

Lemma 7.1 *[4, Lemma 2.1] The following is the truncation error bound for any $\alpha \in (0,1)$, $2 \leq n \leq N$ and $u(t) \in \mathcal{C}^3[0, t_{n+1}]$:*

$$\left|\left({}^{C}\mathcal{D}_t^{\alpha} - {}_{L2}^{C}\mathcal{D}_N^{\alpha}\right) u(t_{n+1})\right| \leq C\tau^{3-\alpha},$$

where $C > 0$ is a constant.

Remark 7.1 *In order to use the L2-discretization for the discretization of ${}^{C}\mathcal{D}_t^{\alpha} u(x, t_{n+1}), n \geq 2$ given in (1.11), one has to know the values of $U^1(x)$ and $U^2(x)$ in advance. Here, the initial value $g(x)$ can be taken as $U^1(x)$ and to calculate $U^2(x)$, we use L1-discretization. As the L1-discretization has an accuracy of order $(2-\alpha)$ in the temporal direction, we will obtain $U^2(x)$ using L1-discretization with an order of accuracy $\mathcal{O}(\tau^{3-\alpha})$ in time with step $\widehat{\tau} = \mathcal{O}\left(\tau^{\frac{3-\alpha}{2-\alpha}}\right)$ on $[0, \tau]$. Over $[0, \tau]$, define grid points as $\widehat{t}_{n_1} = (n_1 - 1)\widehat{\tau}$, $1 \leq n_1 \leq N_1$, where N_1 is chosen such that $\widehat{t}_{N_1} = \tau$.*

To approximate the fractional derivative ${}^{C}\mathcal{D}_t^{\alpha} u(x, \widehat{t}_{n_1})$ for $\widehat{t}_{n_1} \in [0, \tau]$, utilize the L1-discretization as ${}^{C}\mathcal{D}_t^{\alpha} u(x, \widehat{t}_{n_1}) \approx {}_{L1}^{C}\mathcal{D}_{N_1}^{\alpha} \widehat{u}^{n_1}(x)$.

We generate the following semi-discrete problem by discretizing the temporal derivative in (7.1):

$$\begin{cases} {}_{L1}^{C}\mathcal{D}_{N_1}^{\alpha}\widehat{u}^{n_1}(x)+\widehat{u}^{n_1}(x)\dfrac{\partial\widehat{u}^{n_1}}{\partial x}(x)=p\dfrac{\partial^2\widehat{u}^{n_1}}{\partial x^2}(x)+\widehat{f}^{n_1}(x), \quad x\in\Omega, \quad 2\le n_1\le N_1, \\ {}_{L2}^{C}\mathcal{D}_{N}^{\alpha}U^{n+1}(x)+U^{n+1}(x)\dfrac{\partial U^{n+1}}{\partial x}(x)=p\dfrac{\partial^2 U^{n+1}}{\partial x^2}(x)+f^{n+1}(x), \quad x\in\Omega, \quad 2\le n\le N, \\ \widehat{u}^1(x)=U^1(x)=g(x), \quad \forall x\in\overline{\Omega}, \\ U^2(x)=\widehat{u}^{N_1}(x), \quad \forall x\in\overline{\Omega}, \\ \widehat{u}^{n_1}(0)=\widehat{u}^{n_1}(\ell)=U^n(0)=U^n(\ell)=0, \quad 2\le n_1\le N_1, \quad 2\le n\le N. \end{cases} \tag{7.2}$$

Here, we denote $\widehat{f}^{n1}(x)=f(x,\widehat{t}_{n_1})$, $f^n(x)=f(x,t_n)$.

7.2.2 The fully discrete scheme

Here, we employ the NIPG approach to construct a fully discrete scheme by discretizing the spatial variables in the semi-discrete problem (7.2). The weak formulation of (7.2) is now given as: Find $\widehat{u}^{n_1}, U^{n+1}\in H_0^1(\Omega)$ for $2\le n_1\le N_1$, $2\le n\le N$ such that one has for all $\psi\in H_0^1(\Omega)$,

$$\begin{cases} \left\langle {}_{L1}^{C}\mathcal{D}_{N_1}^{\alpha}\widehat{u}^{n_1},\psi\right\rangle+\left\langle \widehat{u}^{n_1}\dfrac{\partial\widehat{u}^{n_1}}{\partial x},\psi\right\rangle+p\left\langle\dfrac{\partial\widehat{u}^{n_1}}{\partial x},\dfrac{\partial\psi}{\partial x}\right\rangle-p\sum_{i=1}^{M}\dfrac{\partial\widehat{u}^{n_1}}{\partial x}\psi|_{x_i}^{x_{i+1}}=\left\langle\widehat{f}^{n_1},\psi\right\rangle, \\ \left\langle {}_{L2}^{C}\mathcal{D}_{N}^{\alpha}U^{n+1},\psi\right\rangle+\left\langle U^{n+1}\dfrac{\partial U^{n+1}}{\partial x},\psi\right\rangle+p\left\langle\dfrac{\partial U^{n+1}}{\partial x},\dfrac{\partial\psi}{\partial x}\right\rangle-p\sum_{i=1}^{M}\dfrac{\partial U^{n+1}}{\partial x}\psi|_{x_i}^{x_{i+1}}=\left\langle f^{n+1},\psi\right\rangle, \\ \langle\widehat{u}^1,\psi\rangle=\langle U^1,\psi\rangle=\langle g,\psi\rangle. \end{cases} \tag{7.3}$$

The following is the fully discrete scheme for the IBVP (7.1) utilizing the NIPG approach for the spatial variable in (7.2): Find $\widehat{u}_h^{n_1}, U_h^{n+1}\in V_{0,h}^k(\Omega)$ for $2\le n_1\le N_1$, $2\le n\le N$ and $\forall\psi_h\in V_{0,h}^k(\Omega)$ such that

$$\begin{cases} \left\langle {}_{L1}^{C}\mathcal{D}_{N_1}^{\alpha}\widehat{u}_h^{n_1},\psi_h\right\rangle+\mathcal{A}(\widehat{u}_h^{n_1},\psi_h)=\left\langle\widehat{f}^{n_1},\psi_h\right\rangle, \\ \left\langle {}_{L2}^{C}\mathcal{D}_{N}^{\alpha}U_h^{n+1},\psi_h\right\rangle+\mathcal{A}(U_h^{n+1},\psi_h)=\left\langle f^{n+1},\psi_h\right\rangle, \\ \left\langle\widehat{u}_h^1,\psi_h\right\rangle=\left\langle U_h^1,\psi_h\right\rangle=\langle g,\psi_h\rangle, \end{cases} \tag{7.4}$$

where

$$\begin{aligned}\mathcal{A}(v,\psi_h) &= \left\langle v\frac{dv}{dx},\psi_h\right\rangle + p\left\langle \frac{dv}{dx},\frac{d\psi_h}{dx}\right\rangle + p\sum_{i=1}^{M+1}\left\{\frac{dv}{dx}(x_i)\right\}[\psi_h(x_i)]\\ &\quad -p\sum_{i=1}^{M+1}\left\{\frac{d\psi_h}{dx}(x_i)\right\}[v(x_i)] + \sum_{i=1}^{M+1}\frac{\sigma_i}{h}[v(x_i)][\psi_h(x_i)].\end{aligned}$$

Here, $\sigma_i \geq 1$ for $1 \leq i \leq M+1$ are called penalty parameter for this problem.

7.2.3 Linearization of the fully discrete scheme

We use the Newton linearization process to tackle the nonlinear term in the study of the error analysis and compute the numerical solution for the fully discrete scheme (7.4). The nonlinear term $\left(v^n\frac{\partial v^n}{\partial x}\right)(x)$ can be linearized as:

$$\left(v^{n,(q+1)}\frac{\partial v^{n,(q+1)}}{\partial x}\right)(x) = v^{n,(q)}(x)\frac{\partial v^{n,(q+1)}}{\partial x}(x) + \frac{\partial v^{n,(q)}}{\partial x}(x)v^{n,(q+1)}(x) - v^{n,(q)}(x)\frac{\partial v^{n,(q)}}{\partial x}(x), \tag{7.5}$$

where we have introduced a new dummy variable $q = 0, 1, 2, \cdots$ and $v^{n,(q+1)}(x)$, $r \geq 0$ are unknowns with an initial guess $v^{n,(0)}(x)$.

Using the technique (7.5) in (7.4), we obtain the following scheme: Find $\widehat{u}_h^{n_1,(q+1)}, U_h^{n+1,(q+1)} \in V_{0,h}^k(\Omega)$ for $2 \leq n_1 \leq N_1$, $2 \leq n \leq N$, $r \geq 0$ and $\forall \psi_h \in V_{0,h}^k(\Omega)$ such that

$$\begin{cases}\left\langle {}_{L1}^{C}\mathcal{D}_{N_1}^{\alpha}\widehat{u}_h^{n_1,(q+1)},\psi_h\right\rangle + \mathcal{B}(\widehat{u}_h^{n_1,(q+1)},\psi_h) = \left\langle \widehat{f}^{n_1} + \widehat{u}_h^{n_1,(q)}\frac{d\widehat{u}_h^{n_1,(q)}}{dx},\psi_h\right\rangle,\\ \left\langle {}_{L2}^{C}\mathcal{D}_{N}^{\alpha}U_h^{n+1,(q+1)},\psi_h\right\rangle + \mathcal{B}(U_h^{n+1,(q+1)},\psi_h) = \left\langle f^{n+1} + U_h^{n+1,(q)}\frac{dU_h^{n+1,(q)}}{dx},\psi_h\right\rangle,\\ \left\langle \widehat{u}^{1,(q+1)},\psi_h\right\rangle = \left\langle U^{1,(q+1)},\psi_h\right\rangle = \langle g,\psi_h\rangle,\end{cases} \tag{7.6}$$

where

$$\begin{aligned}\mathcal{B}(v^{n,(q+1)},\psi_h) &= \left\langle v^{n,(q)}\frac{dv^{n,(q+1)}}{dx},\psi_h\right\rangle + \left\langle \frac{dv^{n,(q)}}{dx}v^{n,(q+1)},\psi_h\right\rangle + p\left\langle \frac{dv^{n,(q+1)}}{dx},\frac{d\psi_h}{dx}\right\rangle\\ &\quad +p\sum_{i=1}^{M+1}\left\{\frac{dv^{n,(q+1)}}{dx}(x_i)\right\}[\psi_h(x_i)] - p\sum_{i=1}^{M+1}\left\{\frac{d\psi_h}{dx}(x_i)\right\}[v^{n,(q+1)}(x_i)]\end{aligned}$$

$$+\sum_{i=1}^{M+1}\frac{\sigma_i}{h}[v^{n,(q+1)}(x_i)][\psi_{_h}(x_i)]+\sum_{i=1}^{M}v^{n,(q)}(x_i)[v^{n,(q+1)}(x_i)]\psi_{_h}(x_i^+), \quad (7.7)$$

where we have introduced the last term as a stabilizer term.

We use the iteration stopping criteria in the Newton linearization process (7.6) as:

$$\max_{\substack{x\in\Omega,\\ n_1}}|\widehat{u}^{n_1,(q+1)}(x)-\widehat{u}^{n_1,(q)}(x)|\le \text{Tol}, \quad \max_{\substack{x\in\Omega,\\ n}}|U_h^{n+1,(q+1)}(x)-U_h^{n+1,(q)}(x)|\le \text{Tol}, \quad q\ge 0,$$

and to perform the computation, we utilized $\text{Tol}=1.0e-10$.

Whenever the above criteria hold true, we denote the computed solution of the fully discrete scheme (7.4) as $\widehat{u}_h^{n_1}:=\widehat{u}_h^{n_1,(q+1)}$ and $U_h^{n+1}:=U_h^{n+1,(q+1)}$. We also introduce the following notations to express the linearized problem (7.6) in a simpler form:

$$\widehat{a}^{n_1}(x):=\widehat{u}_h^{n_1,(q)}(x),\ \widehat{b}^{n_1}(x):=\frac{d\widehat{u}_h^{n_1,(q)}}{dx}(x),\ a^{n+1}(x):=U_h^{n+1,(q)}(x),\ b^{n+1}(x):=\frac{dU_h^{n+1,(q)}}{dx}(x),$$

$$\widehat{\mathcal{G}}^{n_1}(x):=\widehat{f}^{n_1}(x)+\widehat{a}^{n_1}(x)\,\widehat{b}^{n_1}(x), \quad \mathcal{G}^{n+1}(x):=f^{n+1}(x)+a^{n+1}(x)\,b^{n+1}(x).$$

By using the above notations, the linearized equation (7.6) can be written as:

$$\begin{cases} \left\langle {}_{L1}^{C}\mathcal{D}_{N_1}^{\alpha}\widehat{u}_h^{n_1},\psi_{_h}\right\rangle+\mathcal{B}(\widehat{u}_h^{n_1},\psi_{_h})=\left\langle\widehat{\mathcal{G}}^{n_1},\psi_{_h}\right\rangle, \\ \left\langle {}_{L2}^{C}\mathcal{D}_{N}^{\alpha}U_h^{n+1},\psi_{_h}\right\rangle+\mathcal{B}(U_h^{n+1},\psi_{_h})=\left\langle\mathcal{G}^{n+1},\psi_{_h}\right\rangle, \\ \left\langle\widehat{u}_h^{1},\psi_{_h}\right\rangle=\left\langle U_h^{1},\psi_{_h}\right\rangle=\langle g,\psi_{_h}\rangle, \end{cases} \quad (7.8)$$

where

$$\mathcal{B}(\widehat{u}_h^{n_1},\psi_{_h})=\left\langle\widehat{a}^{n_1}\frac{d\widehat{u}_h^{n_1}}{dx},\psi_{_h}\right\rangle+\left\langle\widehat{b}^{n_1}\widehat{u}_h^{n_1},\psi_{_h}\right\rangle+p\left\langle\frac{d\widehat{u}_h^{n_1}}{dx},\frac{d\psi_{_h}}{dx}\right\rangle+p\sum_{i=1}^{M+1}\left\{\frac{d\widehat{u}_h^{n_1}}{dx}(x_i)\right\}[\psi_{_h}(x_i)]$$
$$-p\sum_{i=1}^{M+1}\left\{\frac{d\psi_{_h}}{dx}(x_i)\right\}[\widehat{u}_h^{n_1}(x_i)]+\sum_{i=1}^{M+1}\frac{\sigma_i}{h}[\widehat{u}_h^{n_1}(x_i)][\psi_{_h}(x_i)]+\sum_{i=1}^{M}\widehat{a}^{n_1}(x_i)[\widehat{u}_h^{n_1}(x_i)]\psi_{_h}(x_i^+),$$

and

$$\mathcal{B}(U_h^{n+1},\psi_{_h}) = \left\langle a^{n+1}\frac{dU_h^{n+1}}{dx},\psi_{_h}\right\rangle+\left\langle b^{n+1}U_h^{n+1},\psi_{_h}\right\rangle+p\left\langle\frac{dU_h^{n+1}}{dx},\frac{d\psi_{_h}}{dx}\right\rangle$$
$$+p\sum_{i=1}^{M+1}\left\{\frac{dU_h^{n+1}}{dx}(x_i)\right\}[\psi_{_h}(x_i)]-p\sum_{i=1}^{M+1}\left\{\frac{d\psi_{_h}}{dx}(x_i)\right\}[U_h^{n+1}(x_i)]$$

$$+\sum_{i=1}^{M+1}\frac{\sigma_i}{h}[U_h^{n+1}(x_i)][\psi_{_h}(x_i)]+\sum_{i=1}^{M}a^{n+1}(x_i)[U_h^{n+1}(x_i)]\psi_{_h}(x_i^+).$$

7.3 L^2-stability of the fully discrete scheme

The L^2-stability of the fully discrete scheme developed from the IBVP will be studied in this section. For establish the stability, we assume that $\widehat{a}^{n_1}, a^{n+1} \geq a^* > 0$. Now, define the DG-norm for the bilinear form $\mathcal{B}(\cdot,\cdot)$ as

$$|||u|||_{DG}^2 := p|u|_{1,\Omega}^2 + \frac{\nu^*}{2}\|u\|^2 + \sum_{i=1}^{M+1}(\sigma_i + a^*)[u(x_i)]^2.$$

By using integration by parts, we have the following coercieve property:

$$\mathcal{B}\left(\widehat{u}_h^{n_1}, \widehat{u}_h^{n_1}\right) \geq |||\widehat{u}_h^{n_1}|||_{DG}^2 \quad \text{and} \quad \mathcal{B}(U_h^{n+1}, U_h^{n+1}) \geq |||U_h^{n+1}|||_{DG}^2. \tag{7.9}$$

Lemma 7.2 *The solution of the scheme* (7.8) *is unconditionally stable, i.e.,*

$$\frac{\widehat{d}_{n_1,n_1-1}}{2}\|\widehat{u}_h^{n_1}\|^2 + |||\widehat{u}_h^{n_1}|||_{DG}^2 \leq \frac{2}{\widehat{d}_{n_1,n_1-1}}\left(\left\|\widehat{\mathcal{G}}^{n_1}\right\|^2 + \left\|\widehat{d}_{n_1,1}\widehat{u}_h^1\right\|^2 + 2\sum_{j=2}^{n_1-1}\left[\widehat{d}_{n_1,j} - \widehat{d}_{n_1,j-1}\right]^2\left\|\widehat{u}_h^j\right\|^2\right), \tag{7.10}$$

and

$$\frac{D_{n,n+1}^{(\alpha)}}{2}\left\|U_h^{n+1}\right\|^2 + |||U_h^{n+1}|||_{DG}^2 \leq \frac{2}{D_{n,n+1}^{(\alpha)}}\left(\left\|\mathcal{G}^{n+1}\right\|^2 + \sum_{j=1}^{n}\left(D_{n,j}^{(\alpha)}\right)^2\left\|U_h^j\right\|^2\right). \tag{7.11}$$

Proof. Letting $\psi_{_h} = \widehat{u}_h^{n_1}$ and $\psi_{_h} = U_h^{n+1}$, respectively, in the first and second equation of (7.8), and using (1.10) and (1.11), we have

$$\widehat{d}_{n_1,n_1-1}\left\|\widehat{u}_h^{n_1}\right\|^2 + \mathcal{B}\left(\widehat{u}_h^{n_1}, \widehat{u}_h^{n_1}\right) = \left\langle \widehat{\mathcal{G}}^{n_1} + \widehat{d}_{n_1,1}\widehat{u}_h^1 + \sum_{j=2}^{n_1-1}\left[\widehat{d}_{n_1,j} - \widehat{d}_{n_1,j-1}\right]\widehat{u}_h^j, \widehat{u}_h^{n_1}\right\rangle, \tag{7.12}$$

and

$$D_{n,n+1}^{(\alpha)}\left\|U_h^{n+1}\right\|^2 + \mathcal{B}\left(U_h^{n+1}, U_h^{n+1}\right) = \left\langle \mathcal{G}^{n+1} - \sum_{j=1}^{n}D_{n,j}^{(\alpha)}U_h^j, U_h^{n+1}\right\rangle. \tag{7.13}$$

By using coercieve property (7.9), the Hölder's inequality and the Young's inequality in (7.12) and (7.13), we obtain

$$\widehat{d}_{n_1,n_1-1}\left\|\widehat{u}_h^{n_1}\right\|^2+\left|\left|\left|\widehat{u}_h^{n_1}\right|\right|\right|_{DG}^2\leq\frac{2\left\|\widehat{\mathcal{G}}^{n_1}\right\|^2}{\widehat{d}_{n_1,n_1-1}}+\frac{\widehat{d}_{n_1,n_1-1}}{8}\left\|\widehat{u}_h^{n_1}\right\|^2+\frac{2\left\|\widehat{d}_{n_1,1}\widehat{u}_h^1\right\|^2}{\widehat{d}_{n_1,n_1-1}}$$
$$+\frac{\widehat{d}_{n_1,n_1-1}}{8}\left\|\widehat{u}_h^{n_1}\right\|^2+2\sum_{j=2}^{n_1-1}\left[\widehat{d}_{n_1,j}-\widehat{d}_{n_1,j-1}\right]^2\frac{\left\|\widehat{u}_h^j\right\|^2}{\widehat{d}_{n_1,n_1-1}}+\frac{\widehat{d}_{n_1,n_1-1}}{4}\left\|\widehat{u}_h^{n_1}\right\|^2,\quad(7.14)$$

and

$$D_{n,n+1}^{(\alpha)}\left\|U_h^{n+1}\right\|^2+\left|\left|\left|U_h^{n+1}\right|\right|\right|_{DG}^2\leq\frac{\left\|\mathcal{G}^{n+1}\right\|^2}{D_{n,n+1}^{(\alpha)}}+\frac{D_{n,n+1}^{(\alpha)}}{4}\left\|U_h^{n+1}\right\|^2$$
$$+2\sum_{j=1}^{n}\left(D_{n,j}^{(\alpha)}\right)^2\frac{\left\|U_h^j\right\|^2}{D_{n,n+1}^{(\alpha)}}+\frac{D_{n,n+1}^{(\alpha)}}{4}\left\|U_h^{n+1}\right\|^2.\quad(7.15)$$

By combining (7.14) and (7.15), we have the required result. □

Using Lemma 6.5 and (7.10) of Lemma 7.2, one can obtain the following result.

Lemma 7.3 *The solution $\widehat{u}_h^{n_1}$ of the fully discrete scheme* (7.8) *satisfies the following stability result:*

$$\|\widehat{u}_h^{n_1}\|^2\leq C\left(\|\widehat{u}_h^1\|^2+\max_{1\leq j\leq n_1}\left\|\widehat{\mathcal{G}}^j\right\|^2\right),\quad 2\leq n_1\leq N_1.$$

For $2\leq n\leq N$, $2\leq j\leq n$, we define

$$\mu_{n+1,j}=\tau^{2\alpha}\sum_{m=3}^{n-j+3}\left(D_{n,n-m+3}^{(\alpha)}\right)^2\mu_{n-m+3,j},\quad\text{and}\quad\mu_{n+1,n+1}=1.$$

In the same way as in Lemma 3.4, one can establish the following result, which will be used in the proof of stability and convergence analysis.

Lemma 7.4 *$\mu_{n+1,j}$ satisfies the following bound for $n=2,\cdots,N$ and $\gamma\geq 0$:*

$$\tau^{2\alpha}\sum_{j=2}^{n+1}j^{-\gamma}\mu_{n+1,j}\leq CN^{-\gamma}.$$

Lemma 7.5 *The solution U_h^{n+1} of the fully discrete scheme* (7.8) *satisfies the following*

stability result:

$$\left\|U_h^{n+1}\right\|^2 \leq C\left(\left\|U_h^1\right\|^2 + \max_{1\leq n_1\leq N_1}\left\|\widehat{\mathcal{G}}^{n_1}\right\|^2 + \max_{3\leq j\leq n+1}\left\|\mathcal{G}^j\right\|^2\right), \quad 2\leq n\leq N.$$

Proof. From Lemma 7.2 and using the fact that $\left|\left|\left|U_h^{n+1}\right|\right|\right|_{DG} \geq 0$, we have

$$\begin{aligned}\left\|U_h^{n+1}\right\|^2 &\leq \left(\frac{2}{D_{n,n+1}^{(\alpha)}}\right)^2\left(\left\|\mathcal{G}^{n+1}\right\|^2 + \sum_{j=1}^{n}\left(D_{n,j}^{(\alpha)}\right)^2\left\|U_h^j\right\|^2\right)\\ &\leq C\tau^{2\alpha}\left(\left\|\mathcal{G}^{n+1}\right\|^2 + \sum_{j=1}^{n}\left(D_{n,j}^{(\alpha)}\right)^2\left\|U_h^j\right\|^2\right), \quad 2\leq n\leq N. \qquad (7.16)\end{aligned}$$

As $U_h^2 = \widehat{u}^{N_1}$, so from Lemma 7.3, we have

$$\|U_h^2\|^2 \leq C\left(\|U_h^1\|^2 + \max_{1\leq n_1\leq N_1}\left\|\widehat{\mathcal{G}}^{n_1}\right\|^2\right). \qquad (7.17)$$

Next, we will prove that for $2\leq m\leq N$, the following holds true:

$$\left\|U_h^{m+1}\right\|^2 \leq C\left(\left\|U_h^1\right\|^2 + \max_{1\leq n_1\leq N_1}\left\|\widehat{\mathcal{G}}^{n_1}\right\|^2 + \tau^{2\alpha}\sum_{j=3}^{m+1}\mu_{m+1,j}\left\|\mathcal{G}^j\right\|^2\right). \qquad (7.18)$$

From (7.16) and using (7.17), it is easy to see that (7.18) holds true for $m=2$. Now, we assume that (7.18) holds for $m=2,\cdots,n-1$, $n\geq 3$, i.e., for $2\leq m\leq n-1$, $n\geq 3$, we have

$$\left\|U_h^{m+1}\right\|^2 \leq C\left(\left\|U_h^1\right\|^2 + \max_{1\leq n_1\leq N_1}\left\|\widehat{\mathcal{G}}^{n_1}\right\|^2 + \tau^{2\alpha}\sum_{j=3}^{m+1}\mu_{m+1,j}\left\|\mathcal{G}^j\right\|^2\right). \qquad (7.19)$$

Now, from (7.16) and (7.19), we have

$$\begin{aligned}\left\|U_h^{n+1}\right\|^2 &\leq C\left(\left\|U_h^1\right\|^2 + \max_{1\leq n_1\leq N_1}\left\|\widehat{\mathcal{G}}^{n_1}\right\|^2 + \tau^{2\alpha}\left\|\mathcal{G}^{n+1}\right\|^2\right)\\ &\quad + C\tau^{2\alpha}\sum_{j=3}^{n}\left(D_{n,j}^{(\alpha)}\right)^2\tau^{2\alpha}\sum_{m=3}^{j}\mu_{j,m}\left\|\mathcal{G}^m\right\|^2\\ &= C\left(\left\|U_h^1\right\|^2 + \max_{1\leq n_1\leq N_1}\left\|\widehat{\mathcal{G}}^{n_1}\right\|^2 + \tau^{2\alpha}\mu_{n+1,n+1}\left\|\mathcal{G}^{n+1}\right\|^2\right)\end{aligned}$$

$$+C\tau^{2\alpha}\sum_{j=3}^{n}\left\|\mathcal{G}^{j}\right\|^{2}\left(\tau^{2\alpha}\sum_{m=3}^{n-j+3}\mu_{n-m+3,j}\left(D_{n,n-m+3}^{(\alpha)}\right)^{2}\right)$$

$$= C\left(\left\|U_h^1\right\|^2+\max_{1\le n_1\le N_1}\left\|\widehat{\mathcal{G}}^{n_1}\right\|^2+\tau^{2\alpha}\sum_{j=3}^{n+1}\mu_{n+1,j}\left\|\mathcal{G}^{j}\right\|^2\right)$$

$$\le C\left(\left\|U_h^1\right\|^2+\max_{1\le n_1\le N_1}\left\|\widehat{\mathcal{G}}^{n_1}\right\|^2+\max_{3\le j\le n+1}\left\|\mathcal{G}^{j}\right\|^2\tau^{2\alpha}\sum_{j=3}^{n+1}\mu_{n+1,j}\right). \quad (7.20)$$

Now, by using Lemma 7.4 with $\gamma = 0$, we obtain our required result. □

Remark 7.2 *The fully discrete L2-NIPG method* (7.8) *is well-posed, as Lemma 7.5 states that if* $f = U_h^1 = 0$ *along with our linearization assumption* $U_h^{n,(0)} = 0$*, then one must have trivial solution* $U_h^{n+1,(q+1)} = U_h^{n+1}$ *for the fully discrete scheme* (7.8).

7.4 Error analysis

This section establishes the error analysis for the fully discrete scheme (7.8).

Let $u(x,t_{n+1})$ and U_h^{n+1} be the solutions of IBVP (7.1) and L2-NIPG scheme (7.8) at $t = t_{n+1}$, $n \ge 2$, respectively. The error due to L2-NIPG discretization of (7.1) denotes as

$$e_h^{n+1} := u(x,t_{n+1}) - U_h^{n+1} = \eta_h^{n+1} + \xi_h^{n+1}, \quad n = 2,\cdots,N,$$

where $\eta_h^{n+1} := u(x,t_{n+1}) - \mathbf{P}u(x,t_{n+1})$ and $\xi_h^{n+1} := \mathbf{P}u(x,t_{n+1}) - U_h^{n+1}$. It is clear that $\xi_h^{n+1} \in V_{0,h}^k(\Omega)$.

By using Lemma 1.4, we can obtain the following bound for the projection error.

Lemma 7.6 *Let* $u(x,t_{n+1})$ *be the solution of IBVP* (7.1)*. Then, the projection error have the following bound:*

$$\|\mathbf{P}u(x,t_n) - u(x,t_n)\| \le Ch^{k+1}, \quad 1 \le n \le N+1,$$

where $C > 0$ *is a constant.*

Now, from (7.3) and (7.8), we have the following for all $\psi_h \in V_{0,h}^k(\Omega)$:

$$\left\langle {}_{C}^{}{}_{L2}\mathcal{D}_N^{\alpha}\,\xi_h^{n+1},\psi_h\right\rangle + \mathcal{B}(\xi_h^{n+1},\psi_h) = -\left\langle {}_{C}^{}{}_{L2}\mathcal{D}_N^{\alpha}\,\eta_h^{n+1},\psi_h\right\rangle - \mathcal{B}(\eta_h^{n+1},\psi_h) + \left\langle \mathcal{R}_N^n,\psi_h\right\rangle, \quad (7.21)$$

where $\mathcal{R}_N^n = \left({}_{L2}^{C}\mathcal{D}_N^{\alpha} - {}^{C}\mathcal{D}_t^{\alpha}\right) u(x,t_{n+1})$ and we assume that $u^{(q)}(x,t_{n+1}) = U_h^{n+1,(q)}(x)$, $\dfrac{du^{(q)}}{dx}(x,t_{n+1}) = \dfrac{dU_h^{n+1,(q)}}{dx}(x)$ for the linearization technique (7.5).

Theorem 7.3 *Assume that the solution u of (7.1) satisfies the condition $\left|{}^{C}\mathcal{D}_t^{\alpha}u\right|_{k+1} \leq C$. Then, the discretization error for each $n = 2, \cdots, N$ has the following bound:*

$$\|\xi_h^{n+1}\| \leq C\left(h^{k+1} + \tau^{3-\alpha}\right). \tag{7.22}$$

Proof. By substituting $\psi_h = \xi_h^{n+1}$ in (7.21), we have

$$\left\langle {}_{L2}^{C}\mathcal{D}_N^{\alpha}\,\xi_h^{n+1}, \xi_h^{n+1}\right\rangle + \mathcal{B}(\xi_h^{n+1}, \xi_h^{n+1}) = -\left\langle {}_{L2}^{C}\mathcal{D}_N^{\alpha}\,\eta_h^{n+1}, \xi_h^{n+1}\right\rangle - \mathcal{B}(\eta_h^{n+1}, \xi_h^{n+1}) + \left\langle \mathcal{R}_N^n, \xi_h^{n+1}\right\rangle. \tag{7.23}$$

Now, by using integration by parts and using the fact that $\left\{\dfrac{d\eta_h^{n+1}}{dx}(x_i)\right\} = 0$, $[\eta_h^{n+1}(x_i)] = 0$, we have

$$\begin{aligned}
\mathcal{B}(\eta_h^{n+1}, \xi_h^{n+1}) &= p\sum_{i=1}^{M}\int_{\mathcal{K}_i}\frac{d\eta_h^{n+1}}{dx}\frac{d\xi_h^{n+1}}{dx}dx + \sum_{i=1}^{M}\int_{\mathcal{K}_i}\left(\frac{du^{(q)}}{dx}(x,t_{n+1})\eta_h^{n+1}\right.\\
&\qquad \left. + u^{(q)}(x,t_{n+1})\frac{d\eta_h^{n+1}}{dx}\right)\xi_h^{n+1}dx\\
&= -p\sum_{i=1}^{M}\int_{\mathcal{K}_i}\eta_h^{n+1}\frac{d^2\xi_h^{n+1}}{dx^2}dx - \sum_{i=1}^{M}\int_{\mathcal{K}_i}u^{(q)}(\cdot,t_{n+1})\eta_h^{n+1}\frac{d\xi_h^{n+1}}{dx}dx\\
&= -\sum_{i=1}^{M}\int_{\mathcal{K}_i}w^{(q)}(\cdot,t_{n+1})\eta_h^{n+1}\frac{d\xi_h^{n+1}}{dx}dx,
\end{aligned} \tag{7.24}$$

where the first term is zero by using the fact that $\dfrac{d^2\xi_h^{n+1}}{dx^2} \in V_{0,h}^k(\Omega)$ and Definition 1.11 of L^2-projection $\mathbf{P}$. Now, since for every step of linearization $u^{(q)}(\cdot,t_{n+1})$ is known, whereas the unknown quantity is $u^{(q+1)}(\cdot,t_{n+1})$, and they satisfy stability result, so we assume that there exists a constant $C > 0$ such that $|u^{(q)}(\cdot,t_{n+1})| \leq C$. Therefore, we

have

$$\int_{\mathcal{K}_i} u^{(q)}(\cdot,t_{n+1})\eta_h^{n+1}\frac{d\xi_h^{n+1}}{dx}dx \le C\int_{\mathcal{K}_i}\eta_h^{n+1}\frac{d\xi_h^{n+1}}{dx}dx = 0, \text{ as } \frac{d\xi_h^{n+1}}{dx}\in V_{0,h}^k(\Omega).$$

Hence, $-\mathcal{B}(\eta_h^{n+1},\xi_h^{n+1}) = \sum_{i=1}^{M}\int_{\mathcal{K}_i} u^{(q)}(\cdot,t_{n+1})\eta_h^{n+1}\frac{d\xi_h^{n+1}}{dx}dx \le 0.$

Now, let us consider $\chi_h^{n+1} = -{}_{L2}^{C}\mathcal{D}_N^{\alpha}\,\eta_h^{n+1} + \mathcal{R}_N^n$. Then, by using Lemma 7.1 and Lemma 7.6, we have

$$\begin{aligned}
\left\|\chi_h^{n+1}\right\| &\le \left\|{}_{L2}^{C}\mathcal{D}_N^{\alpha}\,\eta_h^{n+1}\right\| + \left\|\mathcal{R}_N^n\right\| = \left\|{}^{C}\mathcal{D}_t^{\alpha}\,\eta_h^{n+1} + \left({}_{L2}^{C}\mathcal{D}_N^{\alpha} - {}^{C}\mathcal{D}_t^{\alpha}\right)\eta_h^{n+1}\right\| + \left\|\mathcal{R}_N^n\right\| \\
&\le \left\|{}^{C}\mathcal{D}_t^{\alpha}u(\cdot,t_{n+1}) - \mathbf{P}\left({}^{C}\mathcal{D}_t^{\alpha}u(\cdot,t_{n+1})\right)\right\| + 2\left\|\mathcal{R}_N^n\right\| \\
&\le Ch^{k+1}\left|{}^{C}\mathcal{D}_t^{\alpha}u(\cdot,t_{n+1})\right|_{k+1,\Omega} + C\tau^{3-\alpha} \\
&\le C(h^{k+1}+\tau^{3-\alpha}). \qquad (7.25)
\end{aligned}$$

By using (1.11) and (7.9) in (7.23), and also using the Cauchy-Schwartz inequality and the Young's inequality, we obtain the following

$$\begin{aligned}
D_{n,n+1}^{(\alpha)}\left\|\xi_h^{n+1}\right\|^2 + \left|\left|\left|\xi_h^{n+1}\right|\right|\right|_{DG}^2 &\le D_{n,n+1}^{(\alpha)}\left\|\xi_h^{n+1}\right\|^2 + \mathcal{B}(\xi_h^{n+1},\xi_h^{n+1}) \\
&\le \left\langle \chi_h^{n+1} - \sum_{j=1}^{n} D_{n,j}^{(\alpha)}\xi_h^j, \xi_h^{n+1}\right\rangle \\
&\le \left\|\chi_h^{n+1}\right\|\left\|\xi_h^{n+1}\right\| + \sum_{j=1}^{n}\left|D_{n,j}^{(\alpha)}\right|\left\|\xi_h^j\right\|\left\|\xi_h^{n+1}\right\| \\
\le \frac{1}{D_{n,n+1}^{(\alpha)}}\left\|\chi_h^{n+1}\right\|^2 &+ \frac{D_{n,n+1}^{(\alpha)}}{4}\left\|\xi_h^{n+1}\right\|^2 + 2\sum_{j=1}^{n}\left|D_{n,j}^{(\alpha)}\right|^2\frac{\left\|\xi_h^j\right\|^2}{D_{n,n+1}^{(\alpha)}} + \frac{D_{n,n+1}^{(\alpha)}}{4}\left\|\xi_h^{n+1}\right\|^2,
\end{aligned}$$

which can be simplified as

$$\frac{D_{n,n+1}^{(\alpha)}}{2}\left\|\xi_h^{n+1}\right\|^2 + \left|\left|\left|\xi_h^{n+1}\right|\right|\right|_{DG}^2 \le \frac{1}{D_{n,n+1}^{(\alpha)}}\left(\left\|\chi_h^{n+1}\right\|^2 + 2\sum_{j=1}^{n}\left|D_{n,j}^{(\alpha)}\right|^2\left\|\xi_h^j\right\|^2\right). \qquad (7.26)$$

Applying Lemma 7.2, Lemma 7.5 and (7.25) in (7.26), we have

$$\left\|\xi_h^{n+1}\right\| \le C\left\|\chi_h^{n+1}\right\| \le C(h^{k+1}+\tau^{3-\alpha}), \qquad (7.27)$$

where we have used the fact that $\xi_h^1 = 0$. □

Now, as $\|e_h^{n+1}\| \leq \|\eta_h^{n+1}\| + \|\xi_h^{n+1}\|$, using Lemma 7.6 and Lemma 7.3, we obtain the bound for the error due to fully discretization.

Theorem 7.4 *Assume that the solution u of (7.1) satisfies the condition $\left|{}^C\mathcal{D}_t^\alpha u\right|_{k+1} \leq C$. Then, the error due to the fully discretization for each $n = 2, \cdots, N$ has the following bound:*

$$\max_{1\leq n\leq N} \|u(x, t_{n+1}) - U_h^{n+1}\| \leq C\left(h^{k+1} + \tau^{3-\alpha}\right). \tag{7.28}$$

7.5 Experimental results

In this section, we will validate the theoretical results numerically by implementing it to some examples. The error at final time $T = 1$ in the L^2-norm and L^∞-norm defined respectively as

$$\|u^{N+1} - U_h^{N+1}\|_{L^\infty} \quad \text{and} \quad \|u^{N+1} - U_h^{N+1}\|_{L^2}.$$

Further, if $E_{M,N}$ is either the error in L^2-norm or the error in L^∞-norm, then the order of convergence in temporal and spatial direction, denoted by $R_{M,N}^1 = \log_2\left(\dfrac{E_{M,N}}{E_{M,2N}}\right)$ and $R_{M,N}^2 = \log_2\left(\dfrac{E_{M,N}}{E_{2M,N}}\right)$, respectively, are reported.

Example 7.5 *Take into account the following problem:*

$$\begin{cases} {}^C\mathcal{D}_t^\alpha u(x,t) + u(x,t)\dfrac{\partial u}{\partial x}(x,t) = \dfrac{\partial^2 u}{\partial x^2}(x,t) + f(x,t),\ (x,t) \in (0,1)\times(0,1], \\ u(x,0) = \sin(\pi x), \quad \forall x \in [0,1], \\ u(0,t) = u(1,t) = 0, \quad \forall t \in (0,1]. \end{cases} \tag{7.29}$$

In the above problem (7.29), the exact solution is $u(x,t) = \sin(\pi x) - \dfrac{t^{3+\alpha}}{\Gamma(4+\alpha)}\sin(2\pi x)$ which will be used to calculate $f(x,t)$.

For Example 7.5 with $\alpha = 0.4, 0.6, 0.8$, $k = 1$, Table 7.1 and Table 7.2 presents the error and order of convergence in the temporal and the spatial directions respectively. The results in the Tables show that the order of error estimates are second order in space and $(3-\alpha)$-th order in time. Figure 7.1 displays log-log plots of L^∞-norm errors for Example 7.5, where we can observe that temporal order of convergence is $(3-\alpha)$

whereas spatial order of convergence is second order, which also validates the results in Tables 7.1 and 7.2.

Table 7.1: *Error and order of convergence in temporal direction at final time $T = 1$ for Example 7.5 with $h^2 = \tau^{3-\alpha}$ and $k = 1$.*

	N	$\alpha = 0.4$		$\alpha = 0.6$		$\alpha = 0.8$	
		$E_{M,N}$	$R^1_{M,N}$	$E_{M,N}$	$R^1_{M,N}$	$E_{M,N}$	$R^1_{M,N}$
	4	1.3461e-02	3.0765	2.0954e-02	3.0105	2.1047e-02	2.4038
	8	1.5957e-03	2.7799	2.6002e-03	2.6463	3.9771e-03	2.3533
L^2-norm	16	2.3233e-04	2.6691	4.1533e-04	2.4733	7.7830e-04	2.3062
(Present	32	3.6527e-05	2.6159	7.4790e-05	2.4387	1.5737e-04	2.2676
method)	64	5.9585e-06	2.6117	1.3795e-05	2.4198	3.2682e-05	2.2251
	128	9.7483e-07	–	2.5781e-06	–	6.9900e-06	–
	4	2.1591e-02	3.0226	3.1636e-02	2.9194	3.1197e-02	2.3716
	8	2.6570e-03	2.7377	4.1816e-03	2.6111	6.0283e-03	2.2870
L^∞-norm	16	3.9834e-04	2.6560	6.8442e-04	2.4562	1.2352e-03	2.2871
(Present	32	6.3200e-05	2.6100	1.2472e-04	2.4307	2.5308e-04	2.2563
method)	64	1.0352e-05	2.6093	2.3133e-05	2.4162	5.2971e-05	2.2204
	128	1.6965e-06	–	4.3338e-06	–	1.1367e-05	–

Example 7.6 *Consider the following problem:*

$$\begin{cases} {}^{C}\mathcal{D}_t^{\alpha} u(x,t) + u(x,t)\dfrac{\partial u}{\partial x}(x,t) = \dfrac{\partial^2 u}{\partial x^2}(x,t) + f(x,t),\ (x,t) \in (0,1)\times(0,1], \\ u(x,0) = 0, \quad \forall x \in (0,1), \\ u(0,t) = u(1,t) = 0, \quad \forall t \in (0,1]. \end{cases} \tag{7.30}$$

In the above problem (7.30), the exact solution is $u(x,t) = t^2 \sin(2\pi x)$ and

$$f(x,t) = 4\pi^2 t^2 \sin(2\pi x) + \pi t^4 \sin(4\pi x) + \frac{2t^{2-\alpha}}{\Gamma(3-\alpha)} \sin(2\pi x).$$

Table 7.3 and Table 7.4 show the errors at final time $t = 1$ and the orders of convergence for Example 7.6 in the temporal directions with various α and $k = 1$ using the present L2-NIPG method and method discussed in [64]. From Table 7.3 and Table 7.4,

Table 7.2: *Error and order of convergence in spatial direction at final time $T = 1$ for Example 7.5 with $\tau^{3-\alpha} = h^2$ and $k = 1$.*

	M	$\alpha = 0.4$		$\alpha = 0.6$		$\alpha = 0.8$	
		$E_{M,N}$	$R^2_{M,N}$	$E_{M,N}$	$R^2_{M,N}$	$E_{M,N}$	$R^2_{M,N}$
	4	3.9376e-02	2.5597	3.8245e-02	2.5369	3.7805e-02	2.5066
L^2-norm	8	6.6788e-03	2.2694	6.5899e-03	2.2588	6.6525e-03	2.2491
	16	1.3853e-03	2.1380	1.3769e-03	2.1339	1.3994e-03	2.1302
(Present	32	3.1474e-04	2.0707	3.1372e-04	2.0686	3.1966e-04	2.0671
method)	64	7.4922e-05	2.0354	7.4790e-05	2.0349	7.6283e-05	2.0339
	128	1.8276e-05	–	1.8251e-05	–	1.8628e-05	–
	4	5.7380e-02	2.4351	5.2560e-02	2.3538	5.0679e-02	2.3201
L^∞-norm	8	1.0610e-02	2.1877	1.0282e-02	2.2006	1.0149e-02	2.2106
	16	2.3289e-03	2.1168	2.2368e-03	2.1086	2.1926e-03	2.1016
(Present	32	5.3693e-04	2.0545	5.1864e-04	2.0560	5.1089e-04	2.0519
method)	64	1.2926e-04	2.0282	1.2472e-04	2.0276	1.2321e-04	2.0266
	128	3.1689e-05	–	3.0590e-05	–	3.0239e-05	–

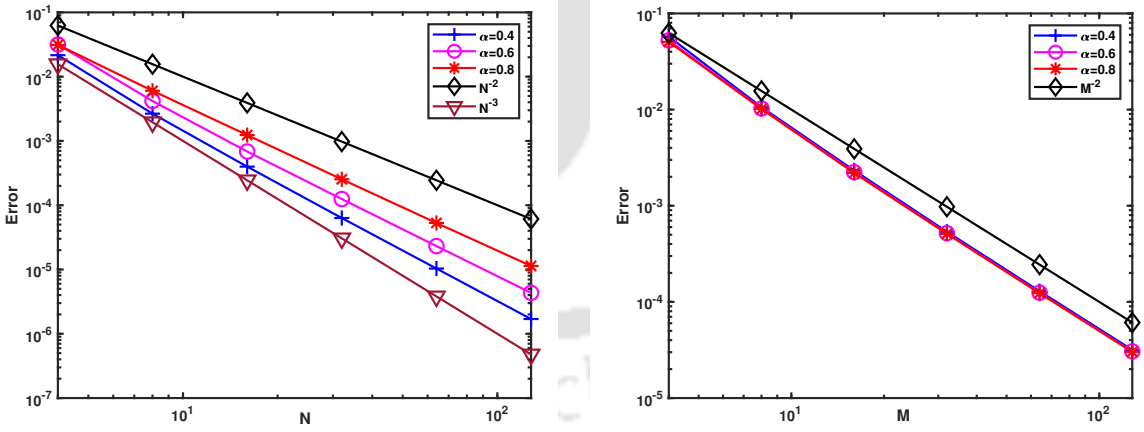

(a) Corresponding to Table 7.1. *(b) Corresponding to Table 7.2.*

Figure 7.1: *Log-log plot of L^∞-norm errors for Example 7.5.*

we can observe that the presented L2-NIPG method has better accuracy in the temporal direction with less number of spatial grid points than the L1/LDG scheme in [64]. Both the present method and the method discussed in [64] have same order of convergence in the spatial direction. Table 7.5 displays the errors at final time $t = 1$ and the orders of convergence for Example 7.6 in the spatial direction. These tables show that numerical solutions using present method agree with exact solutions for various α and the $(3-\alpha)$-th order of convergence in time and $(k+1)$-th order of convergence in space, consistent with the theoretical analysis derived in Theorem 7.4. Figure 7.2 depicts the log-log plot of L^∞-norm errors using present method for Example 7.6.

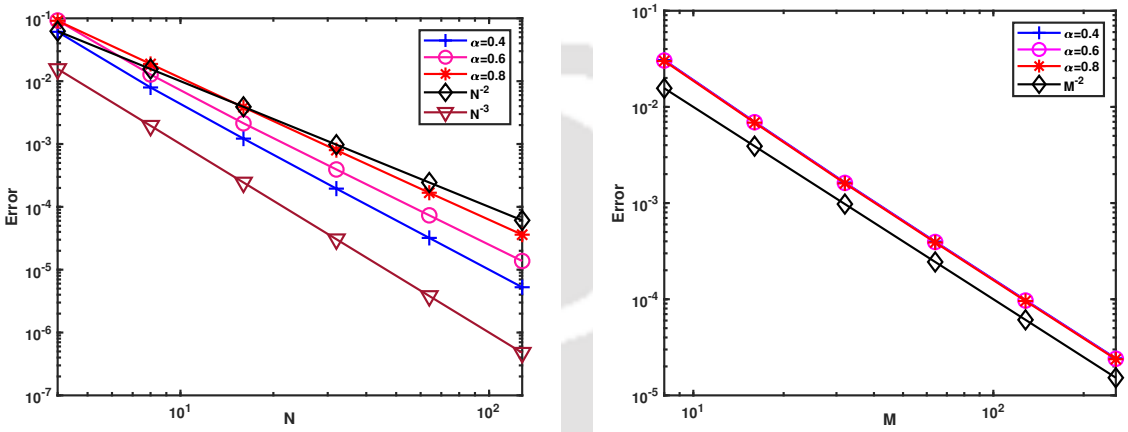

(a) Corresponding to Table 7.4. *(b) Corresponding to Table 7.5.*

Figure 7.2: *Log-log plot of L^∞-norm errors using present method for Example 7.6.*

7.6 Conclusion

This chapter studied the L2-NIPG method for solving the time-fractional Burgers' equation. We used the L2-discretization to discretize the temporal fractional derivative and the NIPG method in space to obtain the fully discrete scheme. We tackled the nonlinearity by applying the Newton's linearization process. We established that the proposed method is numerically stable, and the error estimates are derived. Numerical results are presented to support the theoretical results and compared with previous results available in the literature.

Table 7.3: *Error and order of convergence in temporal direction for Example 7.6 with* $k = 1$.

	N	$\alpha = 0.4$		$\alpha = 0.6$		$\alpha = 0.8$	
		$E_{M,N}$	$R^1_{M,N}$	$E_{M,N}$	$R^1_{M,N}$	$E_{M,N}$	$R^1_{M,N}$
	4	4.7265e-02	3.0093	7.2773e-02	2.9370	7.2099e-02	2.3479
L^2-norm	8	5.8703e-03	2.7644	9.5028e-03	2.6348	1.4163e-02	2.3469
(Present	16	8.6394e-04	2.6623	1.5300e-03	2.4678	2.7839e-03	2.3034
method	32	1.3647e-04	2.6128	2.7658e-04	2.4357	5.6399e-04	2.2655
with	64	2.2310e-05	2.6104	5.1122e-05	2.4182	1.1730e-04	2.2239
$h^2 = \tau^{3-\alpha}$)	128	3.6533e-06	–	9.5641e-06	–	2.5110e-05	–
	4	2.44e-02	1.90	2.62e-02	1.80	3.05e-02	1.63
L^2-norm	8	6.55e-03	1.92	7.49e-03	1.79	9.88e-03	1.54
(method in	16	1.73e-03	1.91	2.17e-03	1.73	3.40e-03	1.44
[64]	32	4.59e-04	1.90	6.54e-04	1.67	1.26e-03	1.35
with	64	1.23e-04	1.89	2.05e-04	1.58	4.91e-04	1.30
$h = 1/1000$)	128	3.32e-05	–	6.69e-05	–	2.00e-04	–

Table 7.4: *Error and order of convergence in temporal direction for Example 7.6 with* $k = 1$.

	N	$\alpha = 0.4$		$\alpha = 0.6$		$\alpha = 0.8$	
		$E_{M,N}$	$R^1_{M,N}$	$E_{M,N}$	$R^1_{M,N}$	$E_{M,N}$	$R^1_{M,N}$
	4	6.1016e-02	2.9415	9.2426e-02	2.8547	9.1430e-02	2.2819
L^∞-norm	8	7.9428e-03	2.7038	1.2777e-02	2.5791	1.8800e-02	2.2895
(Present	16	1.2191e-03	2.6445	2.1381e-03	2.4416	3.8454e-03	2.2678
method	32	1.9497e-04	2.6049	3.9357e-04	2.4248	7.9851e-04	2.2511
with	64	3.2049e-05	2.6074	7.3298e-05	2.4136	1.6774e-04	2.2174
$h^2 = \tau^{3-\alpha}$)	128	5.2589e-06	–	1.3757e-05	–	3.6069e-05	–
	4	4.04e-02	1.93	4.32e-02	1.84	4.98e-02	1.67
L^∞-norm	8	1.06e-02	1.93	1.21e-02	1.81	1.56e-02	1.57
(method	16	2.78e-03	1.92	3.45e-03	1.75	5.25e-03	1.46
in [64]	32	7.34e-04	1.91	1.02e-03	1.69	1.90e-03	1.37
with	64	1.96e-04	1.89	3.17e-04	1.64	7.34e-04	1.31
$h = 1/1000$)	128	5.29e-05	–	1.02e-04	–	2.96e-04	–

Table 7.5: *Error and order of convergence in spatial direction for Example 7.6 with* $\tau^{3-\alpha} = h^2$ *and* $k = 1$.

	M	$\alpha = 0.4$		$\alpha = 0.6$		$\alpha = 0.8$	
		$E_{M,N}$	$R^2_{M,N}$	$E_{M,N}$	$R^2_{M,N}$	$E_{M,N}$	$R^2_{M,N}$
L^2-norm	8	2.4049e-02	2.2372	2.3820e-02	2.2378	2.3597e-02	2.2387
(Present	16	5.1006e-03	2.1259	5.0502e-03	2.1263	4.9995e-03	2.1271
method)	32	1.1686e-03	2.0635	1.1567e-03	2.0642	1.1445e-03	2.0646
	64	2.7957e-04	2.0320	2.7658e-04	2.0322	2.7360e-04	2.0324
	128	6.8359e-05	2.0160	6.7620e-05	2.0160	6.6882e-05	2.0162
	256	1.6901e-05	–	1.6718e-05	–	1.6534e-05	–
	8	3.0682e-02	2.1311	3.0362e-02	2.1309	3.0046e-02	2.1310
	16	7.0040e-03	2.0977	6.9322e-03	2.0979	6.8597e-03	2.0983
L^∞-norm	32	1.6363e-03	2.0403	1.6193e-03	2.0407	1.6020e-03	2.0408
(Present	64	3.9780e-04	2.0221	3.9357e-04	2.0222	3.8932e-04	2.0223
method)	128	9.7940e-05	2.0117	9.6890e-05	2.0117	9.5838e-05	2.0117
	256	2.4288e-05	–	2.4027e-05	–	2.3766e-05	–

CHAPTER 8

Direction splitting discontinuous Galerkin method for the two-dimensional time-fractional diffusion equation

In this chapter, we extend the concept of NIPG method to two-dimensional time-fractional linear diffusion equations. The basic idea for solving the two-dimensional problem is to first use operator splitting approach which split the main problem into two one-dimensional problems. Then we obtain fully discrete scheme for both the problems by applying L2-discretization in the time derivative and NIPG method for the spatial variable. Convergence analysis and numerical experiments are carried out.

8.1 Introduction

Let us consider a rectangular domain $\Omega = \Omega_x \times \Omega_y$, where $\Omega_x = (\ell_1, \ell_2)$, $\Omega_y = (\ell_3, \ell_4)$. We take into account the following two-dimensional time-fractional diffusion IBVP for $0 < \alpha < 1$:

$$\begin{cases} {}^{C}\mathcal{D}_t^{\alpha} u((x,y,t) + \mathcal{L}u(x,y,t) = f(x,y,t),\ (x,y,t) \in \Omega \times (0,T], \\ u(x,y,0) = g(x,y), \quad (x,y) \in \overline{\Omega}, \\ u(x,y,t) = 0, \quad (x,y) \in \partial\Omega,\ t \in (0,T], \end{cases} \tag{8.1}$$

where $p > 0$, $\mathbf{a}(x,y) = (a_1(x,y), a_2(x,y))$ and $b = b_1 + b_2$, and

$$\mathcal{L}u(x,y,t) := -p\Delta u(x,y,t) + \mathbf{a}(x,y) \cdot \nabla u(x,y,t) + b(x,y)u(x,y,t). \tag{8.2}$$

We also assume that

$$a_1 \geq a_1^* > 0,\ a_2 \geq a_2^* > 0, \quad b_1, b_2 \geq 0 \quad \text{in } \overline{\Omega}, \tag{8.3}$$

$$b_1 - \frac{1}{2}\frac{\partial a_1}{\partial x} \geq \gamma_1 > 0, \quad b_2 - \frac{1}{2}\frac{\partial a_2}{\partial y} \geq \gamma_2 > 0. \tag{8.4}$$

The structure of this chapter is as follows: We review the proposed splitting approach and its fully discrete discretization utilizing the L1-discretization and L2-discretization for time and the NIPG method for space in Section 8.2. The stability and convergence analysis is covered in Section 8.3, and some numerical examples are provided in Section 8.4.

8.2 Proposed numerical scheme

In this section, we will describe a numerical scheme which is a proper combination of the locally one-dimensional (LOD) approach and the NIPG method. To accomplish this, we must provide some preliminary information before diving into the usual NIPG approach on Cartesian meshes.

Let us consider the uniform partitions with step size h over Ω_x and Ω_y, respectively,

$$\overline{\Omega}_x^{M_1} = \{\ell_1 = x_1 < x_2 \cdots < x_{M_1} < x_{M_1+1} = \ell_2\},$$

$$\overline{\Omega}_y^{M_2} = \{\ell_3 = y_1 < y_2 < \cdots < y_{M_2} < y_{M_2+1} = \ell_4\},$$

and define $K_i^1 := [x_i, x_{i+1}]$, $i = 1, \cdots, M_1$, and $K_j^2 := [y_j, y_{j+1}]$, $j = 1, \cdots, M_2$, where M_1 and M_2 denote the number of elements in x and y directions, respectively. Consequently, Ω is partitioned into Cartesian grid $\mathcal{T}_h$ consisting of $M_1 \times M_2$ rectangular elements $K_{ij} = K_i^1 \times K_j^2$. Boundary of the domain, $\partial\Omega$, is decomposed into $\partial\Omega^- = \partial\Omega_x^- \cup \partial\Omega_y^-$ and $\partial\Omega^+ = \partial\Omega_x^+ \cup \partial\Omega_y^+$, where

$$\partial\Omega_x^- = \{(\ell_1, y) : y \in [\ell_3, \ell_4]\}, \quad \partial\Omega_x^+ = \{(\ell_2, y) : y \in [\ell_3, \ell_4]\},$$

and $\partial\Omega_y^-$ and $\partial\Omega_y^+$ are defined similarly. Boundary of each arbitrary element $K \in \mathcal{T}_h$ is defined as $\Gamma = \Gamma^- \cup \Gamma^+$ in which

$$\Gamma^+ = \{(x, y) \in \Gamma : \mathbf{v} \cdot \mathbf{n} \geq 0\} = \Gamma_x^+ \cup \Gamma_y^+, \quad \Gamma^- = \Gamma_x^- \cup \Gamma_y^-,$$

where $\mathbf{v}$ is auxiliary fixed vector with positive components and $\mathbf{n} = (n_x, n_y)$ is the unit

outward normal vector.

Let $H^1(K)$ be the standard Sobolev space on the element $K \in \mathcal{T}_h$. Let's define the following broken Sobolev space over Ω as:

$$H^1(\Omega) = \left\{\Phi \in L^2(\Omega) : \Phi|_K \in H^1(K),\ \forall K \in \mathcal{T}_h\right\},$$

and

$$H_0^1(\Omega) = \left\{\Phi \in H^1(\Omega) : \Phi|_{\partial\Omega} = 0\right\}.$$

Further, consider the Sobolev spaces in the x- and y- directions, respectively, as

$$H_0^1(\Omega_x) := \left\{\phi(x) \in L^2(\Omega_x) : \phi|_{K_i^1} \in H^1(K_i^1), \quad i = 1, \cdots, M_1, \quad \phi|_{\partial\Omega_x} = 0\right\},$$

and

$$H_0^1(\Omega_y) := \left\{\psi(y) \in L^2(\Omega_y) : \psi|_{K_j^2} \in H^1(K_j^2), \quad j = 1, \cdots, M_2, \quad \psi|_{\partial\Omega_y} = 0\right\}.$$

The inner product and norm on Ω are defined as $\langle\cdot,\cdot\rangle_\Omega = \sum_{K\in\mathcal{T}_h} \langle\cdot,\cdot\rangle_K$ and $\|\cdot\|_\Omega = \sum_{K\in\mathcal{T}_h} \|\cdot\|_K$, where $\langle\cdot,\cdot\rangle_K$ and $\|\cdot\|_K$ are the standard inner product and norm on the element K. Now, define the inner product and norm on Ω_x as $\langle\cdot,\cdot\rangle_{\Omega_x} = \sum_{i=1}^{M_1} \langle\cdot,\cdot\rangle_{K_i^1}$ and $\|\cdot\|_{\Omega_x} = \sum_{i=1}^{M_1} \|\cdot\|_{K_i^1}$. $\langle\cdot,\cdot\rangle_{\Omega_y}$ and $\|\cdot\|_{\Omega_y}$ are defined in a similar way.

As our main aim is to solve two-dimensional problem by splitting it into two 1D sub-problems and then use NIPG method in both the sub-problems for spatial variables. So, we will introduce certain discontinuous finite element spaces over the domains Ω_x and Ω_y. For a fixed $k \geq 1$, let $\mathcal{P}_x^k(K_i^1)$ be the space of all polynomials of degree up to k in x variable over K_i^1. The finite element space $V_{x,0}^{k,h}$ is defined over Ω_x as follows:

$$V_{x,0}^{k,h} = \left\{\phi_h \in L^2(\Omega_x) : \phi_h|_{K_i^1} \in \mathcal{P}_x^k(K_i^1), \quad \forall i = 1, \cdots, M_1, \quad \text{and} \quad \phi_h|_{\partial\Omega_x} = 0\right\}.$$

The polynomial space $\mathcal{P}_y^k(K_j^2)$, the finite element space $V_{y,0}^{k,h}$ is defined over Ω_y in a similar way. It has been noted that the element surfaces permit discontinuity in the DG approximation space functions. This suggests that, for each piecewise function ϕ, ϕ_i^+ (ϕ_i^-) denotes the value of ϕ at z_i^+ (z_i^-), where z_i belongs to the subinterval K_i^1 or K_i^2. Thus, the following average and jump of any function ϕ are defined on each subinterval

K_i^1 or K_i^2, respectively:

$$\{\phi(z_i)\} = \frac{1}{2}(\phi_i^- + \phi_i^+), \quad \text{and} \quad [\phi(z_i)] = \phi_i^+ - \phi_i^-.$$

Let us consider the time domain discretization as

$$\{t_n = (n-1)\tau,\ n = 1, \cdots, N+1,\ \tau = T/N,\ N \in \mathbb{N}\}.$$

Time-fractional Caputo derivative ${}^C\mathcal{D}_t^\alpha u(t)$ is discretized at $t = t_{n+1}$, $n = 1 \cdots, N$ using L1-discretization as

$${}^C\mathcal{D}_t^\alpha u(t_{n+1}) \approx {}_{L_1}^{C}\mathcal{D}_N^\alpha u(t_{n+1}) = d_{n,n}u^{n+1} - d_{n,1}u^1 + \sum_{k=2}^{n}(d_{n,k-1} - d_{n,k})u^k,$$

where $d_{n,k} = \dfrac{(n-k+1)^{1-\alpha} - (n-k)^{1-\alpha}}{\tau^\alpha \Gamma(2-\alpha)}$, and $\quad u^k = u(t_k) \quad$ for $\quad k = 1, \cdots, n.$

Weak formulation for the IBVP is as follows: Find $u(\cdot,\cdot,t) \in H_0^1(\Omega)$ such that for all $\Phi \in H_0^1(\Omega)$,

$$\begin{cases} \left\langle {}^C\mathcal{D}_t^\alpha u(\cdot,\cdot,t), \Phi \right\rangle + p\left\langle \nabla u(\cdot,\cdot,t), \nabla\Phi \right\rangle + \left\langle \mathbf{a}\cdot u(\cdot,\cdot,t), \Phi \right\rangle + \left\langle bu(\cdot,\cdot,t), \Phi \right\rangle = \left\langle f(\cdot,\cdot,t), \Phi \right\rangle, \\ \left\langle u(\cdot,\cdot,0), \Phi \right\rangle = \left\langle g, \Phi \right\rangle. \end{cases} \tag{8.5}$$

Consider the following two operators

$$\begin{cases} \mathcal{L}_x :\equiv -p\dfrac{\partial^2}{\partial x^2} + a_1(x,y)\dfrac{\partial}{\partial x} + b_1(x,y), \quad \forall y \in \Omega_y, \\ \mathcal{L}_y :\equiv -p\dfrac{\partial^2}{\partial y^2} + a_2(x,y)\dfrac{\partial}{\partial y} + b_2(x,y), \quad \forall x \in \Omega_x, \end{cases} \tag{8.6}$$

in the x- and y- directions, respectively. Now, the equation (8.1) can be written as

$${}^C\mathcal{D}_t^\alpha u(x,y,t) + (\mathcal{L}_x + \mathcal{L}_x)\, u(x,y,t) = f(x,y,t),\ (x,y,t) \in \Omega \times (0,T].$$

8.2.1 Direction splitting scheme

We propose the following direction splitting scheme. Discretization of the domain Ω into a finite number of element can be done separately in each direction. We use two one-dimensional finite element spaces to discretize the 2D finite element space, which reduce the computational complexity. Here we have modified the operator splitting technique

given in [36]. In each time subinterval $(t_n, t_{n+1}], n = 1, \cdots, N$, we solve the following sub-problems:

Step 1 (x-direction)

$$\begin{cases} \text{Find} \quad u^* : \Omega \times (t_n, t_{n+1}] \to \mathbb{R} \quad \text{such that } \forall y \in \Omega_y \\ \frac{1}{2}{}^C\mathcal{D}_t^\alpha u^* + \mathcal{L}_x u^* = \frac{1}{2} f(x,y,t), \text{ in } \Omega \times (t_n, t_{n+1}], \\ u^*(x,y,t) = 0. \quad (x,y,t) \in \partial\Omega_x \times \Omega_y \times (t_n, t_{n+1}], \\ u^*(x,y,t_k) = u(x,y,t_k), \quad (x,y) \in \Omega,\ 1 \le k \le n, \end{cases} \tag{8.7}$$

Step 2 (y-direction)

$$\begin{cases} \text{Find} \quad u : \Omega \times (t_n, t_{n+1}] \to \mathbb{R} \quad \text{such that } \forall x \in \Omega_x \\ \frac{1}{2}{}^C\mathcal{D}_t^\alpha u + \mathcal{L}_y u = \frac{1}{2} f(x,y,t), \text{ in } \Omega \times (t_n, t_{n+1}], \\ u(x,y,t) = 0. \quad (x,y,t) \in \Omega_x \times \partial\Omega_y \times (t_n, t_{n+1}], \\ u(x,y,t_k) = u^*(x,y,t_k), \quad (x,y) \in \Omega,\ 1 \le k \le n. \end{cases} \tag{8.8}$$

Here, we solve the IBVP (8.7) in **Step 1** along x-direction while taking into account y as a parameter. After solving $u^*(x,y,t_k), \forall y \in \Omega_y,\ 1 \le k \le n$, we then use these for the second sub-problem (8.8). **Step 2** involves changing the x-direction to the y-direction and solving the IBVP (8.8) $\forall x \in \Omega_x$. In other words, one may conclude that the two sub-problems discussed above are connected by the condition at previous time step.

8.2.2 L2-NIPG fully discrete scheme

Using the L2-discretization given in (1.11) for discretizing the time-fractional derivative at $t = t_{n+1}$, $n = 2, \cdots, N$ in the equations (8.7)-(8.8), we obtain the following semi-discretized sub-problems:

Step 1 (x-direction)

$$\begin{cases} \text{Find} \quad u^{*,n+1} : \Omega \to \mathbb{R} \quad \text{such that } \forall y \in \Omega_y \\ {}_{L2}^{C}\mathcal{D}_{N}^{\alpha} u^{*,n+1} + 2\mathcal{L}_x u^{*,n+1} = f(x,y,t_{n+1}), \text{ in } \Omega, \\ u^{*,n+1}(x,y) = 0. \quad (x,y) \in \partial\Omega_x \times \Omega_y, \\ u^{*,k}(x,y) = u^{k}(x,y), \quad (x,y) \in \Omega,\ 1 \le k \le n, \end{cases} \tag{8.9}$$

Step 2 (y-direction)

$$\begin{cases} \text{Find} \quad u^{n+1} : \Omega \to \mathbb{R} \quad \text{such that } \forall x \in \Omega_x \\ {}_{L2}^{C}\mathcal{D}_{t}^{\alpha} u^{n+1} + 2\mathcal{L}_y u^{n+1} = f(x,y,t_{n+1}), \text{ in } \Omega, \\ u^{n+1}(x,y) = 0. \quad (x,y) \in \Omega_x \times \partial\Omega_y, \\ u^{k}(x,y) = u^{*,k}(x,y), \quad (x,y) \in \Omega,\ 1 \le k \le n. \end{cases} \tag{8.10}$$

In order to derive the fully discrete scheme, we use NIPG scheme for the semi-discretized sub-problems (8.9) and (8.10), we obtain the following fully discrete scheme:

Step 1 (x-direction)

$$\begin{cases} \text{Find} \quad u_h^{*,n+1}(x,y_j) \in V_{x,0}^{k,h}, \quad \forall y_j \in \overline{\Omega}_y^{M_2}, \forall \phi_h \in V_{x,0}^{k,h} \quad \text{such that} \\ D_{n,n+1}\left\langle u_h^{*,n+1}(\cdot,y_j), \phi_h \right\rangle_{\Omega_x} + \mathcal{A}_x\left(u_h^{*,n+1}(\cdot,y_j), \phi_h\right) \\ \qquad = \left\langle f(\cdot,y_j,t_{n+1}) - \sum_{k=1}^{n} D_{n,k} u_h^{k}(\cdot,y_j), \phi_h \right\rangle_{\Omega_x}, \end{cases} \tag{8.11}$$

Step 2 (y-direction)

$$\begin{cases} \text{Find} \quad u_h^{n+1}(x_i,y) \in V_{y,0}^{k,h}, \quad \forall x_i \in \overline{\Omega}_x^{M_1}, \ \forall \psi_h \in V_{y,0}^{k,h} \quad \text{such that} \\ D_{n,n+1}\left\langle u_h^{n+1}(x_i,\cdot), \psi_h \right\rangle_{\Omega_y} + \mathcal{A}_y\left(u_h^{n+1}(x_i,\cdot), \psi_h\right) \\ \qquad = \left\langle f(x_i,\cdot,t_{n+1}) - \sum_{k=1}^{n} D_{n,k} u_h^{*,k}(x_i,\cdot), \psi_h \right\rangle_{\Omega_y}, \end{cases} \tag{8.12}$$

where

$$\mathcal{A}_x\left(u_h^{*,n+1}(\cdot,y_j),\phi_h\right) = 2p\left\langle \frac{du_h^{*,n+1}}{dx}(\cdot,y_j),\frac{d\phi_h}{dx}\right\rangle_{\Omega_x} + 2\left\langle a_1(\cdot,y_j)\frac{du_h^{*,n+1}}{dx}(\cdot,y_j),\phi_h\right\rangle_{\Omega_x}$$
$$+\left\langle 2b_1(\cdot,y_j)u_h^{*,n+1}(\cdot,y_j),\phi_h\right\rangle_{\Omega_x} + 2p\sum_{i=1}^{M_1+1}\left\{\frac{du_h^{*,n+1}}{dx}(x_i,y_j)\right\}[\phi_h(x_i)]$$
$$-2p\sum_{i=1}^{M_1+1}\left\{\frac{d\phi_h}{dx}(x_i)\right\}[u_h^{*,n+1}(x_i,y_j)] + \sum_{i=1}^{M_1+1}\frac{\sigma_i^1}{h}[u_h^{*,n+1}(x_i,y_j)][\phi_h(x_i)]$$
$$+2\sum_{i=1}^{M_1} a_1(x_i,y_j)[u_h^{*,n+1}(x_i,y_j)]\phi_h(x_i^+), \tag{8.13}$$

and

$$\mathcal{A}_y\left(u_h^{n+1}(x_i,\cdot),\psi_h\right) = 2p\left\langle \frac{du_h^{n+1}}{dy}(x_i,\cdot),\frac{d\psi_h}{dy}\right\rangle_{\Omega_y} + 2\left\langle a_2(x_i,\cdot)\frac{du_h^{n+1}}{dy}(x_i,\cdot),\psi_h\right\rangle_{\Omega_y}$$
$$+\left\langle 2b_2(x_i,\cdot)u_h^{n+1}(x_i,\cdot),\psi_h\right\rangle_{\Omega_y} + 2p\sum_{j=1}^{M_2+1}\left\{\frac{du_h^{n+1}}{dy}(x_i,y_j)\right\}[\psi_h(y_j)]$$
$$-2p\sum_{j=1}^{M_2+1}\left\{\frac{d\psi_h}{dy}(y_j)\right\}[u_h^{n+1}(x_i,y_j)] + \sum_{j=1}^{M_2+1}\frac{\sigma_j^2}{h}[u_h^{n+1}(x_i,y_j)][\psi_h(y_j)]$$
$$+2\sum_{j=1}^{M_2} a_2(x_i,y_j)[u_h^{n+1}(x_i,y_j)]\psi_h(y_j^+). \tag{8.14}$$

We define the DG norm in x-direction as

$$|||u|||_{DG,x}^2 := 2p|u|_{H^1(\Omega_x)}^2 + 2\gamma_1\|u\|_{\Omega_x}^2 + \sum_{i=1}^{M_1+1}(a_1^* + \sigma_i^1)[u(x_i)]^2.$$

The norm $|||\cdot|||_{DG,y}$ in the y-direction can be defined in a similar way. It is clear that

$$\mathcal{A}_x(u,u) \geq |||u|||_{DG,x}^2 \quad \text{and} \quad \mathcal{A}_y(u,u) \geq |||u|||_{DG,y}^2. \tag{8.15}$$

8.3 Stability and convergence

This part will discuss the aforementioned two-step scheme's stability findings and convergence analyses. There are typically two different methods for determining these operator-splitting techniques' stability and error estimation. The study can either be performed using a one-step equivalent method and an operator splitting consistency error, or the results can be obtained separately for each sub-problem and combined to determine the overall stability and error estimates for the two-step operator splitting method. Here, we choose the latter strategy.

Lemma 8.1 *Suppose* $u_h^{*,n+1}$ *and* u_h^{n+1} *are the solutions obtained from the two-step method* (8.11) *and* (8.12)*, respectively. Then for each* $n = 2, \cdots, N$*, we have the following:*

$$\begin{aligned}\frac{D_{n,n+1}}{2}&\left(\left\|u_h^{*,n+1}(\cdot,y_j)\right\|_{\Omega_x}^2+\left\|u_h^{n+1}(x_i,\cdot)\right\|_{\Omega_y}^2\right)+\left|\left|\left|u_h^{*,n+1}(\cdot,y_j)\right|\right|\right|_{DG,x}^2+\left|\left|\left|u_h^{n+1}(x_i,\cdot)\right|\right|\right|_{DG,y}^2\\ &\leq\frac{1}{D_{n,n+1}}\left(\left\|f(\cdot,y_j,t_{n+1})\right\|_{\Omega_x}^2+\left\|f(x_i,\cdot,t_{n+1})\right\|_{\Omega_y}^2\right.\\ &\qquad\left.+2\sum_{k=1}^{n}|D_{n,k}|^2\left(\left\|u_h^{k}(\cdot,y_j)\right\|_{\Omega_x}^2+\left\|u_h^{*,k}(x_i,\cdot)\right\|_{\Omega_y}^2\right)\right).\end{aligned}$$

Proof. Substituting $\phi_h = u_h^{*,n+1}(\cdot,y_j), \forall y_j \in \overline{\Omega}_y^{M_2}$ in (8.11) and using the notation $u_h^{*,n+1} = u_h^{*,n+1}(\cdot,y_j)$, we obtain

$$\begin{aligned}2p\left|u_h^{*,n+1}\right|_{H^1(\Omega_x)}^2&+2\left\langle a_1(\cdot,y_j)\frac{du_h^{*,n+1}}{dx},u_h^{*,n+1}\right\rangle_{\Omega_x}+\left\langle(2b_1(\cdot,y_j)+D_{n,n+1})u_h^{*,n+1},u_h^{*,n+1}\right\rangle_{\Omega_x}\\ &+\sum_{i=1}^{M_1+1}\frac{\sigma_i^1}{h}\left[u_h^{*,n+1}(x_i,y_j)\right]^2+2\sum_{i=1}^{M_1}a_1(x_i,y_j)\left[u_h^{*,n+1}(x_i,y_j)\right]u_h^{*,n+1}(x_i^+,y_j)\\ &=\left\langle f(\cdot,y_j,t_{n+1})-\sum_{k=1}^{n}D_{n,k}u_h^{k}(\cdot,y_j),u_h^{*,n+1}\right\rangle_{\Omega_x}.\end{aligned}\tag{8.16}$$

Now, by using integration by parts, the second term in (8.16) can be written as

$$2\left\langle a_1(\cdot,y_j)\frac{du_h^{*,n+1}}{dx},u_h^{*,n+1}\right\rangle_{\Omega_x}=-\left\langle\frac{da_1}{dx}(\cdot,y_j)u_h^{*,n+1},u_h^{*,n+1}\right\rangle_{\Omega_x}$$

$$-2\sum_{i=1}^{M_1+1}\left[\left(a_1\left(u_h^{*,n+1}\right)^2\right)(x_i,y_j)\right]. \quad (8.17)$$

It is clear that, $D_{n,n+1} > 0$ for all $n \geq 2$. Therefore, by using (8.3) and (8.17), we have

$$\begin{aligned}
&2\left\langle a_1(\cdot,y_j)\frac{du_h^{*,n+1}}{dx}, u_h^{*,n+1}\right\rangle_{\Omega_x} + \left\langle 2b_1(\cdot,y_j)u_h^{*,n+1}, u_h^{*,n+1}\right\rangle_{\Omega_x} \\
&\qquad +2\sum_{i=1}^{M_1} a_1(x_i,y_j)\left[u_h^{*,n+1}(x_i,y_j)\right]u_h^{*,n+1}(x_i^+,y_j) \\
&= 2\left\langle\left(b_1-\frac{1}{2}\frac{da_1}{dx}\right)(\cdot,y_j)u_h^{*,n+1}, u_h^{*,n+1}\right\rangle_{\Omega_x} - 2\sum_{i=1}^{M_1+1}\left[\left(a_1\left(u_h^{*,n+1}\right)^2\right)(x_i,y_j)\right] \\
&\qquad +2\sum_{i=1}^{M_1} a_1(x_i,y_j)\left[u_h^{*,n+1}(x_i,y_j)\right]u_h^{*,n+1}(x_i^+,y_j) \\
&\geq 2\gamma_1\left\|u_h^{*,n+1}\right\|_{\Omega_x}^2 + \sum_{i=1}^{M_1+1} a_1(x_i,y_j)\left[u_h^{*,n+1}(x_i,y_j)\right]^2 \\
&\geq 2\gamma_1\left\|u_h^{*,n+1}\right\|_{\Omega_x}^2 + a_1^*\sum_{i=1}^{M_1+1}\left[u_h^{*,n+1}(x_i,y_j)\right]^2. \quad (8.18)
\end{aligned}$$

Using the Hölder's inequality and the Young's inequality, the term on the right-hand side of the equation now reads as follows:

$$\begin{aligned}
&\left\langle f(\cdot,y_j,t_{n+1}) - \sum_{k=1}^{n} D_{n,k}u_h^k(\cdot,y_j), u_h^{*,n+1}\right\rangle_{\Omega_x} \\
&\leq \left(\left\|f(\cdot,y_j,t_{n+1})\right\|_{\Omega_x} + \sum_{k=1}^{n}|D_{n,k}|\left\|u_h^k(x,y_j)\right\|_{\Omega_x}\right)\left\|u_h^{*,n+1}\right\|_{\Omega_x} \\
&\leq \frac{\left\|f(\cdot,y_j,t_{n+1})\right\|_{\Omega_x}^2}{D_{n,n+1}} + \frac{D_{n,n+1}}{2}\left\|u_h^{*,n+1}\right\|_{\Omega_x}^2 + \frac{\left(\sum_{k=1}^{n}|D_{n,k}|\left\|u_h^k(x,y_j)\right\|_{\Omega_x}\right)^2}{D_{n,n+1}} \\
&\leq \frac{\left\|f(\cdot,y_j,t_{n+1})\right\|_{\Omega_x}^2}{D_{n,n+1}} + \frac{D_{n,n+1}}{2}\left\|u_h^{*,n+1}\right\|_{\Omega_x}^2 + \frac{2}{D_{n,n+1}}\left(\sum_{k=1}^{n}|D_{n,k}|^2\left\|u_h^k(\cdot,y_j)\right\|_{\Omega_x}^2\right). \quad (8.19)
\end{aligned}$$

Therefore, using (8.18)-(8.19) in (8.16) and by simplifying, we obtain the following

$$\frac{D_{n,n+1}}{2}\left\|u_h^{*,n+1}\right\|_{\Omega_x}^2 + \left|\left|\left|u_h^{*,n+1}\right|\right|\right|_{DG,x}^2$$

$$\leq \frac{1}{D_{n,n+1}} \left(\left\| f(\cdot, y_j, t_{n+1}) \right\|_{\Omega_x}^2 + 2 \sum_{k=1}^{n} |D_{n,k}|^2 \left\| u_h^k(\cdot, y_j) \right\|_{\Omega_x}^2 \right). \tag{8.20}$$

Using the notation $u_h^n = u_h^n(x_i, y)$, we obtain the following in a similar way in the y-direction:

$$\begin{aligned} &\frac{D_{n,n+1}}{2} \left\| u_h^{n+1} \right\|_{\Omega_y}^2 + \left\| \left| u_h^{n+1} \right| \right\|_{DG,y}^2 \\ &\leq \frac{1}{D_{n,n+1}} \left(\left\| f(x_i, \cdot, t_{n+1}) \right\|_{\Omega_y}^2 + 2 \sum_{k=1}^{n} |D_{n,k}|^2 \left\| u_h^{*,k}(x_i, \cdot) \right\|_{\Omega_y}^2 \right). \end{aligned} \tag{8.21}$$

Hence, by combining (8.20) and (8.21), we obtain the required result. □

Theorem 8.1 *Let $u_h^{*,n+1}$ and u_h^{n+1} be the solutions obtained from the two-step method* (8.11) *and* (8.12)*, respectively. Then for each $n = 2, \cdots, N$, we have the following stability result:*

$$\begin{aligned} \left\| u_h^{*,n+1}(\cdot, y_j) \right\|_{\Omega_x}^2 + \left\| u_h^{n+1}(x_i, \cdot) \right\|_{\Omega_y}^2 \leq\ & C \left(\left\| u_h^1(\cdot, y_j) \right\|_{\Omega_x}^2 + \left\| u_h^{*,1}(x_i, \cdot) \right\|_{\Omega_y}^2 \right. \\ & \left. + \max_{1 \leq m \leq n+1} \left(\left\| f(\cdot, y_j, t_m) \right\|_{\Omega_x}^2 + \left\| f(x_i, \cdot, t_m) \right\|_{\Omega_y}^2 \right) \right). \end{aligned}$$

Proof. From Lemma 8.1 and using the fact that $\left\| \left| u_h^{*,n+1}(\cdot, y_j) \right| \right\|_{DG,x}^2 \geq 0$ and $\left\| \left| u_h^{n+1}(x_i, \cdot) \right| \right\|_{DG,y}^2 \geq 0$, we have

$$\begin{aligned} &\left(\left\| u_h^{*,n+1}(\cdot, y_j) \right\|_{\Omega_x}^2 + \left\| u_h^{n+1}(x_i, \cdot) \right\|_{\Omega_y}^2 \right) \\ &\leq \frac{2}{(D_{n,n+1})^2} \left(\left\| f(\cdot, y_j, t_{n+1}) \right\|_{\Omega_x}^2 + \left\| f(x_i, \cdot, t_{n+1}) \right\|_{\Omega_y}^2 \right. \\ &\qquad \left. + 2 \sum_{m=1}^{n} |D_{n,m}|^2 \left(\left\| u_h^m(\cdot, y_j) \right\|_{\Omega_x}^2 + \left\| u_h^{*,m}(x_i, \cdot) \right\|_{\Omega_y}^2 \right) \right) \\ &\leq C\tau^{2\alpha} \left(\left\| f(\cdot, y_j, t_{n+1}) \right\|_{\Omega_x}^2 + \left\| f(x_i, \cdot, t_{n+1}) \right\|_{\Omega_y}^2 \right. \\ &\qquad \left. + 2 \sum_{m=1}^{n} |D_{n,m}|^2 \left(\left\| u_h^m(\cdot, y_j) \right\|_{\Omega_x}^2 + \left\| u_h^{*,m}(x_i, \cdot) \right\|_{\Omega_y}^2 \right) \right). \end{aligned} \tag{8.22}$$

Using the notation $\nu_{n+1,n+1} = 1,\ \nu_{n+1,n_1} = \tau^{2\alpha} \sum_{m=2}^{n-n_1+2} (D_{n,n-n_1+2})^2 \nu_{n-m+2,n_1}$, for $2 \leq n_1 \leq n$, $1 \leq n \leq N$, we will first establish the following: For $n = 1, \cdots, N$,

$$\left\| u_h^{*,n+1}(\cdot, y_j) \right\|_{\Omega_x}^2 + \left\| u_h^{n+1}(x_i, \cdot) \right\|_{\Omega_y}^2 \leq C \left(\left\| u_h^{1}(\cdot, y_j) \right\|_{\Omega_x}^2 + \left\| u_h^{*,1}(x_i, \cdot) \right\|_{\Omega_y}^2 + \tau^{2\alpha} \sum_{m=2}^{n+1} \nu_{n+1,m} \left(\left\| f(\cdot, y_j, t_m) \right\|_{\Omega_x}^2 + \left\| f(x_i, \cdot, t_m) \right\|_{\Omega_y}^2 \right) \right). \quad (8.23)$$

It is clear that (8.23) holds true for $n = 1$. Now, assume that (8.23) is true for $n = 1, \cdots, k-1$. Then, from (8.22) with $n = k$, we have

$$\begin{aligned}
&\left\| u_h^{*,k+1}(\cdot, y_j) \right\|_{\Omega_x}^2 + \left\| u_h^{k+1}(x_i, \cdot) \right\|_{\Omega_y}^2 \leq C \left(\tau^{2\alpha} \left(\left\| f(\cdot, y_j, t_{k+1}) \right\|_{\Omega_x}^2 + \left\| f(x_i, \cdot, t_{k+1}) \right\|_{\Omega_y}^2 \right) \right. \\
&\left. + \left\| u_h^{1}(\cdot, y_j) \right\|_{\Omega_x}^2 + \left\| u_h^{*,1}(x_i, \cdot) \right\|_{\Omega_y}^2 + \tau^{2\alpha} \sum_{m=2}^{k} |D_{k,m}|^2 \left(\| u_h^{m}(\cdot, y_j) \|_{\Omega_x}^2 + \| u_h^{*,m}(x_i, \cdot) \|_{\Omega_y}^2 \right) \right) \\
&\leq C \left(\tau^{2\alpha} \left(\left\| f(\cdot, y_j, t_{k+1}) \right\|_{\Omega_x}^2 + \left\| f(x_i, \cdot, t_{k+1}) \right\|_{\Omega_y}^2 \right) + \left\| u_h^{1}(\cdot, y_j) \right\|_{\Omega_x}^2 + \left\| u_h^{*,1}(x_i, \cdot) \right\|_{\Omega_y}^2 \right) \\
&\quad + C\tau^{2\alpha} \sum_{m=2}^{k} |D_{k,m}|^2 \left(\left\| u_h^{1}(\cdot, y_j) \right\|_{\Omega_x}^2 + \left\| u_h^{*,1}(x_i, \cdot) \right\|_{\Omega_y}^2 \right. \\
&\qquad \left. + \tau^{2\alpha} \sum_{n_1=2}^{m} \nu_{m,n_1} \left(\left\| f(\cdot, y_j, t_{n_1}) \right\|_{\Omega_x}^2 + \left\| f(x_i, \cdot, t_{n_1}) \right\|_{\Omega_y}^2 \right) \right) \\
&\leq C \left(\tau^{2\alpha} \left(\left\| f(\cdot, y_j, t_{k+1}) \right\|_{\Omega_x}^2 + \left\| f(x_i, \cdot, t_{k+1}) \right\|_{\Omega_y}^2 \right) + \left\| u_h^{1}(\cdot, y_j) \right\|_{\Omega_x}^2 + \left\| u_h^{*,1}(x_i, \cdot) \right\|_{\Omega_y}^2 \right) \\
&\qquad + C\tau^{2\alpha} \sum_{m=2}^{k} \nu_{k+1,m} \left(\left\| f(\cdot, y_j, t_m) \right\|_{\Omega_x}^2 + \left\| f(x_i, \cdot, t_m) \right\|_{\Omega_y}^2 \right) \\
&= C \left(\left\| u_h^{1}(\cdot, y_j) \right\|_{\Omega_x}^2 + \left\| u_h^{*,1}(x_i, \cdot) \right\|_{\Omega_y}^2 \right. \\
&\qquad \left. + \tau^{2\alpha} \sum_{m=2}^{k+1} \nu_{k+1,m} \left(\left\| f(\cdot, y_j, t_m) \right\|_{\Omega_x}^2 + \left\| f(x_i, \cdot, t_m) \right\|_{\Omega_y}^2 \right) \right). \quad (8.24)
\end{aligned}$$

Therefore, from (8.24), we can see that (8.23) holds true for $n = k+1$. Then by mathematical induction, one can say that (8.23) holds true for any $n = 1, \cdots, N$.

In the same way as in Lemma 3.4, one can establish that for $n = 2, \cdots, N$ and $\gamma \geq 0$:

$$\tau^{2\alpha} \sum_{m=2}^{n+1} j^{-\gamma} \nu_{n+1,m} \leq C N^{-\gamma}. \tag{8.25}$$

Hence, from (8.23) and (8.25) with $\gamma = 0$, we have

$$\left\| u_h^{*,n+1}(\cdot, y_j) \right\|_{\Omega_x}^2 + \left\| u_h^{n+1}(x_i, \cdot) \right\|_{\Omega_y}^2 \leq C \left(\left\| u_h^{1}(\cdot, y_j) \right\|_{\Omega_x}^2 + \left\| u_h^{*,1}(x_i, \cdot) \right\|_{\Omega_y}^2 + \max_{1 \leq m \leq n+1} \left(\left\| f(\cdot, y_j, t_m) \right\|_{\Omega_x}^2 + \left\| f(x_i, \cdot, t_m) \right\|_{\Omega_y}^2 \right) \tau^{2\alpha} \sum_{m=2}^{n+1} \nu_{n+1,m} \right),$$

and we obtain the required result. □

Next, we will study the error analysis of the above discussed numerical scheme (8.11) and (8.12). In order to begin our analysis, we first divide the error into two components as follows:

$$\begin{aligned} Er_{i,j}^{n+1} &= \left(u^*(x, y_j, t_{n+1}) - u_h^{*,n+1}(x, y_j) \right) + \left(u(x_i, y, t_{n+1}) - u_h^{n+1}(x_i, y) \right) \\ &=: \xi_j^{*,n+1} + \xi_i^{n+1}, \quad i = 1, \cdots, M_1 + 1, \quad j = 1, \cdots, M_2 + 1, \end{aligned} \tag{8.26}$$

where $\xi_j^{*,n+1}$ and ξ_i^{n+1} are the errors due to the discretization (8.11) and (8.12), respectively at time level t_{n+1}. Further, we split up these errors into the following parts:

$$\begin{aligned} \xi_j^{*,n+1} &= u^*(x, y_j, t_{n+1}) - \mathbf{P}_x u^*(x, y_j, t_{n+1}) + \mathbf{P}_x u^*(x, y_j, t_{n+1}) - u_h^{*,n+1}(x, y_j) \\ &=: \mu_j^{*,n+1} + \eta_j^{*,n+1}, \quad j = 1, \cdots, M_2 + 1, \end{aligned} \tag{8.27}$$

$$\begin{aligned} \xi_i^{n+1} &= u(x_i, y, t_{n+1}) - \mathbf{P}_y u(x_i, y, t_{n+1}) + \mathbf{P}_y u(x_i, y, t_{n+1}) - u_h^{n+1}(x_i, y) \\ &=: \mu_i^{n+1} + \eta_i^{n+1}, \quad i = 1, \cdots, M_1 + 1, \end{aligned} \tag{8.28}$$

where $\mathbf{P}_x u^*(x, y_j, t_{n+1})$ signifies the L^2-projection of $u^*(x, y_j, t_{n+1})$ in the space $V_{x,0}^{k,h}$ along x-direction, and $\mu_j^{*,n+1}$ and $\eta_j^{*,n+1}$ represent the projection and discretization errors at time level t_{n+1} for the sub-problem (8.11). For the sub-problem (8.12), an analogous notation has been employed.

Lemma 8.2 *For the corresponding solutions to the sub-problems* (8.11) *and* (8.12)*, the*

projection error bounds are as follows:

$$\|u^*(x, y_j, t_{n+1}) - \mathbf{P}_x u^*(x, y_j, t_{n+1})\|_{\Omega_x} \leq Ch^{k+1}, \tag{8.29}$$

$$\|u(x_i, y, t_{n+1}) - \mathbf{P}_y u(x_i, y, t_{n+1})\|_{\Omega_y} \leq Ch^{k+1}, \tag{8.30}$$

for $n = 1, \cdots, N$, *and* $i = 1, \cdots, M_1 + 1$, $j = 1, \cdots, M_2 + 1$.

Proof. The projection error bounds in both directions can be obtained similarly as in Lemma 1.4. □

Theorem 8.2 *The following discretization error bound holds true for* $1 \leq i \leq M_1 + 1$, $1 \leq j \leq M_2 + 1$, $1 \leq n \leq N$*:*

$$\|\eta_j^{*,n+1}\|_{\Omega_x} + \|\eta_i^{n+1}\|_{\Omega_y} \leq C\left(h^{k+1} + \tau^{3-\alpha}\right).$$

Proof. From (8.7) and (8.11), we obtain the following error equation for the fully discrete scheme

$$\begin{aligned}
&\left\langle {}_{L2}^{C}\mathcal{D}_N^{\alpha}\left(\mu_j^{*,n+1} + \eta_j^{*,n+1}\right), \phi_h\right\rangle_{\Omega_x} + \mathcal{A}_x\left(\mu_j^{*,n+1} + \eta_j^{*,n+1}, \phi_h\right) \\
&= -\left\langle \left({}^{C}\mathcal{D}_t^{\alpha} - {}_{L2}^{C}\mathcal{D}_N^{\alpha}\right) u^*(\cdot, y_j, t_{n+1}), \phi_h\right\rangle_{\Omega_x},
\end{aligned}$$

which can be written as

$$\begin{aligned}
&\left\langle {}_{L2}^{C}\mathcal{D}_N^{\alpha}\,\eta_j^{*,n+1}, \phi_h\right\rangle_{\Omega_x} + \mathcal{A}_x\left(\eta_j^{*,n+1}, \phi_h\right) \\
&= -\left\langle \mathcal{R}_N^*, \phi_h\right\rangle_{\Omega_x} - \left\langle {}_{L2}^{C}\mathcal{D}_N^{\alpha}\,\mu_j^{*,n+1}, \phi_h\right\rangle_{\Omega_x} - \mathcal{A}_x\left(\mu_j^{*,n+1}, \phi_h\right),
\end{aligned}$$

where $\mathcal{R}_N^{*,n+1} = \left({}^{C}\mathcal{D}_t^{\alpha} - {}_{L2}^{C}\mathcal{D}_N^{\alpha}\right) u^*(\cdot, y_j, t_{n+1})$. By substituting $\phi_h = \eta_j^{*,n+1}$ in the above error equation, we obtain

$$\begin{aligned}
&\left\langle {}_{L2}^{C}\mathcal{D}_N^{\alpha}\,\eta_j^{*,n+1}, \eta_j^{*,n+1}\right\rangle_{\Omega_x} + \mathcal{A}_x\left(\eta_j^{*,n+1}, \eta_j^{*,n+1}\right) \\
&= -\left\langle \mathcal{R}_N^{*,n+1} + {}_{L2}^{C}\mathcal{D}_N^{\alpha}\,\mu_j^{*,n+1}, \eta_j^{*,n+1}\right\rangle_{\Omega_x} - \mathcal{A}_x\left(\mu_j^{*,n+1}, \eta_j^{*,n+1}\right).
\end{aligned} \tag{8.31}$$

Now, by using integration by parts and using the fact that $\left\{\dfrac{d\mu_j^{*,n+1}}{dx}(x_i)\right\} =$

$[\mu_j^{*,n+1}(x_i)] = 0$, we have

$$\begin{aligned}
-\mathcal{A}_x\left(\mu_j^{*,n+1}, \eta_j^{*,n+1}\right) &= 2p\sum_{i=1}^{M_1}\int_{K_i^1}\mu_j^{*,n+1}\frac{d^2\eta_j^{*,n+1}}{dx^2}dx + 2\sum_{i=1}^{M_1}\int_{K_i^1}a_1(\cdot,y_j)\mu_j^{*,n+1}\frac{d\eta_j^{*,n+1}}{dx}dx \\
&\quad +2\sum_{i=1}^{M_1}\int_{K_i^1}\left(\frac{da_1}{dx}-b_1\right)(\cdot,y_j)\eta_j^{*,n+1}\mu_j^{*,n+1}dx \\
&\leq 2p\sum_{i=1}^{M_1}\int_{K_i^1}\mu_j^{*,n+1}\frac{d^2\eta_j^{*,n+1}}{dx^2}dx + 2\sum_{i=1}^{M_1}\int_{K_i^1}a_1(\cdot,y_j)\mu_j^{*,n+1}\frac{d\eta_j^{*,n+1}}{dx}dx \\
&\quad +2\sum_{i=1}^{M_1}\int_{K_i^1}\frac{da_1}{dx}(\cdot,y_j)\eta_j^{*,n+1}\mu_j^{*,n+1}dx \\
&\leq 2p\sum_{i=1}^{M_1}\int_{K_i^1}\mu_j^{*,n+1}\frac{d^2\eta_j^{*,n+1}}{dx^2}dx + 2C\sum_{i=1}^{M_1}\int_{K_i^1}\mu_j^{*,n+1}\frac{d\eta_j^{*,n+1}}{dx}dx + 2C\sum_{i=1}^{M_1}\int_{K_i^1}\eta_j^{*,n+1}\mu_j^{*,n+1}dx \\
&= 0, \qquad (8.32)
\end{aligned}$$

where we have used the definition of L^2-projection, and the facts $a_1 \in \mathcal{C}(\overline{\Omega})$, $\eta_j^{*,n+1}$, $\dfrac{d\eta_j^{*,n+1}}{dx}$ $\dfrac{d^2\eta_j^{*,n+1}}{dx^2} \in V_{x,0}^{k,h}$.

By considering $\chi_j^{*,n+1} = \mathcal{R}_N^{*,n+1} + {}_{L2}^{C}\mathcal{D}_N^{\alpha}\,\mu_j^{*,n+1}$, and using (1.11) and (8.15) in (8.31), also using the Cauchy-Schwartz inequality and the Young's inequality, we have

$$\begin{aligned}
D_{n,n+1}\left\|\eta_j^{*,n+1}\right\|_{\Omega_x}^2 + \left|\left|\left|\eta_j^{*,n+1}\right|\right|\right|_{DG,x}^2 &\leq D_{n,n+1}\left\|\eta_j^{*,n+1}\right\|_{\Omega_x}^2 + \mathcal{A}_x\left(\eta_j^{*,n+1}, \eta_j^{*,n+1}\right) \\
&\leq -\left\langle \chi_j^{*,n+1} + \sum_{k=1}^{n} D_{n,k}\,\eta_j^{*,k}, \eta_j^{*,n+1}\right\rangle_{\Omega_x} \\
&\leq \left(\left\|\chi_j^{*,n+1}\right\|_{\Omega_x} + \sum_{k=1}^{n}|D_{n,k}|\left\|\eta_j^{*,k}\right\|_{\Omega_x}\right)\left\|\eta_j^{*,n+1}\right\| \\
&\leq \frac{1}{D_{n,n+1}}\left\|\chi_j^{*,n+1}\right\|_{\Omega_x}^2 + \frac{D_{n,n+1}}{2}\left\|\eta_j^{*,n+1}\right\|_{\Omega_x}^2 + \frac{2}{D_{n,n+1}}\sum_{k=1}^{n}|D_{n,k}|^2\left\|\eta_j^{*,k}\right\|_{\Omega_x}^2,
\end{aligned}$$

which can be simplified as

$$\frac{D_{n,n+1}}{2}\left\|\eta_j^{*,n+1}\right\|_{\Omega_x}^2+\left|\left|\left|\eta_j^{*,n+1}\right|\right|\right|_{DG,x}^2\leq\frac{1}{D_{n,n+1}}\left(\left\|\chi_j^{*,n+1}\right\|_{\Omega_x}^2+2\sum_{k=1}^{n}|D_{n,k}|^2\left\|\eta_j^{*,k}\right\|_{\Omega_x}^2\right). \tag{8.33}$$

Now, by using Lemma 1.6 and Lemma 8.2, we have

$$\begin{aligned}\left\|\chi_j^{*,n+1}\right\|_{\Omega_x} &\leq \left\|\mathcal{R}_N^{*,n+1}\right\|_{\Omega_x}+\left\|{}_{L2}^{C}\mathcal{D}_N^{\alpha}\,\mu_j^{*,n+1}\right\|_{\Omega_x}\\ &= \left\|\mathcal{R}_N^{*,n+1}\right\|_{\Omega_x}+\left\|{}^{C}\mathcal{D}_t^{\alpha}\,\mu_j^{*,n+1}-\left({}^{C}\mathcal{D}_t^{\alpha}-{}_{L2}^{C}\mathcal{D}_N^{\alpha}\right)\,\mu_j^{*,n+1}\right\|_{\Omega_x}\\ &\leq 2\left\|\mathcal{R}_N^{*,n+1}\right\|_{\Omega_x}+\left\|{}^{C}\mathcal{D}_t^{\alpha}\,u^*(\cdot,y_j,t_{n+1})-\mathbf{P}_x\left({}^{C}\mathcal{D}_t^{\alpha}u^*(\cdot,y_j,t_{n+1})\right)\right\|_{\Omega_x}\\ &\leq C(\tau^{3-\alpha}+h^{k+1}).\end{aligned} \tag{8.34}$$

Applying Lemma 8.1, Theorem 8.1 and (8.34) in (8.33), we obtain

$$\left\|\eta_j^{*,n+1}\right\|_{\Omega_x}\leq C\left\|\chi_j^{*,n+1}\right\|_{\Omega_x}\leq C(\tau^{3-\alpha}+h^{k+1}). \tag{8.35}$$

In the similar way, one can obtain

$$\left\|\eta_i^{n+1}\right\|_{\Omega_y}\leq C(\tau^{3-\alpha}+h^{k+1}). \tag{8.36}$$

By combining (8.35) and (8.36), the proof is done. □

Now we proceed to the error estimate of the proposed scheme.

Theorem 8.3 *If $\xi_j^{*,n+1}$ and ξ_i^{n+1} denote the errors of the sub-problems* (8.11) *and* (8.12)*, respectively, then the error of the fully discrete operator splitting L2-NIPG scheme satisfies the following bound:*

$$\|\xi_j^{*,n+1}\|_{\Omega_x}+\|\xi_i^{n+1}\|_{\Omega_y}\leq C\left(h^{k+1}+\tau^{3-\alpha}\right),\quad 1\leq i\leq M_1+1,\ 1\leq j\leq M_2+1,\ 1\leq n\leq N.$$

Proof. Proof of this theorem follows from Lemma 8.2 and Theorem 8.2. □

8.4 Numerical tests

In this section, we discuss the numerical results to validate the theoretical results. The error and order of convergence can be calculated using

$$\mathcal{E}_{M,N}=\|u(\cdot,\cdot,t_{N+1})-u_h^{N+1}\|_{\Omega},\quad\text{and}\quad R_{M,N}=\log_2\left(\frac{\mathcal{E}_{M,N}}{\mathcal{E}_{2M,2N}}\right),$$

where $M = M_1 = M_2$.

Example 8.4 *Consider the following problem:*

$$\begin{cases} {}^{C}\mathcal{D}_t^{\alpha} u - \Delta u = f(x,y,t), \quad (x,y,t) \in \Omega \times (0,1], \\ u(x,y,0) = 0, \quad (x,y) \in \overline{\Omega}, \\ u(x,y,t) = 0, \quad (x,y) \in \partial\Omega, \end{cases} \tag{8.37}$$

where $\Omega = (0,1) \times (0,1)$. *Exact solution and source function for the problem* (8.37) *are respectively,* $u(x,y,t) = t^2 \sin(\pi x)\sin(\pi y)$ *and* $f(x,y,t) = 2\left(\pi^2 t^2 + \dfrac{t^{2-\alpha}}{\Gamma(3-\alpha)}\right)\sin(\pi x)\sin(\pi y)$.

Table 8.1 and Table 8.2 show the errors and order of convergences for Example 8.4 for various values of α in the spatial and the temporal direction, respectively. Figure 8.1 displays the exact and numerical solutions for Example 8.4 with $\alpha = 0.4$ at $t = 1$, whereas Figure 8.2 depict the corresponding error surface.

Table 8.1: $\mathcal{E}_{M,N}$ *and* $R_{M,N}$ *for Example 8.4 with* $M = M_1 = M_2$, $N = M$ *and* $k = 1$.

$\alpha \downarrow$	$M \rightarrow$	8	16	32	64
0.2	$\mathcal{E}_{M,N}$	1.7598e-02	4.2748e-03	1.0549e-03	2.6236e-04
	$R_{M,N}$	2.0415	2.0187	2.0075	–
0.4	$\mathcal{E}_{M,N}$	1.7582e-02	4.2920e-03	1.0654e-03	2.6697e-04
	$R_{M,N}$	2.0344	2.0103	1.9966	–
0.6	$\mathcal{E}_{M,N}$	1.7627e-02	4.3483e-03	1.0957e-03	2.8086e-04
	$R_{M,N}$	2.0192	1.9886	1.9639	–
0.8	$\mathcal{E}_{M,N}$	3.8217e-03	9.4289e-04	5.6679e-05	1.3898e-05
	$R_{M,N}$	2.0191	2.0272	2.0290	–

8.5 Conclusions

To solve the two-dimensional time-factional diffusion problem, a combined LOD, L2 and NIPG approach has been presented. An investigation has been conducted into the stability and convergence studies of the suggested approach. With k being the degree

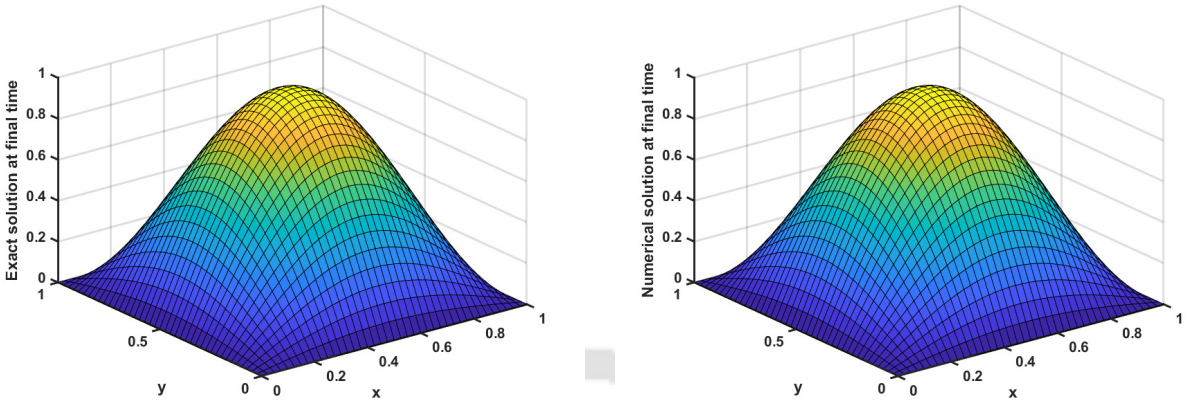

(a) Exact solution surface at $t = 1$. *(b) Numerical solution surface at $t = 1$.*

Figure 8.1: *Exact and numerical solution at $t = 1$ for Example 8.4 with $\alpha = 0.4$ and $M_1 = M_2 = N = 40$.*

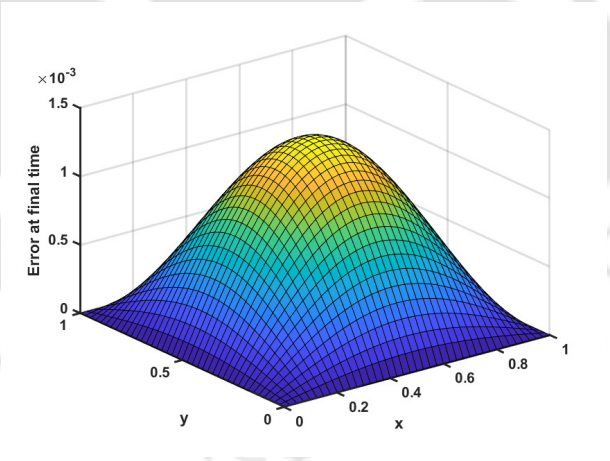

Figure 8.2: *Error surface at $t = 1$ for Example 8.4 with $\alpha = 0.4$ and $M_1 = M_2 = N = 40$.*

Table 8.2: *$\mathcal{E}_{M,N}$ and $R_{M,N}$ for Example 8.4 with $M = M_1 = M_2$ and $k = 1$.*

$\alpha \downarrow$	$M \rightarrow$	4	8	16	32
0.2	$\mathcal{E}_{M,N}$	2.3111e-02	3.3573e-03	4.4681e-04	6.5202e-05
	$R_{M,N}$	2.7832	2.9096	2.7767	–
0.4	$\mathcal{E}_{M,N}$	3.1780e-02	4.8639e-03	7.8954e-04	1.3051e-04
	$R_{M,N}$	2.7079	2.6230	2.5969	–
0.6	$\mathcal{E}_{M,N}$	4.6333e-02	7.6903e-03	1.4031e-03	2.7199e-04
	$R_{M,N}$	2.5909	2.4545	2.3670	–
0.8	$\mathcal{E}_{M,N}$	4.6118e-02	1.1254e-02	2.5801e-03	5.8721e-04
	$R_{M,N}$	2.0349	2.1250	2.1355	–

of the piecewise polynomial in the finite element space and α denoting the order of the fractional derivative, the proposed technique is convergent of order $(k+1)$ in the spatial direction and of order $(3-\alpha)$ in the temporal direction. We verified the theoretical results with the numerical results.

CHAPTER 9

Summary and Future Scopes

The thesis finishes in this chapter with an overview and some suggestions for further developing the concepts from the earlier chapters.

9.1 Summary of the Results

Some important results of this thesis are highlighted below:

- In Chapter 2, we considered linear and semi-linear fractional differential BVPs with RLC type fractional derivative. By converting the BVP into an IVP using the shooting technique based on the secant method, we discretize the resultant IVP to obtain a numerical solution. Stability of the proposed scheme is studied and error analysis is carried out. The error bound CM^{-1} for the present method is better than the convergence result of $CM^{-1} \ln M$ that was obtained in reference [38] for their finite difference scheme. The numerical outcomes show that the current method is more effective and accurate than the prior result Gracia et al. [38].

- The separation of variables method and the Mittag-Leffler analysis are commonly used for the existence of the solution to autonomous TF-ADR. But these methods are not sufficient for proving the existence of solution for non-autonomous TF-ADR equation, and therefore, one has to use some other suitable techniques. To the best of our knowledge, in literature, there is no work has been done towards the existence and uniqueness of the classical solution of non-autonomous Caputo TF-ADR IBVPs of the form (3.1). Chapter 3 established the existence of

unique solution of the linear non-autonomous time-fractional IBVP by using the Sumudu decomposition method and the maximum-minimum principle. Based on L1-discretization for fractional temporal derivative and cubic spline approximation for spatial variables, we also proposed a numerical solution technique for solving the IBVP. The proposed method is of $O\big(N^{-(2-\alpha)} + M^{-2}\big)$, where N and M are respectively the number of sub-intervals in temporal and spatial direction. We extended the proposed method to solve semi-linear problems after linearizing by the Newton's linearization process. Numerical experiments support the theoretical results and also compared the numerical results with previous results available in the literature.

- Chapter 4 discussed the well-posedness of the TF-IPDE by utilizing the Sumudu decomposition technique and the maximum-minimum principle. Further, we proposed a numerical technique for solving the IBVP, which comprises the L1-discretization for the fractional-time derivative, trapezoidal rule for the integral term and the cubic spline approximation for the spatial derivatives. The stability of the fully discrete scheme is analyzed through the discrete maximum principle, and error estimates are obtained. Theoretical results are validated through several numerical examples and we demonstrated the accuracy and efficiency of the propose method over the previous method described in [95] by the comparison of numerical results.

- We considered linear and semi-linear non-autonomous TF-ADR equations with Caputo-type fractional derivative in Chapter 5. We obtained a stable fully discrete scheme by applying the NIPG method in space on a uniform mesh and the L1-discretization in time on a graded mesh. Superconvergence of error estimates for the proposed method is obtained using the discrete energy-norm. Newton's linearization process used to linearizing semi-linear problem and then we have applied the proposed method. The theoretical results are verified through numerical experiments.

- Next, Chapter 6 studied the numerical solution of the nonlinear time-fractional integro-partial differential IBVP by using the L1-NIPG and L2-NIPG methods. By linearizing the nonlinear model problem, we apply the NIPG method for the spatial variable and use both L1-discretization and L2-discretization for the time-

fractional derivative, and the trapezoidal rule for the integral term and obtained two fully discrete schemes. Further, we study the L^2-norm stability of the proposed methods and derive the required error estimates. In the study of convergence analysis, we will find that when we discretize the Caputo derivative using the L1-discretization, the order of convergence for the suggested technique is $(2-\alpha)$ in the time direction, however, the order will increase by one, *i.e.*, $(3-\alpha)$ when we do the same using the L2-discretization. To support the proposed approach and demonstrate the theoretical error bounds, numerical experiments will be carried out.

- Then, in Chapter 7, we arrived at a numerical scheme for the nonlinear time-fractional Burgers' equation by applying the NIPG approach for spatial variable and the L2-discretization for time derivative discretization. We further examine the suggested method's stability under the L^2-norm, and we calculate the necessary error estimates with an order of convergence of $(h^{k+1}+\tau^{3-\alpha})$, where h and τ are the step-lengths in space and time, respectively. Numerical experiments will be carried out to validate the suggested approach and show the theoretical error bounds.

- Finally, the alternating direction implicit type operator splitting discontinuous Galerkin finite element method is proposed to numerically solve a class of two-dimensional time-factional diffusion equations in Chapter 8. By using the operator splitting method, we splitted the two-dimensional diffusion problem into two separate one-dimensional problems. The time-fractional derivative term is discretized over uniform mesh using the well-known L2-discretization and for the discretization of the spatial derivatives, the discontinuous Galerkin finite element method is used in both one-dimensional problems over the uniform mesh. The stability and the error estimate of the proposed scheme are addressed. Finally, we give some numerical experiments to validate the proposed method.

9.2 Scope for Future Work

A brief outline, describing the possible extensions of the current work to be carried out in the future with suitable model problems, are presented below:

- In this thesis, we have studied the numerical solution techniques for the one-dimensional time-fractional problems with time-fractional derivative of order $\alpha \in (0,1)$. We wish to extends the numerical techniques to the following one-dimensional and the two-dimensional time-fractional diffusion-wave problems [49, 68] with the time-fractional derivative of order $\alpha \in (1,2)$:

$$\begin{cases} {}^{C}\mathcal{D}_t^{\alpha} u(x,t) - p\Delta u(x,t) = f(x,t),\ (x,t) \in \Omega \times (0,T], \\ u(x,0) = g_1(x),\ \dfrac{\partial u}{\partial t}(x,0) = g_2(x),\ x \in \overline{\Omega}, \\ u(x,t) = 0,\ (x) \in \partial\Omega,\ t \in (0,T], \end{cases} \tag{9.1}$$

  where $\Omega \subset \mathbb{R}^d (d = 1 \text{ or } 2)$ is a bounded domain with smooth boundary $\partial\Omega$ and $p > 0$.

- We wish to extend the numerical solution techniques used in this thesis to the following multi-term time-fractional diffusion problem [73]:

$$\begin{cases} {}^{C}\mathcal{D}_t^{\alpha} u(x,y,t) + \displaystyle\sum_{j=1}^{J} a_j {}^{C}\mathcal{D}_t^{\alpha_j} u(x,y,t) - p\Delta u(x,y,t) \\ = f(x,y,t),\ (x,y,t) \in \Omega \times (0,T], \\ u(x,y,0) = g_1(x,y),\ \dfrac{\partial u}{\partial t}(x,y,0) = g_2(x,y),\ (x,y) \in \overline{\Omega}, \\ u(x,y,t) = 0,\ (x,y) \in \partial\Omega,\ t \in (0,T], \end{cases} \tag{9.2}$$

  where $\Omega = (0,\ell_1) \times (0,\ell_2) \subset \mathbb{R}^2$ with $\partial\Omega$ being the boundary, $p > 0$, and $0 < \alpha_{J} < \alpha_{J-1} < \cdots < \alpha_{J'+1} \leq 1 < \alpha_{J'} < \cdots < \alpha_1 < \alpha < 2$ with $J' < J$.

- The following two-dimensional time-fractional Burgers' equation [121] can be resolved using the numerical scheme discussed in Chapter 7:

$$\begin{cases} {}^{C}\mathcal{D}_t^{\alpha} u(x,y,t) + \left(\dfrac{\partial}{\partial x} + \dfrac{\partial}{\partial y}\right)\left(\dfrac{u^2}{2}\right)(x,y,t) - p\left(\dfrac{\partial^2 u}{\partial x^2} + \dfrac{\partial^2 u}{\partial y^2}\right)(x,y,t) \\ = f(x,y,t),\ (x,y,t) \in \Omega \times (0,T], \\ u(x,y,0) = g(x,y), \quad (x,y) \in \overline{\Omega}, \\ u(x,y,t) = 0, \quad (x,y) \in \partial\Omega,\ t \in (0,T], \end{cases} \tag{9.3}$$

where $\Omega = (0, \ell_1) \times (0, \ell_2) \subset \mathbb{R}^2$ with $\partial\Omega$ being the boundary, $p > 0$, and $0 < \alpha < 1$.

- One can apply the numerical solution methods employed in this thesis to the following nonlinear time-fractional mobile/immobile transport equation [39, 52] in multi-dimension:

$$\begin{cases} \dfrac{\partial u}{\partial t} + {}^{C}\mathcal{D}_t^{\alpha} u - p\Delta u + b(u) = f(x,t),\ (x,t) \in \Omega \times (0,T], \\ u(x,0) = g(x),\ x \in \Omega, \\ u(x,t) = 0,\ (x,t) \in \partial\Omega \times (0,T], \end{cases} \tag{9.4}$$

where $0 < \alpha < 1$, p is a positive constant, $b \in \mathcal{C}^2(\mathbb{R})$ represents the nonlinear reaction function, $\Omega \subset \mathbb{R}^d\,(d = 2, 3)$ is a bounded and convex domain with a polygonal (polyhedral) boundary $\partial\Omega$.

Bibliography

[1] G. Adomian. *Solving frontier problems of physics: the decomposition method*, volume 60 of *Fundamental Theories of Physics*. Kluwer Academic Publishers Group, Dordrecht, 1994.

[2] R. P. Agarwal. Some inversion formulae for the generalised Hankel transform. *Bull. Calcutta Math. Soc.*, 45:69–73, 1953.

[3] Q. M. Al-Mdallal, M. I. Syam, and M. N. Anwar. A collocation-shooting method for solving fractional boundary value problems. *Commun. Nonlinear Sci. Numer. Simul.*, 15(12):3814–3822, 2010.

[4] A. A. Alikhanov and C. Huang. A high-order L2 type difference scheme for the time-fractional diffusion equation. *Appl. Math. Comput.*, 411:126545, 19, 2021.

[5] D. N. Arnold. An interior penalty finite element method with discontinuous elements. *SIAM J. Numer. Anal.*, 19(4):742–760, 1982.

[6] M. A. Asiru. Sumudu transform and the solution of integral equations of convolution type. *Internat. J. Math. Ed. Sci. Tech.*, 32(6):906–910, 2001.

[7] D. Avijit and S. Natesan. A novel two-step streamline-diffusion FEM for singularly perturbed 2D parabolic PDEs. *Appl. Numer. Math.*, 172:259–278, 2022.

[8] G. A. Baker. Finite element methods for elliptic equations using nonconforming elements. *Math. Comp.*, 31(137):45–59, 1977.

[9] F. Bassi and S. Rebay. A high-order accurate discontinuous finite element method for the numerical solution of the compressible Navier-Stokes equations. *J. Comput. Phys.*, 131(2):267–279, 1997.

[10] H. Bateman. Some recent researches on the motion of fluids. *Mon. Weather Rev.*, 43(4):163–170, 1915.

[11] C. E. Baumann and J. T. Oden. A discontinuous *hp* finite element method for convection-diffusion problems. *Comput. Methods Appl. Mech. Engrg.*, 175(3-4):311–341, 1999.

[12] C. E. Baumann and J. T. Oden. A discontinuous *hp* finite element method for the Euler and Navier-Stokes equations. *Internat. J. Numer. Methods Fluids*, 31(1):79–95, 1999.

[13] F. B. M. Belgacem and A. Karaballi. Sumudu transform fundamental properties investigations and applications. *J. Appl. Math. Stoch. Anal.*, 2006:91083, 1–23, 2006.

[14] D. A. Benson, S. W. Wheatcraft, and M. M. Meerschaert. Application of a fractional advection-dispersion equation. *Water Resour. Res.*, 36(6):1403–1412, 2000.

[15] J. M. Burgers. Mathematical examples illustrating relations occurring in the theory of turbulent fluid motion. *Verh. Nederl. Akad. Wetensch. Afd. Natuurk. Sect. 1*, 17(2):53, 1939.

[16] J. M. Burgers. A mathematical model illustrating the theory of turbulence. *Adv. in Appl. Mechanics*, 1:171–199, 1948.

[17] J. Caballero, A. B. Mingarelli, and K. Sadarangani. Existence of solutions of an integral equation of Chandrasekhar type in the theory of radiative transfer. *Electron. J. Differential Equations*, 2006:57, 1–11, 2006.

[18] Z. Cen, J. Huang, and A. Xu. An efficient numerical method for a two-point boundary value problem with a Caputo fractional derivative. *J. Comput. Appl. Math.*, 336:1–7, 2018.

[19] Z. Cen, J. Huang, A. Xu, and A. Le. A modified integral discretization scheme for a two-point boundary value problem with a Caputo fractional derivative. *J. Comput. Appl. Math.*, 367:112465, 10, 2020.

[20] Z. Cen, L.-B. Liu, and J. Huang. A posteriori error estimation in maximum norm for a two-point boundary value problem with a Riemann-Liouville fractional derivative. *Appl. Math. Lett.*, 102:106086, 8, 2020.

[21] J. Chen and Y. Ge. High order locally one-dimensional methods for solving two-dimensional parabolic equations. *Adv. Difference Equ.*, 2018:361, 1–17, 2018.

[22] Y. Cherruault. Convergence of Adomian's method. *Kybernetes*, 18(2):31–38, 1989.

[23] B. Cockburn, S. Hou, and C.-W. Shu. The Runge-Kutta local projection discontinuous Galerkin finite element method for conservation laws. IV. The multidimensional case. *Math. Comp.*, 54(190):545–581, 1990.

[24] B. Cockburn, S. Y. Lin, and C.-W. Shu. TVB Runge-Kutta local projection discontinuous Galerkin finite element method for conservation laws. III. One-dimensional systems. *J. Comput. Phys.*, 84(1):90–113, 1989.

[25] B. Cockburn and C.-W. Shu. TVB Runge-Kutta local projection discontinuous Galerkin finite element method for conservation laws. II. General framework. *Math. Comp.*, 52(186):411–435, 1989.

[26] B. Cockburn and C.-W. Shu. The Runge-Kutta local projection P^1-discontinuous-Galerkin finite element method for scalar conservation laws. *RAIRO Modél. Math. Anal. Numér.*, 25(3):337–361, 1991.

[27] B. Cockburn and C.-W. Shu. The local discontinuous Galerkin method for time-dependent convection-diffusion systems. *SIAM J. Numer. Anal.*, 35(6):2440–2463, 1998.

[28] C. Cui, J. Liu, Y. Mo, and S. Zhai. An effective operator splitting scheme for two-dimensional conservative nonlocal Allen-Cahn equation. *Appl. Math. Lett.*, 130:108016, 1–10, 2022.

[29] R. Gencoy U. Müller R.B. Olsen Dacorogna, M.M. and O.V. Pictet. *An introduction to high frequency finance*. Academic Press, San Diego, CA, 2001.

[30] G. Dahlquist and Å. Björck. *Numerical methods in scientific computing. Vol. I.* SIAM, Philadelphia, PA, 2008.

[31] K. Diethelm. *The analysis of fractional differential equations: An application-oriented exposition using differential operators of Caputo type*, volume 2004 of *Lecture Notes in Mathematics*. Springer-Verlag, Berlin, 2010.

[32] K. Diethelm and N. J. Ford. Volterra integral equations and fractional calculus: do neighboring solutions intersect? *J. Integral Equations Appl.*, 24(1):25–37, 2012.

[33] K. Diethelm and G. Walz. Numerical solution of fractional order differential equations by extrapolation. *Numer. Algorithms*, 16(3-4):231–253 (1998), 1997.

[34] J. Dixon and S. McKee. Weakly singular discrete Gronwall inequalities. *Z. Angew. Math. Mech.*, 66(11):535–544, 1986.

[35] J. Douglas, Jr. and T. Dupont. Interior penalty procedures for elliptic and parabolic Galerkin methods. In *Computing methods in applied sciences (Second Internat. Sympos., Versailles, 1975)*, volume Vol. 58 of *Lecture Notes in Phys.*, pages 207–216. Springer, Berlin-New York, 1976.

[36] S. Fouladi, R. Mokhtari, and M. S. Dahaghin. Operator-splitting local discontinuous Galerkin method for multi-dimensional linear convection-diffusion equations. *Numer. Algorithms*, 92(2):1425–1449, 2023.

[37] S. Ganesan and L. Tobiska. Operator-splitting finite element algorithms for computations of high-dimensional parabolic problems. *Appl. Math. Comput.*, 219(11):6182–6196, 2013.

[38] J. L. Gracia, E. O'Riordan, and M. Stynes. Convergence analysis of a finite difference scheme for a two-point boundary value problem with a Riemann-Liouville-Caputo fractional derivative. *BIT*, 60(2):411–439, 2020.

[39] Z. Guan, J. Wang, Y. Liu, and Y. Nie. Unconditionally optimal convergence of a linearized Galerkin FEM for the nonlinear time-fractional mobile/immobile transport equation. *Appl. Numer. Math.*, 172:133–156, 2022.

[40] J. Guo, D. Xu, and W. Qiu. A finite difference scheme for the nonlinear time-fractional partial integro-differential equation. *Math. Methods Appl. Sci.*, 43(6):3392–3412, 2020.

[41] A. Hellander, M. J. Lawson, B. Drawert, and L. Petzold. Local error estimates for adaptive simulation of the reaction-diffusion master equation via operator splitting. *J. Comput. Phys.*, 266:89–100, 2014.

[42] M. Hemami, J. A. Rad, and K. Parand. The use of space-splitting RBF-FD technique to simulate the controlled synchronization of neural networks arising from brain activity modeling in epileptic seizures. *J. Comput. Sci.*, 42:101090, 1–17, 2020.

[43] H. Holden, K. H. Karlsen, K.-A. Lie, and N. H. Risebro. *Splitting methods for partial differential equations with rough solutions: Analysis and MATLAB programs.* EMS Series of Lectures in Mathematics. European Mathematical Society (EMS), Zürich, 2010.

[44] Y. Hu, Y. Luo, and Z. Lu. Analytical solution of the linear fractional differential equation by Adomian decomposition method. *J. Comput. Appl. Math.*, 215(1):220–229, 2008.

[45] C. Huang, N. An, X. Yu, and H. Zhang. A direct discontinuous Galerkin method for time-fractional diffusion equation with discontinuous diffusive coefficient. *Complex Var. Elliptic Equ.*, 65(9):1445–1461, 2020.

[46] C. Huang and M. Stynes. Superconvergence of the direct discontinuous Galerkin method for a time-fractional initial-boundary value problem. *Numer. Methods Partial Differential Equations*, 35(6):2076–2090, 2019.

[47] C. Huang, M. Stynes, and N. An. Optimal $L^\infty(L^2)$ error analysis of a direct discontinuous Galerkin method for a time-fractional reaction-diffusion problem. *BIT*, 58(3):661–690, 2018.

[48] J. Huang, Z. Cen, L.-B. Liu, and J. Zhao. An efficient numerical method for a Riemann-Liouville two-point boundary value problem. *Appl. Math. Lett.*, 103:106201, 1–8, 2020.

[49] Q. Huang, R.-J. Qi, and W. Qiu. The efficient alternating direction implicit Galerkin method for the nonlocal diffusion-wave equation in three dimensions. *J. Appl. Math. Comput.*, 68(5):3067–3087, 2022.

[50] A. Jaishankar and G. H. McKinley. Power-law rheology in the bulk and at the interface: quasi-properties and fractional constitutive equations. *Proc. R. Soc. Lond. Ser. A Math. Phys. Eng. Sci.*, 469(2149):20120284, 1–18, 2013.

[51] L. Jia, H. Chen, and V. J. Ervin. Existence and regularity of solutions to 1-D fractional order diffusion equations. *Electron. J. Differential Equations*, 2019:93, 1–21, 2019.

[52] H. Jiang, D. Xu, W. Qiu, and J. Zhou. An ADI compact difference scheme for the two-dimensional semilinear time-fractional mobile-immobile equation. *Comput. Appl. Math.*, 39(4):287, 17, 2020.

[53] B. Jin, B. Li, and Z. Zhou. Numerical analysis of nonlinear subdiffusion equations. *SIAM J. Numer. Anal.*, 56(1):1–23, 2018.

[54] C. Johnson and J. Pitkäranta. An analysis of the discontinuous Galerkin method for a scalar hyperbolic equation. *Math. Comp.*, 46(173):1–26, 1986.

[55] Q. D. Katatbeh and F. B. M. Belgacem. Applications of the Sumudu transform to fractional differential equations. *Nonlinear Stud.*, 18(1):99–112, 2011.

[56] H. B. Keller. *Numerical methods for two-point boundary-value problems*. Blaisdell Publishing Co. [Ginn and Co.], Waltham, Mass.-Toronto, Ont.-London, 1968.

[57] H. B. Keller. *Numerical solution of two point boundary value problems*, volume No. 24 of *Regional Conference Series in Applied Mathematics*. SIAM, Philadelphia, PA, 1976.

[58] J. F. Kelly, H. Sankaranarayanan, and M. M. Meerschaert. Boundary conditions for two-sided fractional diffusion. *J. Comput. Phys.*, 376:1089–1107, 2019.

[59] A. A. Kilbas, H. M. Srivastava, and J. J. Trujillo. *Theory and applications of fractional differential equations*, volume 204 of *North-Holland Mathematics Studies*. Elsevier Science B.V., Amsterdam, 2006.

[60] C. Kirches, H. G. Bock, J. P. Schlöder, and S. Sager. Block-structured quadratic programming for the direct multiple shooting method for optimal control. *Optim. Methods Softw.*, 26(2):239–257, 2011.

[61] L. Kong, P. Zhu, Y. Wang, and Z. Zeng. Efficient and accurate numerical methods for the multidimensional convection-diffusion equations. *Math. Comput. Simulation*, 162:179–194, 2019.

[62] P. Lasaint and P.-A. Raviart. On a finite element method for solving the neutron transport equation. In *Mathematical aspects of finite elements in partial differential equations (Proc. Sympos., Math. Res. Center, Univ. Wisconsin, Madison, Wis., 1974)*, pages 89–123. Academic Press, New York-London, 1974.

[63] B. Q. Li. *Discontinuous finite elements in fluid dynamics and heat transfer*. Computational Fluid and Solid Mechanics. Springer-Verlag London, Ltd., London, 2006.

[64] C. Li, D. Li, and Z. Wang. L1/LDG method for the generalized time-fractional Burgers' equation. *Math. Comput. Simulation*, 187:357–378, 2021.

[65] C. Li and F. Zeng. *Numerical methods for fractional calculus*. Chapman & Hall/CRC Numerical Analysis and Scientific Computing. CRC Press, Boca Raton, FL, 2015.

[66] D. Li, H.-L. Liao, W. Sun, J. Wang, and J. Zhang. Analysis of $L1$-Galerkin FEMs for time-fractional nonlinear parabolic problems. *Commun. Comput. Phys.*, 24(1):86–103, 2018.

[67] D. Li, C. Zhang, and M. Ran. A linear finite difference scheme for generalized time fractional Burgers' equation. *Appl. Math. Model.*, 40(11-12):6069–6081, 2016.

[68] L. Li, D. Xu, and M. Luo. Alternating direction implicit Galerkin finite element method for the two-dimensional fractional diffusion-wave equation. *J. Comput. Phys.*, 255:471–485, 2013.

[69] C.-S. Liu. Efficient shooting methods for the second-order ordinary differential equations. *CMES Comput. Model. Eng. Sci.*, 15(2):69–86, 2006.

[70] C.-S. Liu. The Lie-group shooting method for nonlinear two-point boundary value problems exhibiting multiple solutions. *CMES Comput. Model. Eng. Sci.*, 13(2):149–163, 2006.

[71] C.-S. Liu. The Lie-group shooting method for singularly perturbed two-point boundary value problems. *CMES Comput. Model. Eng. Sci.*, 15(3):179–196, 2006.

[72] H. Liu and J. Yan. The direct discontinuous Galerkin (DDG) methods for diffusion problems. *SIAM J. Numer. Anal.*, 47(1):675–698, 2008/09.

[73] Z. Liu, F. Liu, and F. Zeng. An alternating direction implicit spectral method for solving two dimensional multi-term time fractional mixed diffusion and diffusion-wave equations. *Appl. Numer. Math.*, 136:139–151, 2019.

[74] Y. Luchko. Maximum principle for the generalized time-fractional diffusion equation. *J. Math. Anal. Appl.*, 351(1):218–223, 2009.

[75] Y. Luchko and A. Punzi. Modeling anomalous heat transport in geothermal reservoirs via fractional diffusion equations. *GEM Int. J. Geomath.*, 1(2):257–276, 2011.

[76] A. A. Lukassen and M. Kiehl. Operator splitting for chemical reaction systems with fast chemistry. *J. Comput. Appl. Math.*, 344:495–511, 2018.

[77] Z. Luo, X. Zhang, S. Wang, and L. Yao. Numerical approximation of time fractional partial integro-differential equation based on compact finite difference scheme. *Chaos Solitons Fractals*, 161:112395, 8, 2022.

[78] R. L. Magin. *Fractional calculus in bioengineering*, volume 2. Begell House Redding, Danbury, CT, 2006.

[79] J. Mazloum and B. Hadian Siahkal-Mahalle. A time-splitting local meshfree approach for time-fractional anisotropic diffusion equation: application in image denoising. *Adv. Contin. Discrete Models*, 2022:56, 1–19, 2022.

[80] G. M. Mittag-Leffler. Sur la représentation analytique d'une branche uniforme d'une fonction monogène. *Acta Math.*, 29(1):101–181, 1905.

[81] D. D. Morrison, J. D. Riley, and J. F. Zancanaro. Multiple shooting method for two-point boundary value problems. *Comm. ACM*, 5:613–614, 1962.

[82] K. Mustapha, B. Abdallah, K. M. Furati, and M. Nour. A discontinuous Galerkin method for time fractional diffusion equations with variable coefficients. *Numer. Algorithms*, 73(2):517–534, 2016.

[83] R. Nigmatullin. The realization of the generalized transfer equation in a medium with fractal geometry. *Phys. Status Solidi (B)*, 133(1):425–430, 1986.

[84] P. Patie and T. Simon. Intertwining certain fractional derivatives. *Potential Anal.*, 36(4):569–587, 2012.

[85] A. Pedas, E. Tamme, and M. Vikerpuur. Numerical solution of linear fractional weakly singular integro-differential equations with integral boundary conditions. *Appl. Numer. Math.*, 149:124–140, 2020.

[86] W. Qiu, H. Chen, and X. Zheng. An implicit difference scheme and algorithm implementation for the one-dimensional time-fractional Burgers' equations. *Math. Comput. Simulation*, 166:298–314, 2019.

[87] G. F. Raggett. On the solution of hyperbolic partial differential equations using cubic splines. In *International Congress of Mathematicians, Vancouver, Canada*, volume 31, pages 297–319. 1974.

[88] G. F. Raggett and P. D. Wilson. A fully implicit finite difference approximation to the one-dimensional wave equation using a cubic spline technique. *J. Inst. Math. Appl.*, 14:75–77, 1974.

[89] W. H Reed and T. R Hill. Triangular mesh methods for the neutron transport equation. Technical report, Los Alamos Scientific Lab., N. Mex.(USA), 1973.

[90] G. R. Richter. An optimal-order error estimate for the discontinuous Galerkin method. *Math. Comp.*, 50(181):75–88, 1988.

[91] G. R. Richter. The discontinuous Galerkin method with diffusion. *Math. Comp.*, 58(198):631–643, 1992.

[92] S. Z. Rida, A. A. Yahya, N. A. Zidan, and H. M. Bakry. Fractional order of mathematical systems for some bio-chemical application. *J. Fract. Calc. Appl.*, 5(3S):25, 17, 2014.

[93] B. Rivière. *Discontinuous Galerkin methods for solving elliptic and parabolic equations: Theory and implementation*, volume 35 of *Frontiers in Applied Mathematics*. Society for Industrial and Applied Mathematics (SIAM), Philadelphia, PA, 2008.

[94] B. Rivière, M. F. Wheeler, and V. Girault. Improved energy estimates for interior penalty, constrained and discontinuous Galerkin methods for elliptic problems. I. *Comput. Geosci.*, 3(3-4):337–360, 1999.

[95] S. Santra and J. Mohapatra. A novel finite difference technique with error estimate for time fractional partial integro-differential equation of Volterra type. *J. Comput. Appl. Math.*, 400:113746, 1–13, 2022.

[96] M. Saqib, I. Khan, and S. Shafie. Application of fractional differential equations to heat transfer in hybrid nanofluid: modeling and solution via integral transforms. *Adv. Difference Equ.*, 2019:52, 1–18, 2019.

[97] M. Kh. Shkhanukov. On the convergence of difference schemes for differential equations with a fractional derivative. *Dokl. Akad. Nauk*, 348(6):746–748, 1996.

[98] M. Kh. Shkhanukov, A. A. Kerefov, and A. A. Berezovskiĭ. Boundary value problems for the heat equation with a fractional derivative in the boundary conditions, and difference methods for their numerical realization. *Ukraïn. Mat. Zh.*, 45(9):1289–1298, 1993.

[99] G. Singh and S. Natesan. Superconvergence of discontinuous Galerkin method with interior penalties for singularly perturbed two-point boundary-value problems. *Calcolo*, 55(4):54, 1–30, 2018.

[100] G. Singh and S. Natesan. Study of the NIPG method for two-parameter singular perturbation problems on several layer adapted grids. *J. Appl. Math. Comput.*, 63(1-2):683–705, 2020.

[101] I. H. Sloan and V. Thomée. Time discretization of an integro-differential equation of parabolic type. *SIAM J. Numer. Anal.*, 23(5):1052–1061, 1986.

[102] F. Song and C. Xu. Spectral direction splitting methods for two-dimensional space fractional diffusion equations. *J. Comput. Phys.*, 299:196–214, 2015.

[103] D. Sornette. Critical market crashes. *Physics Reports*, 378(1):1–98, 2003.

[104] H. E. Stanley and R. N. Mantegna. *An introduction to econophysics.* Cambridge University Press, Cambridge, 2000.

[105] J.P. Sturmberg and C.M. Martin. *Handbook of Systems and Complexity in Health.* Springer, New York, 2013.

[106] M. Stynes, E. O'Riordan, and J. L. Gracia. Error analysis of a finite difference method on graded meshes for a time-fractional diffusion equation. *SIAM J. Numer. Anal.*, 55(2):1057–1079, 2017.

[107] M. Turalska, M. Lukovic, B. J. West, and P. Grigolini. Complexity and synchronization. *Phys. Rev. E*, 80:021110, 2009.

[108] S. Wang, J. Yuan, W. Deng, and Y. Wu. A hybridized discontinuous Galerkin method for 2D fractional convection-diffusion equations. *J. Sci. Comput.*, 68(2):826–847, 2016.

[109] T. Wang and Y.-M. Wang. A higher-order compact LOD method and its extrapolations for nonhomogeneous parabolic differential equations. *Appl. Math. Comput.*, 237:512–530, 2014.

[110] Y.-M. Wang. Error and extrapolation of a compact LOD method for parabolic differential equations. *J. Comput. Appl. Math.*, 235(5):1367–1382, 2011.

[111] Y.-M. Wang and L. Ren. A high-order $L2$-compact difference method for Caputo-type time-fractional sub-diffusion equations with variable coefficients. *Appl. Math. Comput.*, 342:71–93, 2019.

[112] G. K. Watugala. Sumudu transform: a new integral transform to solve differential equations and control engineering problems. *Internat. J. Math. Ed. Sci. Tech.*, 24(1):35–43, 1993.

[113] M. Waurick. Homogenization in fractional elasticity. *SIAM J. Math. Anal.*, 46(2):1551–1576, 2014.

[114] S. Weerakoon. Application of Sumudu transform to partial differential equations. *Internat. J. Math. Ed. Sci. Tech.*, 25(2):277–283, 1994.

[115] B.J. West and P. Grigolini. Habituation and 1/f-noise. *Physica A: Statistical Mechanics and its Applications*, 389(24):5706–5718, 2010.

[116] M. F. Wheeler. An elliptic collocation-finite element method with interior penalties. *SIAM J. Numer. Anal.*, 15(1):152–161, 1978.

[117] Q. Xu and J. S. Hesthaven. Discontinuous Galerkin method for fractional convection-diffusion equations. *SIAM J. Numer. Anal.*, 52(1):405–423, 2014.

[118] S. Yaghoobi, B. P. Moghaddam, and K. Ivaz. An efficient cubic spline approximation for variable-order fractional differential equations with time delay. *Nonlinear Dynam.*, 87(2):815–826, 2017.

[119] N. N. Yanenko. *The method of fractional steps: The solution of problems of mathematical physics in several variables*. Springer-Verlag, New York-Heidelberg, 1971.

[120] W. K. Zahra and S. M. Elkholy. The use of cubic splines in the numerical solution of fractional differential equations. *Int. J. Math. Math. Sci.*, 2012:638026, 1–16, 2012.

[121] Z. Zhao and H. Li. Numerical study of two-dimensional Burgers' equation by using a continuous Galerkin method. *Comput. Math. Appl.*, 149:38–48, 2023.

Publications from this Thesis

Published Papers

1. **Sandip Maji, Srinivasan Natesan:** *An Efficient Numerical Method for Fractional Advection-Diffusion-Reaction Problem with RLC Fractional Derivative*, **Mediterranean Journal of Mathematics** (2023) 20:297.
2. **Sandip Maji, Srinivasan Natesan:** *Analytical and Numerical Solutions of Time-Fractional Advection-Diffusion-Reaction Equations*, **Applied Numerical Mathematics** 185 (2023), 549–570.
3. **Sandip Maji, Srinivasan Natesan:** *Nonsymmetric interior penalty Galerkin method for nonlinear time-fractional integro-partial differential equations*, **Mathematics and Computers in Simulation** 213 (2023), 1–17.
4. **Sandip Maji, Srinivasan Natesan:** *Analytical and numerical solution techniques for a class of time-fractional integro-partial differential equations*, **Numerical Algorithms** 94 (2023), 229–256.
5. **Sandip Maji, Srinivasan Natesan:** *Adaptive-grid technique for the numerical solution of a class of fractional boundary-value-problems*, **Computational Methods for Differential Equations** 12(2), 338–349, 2024.
6. **Sandip Maji, Srinivasan Natesan:** *Superconvergence analysis of interior penalty discontinuous Galerkin method for a class of time-fractional diffusion problems*, **Computational and Applied Mathematics** (2024) 43:133.
7. **Sandip Maji, Srinivasan Natesan:** *Error analysis for discontinuous Galerkin method for time-fractional Burgers' equation*, **Mathematical Methods in the Applied Sciences** (2024) (Accepted).

Submitted Papers

1. **Sandip Maji, Srinivasan Natesan:** *Error estimate for the direction splitting discontinuous Galerkin methods for two-dimensional time-fractional diffusion equations.* (Under Review)